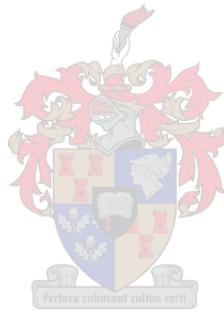


# INVESTIGATION INTO THE EFFECTIVE LENGTHS OF WEB COMPRESSION ELEMENTS IN PARALLEL CHORD TRUSSES

by

Wibke Dunaiski

Thesis presented in partial fulfillment of the requirements for the degree  
of



Master of Science in Engineering at Stellenbosch University

Professor PE Dunaiski  
Professor PJ Pahl  
Professor GPAG van Zijl

December 2008

**DECLARATION**

By submitting this thesis electronically, I declare that the entirety of the work contained therein is my own, original work, that I am the owner of the copyright thereof (unless to the extent explicitly otherwise stated) and that I have not previously in its entirety or in part submitted it for obtaining any qualification.

Signature : .....

Date : .....

## SYNOPSIS

The Southern African Institute of Steel Construction expressed concern with regard to the unit definition of the effective length factor,  $K$ , stipulated for compressive elements of parallel chord trusses in Clause 15 of SANS 10162-1:2005 - Limit state design of hot-rolled steelwork. The simplified method for truss design specified in the code assumes all compression members are pin-connected, which allows for greater design simplicity and reduces the amount of code interpretation required by the designer. In addition to this, Clause 15 requires the additional reduction in resistance of the first web compression members by a factor of 0.85. However, this approach may be considered overly conservative and in current design practice the effective length factor is often reduced to less than 1.0.

This research investigates the effective length factor of web compression members in parallel chord trusses, by means of investigative structural analyses of representative trusses using ANGELINE and Prokon analytical programs, and by designing, constructing and testing six representative trusses, using current design practices. A comparative study of a number of different countries' codified approaches to truss design is also included.

The structural analyses revealed that in-plane buckling of the web compression members was the consistent mode of failure, however at a much greater applied load than the design load determined according to SANS 10162-1:2005. Contrary to the expected mode of failure, all six tests performed on the representative trusses exhibited elastic out-of-plane buckling, or strong-axis buckling, of the web compression members, but still at a much greater applied load than the design load. The unexpected out-of-plane buckling of the web members is due to the in-plane stiffness of the end connections used. In order to stay true to current design practice, gusset plates and longitudinal welds were used to join the web members to the chords. The stiffness of the gusset plates therefore significantly reduced the effective length of the web compression members in-plane, but did not reduce the effective length out-of-plane.

Despite the unanticipated behaviour of the tests performed, certain conclusions can still be drawn from the results. The unit definition of the effective length factor for in-plane buckling of web compression members is too conservative and a  $K$  factor of 0.8 is recommended. In addition to this an effective length factor for out-of-plane-buckling of web compression members of 1.1 is recommended for trusses with welded connections. The necessity of the reduction in resistance of 0.85 of the first web compression members requires further investigation. The most important conclusion to be drawn is that out-of-plane buckling of web compression members can be the dominant failure mode, which is not taken into consideration in current design practice.

## SAMEVATTING

Navorsing is gedoen op die eenheidsdefinisie van die effektiewe lengte faktor,  $K$ , vir drukelemente in die web van parallel-koord vakwerke, soos voorgeskryf in Klousule 15 van SANS 10162-1:2005 - Limit state design of hot-rolled steelwork. Die navorsing is gedoen as gevolg van besorgdheid wat deur die Suidelike Afrikaanse Instituut vir Staal Konstruksie uitgedruk is ten opsigte van die huidige aanwending van hierdie klousule in die praktyk. Die vereenvoudigde metode vir die ontwerp van vakwerke, soos voorgeskryf in die kode, is gebaseer op die aanname dat die drukelemente in 'n vakwerk by hul verbindingspunte nie teen rotasie ingeklem is nie. Dit vereenvoudig die ontwerpprosedure en minimaliseer die benodigde interpretasie van die kode. Bykomstig tot die eenheidsdefinisie van die  $K$ -faktor, moet die weerstand van die eerste drukelemente in die web met 'n faktor 0.85 gereduseer word. Hierdie benadering tot die ontwerp van die drukelemente word dikwels as te konserwatief beskou. 'n  $K$ -faktor van minder as een word gevolglik dikwels in die praktyk toegepas.

Die effektiewe lengte faktor van parallel-koord vakwerke word ondersoek deur middel van strukturele analyses, deur gebruik te maak van ANGELINE en Prokon. Ses verteenwoordigende vakwerke is ontwerp, vervaardig en getoets, met die toepassing van huidige ontwerpgebruike. Daar is ook 'n vergelykende studie gedoen op die verskillende ontwerpkode benaderings van verskeie lande. Die strukturele analyses het aangetoon dat knik van die drukelemente in die web, in die vlak van die vakwerk, die oorheersende swigtingsvorm is, maar by 'n baie hoër aangewende las as die ontwerplas wat bepaal is deur SANS 10162-1:2005. Teen die verwagting het in al ses vakwerke wat getoets is, die kritieke elemente uit die vlak van die vakwerk elasties geknik, maar steeds by 'n baie hoër aangewende las as die ontwerplas.

Die onverwagte knik van die webelemente uit die vlak van die vakwerk is as gevolg van die styfheid van die endverbindings van die elemente. Knoopplate en langssweisnate is gebruik om die webelemente aan die koorde te verbind, om sodanig so getrou as moontlik aan huidige ontwerpgebruike te bly. Die styfheid van die verbindings het dus die effektiewe lengte van die drukelemente in die vlak van die vakwerk beduidend verminder, maar nie die effektiewe lengte uit die vlak nie. Ten spyte van die onverwagte gedrag tydens die toetse kan sekere gevolgtrekkings gemaak word. Die eenheidsdefinisie van die effektiewe lengte faktor vir knik van webelemente in die vlak van die vakwerk is te konserwatief en 'n  $K$ -faktor van 0.8 word aanbeveel. 'n Effektiewe lengte faktor vir knik uit die vlak van die vakwerk vir web-drukelemente van 1.1 word aanbeveel vir vakwerke met gesweiste endverbindings. Die kwessie van die vermindering van die weerstand van die eerste web-drukelemente met 'n faktor 0.85 benodig addisionele ondersoek. Die belangrikste gevolgtrekking wat gemaak kan word is dat knik van die web-drukelemente uit die vlak van die vakwerk die oorheersende swigtingsvorm van gesweiste parallel-koord vakwerke kan wees, wat huidig nie in die praktyk in ag geneem word nie.

## **ACKNOWLEDGEMENTS**

The author of this thesis would like to express her gratitude to the following people:

- Professor PE Dunaiski for his guidance and support
- Professor PJ Pahl for his invaluable expert knowledge, time and effort
- Dion Viljoen for his dedication and advice
- Arthur Layman for his patience and support
- The Southern African Institute of Steel Construction and the Frank Wilhelm Trust for their financial support

## TABLE OF CONTENTS

<b>LIST OF FIGURES.....</b>	<b>IX</b>
<b>LIST OF TABLES .....</b>	<b>XI</b>
<b>LIST OF SYMBOLS.....</b>	<b>XII</b>
<b>LIST OF ABBREVIATIONS.....</b>	<b>XIV</b>
<b>1. INTRODUCTION.....</b>	<b>1.1</b>
1.1 OBJECTIVES.....	1.1
1.2 APPROACH .....	1.2
1.3 SCOPE.....	1.3
<b>2. LITERATURE STUDY .....</b>	<b>2.1</b>
2.1 BACKGROUND.....	2.1
2.2 GENERAL ANALYSIS CONSIDERATIONS.....	2.1
2.3 EFFECTIVE LENGTHS OF COMPRESSION MEMBERS .....	2.2
2.4 END CONNECTION DESIGN .....	2.3
2.5 ANGLES IN COMPRESSION .....	2.4
2.6 BUCKLING .....	2.5
2.7 OUT-OF-PLANE STABILITY.....	2.6
2.8 NONLINEAR STRUCTURAL BEHAVIOUR .....	2.7
<b>3. DESIGN CODE SURVEY .....</b>	<b>3.1</b>
3.1 BENCHMARK PROBLEM.....	3.1
3.2 SANS 10162-1 : THE STRUCTURAL USE OF STEEL : PART 1 (2005) .....	3.1
3.3 BS 5950 : STRUCTURAL USE OF STEELWORK IN BUILDING : PART 1 (2000).....	3.3
3.4 SIA 263 : STEEL CONSTRUCTION (2003) .....	3.5
3.5 ANSI / AISC 360 – 05 : SPECIFICATION FOR STRUCTURAL STEEL BUILDINGS (2005) ....	3.7
3.6 CAN/CSA – S16-01 : LIMIT STATES DESIGN OF STEEL STRUCTURES (2005) .....	3.9
3.7 SUMMARY OF RESULTS.....	3.9
<b>4. INVESTIGATIVE ANALYSES .....</b>	<b>4.1</b>
4.1 EFFECTS TO BE INVESTIGATED .....	4.1
4.2 PRACTICAL CONSIDERATIONS .....	4.2
4.3 CHOICE OF SOFTWARE .....	4.3
4.4 THEORY BASIS OF ANGELINE .....	4.3
4.5 APPLICATION OF ANGELINE TO INVESTIGATIVE ANALYSES .....	4.5
4.6 INVESTIGATIVE ANALYSES PERFORMED.....	4.10
4.7 RESULTS OF FRAMEVERTICAL ANALYSES .....	4.12
4.8 RESULTS OF FRAMEDIAGONAL ANALYSES .....	4.18
4.9 CONCLUSIONS OF ANALYSES .....	4.24

---

<b>5.</b>	<b>STRUCTURAL ANALYSES .....</b>	<b>5.1</b>
5.1	PROKON STRUCTURAL ANALYSES .....	5.1
5.2	ANGELINE STRUCTURAL ANALYSES .....	5.5
5.3	COMPARISON OF RESULTS .....	5.7
5.4	INVESTIGATION INTO SIGNIFICANCE OF OWN WEIGHT ON BUCKLING LOAD.....	5.9
<b>6.</b>	<b>DESIGN, CONSTRUCTION AND EXECUTION OF EXPERIMENTS.....</b>	<b>6.1</b>
6.1	DESIGN OF TRUSSES.....	6.1
6.2	DESIGN OF CONNECTIONS .....	6.2
6.3	DESIGN OF SUPPORTS.....	6.3
6.4	DETERMINATION OF MATERIAL PROPERTIES.....	6.4
6.5	SETUP OF TEST .....	6.7
6.6	TEST PROCEDURE .....	6.12
6.7	RESULTS OF WIND LOAD CASE TESTS .....	6.14
6.8	RESULTS OF GRAVITY LOAD CASE TESTS .....	6.19
<b>7.</b>	<b>COMPARISON OF ANALYTICAL AND EXPERIMENTAL RESULTS .....</b>	<b>7.1</b>
7.1	GRAVITY LOAD CASE .....	7.2
7.2	WIND LOAD CASE .....	7.4
7.3	COMPARISON OF EXPERIMENTAL RESULTS TO CODE APPROACH.....	7.5
<b>8.</b>	<b>CONCLUSIONS AND RECOMMENDATIONS .....</b>	<b>8.1</b>
8.1	CONCLUSIONS .....	8.1
8.2	RECOMMENDATIONS .....	8.3
<b>9.</b>	<b>REFERENCES .....</b>	<b>9.1</b>
9.1	BOOKS.....	9.1
9.2	PUBLICATIONS .....	9.2
9.3	DESIGN CODES.....	9.3
<b>A.</b>	<b>APPENDIX : DETAILED BENCHMARK PROBLEM CALCULATIONS .....</b>	<b>I</b>
	GENERAL SECTION PROPERTIES : 60 X 60 X 5 DOUBLE ANGLE .....	I
	SANS 10162-1 : 2005 & CSA/CAN S16-01 .....	II
	BS 5950-1 : 2000 .....	IV
	SIA 263 : 2003 .....	VI
	ANSI / AISC 360 - 05.....	VII
<b>B.</b>	<b>APPENDIX : DETERMINATION OF CRITICAL ELEMENT DESIGN LOADS.....</b>	<b>I</b>
	GRAVITY LOAD CASE.....	I
	WIND LOAD CASE.....	III
<b>C.</b>	<b>APPENDIX : DRAWINGS FOR GRAVITY LOAD CASE TRUSS .....</b>	<b>I</b>
	GENERAL NOTES TO WORKSHOP DRAWINGS.....	I
	LIST OF WORKSHOP DRAWINGS .....	I

---

<b>D.</b>	<b>APPENDIX : DRAWINGS FOR WIND LOAD CASE TRUSS.....</b>	<b>I</b>
	GENERAL NOTES TO WORKSHOP DRAWINGS.....	I
	LIST OF WORKSHOP DRAWINGS .....	I
<b>E.</b>	<b>APPENDIX : RESULTS OF GRAVITY LOAD CASE TESTS.....</b>	<b>I</b>
	DISPLACEMENT OF SUPPORTS .....	I
	INFLUENCE OF TEMPERATURE ON STRAIN MEASUREMENTS .....	II
	TEST 1 : GREEN.....	III
	TEST 2 : YELLOW.....	IV
	TEST 3 : ORANGE .....	V
<b>F.</b>	<b>APPENDIX : RESULTS OF WIND LOAD CASE.....</b>	<b>I</b>
	DISPLACEMENT OF SUPPORTS .....	I
	INFLUENCE OF TEMPERATURE ON STRAIN MEASUREMENTS.....	II
	TEST 1 : GREEN.....	III
	TEST 2 : YELLOW.....	IV
	TEST 3 : ORANGE .....	V

**LIST OF FIGURES**

Figure 1.1 : Road map .....	1.2
Figure 3.1 : Buckling curves used to determine buckling stress of compression members .....	3.6
Figure 3.2 : Comparison of axial compressive resistance for varying slenderness ratios .....	3.10
Figure 3.3 : Comparison of axial compressive resistance excluding Euler buckling curves.....	3.10
Figure 4.1 : Definition of connection types.....	4.5
Figure 4.2 : Graphical user interface specifically developed for investigative analyses .....	4.6
Figure 4.3 : Graphical verification of input specified for a specific analysis.....	4.6
Figure 4.4 : Specification of graphical results to be shown.....	4.7
Figure 4.5 : Graphical representation of displacements .....	4.8
Figure 4.6 : Graphical representation of axial forces .....	4.8
Figure 4.7 : Graphical representation of bending moments.....	4.8
Figure 4.8 : Distribution of axial forces in 6 bay truss .....	4.10
Figure 4.9 : Distribution of axial forces in 10 bay truss .....	4.10
Figure 4.10 : Load cases A, B and C for six bay truss.....	4.11
Figure 4.11 : Load cases A, B and C for eight bay truss .....	4.11
Figure 4.12 : Load cases A, B and C for ten bay truss .....	4.11
Figure 4.13 : Effect of node fixity on the critical element buckling load .....	4.12
Figure 4.14 : Effect of stiffness of neighbouring elements on node fixity.....	4.13
Figure 4.15 : Illustration of first and middle elements of frameVertical.....	4.14
Figure 4.16 : Effect of node fixity on the distribution of axial forces in the truss.....	4.15
Figure 4.17 : Maximum bending moments which occur in each element type .....	4.16
Figure 4.18 : Effect of reducing a distributed load to a single point load at midspan .....	4.17
Figure 4.19 : Effect of Node fixity on the critical element buckling load.....	4.18
Figure 4.20 : Effect of stiffness of neighbouring elements on node fixity.....	4.19
Figure 4.21 : Illustration of first and middle elements of frameDiagonal.....	4.20
Figure 4.22 : Effect of node rigidity on distribution of axial forces in the truss.....	4.21
Figure 4.23 : Maximum bending moments which occur in each element type .....	4.22
Figure 4.24 : Effect of reducing a distributed load to a single point load at midspan .....	4.23
Figure 4.25 : Truss configuration for gravity load case .....	4.26
Figure 4.26 : Truss configuration for wind load case .....	4.26
Figure 5.1 : Output of buckling analysis for gravity load case.....	5.2
Figure 5.2 : Output of second order analysis for gravity load case.....	5.3
Figure 5.3 : Output of buckling analysis for wind load case.....	5.3
Figure 5.4 : Output of second order analysis for wind load case.....	5.4
Figure 5.5 : Output of frameVertical analysis.....	5.5
Figure 5.6 : Output of frameDiagonal analysis.....	5.6
Figure 5.7 : Identification of material failure point for gravity load case.....	5.8
Figure 5.8 : Identification of material failure point for wind load case .....	5.9

---

Figure 6.1 : Truss layout for gravity load case as determined by frameVertical analyses.....	6.1
Figure 6.2 : Truss layout for wind load case as determined by frameDiagonal analyses.....	6.2
Figure 6.3 : Cross-section of Glacier pot supports.....	6.3
Figure 6.4 : Glacier pot support used to create pin support (left) and roller support (right).....	6.4
Figure 6.5 : Tensile test of coupon performed in Zwick Z250.....	6.5
Figure 6.6 : Results of tensile tests of 25 x 25 x 3 angle coupons.....	6.6
Figure 6.7 : Results of tensile tests of 30 x 30 x 3 angle coupons.....	6.6
Figure 6.8 : Results of tensile tests of 40 x 40 x 6 angle coupons.....	6.6
Figure 6.9 : Distribution of yield stresses achieved in material tests .....	6.6
Figure 6.10 : Setup of test frame within multi-purpose beam/column testing apparatus.....	6.7
Figure 6.11 : Setup of test frame within multi-purpose beam/column testing apparatus.....	6.7
Figure 6.12 : Fork and steel pin used to transfer load from tensile rod to bottom chord .....	6.8
Figure 6.13 : Frame designed for load application and to support actuator and load cell .....	6.9
Figure 6.14 : Frame designed for load application and to support actuator and load cell .....	6.9
Figure 6.15 : Positioning of strain gauges at mid-length of critical elements.....	6.10
Figure 6.16 : Positioning of measuring devices for the gravity load case tests .....	6.11
Figure 6.17 : Expected behaviour during testing of gravity load case .....	6.13
Figure 6.18 : Expected behaviour during testing of wind load case .....	6.13
Figure 6.19: Out-of-plane buckling mode of failed diagonal compression members.....	6.14
Figure 6.20 : Post-buckling condition of gusset plates supporting failed diagonal members ..	6.15
Figure 6.21 : Comparison of location of failed diagonal compression members .....	6.15
Figure 6.22 : Revised strain gauge configuration .....	6.16
Figure 6.23 : Stresses in buckled diagonal compression members .....	6.18
Figure 6.24 : Comparison of vertical deflection of top chord at midspan.....	6.18
Figure 6.25 : Strain gauge configuration for vertical members .....	6.19
Figure 6.26 : Out-of-plane buckling mode of failed vertical compression members.....	6.20
Figure 6.27 : Post-buckling condition of gusset plates supporting failed vertical members ....	6.20
Figure 6.28 : Comparison of location of failed vertical compression members .....	6.21
Figure 6.29 : Stresses in buckled vertical compression members.....	6.22
Figure 6.30 : Comparison of test results of vertical deflection of top chord at midspan .....	6.22
Figure 7.1 : Definition of axes of double-angle sections used for web compression members.	7.1
Figure 7.2 : Comparison of location of failed vertical compression members .....	7.2
Figure 7.3 : Comparison of analytical and experimental vertical deflection of top chord.....	7.3
Figure 7.4 : Comparison of location of failed diagonal compression members .....	7.4
Figure 7.5 : Comparison of analytical and experimental vertical deflection of top chord.....	7.4

**LIST OF TABLES**

Table 3.1 : Nominal effective length $L_E$ for a compression member, BS 5950-1:2000 .....	3.3
Table 3.2 : Reduced buckling lengths for compressive truss members, Table 13, SIA 263 .....	3.5
Table 3.3 : Summary of effective length factors and axial compressive resistances in kN .....	3.9
Table 4.1 : Excel sheet extract of results corresponding to input depicted in Figure 4.2 .....	4.9
Table 4.2 : Summary of analyses performed in ANGELINE .....	4.11
Table 4.3 : Summary of results obtained for frameVertical and frameDiagonal .....	4.24
Table 4.4 : Section sizes of truss elements for both truss configurations.....	4.27
Table 5.1 : Member forces in vertical elements at buckling point of critical element.....	5.3
Table 5.2 : Member forces in diagonal elements at buckling point of critical element.....	5.4
Table 5.3 : Member forces in vertical elements at buckling point of critical element.....	5.5
Table 5.4 : Member forces in diagonal elements at buckling point of critical element.....	5.6
Table 5.5 : Comparison of results obtained from structural analyses .....	5.7
Table 5.6 : Axial forces in elements due to own weight in gravity load case configuration .....	5.10
Table 5.7 : Axial forces in elements due to own weight in wind load case configuration .....	5.10
Table 6.1 : Truss dimensions and section sizes for gravity load case .....	6.1
Table 6.2 : Truss dimensions and section sizes for wind load case: .....	6.2
Table 6.3 : Samples tested for material property verification.....	6.5
Table 6.4 : Summary of statistical data of yield stress .....	6.5
Table 6.5 : Summary of measuring program .....	6.11
Table 6.6 : Expected values of measurements during testing of gravity load case .....	6.12
Table 6.7 : Expected values of measurements during testing of wind load case .....	6.13
Table 6.8 : Comparison of principle measurement results of wind load case tests .....	6.17
Table 6.9 : Comparison of principle measurement results of gravity load case tests.....	6.21
Table 7.1 : Comparison of principle analytical and experimental results of gravity load case...	7.3
Table 7.2 : Comparison of principle analytical and experimental results of wind load case.....	7.5
Table 7.3 : Comparison of critical loads and effective length factors for gravity load case .....	7.6
Table 7.4 : Comparison of critical loads and effective length factors for wind load case .....	7.6

**LIST OF SYMBOLS**

$A$	cross-sectional area
$A_{\text{eff}}$	effective cross-sectional area
$A_g$	gross cross-sectional area
$C_r$	factored compressive resistance of member
$C_w$	warping torsional constant
$E$	elastic modulus of steel
$F_{\text{cr}}$	critical stress
$F_e$	elastic critical buckling stress
$F_y$	yield stress
$G$	Shear modulus of steel
$J$	St Venant torsional constant of a cross-section
$K$	effective length factor
$L$	gross length of member
$L_E$	nominal effective length
$L_K$	effective length
$N_{b,Rd}$	design buckling resistance
$N_{\text{cr}}$	elastic critical force for relevant buckling mode
$P_c$	compression resistance
$P_n$	nominal compressive strength
$a$	Robertson strut curve constant, distance between members in a built-up member
$f_e$	elastic critical buckling stress in axial compression
$f_y$	yield stress
$h$	distance between centroids of individual components perpendicular to the member axis of buckling
$i$	radius of gyration
$l_k$	effective length
$n$	material regression factor
$p_c$	compressive strength
$p_{\text{cs}}$	value of $p_c$ for a reduced slenderness
$p_Y$	design strength
$r$	radius of gyration
$r_{\text{ib}}$	radius of gyration
$x_o$	principal x-coordinate of shear centre with respect to centroid of cross-section
$y_o$	principal y-coordinate of shear centre with respect to centroid of cross-section

$\Phi$	value to determine the reduction factor $X$
$\Phi_K$	value to determine the reduction factor $X_K$
$X$	reduction factor for relevant buckling mode
$X_K$	reduction factor for relevant buckling mode
$\alpha$	imperfection factor, separation ratio
$\gamma_{M1}$	partial factor for resistance
$\lambda$	non-dimensional slenderness ratio
$\lambda_c$	slenderness ratio of main components centre-to-centre of interconnections
$\lambda_{f,e}$	yield slenderness ratio
$\lambda_k$	effective slenderness ratio
$\lambda_o$	limiting slenderness
$\sigma_{cr,K}$	critical elastic buckling stress
$\Phi$	resistance factor for structural steel
$\eta$	Perry factor for flexural buckling under axial force

**LIST OF ABBREVIATIONS**

ANGELINE	Analysis of geometrically nonlinear structures
AISC	American Institute of Steel Construction
ANSI	American National Standards Institute
ASCE	American Society of Civil Engineers
BS	British Standard
BSI	British Standards Institute
CAN	Canada
CSA	Canadian Standards Association
EN	Europäische Norm
GUI	graphical user interface
HBM	Hottinger Baldwin Messtechnik
LVDT	linearly varying displacement transducer
SAISC	Southern African Institute of Steel Construction
SANS	South African National Standards
SIA	Schweizerischer Ingenieur- und Architektenverein
SN	Schweizer Norm
TUB	Technical University Berlin

## 1. INTRODUCTION

The research was conducted as a result of concern, expressed by the Southern African Institute of Steel Construction (SAISC), with regard to the unit effective length factor,  $K$ , as defined for compressive elements of parallel chord trusses in Clause 15 of SANS 10162-1 : 2005<sup>[30]</sup>, Limit-state design of hot-rolled steelwork.

The simplified method for the design of parallel chord trusses allowed for in the clause, assumes that all members in a parallel chord truss are pin-connected. The effective length of the compression members for buckling in the plane of the truss is defined as the distance between the lines of intersection of the working points of the web members and the chords. The clause also makes allowance for the reduction of the factored resistance of the first web compression members and its connections by a factor of 0.85.

This unit definition of the effective length factor allows for greater design simplicity and reduces the amount of code interpretation required but, together with the 0.85 reduction of the factored resistance of the first web compression members, could be overly-conservative, and thereby result in excessive use of material. The current practice is sometimes not to take into account the unit definition regulation and replace it with a factor of less than one, as well as disregard the reduced resistance of the first web compression members, due to the perception of its conservativeness, with unpredictable consequences.

### 1.1 OBJECTIVES

The objective of the research is to provide answers to the following questions:

- What is the influence of the node fixity on the effective length of the compression elements and the distribution of the forces through the truss?
- Does the fixity of the nodes induce significant bending moments in the elements and would the elements subsequently have to be designed as beam-columns instead of simple columns?
- Can the effective length factor,  $K$ , as defined in Clause 15 of SANS 10162 – 1 : 2005, be reduced to less than 1.0?
- And, is the reduced resistance by a factor of 0.85 of the first web compression elements necessary?

## 1.2 APPROACH

The research consists of a literature study, as well as a survey of foreign codes of practice. The design approach of each code of practice is quantitatively compared by means of a benchmark problem. Investigative analyses are done by means of analyzing a range of different truss configurations and load patterns using the analytical program ANGELINE, in order to determine the optimum representative truss design for the experiments to be conducted.

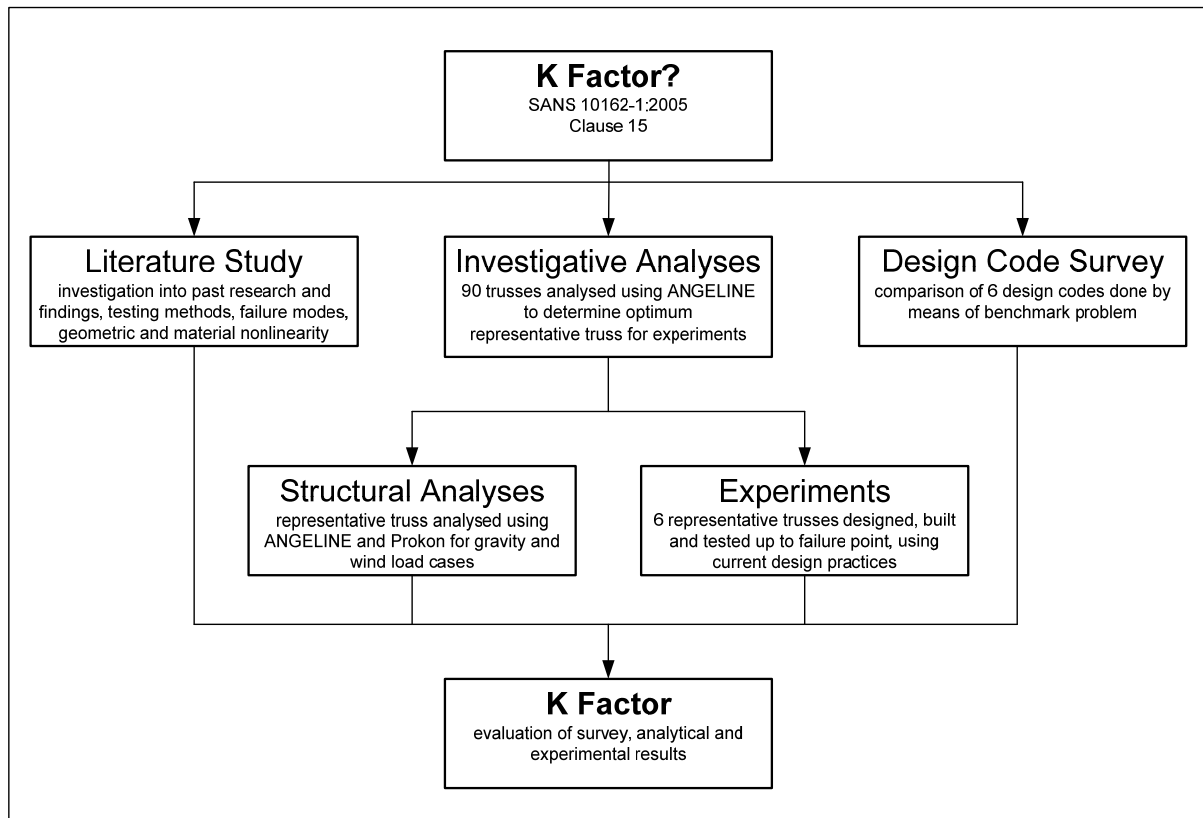


**Figure 1.1** : Road map

Theoretical and experimental analyses of the system are conducted. The theoretical analysis is done using two analytical programs, namely ANGELINE and Prokon. Two load cases are included in the structural analyses, a gravity load case as well as a wind load case. The experimental verification of the analytical results is conducted by designing, constructing and testing six representative trusses, three for each load case, using current design practices.

The results obtained from the design code survey, structural analyses and tests are compared and evaluated in order to draw conclusions.

### **1.3 SCOPE**

The research purposely excludes compression elements in the chords of the truss and focuses on the web compression elements, as it is the effective length of the web compression elements which is under consideration.

Both the analytical and experimental investigations are restricted to two dimensions, investigating only the in-plane behaviour of the truss. Several measures are taken in the experimental setup to ensure two dimensional behaviour of the system.

The load patterns applied are limited to two simulations. The first is an approximation of a gravity load, in which case the vertical web elements are in compression. The second is an approximation of a wind load, in which case the diagonal web elements are in compression. These load patterns allow for both types of web elements to be critical, as they would be in practice.

## 2. LITERATURE STUDY

### 2.1 BACKGROUND

A truss consists of tensile members (ties) and compressive members (struts) in the web, as well as top and bottom chords and carries loads by developing axial forces in these members. Despite this, the truss as a whole still behaves as a beam. For the same span and load as a beam, a truss has greater depth and is lighter due to its skeletal nature. The use of beams becomes uneconomical as the required span increases. Hence trusses become economically viable at spans greater than 20m, especially in large industrial structures. An economical depth to span ratio for a truss ranges between 1:10 and 1:20.

To determine initial member sizes, the beam behaviour of the truss can be used to approximate the force in a web member. The overall shear force at a point is an adequate indication of the force in the vertical member located at that point and the diagonal component of the shear force is an indication of the axial force in the diagonal member at that point. Likewise, the chord force can be approximated by dividing the overall bending moment at a point by the distance between the top and bottom chords.

The choice of node spacing must satisfy different criteria. Large node spacing is required to reduce fabrication costs and the complexity of the truss. However, the spacing of purlins, carrying the roof sheeting, determines the node spacing to a large extent. Members which meet at a node should be arranged in such a way to avoid or minimize eccentricities by ensuring that their centroidal axes intersect in one point at a node. If this is not possible, the connections must be designed to resist the bending moments induced by the eccentricities of the connections, in addition to the axial loads. Bending moments resulting from loads applied between nodes, apart from self weight, must also be taken into consideration.

### 2.2 GENERAL ANALYSIS CONSIDERATIONS

When the truss is subjected predominantly to static loading, the analysis can be done on the assumption of pinned member connections and internal forces and moments found by this simplified method are primary forces. If the truss is statically determinate, method of joints, method of sections or graphical methods can be used for hand calculations. If the truss is statically indeterminate, manual methods in conjunction with energy or virtual work theorems can be used for hand calculations.

Generally a first order elastic analysis is considered sufficient for technical purposes. A second order analysis, in the elastic or inelastic range, is required to obtain reliable information with respect to the ultimate capacity of the truss. There are a number of obstacles to reliable nonlinear structural analysis programs which take into account second order and inelastic effects. These include a complex

mathematical model of the structure, all types of imperfections such as material or geometric, the loading process in a nonlinear analysis and the stress-strain relationship of the material.

If loads are applied to members away from the joints, the members act as continuous beams with unknown moments and shear forces, in addition to the axial forces over the full length of the members, giving it a degree of static indeterminacy. However, if the loads and supports are applied at the joints and these joints are considered to be pinned, as specified in the simplified method in Clause 15 of SANS 10162-1:2005<sup>[30]</sup>, the moments and shear forces are considered to be negligibly small, compared to the axial forces. It is important to remain consistent in design: if the analysis is based on pinned connections, the members are designed to resist primary forces only. If the analysis is done including secondary forces, the members must be designed as either beam-columns or as beams in tension and bending.

### **2.3 EFFECTIVE LENGTHS OF COMPRESSION MEMBERS**

In the design of a truss, the compression members provide the main design challenges. These are determining the effective lengths of the members, the maximum slenderness ratios as well as the effective length of the unbraced compression chords. In the plane of the truss, all members are held in position by virtue of triangulation and therefore the effective length factor can never exceed 1.0<sup>[6]</sup>. The American Institute of Steel Construction (AISC) recommends the use of the full unbraced length in the design of compression members in trusses<sup>[7]</sup>.

The effective length depends on whether or not the member in compression and the other members in the joint fail simultaneously, and hence provide some end restraint to the compression member or not. If all the members fail simultaneously, there is no restraining effect and the length is taken as the distance between the brace points. If the compression member fails before the restraining member, the favourable restraining effect of the other members can be taken into account<sup>[2]</sup>. However, it is not specified how this restraining effect is to be quantified and applied.

“The effect of secondary moments on the stability of a truss has been found to be small and may be neglected in buckling analyses. Thus the compression members on rigid-jointed trusses may be treated as columns elastically restrained at both ends.”<sup>[7]</sup>

The effective length factor for buckling of the web members is taken as 1.0. However, some codes prescribe the effective length factor of web members to be a value less than the distance between the nodes, commonly taken as 0.75<sup>[2]</sup>, and as 0.85<sup>[6]</sup> for web members in trusses which are designed for moving live load systems. The use of effective length factors of less than unit generally results in smaller cross-sections for compression members. Conversely SANS 10162-1:2005, Clause 15.2 requires that the first web compression elements be oversized by 15%. For the sake of uniformity

and practicality, all vertical or diagonal compression members would sometimes consist of the same section, therefore effectively applying this 15% overdesign to all compression members.

The chords are almost always stiffer than the web members, therefore in considering the chord elements, no rotational restraint is assumed at the ends and the effective length factor is taken as 1.0, i.e. the effective length of the compression chord is set to the theoretical distance between the braced panel points. For a truss of balanced design, where buckling stresses in compression chords and yield forces in tension chords will be reached more or less simultaneously,  $K$  is taken as 1.0. In a roof truss of constant depth and a single chord of constant section used for the full length of the truss, an effective length factor of 0.9 is suggested<sup>[7]</sup>.

Double angles for chords and single angle or T-sections are popular internal members. Both provide efficient bolted connections, used in conjunction with gusset plates. Circular hollow sections provide the best resistance to buckling of all the sections but their connections are the most expensive and time consuming to make. Rectangular hollow sections also provide fair resistance to buckling with easier connections than circular hollow sections, but collection of debris and moisture can be a problem.

## 2.4 END CONNECTION DESIGN

In the design of truss connections, the ideal, which is what analysis programs and manual methods assume, is that the centroidal axes of all members at a node intersect at a single point, but this is seldom achieved in practice due to the complexity of the joint<sup>[6]</sup>.

In practice, trusses are not pin-jointed but actually bolted or welded. The joints are therefore semi-rigid or rigid depending on the type of connection. If a member is eccentrically loaded or the connection is subject to eccentricities, the resulting bending moment and end connection stiffness must be taken into consideration. Such a moment is shared by the intersecting members according to their respective stiffnesses. The effects of member continuity and joint rigidity can be disregarded if slenderness of the chord members in the plane of the truss is greater than 50 and that of most of the web members is greater than 100<sup>[2]</sup>.

Gusset plates can be used to ensure that member centerlines intersect at one point but add considerable cost and may not be architecturally acceptable. In addition to this, the analysis of gusset plates is complicated. Simplified design methods give satisfactory results, theoretical and experimental investigations give conservative models of stress distributions in gusset plates<sup>[2]</sup>. In practice, gusset plates are used in most cases, using simplified design methods. This implies that the effect of gusset plates is generally not taken into consideration in the global analysis of a truss.

Gusset plates lead to complex connections, rendering the evaluation of their strength a difficult process. In the design of gusset plates it is generally assumed that only axial forces are transferred through them. However, in transferring the loads from the web compression members to the chords, bending moments, shear forces and normal forces are produced.

A series of full-scale compression tests on gusset plates was conducted by Yam et al<sup>[25]</sup> in order to determine the compressive behaviour and ultimate strength capacity of gusset plate connections. The most common mode of failure was found to be sway buckling of the connection. However, if the connection is restrained out-of-plane, the failure mode becomes local buckling of the free edges of the plate. It was generally found that significant yielding of the gusset plate occurs prior to reaching the ultimate load.

## 2.5 ANGLES IN COMPRESSION

Various experiments have been conducted with respect to the compressive resistance of single-angles, including work done by Temple et al<sup>[20]</sup> and Woolcock et al<sup>[24]</sup>. This member may appear relatively simple to analyze but there are several factors that lead to a more complex process. Firstly, the load is applied eccentrically to the angle, because it is attached by one leg only. The principal axis of the angle cross-section does not coincide with that of the frame or truss in which it is found, and there is some fixity at the ends of the angle which is difficult to account for, since the magnitude of the end restraints is unknown in most practical cases. These problems have been solved for the design of tensile members because tests have shown that the difference between the eccentric ultimate capacity and the concentric ultimate capacity of a tensile member is insignificant. However, these design difficulties have not been resolved in compression members<sup>[24]</sup>.

### 2.5.1 DESIGN APPROACHES

There does not appear to be a generally accepted design approach which takes both the load eccentricity and in- and out-of-plane end restraints into consideration. A single angle compression member can either be approximated as a concentrically loaded column or a pin-ended beam-column. The concentrically loaded column approximation, known as the simple column design approach, assumes a concentrically loaded member, with buckling around the principal axis and the effective length factor generally taken as 1.0 but also as low as 0.9.<sup>[21]</sup>

Most current design practices recommend that the eccentricity in loading be accounted for by considering bending about both principal axes, but the problem lies in determining where to apply the loads<sup>[24]</sup>. By treating the single angle as a beam-column, the eccentricity of the loading about the principal axis is not ignored. The load is assumed to act at the centre of the gusset and the subsequent moments about the principal axes are determined.<sup>[21]</sup>

Although the beam-column approach, strictly speaking, is more correct than the simple column as the latter approach has some shortcomings, such as disregarding the effect of bending moments in the member, the simple column often results in a better estimation of the compressive resistance of the angle because the beam-column approach generally underestimates the capacity. The beam-column approach assumes that the angle is pin-ended and that the maximum stresses due to axial loading and bending about the principal axis occur at the same point.

The effective length factor of a member ranges from 0.5 for fixed end conditions to 1.0 for a pin-ended member. The lower the value for the effective length factor, the higher the calculated compressive resistance. The higher compressive resistance requires more welding at the connection. In turn this results in a connection with a higher fixity. Therefore the end restraint as determined by the assumption of an effective length factor has an influence on the load carrying capacity of compression angles. <sup>[22]</sup>

### **2.5.2 DOUBLE ANGLE COMPRESSION MEMBERS**

Double angle compression members offer several advantages over their single angle counterparts. The double angle section can be connected in such a way to avoid eccentricities between the centerline of the section and the joint and subsequent bending moments. The two angles which comprise a double angle compression member are connected at third points of the member to ensure uniform behaviour of the section.

The orientation of the principle axes of equal leg angles ensures that weak axis buckling coincides with in-plane buckling, unlike weak axis bending of single angle compression members which occurs at 45 degrees to the plane of the truss. Strong axis bending of double angle compression members therefore occurs at right angles to the plane of the truss. It is therefore favourable to use double angle sections for the web compression members of a truss.

## **2.6 BUCKLING**

Research with respect to the buckling phenomenon encounters a number of obstacles. General structural design is based on the assumption that a stable equilibrium exists between the internal and external forces of a structure, i.e. that within certain limits a small change in the loading condition will lead to a proportionately small change in the stresses or elastic deformations of the system. According to this assumption the premise is set that provided a certain allowable stress is adhered to in the design of the structure, the structure is deemed safe. However, in the case of buckling, a potentially unstable equilibrium exists between the applied load, i.e. external forces, and the response of the structure or internal forces. In addition to this, the behaviour is controlled by the complex stress/strain relationship of the material.

Buckling is a failure mode characterized by sudden failure of a structural member subjected to high compressive stresses, often referred to as a failure mode due to elastic instability. For the purpose of mathematical analysis of buckling of a structural member, a perturbation load is applied to introduce a bending moment in the member, which does not form part of the primary forces to which the member is subjected.

Buckling of a structural section generally occurs before the theoretical buckling load, as devised by Euler is reached, due to imperfections causing bending moments. As the compressive load nears the buckling load, the member bows and the material approaches its yield point. The stress-strain relationship of the material is not strictly linear, even before the yield point. The modulus of elasticity decreases as the stresses increase. Therefore the lower stiffness of the member leads to a lower buckling strength and subsequently premature buckling.

A short column, with a low slenderness ratio, fails in direct compression before it buckles. A slender column, with slenderness ratio greater than 200, fails in buckling. An intermediate column, i.e. a column with an intermediate slenderness ratio, generally fails in combined direct compressive stress and bending. Typically intermediate columns are used for structural columns. In this case the critical Euler load is of little practical application. Generally empirical formulae are developed to agree with test data obtained.

## **2.7 OUT-OF-PLANE STABILITY**

Under gravitational loading the top chord is the largest and longest compression member of the truss and requires additional out-of-plane stabilization which is generally provided by purlins. The effective length of the top chord is taken as the distance between members in the plane of the roof cladding, offering lateral support to the chord. Purlins, generally located at the member joints or nodes, usually offer sufficient lateral support to the top chord. Each set of purlins offering lateral restraint must be connected to a bracing system.

As the bottom chord is expected to be in tension during normal loading conditions, its lateral stability should be checked for load reversal due to wind uplift, and subsequent compression loading. Tension members subjected to load reversal must have a slenderness ratio of less than 200, but this maximum slenderness ratio is imposed mainly for serviceability considerations. In order to provide sufficient lateral stability to the bottom chord, longitudinal ties should run the length of the building, linking the gable and eaves bracing at each end. Typically a truss is knee-braced at every other purlin against load reversal.

Apart from ensuring the stability of the truss itself, the chords have an important function in supplying lateral support to the compression members of the web. It is common practice to take the out-of-plane effective length of the web compression members as equal to their geometric length<sup>[14]</sup>. However, this

practice is based on the assumption that the chords provide sufficient lateral support. If the bottom chord, generally seen as the tension chord, is not supported at every panel point, which is generally the case, then the chord members at the unsupported points must act as elastic support to the web compression member.

In considering the lateral restraining effect of the chord on the web compression members, the stiffening effect of the tensile force in the tensile chord can be taken into consideration. However, in the case of load reversal the bottom chord is subject to compressive forces. The effective lateral support provided by the bottom chord is then compromised by both the destabilizing effect of the compressive force and the lack of adequate lateral bracing to the bottom chord. Chen et al.<sup>[14]</sup> propose practical formulae for verifying the adequacy of the chord stiffness for providing lateral support and for determining the effective length of the web compression members in the event of inadequate stiffness.

## **2.8 NONLINEAR STRUCTURAL BEHAVIOUR**

In general an adequate analysis of a truss system can only be performed if structural nonlinearities are taken into account. The most important sources of structural nonlinear behaviour, with respect to the research topic, are geometric and material nonlinearities.

As load is applied to a truss and deflections or deformations occur, the initial geometric configuration of the truss is no longer valid, and the current or deformed geometric configuration should replace the original configuration. If this is done for each load step the geometrical nonlinear behaviour of the truss is taken into account.

Likewise, the nonlinear material properties of the truss must be taken into account. In the case of steel, the initial material behaviour, up to the point of yielding, is considered linear, beyond which nonlinear material behaviour comes into play. Therefore it is necessary to include material nonlinearity in the analysis of a structure that may undergo nonlinear elasticity, plasticity, creep or inelastic rate effects. These may give rise to very complex phenomena such as path dependence, localization or progressive failure.

### **3. DESIGN CODE SURVEY**

#### **3.1 BENCHMARK PROBLEM**

In order to compare the different design codes quantitatively, a benchmark problem is established. This problem consists of a truss web compression element, with end restraints as they would typically be in a truss, i.e. two longitudinal welds at either end. The capacity of the element is then determined as stipulated by each code of practice and the results are compared.

Using a practical example for a benchmark problem, instead of defining theoretical end restraints as either pinned or rigid, allows the assumptions or approximations made by each code approach, regarding end conditions and effective slenderness ratios, to be brought to light. By varying the slenderness ratio of the truss element, the sensitivity of each code's approach to this variance can also be compared.

The effective length factor, as determined according to the end restraints, has a significant influence on the ultimate capacity as determined by each code, but there are other factors, unique to each code, which also affect the calculated ultimate capacity of the element, such as the conservativeness of the column curve employed.

A 60 x 60 x 5 double angle 1000mm in length, with a 5mm thick gusset plate, is selected as the initial benchmark problem. The length of the element is then increased in 500mm increments to 3000mm, to ensure a range of slenderness ratios. The slenderness ratio therefore varies between 54.6 and 163.9. Sufficient 5mm thick intermediate connectors between the two angles are provided to ensure that the section behaves as a unit, instead of two single angles. See Appendix A for detailed calculations. The design codes taken into consideration are as follows:

- SANS 10162-1 : The Structural Use of Steel : Part 1 (2005)
- BS 5950 : Structural Use of Steelwork in Building : Part 1 (2000)
- SIA 263 : Steel Construction (2003)
- AISC/ASCE 360-05 : Specification for Structural Steel Buildings (2005)
- CAN/CSA-S16-01 : Limit States Design of Steel Structures (2005)

#### **3.2 SANS 10162–1 : THE STRUCTURAL USE OF STEEL : PART 1 (2005)**

The simplified method for the design of trusses in Clause 15 of SANS 10162-1:2005 assumes that all members are pin connected and that all loads are applied at the nodal points. This method may be used when the out-of-plan resistance of all compression members is larger than the in-plane resistance and the compression members are at least class 3. The minimum requirement of a class 3

member ensures that the  $b/t$  ratio of the components of the cross-section is such that the possibility of local buckling is eliminated. The slenderness ratio is restricted to 200.

The effective length for buckling in the plane of the truss is taken as the distance between the lines of intersection of the working points of the web members and the chord, i.e. an effective length factor,  $K$ , of 1.0. Bending moments due to joint eccentricities must be taken into account in the design of the members and end connections. In addition to this, the factored resistances of the first compression web member and its connections are determined with their respective resistance factors multiplied by 0.85.

To determine the critical axial load, the following procedure is followed :

$$C_r = \phi A f_y (1 + \lambda^{2n})^{-1} \quad (\text{Equation 3.1})$$

$$\text{Where } \lambda = \sqrt{\frac{f_y}{f_e}} \quad (\text{Equation 3.2})$$

And  $f_e$  is taken as the least of

$$f_{ex} = \frac{\pi^2 E}{\left( \frac{K_x L_x}{r_x} \right)^2} \quad (\text{Equation 3.3})$$

$$\text{And } f_{eyz} = \frac{f_{ey} + f_{ez}}{2\Omega} \left( 1 - \sqrt{1 - \frac{4f_{ey}f_{ez}\Omega}{(f_{ey} + f_{ez})^2}} \right) \quad (\text{Equation 3.4})$$

$$\text{Where } f_{ey} = \frac{\pi^2 E}{\left( \frac{K_y L_y}{r_y} \right)^2} \quad (\text{Equation 3.5})$$

$$\text{And } f_{ez} = \left( \frac{\pi^2 E C_w}{K_z^2 L_z^2} + GJ \right) \frac{1}{A r_o^2} \quad (\text{Equation 3.6})$$

$$\text{Where } \Omega = 1 - \left( \frac{x_o^2 + y_o^2}{r_o^2} \right) \quad (\text{Equation 3.7})$$

$$\text{And } r_o^2 = x_o^2 + y_o^2 + r_x^2 + r_y^2 \quad (\text{Equation 3.8})$$

SANS 10162-1 therefore makes provision for the possibility that torsional-flexural buckling could determine the critical stress. It should be noted that in the case of the shortest element of the benchmark problem, i.e. the 1000mm element, torsional-flexural buckling was dominant but in all other cases flexural buckling dominated.

### 3.3 BS 5950 : STRUCTURAL USE OF STEELWORK IN BUILDING : PART 1 (2000)

The BS 5950 is soon to be superseded by the advent of the Eurocode, EN 1993-1-1. However, it is still pertinent to include the British approach in the comparison, as the Eurocode is based in part on it and the British are leaders in development in many aspects of steel design. In addition, the national annex to the EN 1993-1-1 has as yet not been published and therefore the Eurocode cannot be included in the comparison of design codes.

The BS 5950 provides a fair amount of guidance on the design of truss web members. It is mentioned in Clause 4.10 of BS 5950 that the connections may be taken as pinned for the purpose of calculating the forces in the members. It also states that the fixity of the connections and the rigidity of the adjacent members may be taken into account in the determination of the effective lengths of the members.

How this is to be done is outlined in Clause 4.7 of BS 5950 in greater detail. The segment length,  $L$ , of a compression member should be taken as the length between the points at which it is restrained against buckling in a certain plane. The effective lengths of compression members are selected according to the following table, depending on the conditions of restraint in the relevant plane. Table 3.1 is taken from BS 5950-1:2000 as is. The term “restrained in direction” describes the restraint against rotation about the axis perpendicular to the plane under consideration.

**Table 3.1** : Nominal effective length  $L_E$  for a compression member, BS 5950-1:2000

a) non-sway mode			
Restraint (in the plane under consideration) by other parts of the structure			$L_E$
Effectively held in position at both ends	Effectively restrained in direction at both ends		0.7L
	Partially restrained in direction at both ends		0.85L
	Restrained in direction at one end		0.85L
	Not restrained in direction at either end		1.0L
b) sway mode			
One end	Other End		$L_E$
Effectively held in position and restrained in direction	Not held in position	Effectively restrained in direction	1.2L
		Partially restrained in direction	1.5L
		Not restrained in direction	2.0L

Therefore the degree of restraint at the member ends is left to the discretion of the designer. For example, the end restraints of a welded web element would be “effectively held in position at both ends”, and both ends are equally restrained, but the decision lies with the designer whether the ends are “partially” or “effectively” restrained. Generally UK designers consider “effectively” restrained too unconservative and resort to “partially”, i.e. an effective length of 0.85L. It is not specified, if the

restraint is chosen to be “partial” or “effective”, whether the member should then be designed as a member with combined moment and axial force, or as a simple compression element.

The above table is not applicable to angles, channels or T-sections but it still included to demonstrate the standard design approach and illustrate the fact that provision is made for a reduced effective length under certain conditions. As the benchmark problem makes use of a double angle section, it is necessary to consider the requirements for these sections. For this, Clause 4.7.10 is applicable, which defines slenderness ratios, and thereby effective lengths, for specific connection types, for each of the sections. Applicable to the benchmark problem is the following description :

4.7.10.3 c) to both sides of a gusset member by two or more bolts in standard clearance hole (or equivalent weld), in line along the angles, the slenderness should be taken as the greater of :

$$1) 0.85L_x / r_x \quad \text{but } \geq 0.7L_x / r_x + 30, \quad (\text{Equation 3.9})$$

$$2) \left[ (L_y / r_y)^2 + \lambda_c^2 \right]^{0.5} \quad \text{but } \geq 1.4\lambda_c, \quad (\text{Equation 3.10})$$

$$\text{where } \lambda_c = L_v / r_v. \quad (\text{Equation 3.11})$$

The compression resistance  $P_c$  of a member, depending on the classification of the section, is obtained from :

$$P_c = A_g p_c \quad \text{for Class 1 plastic, Class 2 compact or Class 3 semi-compact} \quad (\text{Equation 3.12})$$

$$\text{or } P_c = A_{\text{eff}} p_{\text{cs}} \quad \text{for Class 4 slender cross sections.} \quad (\text{Equation 3.13})$$

The compressive strength  $p_c$  should be based on the appropriate strut curve for buckling about the relevant axis, depending on the type of cross-section and the maximum thickness. Once the appropriate curve is selected, the value of the compressive strength is then determined according to the design strength  $p_y$  and the slenderness  $\lambda$  for buckling about the relevant axis, as follows:

$$p_c = \frac{p_E p_y}{\phi + (\phi^2 - p_E p_y)^{0.5}} \quad (\text{Equation 3.14})$$

$$\text{where } \phi = \frac{p_y + (\eta + 1)p_E}{2} \quad (\text{Equation 3.15})$$

$$p_E = \frac{\pi^2 E}{\lambda^2} \quad (\text{Equation 3.16})$$

$$\eta = \frac{a(\lambda - \lambda_o)}{1000} \quad (\text{Equation 3.17})$$

$$\lambda_o = 0.2 \left( \frac{\pi^2 E}{p_y} \right)^{0.5} \quad (\text{Equation 3.18})$$

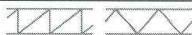
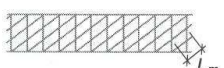
and  $\lambda_o$  is dependent on the strut curve selected.

It is important to note that BS 5950 makes no provision for taking flexural torsional buckling into account. Another aspect relevant to the section selected for the benchmark problem is whether or not the two angles can be considered to behave as a single section. According to Clause 4.7.13.1 the section may be designed as a single integral compression member, subject to certain conditions, the most important of which are highlighted. The main components should be connected by bolts. If they are connected by welding, the member should be designed as a battened strut. The main components should be connected at intervals so that the member is divided into at least three sections of approximately equal length.

### 3.4 SIA 263 : STEEL CONSTRUCTION (2003)

For the design of truss members, SIA 263 recognizes that the effective lengths  $L_K$  are usually less than the distance between nodes, length  $L$ , due to partial restraint at the ends. In general the code stipulates that the effective length is equal to the theoretical length of the member, measured between fixed nodal points. However, the effective length may be reduced if the maximum compression loads do not act simultaneously on the adjacent members and if the end restraints justify such a reduction, i.e. if the connections are sufficiently rigid. If these criteria are met, the effective lengths of both the diagonal and vertical members, in a simple truss, can be reduced to  $0.8L$ , as shown in Table 3.2. Additionally, the effective slenderness ratio is limited to 200 for main structural elements.

**Table 3.2** : Reduced buckling lengths for compressive truss members, Table 13, SIA 263

Member	Brace arrangement	Buckling length $L_K$ for buckling	
		in-plane	out-of-plane <sup>1)</sup>
Chords		$0,9 L$	$1,0 L$
Diagonals	simple 	$0,8 L$	$1,0 L$
	double (a)  (b) 	$0,4 L$	$0,5 L^{2)}$
	multiple 	$1,0 L_m^{3)}$	$1,5 L_m^{3)}$
	K shaped 	$0,9 L$	$1,0 L^{2)}$
Struts	simple and double (a)	$0,8 L$	$1,0 L$
	double (b)	$0,4 L$	$0,5 L^{2)}$
	K shaped	$0,4 L$	$0,5 L^{2)}$

<sup>1)</sup>  $L$ : theoretical distance between joints restrained in buckling direction  
<sup>2)</sup> valid only for identical tension and compression members  
<sup>3)</sup>  $L_m$ : truss mesh dimension

Once the effective length of the member has been established, the stability of the member in compression is verified for both principal axes. In special cases torsional-flexural buckling can be determinant. The capacity of the member is determined either empirically by means of buckling curves, depicted in Figure 3.1, or analytically. The choice of buckling curve depends on the residual stresses and their distribution over the cross section, as well as the direction of buckling under consideration.

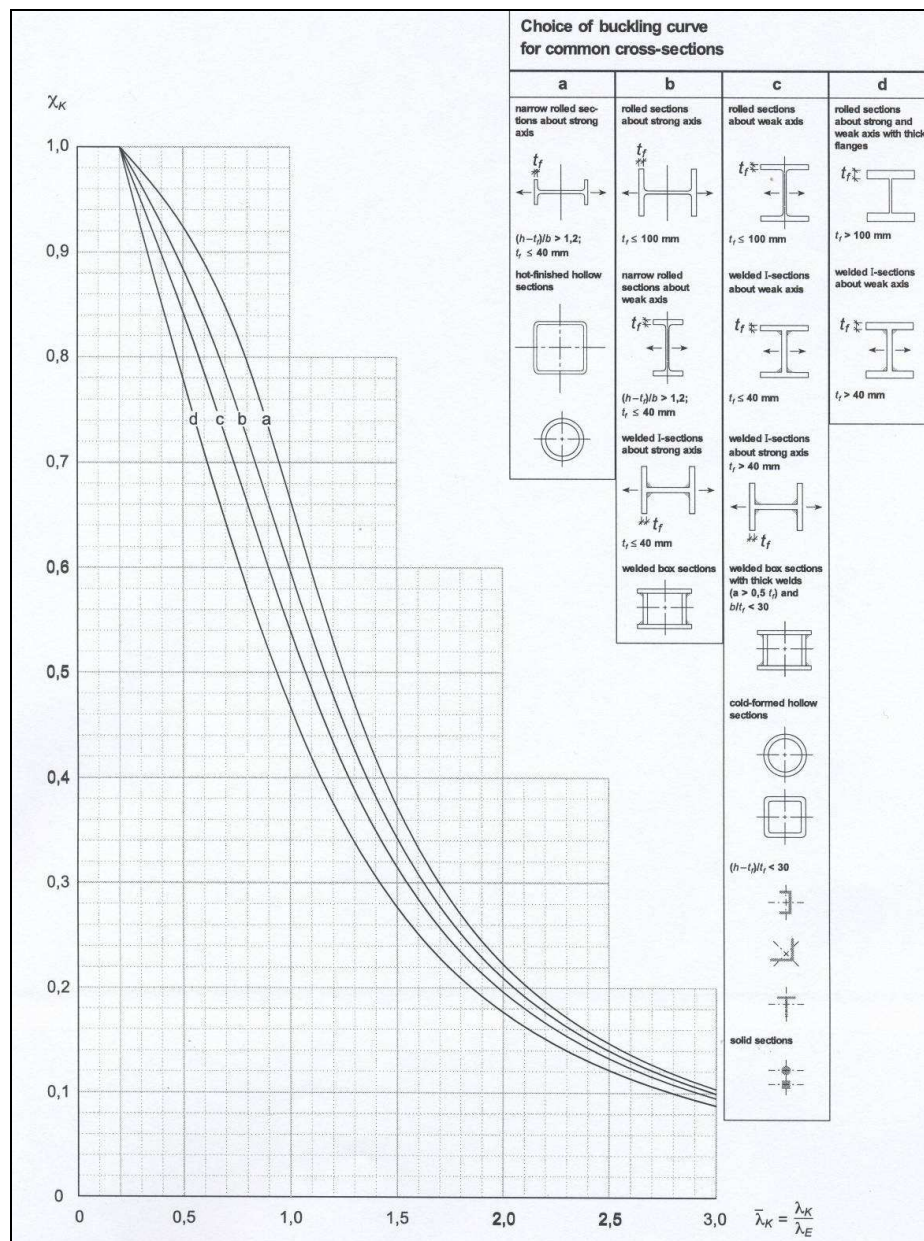


Figure 3.1 : Buckling curves used to determine buckling stress of compression members

This is a dimensionless representation of the buckling slenderness  $\bar{\lambda}_K$  in relation to the reduction factor for buckling  $\chi_K$ .

Where  $\bar{\lambda}_K = \sqrt{\frac{f_y}{\sigma_{cr,K}}}$ ,  $\sigma_{cr,K}$  : critical elastic buckling stress (Equation 3.19)

The section to be used is an angle, which has compressive residual stresses in the extreme fibres. Therefore the buckling curve to be used is curve c. This results in an imperfection factor,  $\alpha$ , of 0.49. Analytical representation of the buckling curves is as follows:

$$\bar{\lambda}_K = \sqrt{\frac{f_y}{\sigma_{cr,K}}} \quad \text{where } \sigma_{cr,K} \text{ is the critical of the two axes} \quad (\text{Equation 3.20})$$

$$\Phi_K = 0.5 \left[ 1 + \alpha(\bar{\lambda}_K - 0.2) + \bar{\lambda}_K^2 \right] \quad (\text{Equation 3.21})$$

$$\chi_K = \frac{1}{\Phi_K + \sqrt{\Phi_K^2 - \bar{\lambda}_K^2}} \leq 1.0 \quad (\text{Equation 3.22})$$

The capacity of the compression member is therefore as follows :

$$N_{K,Rd} = \frac{\chi_K f_y A}{\gamma_{M1}} \quad (\text{Equation 3.23})$$

### 3.5 ANSI / AISC 360 – 05 : SPECIFICATION FOR STRUCTURAL STEEL BUILDINGS (2005)

The AISC 360-05 does not give guidance specifically on the design of web compression members in trusses. The slenderness ratio of compression elements is restricted to 200. For compression members in general the effective length is dependent on the type of section and the type of end and intermediate connections.

The nominal compressive strength  $P_n$  is determined based on the limit state of flexural buckling :

$$P_n = F_{cr} A_g \quad (\text{Equation 3.24})$$

The flexural buckling stress is determined as follows, in Clause E3 and E4 :

$$\text{when } \frac{KL}{r} \leq 4.71 \sqrt{\frac{E}{F_y}} \quad (\text{or } F_e \geq 0.44F_y) \quad F_{cr} = \left[ 0.658 \frac{F_y}{F_e} \right] F_y \quad (\text{Equation 3.25})$$

$$\text{when } \frac{KL}{r} > 4.71 \sqrt{\frac{E}{F_y}} \quad (\text{or } F_e < 0.44F_y) \quad F_{cr} = 0.877F_e \quad (\text{Equation 3.26})$$

Similar to the SANS 10162-1:2005 approach the elastic critical buckling stress,  $F_e$  taken as the lesser of  $F_{cr}$  for flexural buckling and  $F_{cr}$  for flexural-torsional buckling, is determined according to the following :

Flexural Buckling :

$$F_e = \frac{\pi^2 E}{\left(\frac{KL}{r}\right)_x^2} \quad (\text{Equation 3.27})$$

Flexural Torsional Buckling :

$$F_{cry} = \frac{\pi^2 E}{\left(\frac{KL}{r}\right)_y^2} \quad (\text{Equation 3.28})$$

$$F_{crz} = \frac{GJ}{A_g r_o^2} \quad (\text{Equation 3.29})$$

$$F_e = \left(\frac{F_{cry} + F_{crz}}{2H}\right) \left[1 - \sqrt{1 - \frac{4F_{cry}F_{crz}H}{(F_{cry} + F_{crz})^2}}\right] \quad (\text{Equation 3.30})$$

$$\text{Where } H = 1 - \frac{x_o^2 + y_o^2}{r_o^2} \quad (\text{Equation 3.31})$$

However, in the case of built up members, as is the case for the benchmark problem, the effective slenderness ratio is determined as follows :

$$\left(\frac{KL}{r}\right)_m = \sqrt{\left(\frac{KL}{r}\right)_o^2 + 0.82 \frac{\alpha^2}{(1 + \alpha^2)} \left(\frac{a}{r_{ib}}\right)^2} \quad (\text{Equation 3.32})$$

where subscript  $m$  denotes the modified slenderness of the built up member and subscript  $o$  denotes the slenderness of the element behaving as a unit.  $a$  is the distance between the connectors.  $r_{ib}$  is the radius of gyration of the individual component relative to its centroidal axis, parallel to the member axis of buckling.  $\alpha$  is the separation ratio,  $h/2r_{ib}$ , and  $h$  is the distance between centroids of the individual components perpendicular to the member axis of buckling.

Therefore, similar to SANS 10162-1:2005, provision for flexural-torsional buckling is made in AISC 360-05. In the case of the shortest element of the benchmark problem, i.e. the 1000mm element, torsional-flexural buckling was dominant but in all other cases flexural buckling dominated.

### 3.6 CAN/CSA – S16-01 : LIMIT STATES DESIGN OF STEEL STRUCTURES (2005)

The Canadian standard on limit states design of steel structures was developed in collaboration with the South African SANS 10162-1, as a result of an initiative by and cooperation between the Canadian Institute of Steel Construction and the Southern African Institute of Steel Construction. The outcome is an identical standard being applied in both countries.

Therefore the approach to the design of truss web members is identical. The argument may be made that it is redundant to include the Canadian approach in the comparison, as the results are the same. However, it does illustrate the point that other countries, well respected in the steel industry, chose the same approach, and maintain their stand point. The Canadian standard was reaffirmed in 2007, with some changes. None of these changes affect the clauses under consideration.

### 3.7 SUMMARY OF RESULTS

The results of the benchmark calculations are provided in Table 3.3 for each of the design codes taken into consideration, using a constant section, 60 x 60 x 5 double angle with a 5mm gusset plate, but increasing the length from 1000mm in 500mm increments to 3000mm, to vary the slenderness ratio. The Euler buckling load for each slenderness ratio, for pinned as well as rigid end conditions are also given to provide a frame of reference. However, Euler buckling only considers flexural buckling and does not account for inelastic buckling of shorter columns.

**Table 3.3 :** Summary of effective length factors and axial compressive resistances in kN

	Length (mm)	1000	1500	2000	2500	3000
	Dimensionless Slenderness Ratio	54.6	82.0	109.3	136.6	163.9
Design Code	K Factor	Compressive Capacity (kN)				
Euler Pinned	1.0	765.9	340.4	191.5	122.5	85.1
Euler Rigid	0.5	3063.5	1361.6	765.9	490.2	340.4
SANS 10162-1	1.0	176.7	147.7	112.9	85.0	64.7
BS 5950 : 1	0.85	166.1	138.1	112.4	91.1	74.3
SIA 263 : 2003	0.8	194.1	165.9	135.4	107.1	84.1
ASCE 360-05	1.0	202.5	172.8	138.5	104.1	74.1
CSA – S16.1-94	1.0	176.7	147.7	112.9	85.0	64.7

The results are represented graphically in Figures 3.2 and 3.3. Figure 3.2 includes the Euler buckling curves of a pin-connected member ( $K = 1.0$ ), as well as a rigidly connected member ( $K = 0.5$ ), in order to illustrate the difference in magnitude. Figure 3.3 excludes the Euler buckling curve for a rigidly connected member in order for the area of interest on the graph to be magnified.

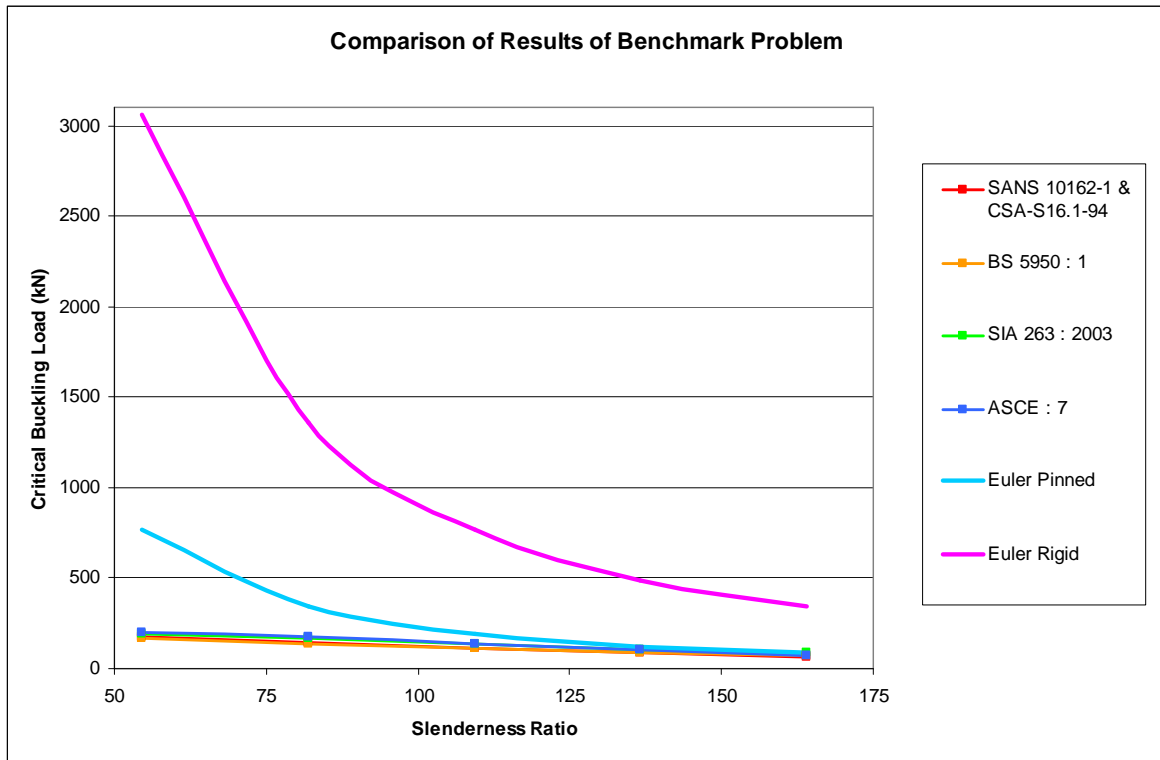


Figure 3.2 : Comparison of axial compressive resistance for varying slenderness ratios

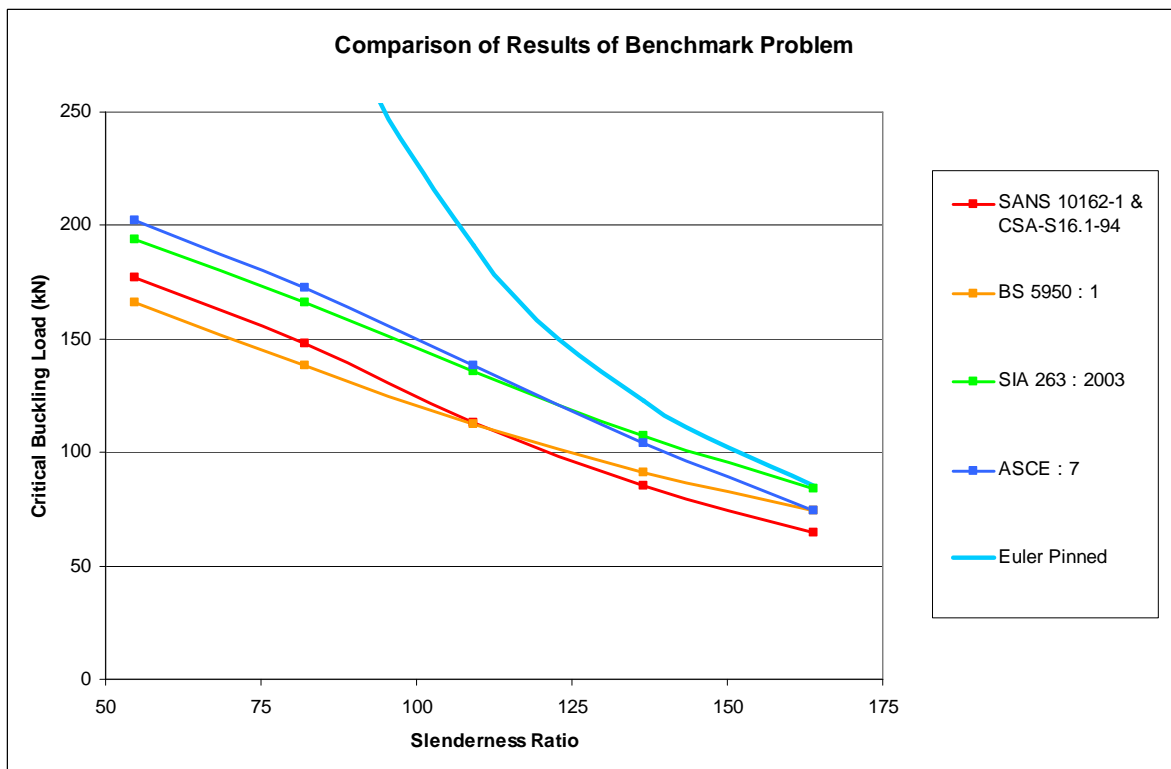


Figure 3.3 : Comparison of axial compressive resistance excluding Euler buckling curves

In general, all code approaches fall within a distinct band, which gradually approaches the curve obtained for a pin-connected Euler column with increasing slenderness ratio. However, the band is fairly wide, i.e. there is a large discrepancy in the calculated capacity between the different code approaches. The two extremes vary by as much as 36kN in some cases, i.e. in this instance the ASCE approach describes a 22% higher buckling load than the BS 5950 approach. The results using the British, South African and Canadian approaches prove to be the most conservative, whereas the results using the Swiss and American design approaches are the most unconservative.

As mentioned previously, each code approach takes different factors into consideration. These factors are also weighted differently, which means that the effective slenderness ratio used is not necessarily the largest contributing factor. For example, the British code approach employs a K factor of 0.85 but results in more conservative capacities than the American code approach which uses a K factor of 1.0.

The South African and Canadian approach is to assume pinned end connections and therefore an effective length factor of 1.0. This is a simple approach, with little design effort, but with conservative results. The British approach is fairly complex, leading to a lengthy calculation process, and yet results in similar capacities compared to the South African or Canadian approach. The American design approach is also relatively complex, involving a number of different steps, and despite employing an effective length factor of 1.0, results in capacities as unconservative as the Swiss approach. The Swiss design approach allows the effective lengths of compression members to be reduced by a factor of 0.8, if the end conditions justify it. This is a simple adjustment, keeping the design effort to a minimum, with visible differences in results. The only drawback is that the onus still lies with the designer to decide whether or not the end conditions can be considered sufficiently rigid to warrant a reduction in the effective length.

## **4. INVESTIGATIVE ANALYSES**

This research is focused on a specific aspect of the behaviour of a truss and in order to maximize the possibility of successful experimental executions and interpretation of results, it is necessary to develop truss dimensions and configurations for the experimental setup which will induce the anticipated behaviour. For example, to investigate the influence of the chord stiffness on the buckling capacity of the web compression members, or to determine the number of bays required to induce optimum truss behaviour.

A number of different factors can influence the load at which the web compression elements buckle, most notably the degree of the rigidity of the nodes, but also the stiffness of neighbouring elements, or the way in which the load is applied to the truss. It is therefore important to separate and isolate these effects by means of investigative analyses, prior to designing the experiment.

Such a priori numerical analyses not only allow for the design optimization of the experiment, taking practical aspects into consideration, but may also reveal unforeseen structural behaviour. Being made aware of unexpected effects prior to the execution of experiments is invaluable to the success of the experimental work.

### **4.1 EFFECTS TO BE INVESTIGATED**

#### **1. Node Rigidity on the Effective Length**

The degree of rigidity of the end nodes of a member has the largest influence on the effective length. The members are considered pin-connected for the benefit of a simplified design method, but this is rarely the case. Typically truss members are welded, using gusset plates, creating connections with a significant degree of rigidity.

#### **2. Stiffness of Neighbouring Elements on Node Fixity**

A number of elements are connected to a node, or gusset plate. Each of these elements contributes to the fixity of the connection, depending on their respective stiffnesses. An element carrying an axial force in close proximity to its buckling load contributes little stiffness to a connection. However, an element carrying only a fraction of its capacity contributes a significant amount of stiffness to a connection and can therefore influence the effective length of a neighbouring element.

### **3. Node Rigidity on the Distribution of Axial Forces in Truss**

The rigidity of a node determines the transfer of forces from one element to a neighbouring one, and therefore can alter the distribution of axial forces in a truss. However, it is not certain whether the altered distribution of forces, created by changing the rigidity of the nodes from 'pinned' to 'rigid', is significant, or not.

### **4. Rigid Nodes on the Magnitude of the Subsequent Bending Moments**

Rigid nodes, as opposed to pinned nodes, cause bending moments in the members of a truss. If the induced bending moments are insignificant, the members can be designed as simple columns. However, if the bending moments are substantial, it might warrant the members being designed as beam-columns, resulting in a considerable amount of additional design effort.

### **5. Reducing Distributed Load to Single Point Load at Midspan**

For practical purposes and due to the importance of control of load application it is most effective to apply a single point load at midspan of the truss. It is therefore necessary to investigate whether reducing a distributed load, such as a wind load, to a single point load causes significantly different behaviour in the truss.

## **4.2 PRACTICAL CONSIDERATIONS**

In determining which truss configurations to include in the investigative analyses, a number of practical aspects needed to be considered. The investigations were restricted to one bay size, 1.05m x 1.05m, and three different numbers of bays, namely six, eight and ten bays. Six is the minimum number of bays necessary to attain full truss behaviour and extending this to eight and ten bays allows for variation of the depth to span ratio of the truss, whilst maintaining a constant bay size. This constant bay size ensures a constant slenderness ratio of the compression members between the different bay numbers, which facilitates the comparison of the results between the different truss sizes.

The section sizes selected for the compression members, and subsequently the bay size, were largely determined by the availability of standard sections sizes. To ensure buckling of the critical elements, these need to be sufficiently slender. The smallest commercially produced, and hence available, angle section is a 25 x 25 x 3 equal leg angle. These were selected for the critical, i.e. vertical elements, of the gravity load case. This results in a slenderness ratio of 140.2. The diagonal, upper and lower chord element sections are then chosen with a sufficiently greater capacity to ensure that they are non-critical.

The diagonal, i.e. critical, elements of the wind load case are longer than the vertical elements of the gravity load case and therefore the section size is slightly larger, namely 30 x 30 x 3 angle, to achieve a similar slenderness ratio, given certain limitations, of 165.2. Again, the vertical, upper and lower chord element sections are then chosen with a sufficiently greater capacity to ensure that they are non-critical.

### **4.3 CHOICE OF SOFTWARE**

The software chosen with which to perform the investigative analyses is ANGELINE (**A**nalysis of **G**eometrically **N**onlinear Structures). This is a non-commercial software package which caters for the geometrically nonlinear analysis of plane trusses and frames. The development of the software is the result of the academic co-operation between the Technical University of Berlin (TUB), the Volgograd State University of Architecture and Civil Engineering and the University of Stellenbosch.

Under the leadership of Professor Peter Jan Pahl of TUB, a set of subsidiary classes were developed in addition to the existing software, developed specifically to the requirements of the investigative analyses. These classes were developed with the aim for the user to be able to execute analyses with minimum input but optimum output. Thereby a range of analyses of the truss system was made possible in order to investigate certain effects and variations of the experimental setup, without incurring the time and monetary costs of extensive experimental work.

The greatest benefit of using ANGELINE for the investigative analyses is the combination of geometrically nonlinear analysis of structural behaviour and the transparency of the theory employed in the development of the software. A brief description of the software, as well as of the importance of nonlinear analysis, is provided in the following section.

### **4.4 THEORY BASIS OF ANGELINE**

The nonlinear analysis of a structure allows for a significantly more reliable prediction of the real structural behaviour, as compared to a linear analysis. This results in a more economic and energy efficient design. However, this improvement in reliability comes at the cost of a far more complex and demanding method of analysis.

Nonlinear structural behaviour encompasses five different phases, the first three of which are applicable to the analyses at hand. These are the nonlinear deformation analysis, the identification of nearly-singular configurations and the computation of the singular point. The last two phases, namely the first step following a singular point and the continuation of the load path beyond the singular point, fall beyond the scope of the analyses of the experimental planning.

#### **4.4.1 LINEAR VS NONLINEAR ANALYSIS OF STRUCTURAL BEHAVIOUR**

As implied by the name, ANGELINE only takes into consideration the geometric nonlinearity of a structure. Geometrically nonlinear structural analysis differs from geometrically linear analysis in four critical areas. Linear theory ignores the nonlinear relationship between the displacements of a structure and the strain in its members. Small strains can lead to relatively large translations and rotations, an effect which is taken into consideration in nonlinear analysis.

The geometry of a truss is constantly changing while being loaded, due to structural deformations. The equilibrium equations of linear frame theory are formulated for the reference, or original geometry, configuration of the frame, whereas nonlinear frame theory equilibrium equations are formulated for the instant configuration of the frame. In addition to this the linear equilibrium equations can be solved directly as they contain the same number of unknowns and equations. The nonlinear problem cannot be solved directly as the governing equations contain nonlinear expressions which need to be solved iteratively. The most frequently used approach to this problem is to treat the nonlinear behaviour as an initial value problem. The tangent stiffness matrix is used to establish the displacement increment in each load step.

The solution obtained for the linear frame theory is independent of the load level. The solution obtained for the nonlinear frame theory, in contrast, is strongly dependent on the load level. It is therefore necessary to determine the point at which the tangent stiffness matrix reaches singularity, which is typically done treating it as an Eigenvalue problem.

#### **4.4.2 ADDITIONAL EFFECTS OF NONLINEAR ANALYSIS**

In the nonlinear analysis of a structure, superposition is no longer valid. Therefore efficiency of the solution is of utmost importance as each step in a step wise solution requires a full analysis, i.e. each loading condition requires a complete solution of the initial value problem for the governing equations.

The reliability and accuracy of the solution of this initial value problem depend on the size of the load steps. The smaller the load step, the greater the accuracy and reliability become. This in turn results in a large amount of data requiring handling and storage. The solution of the Eigenvalue problem, which determines the singular point and the continuation of the load path beyond the singular point, requires special numerical methods and data structures.

Due to the fact that nonlinear structural behaviour is less predictable and perhaps less intuitive, unexpected modes of behaviour are more difficult to detect. In order to facilitate this detection of unforeseen behaviour, a powerful graphical user interface is required.

## 4.5 APPLICATION OF ANGELINE TO INVESTIGATIVE ANALYSES

As mentioned before specialized classes were developed for the purpose of the investigative analyses. Separate classes were developed for the two load cases to be applied during the experiments. The first is the gravity load case, under which the vertical elements are in compression, and the class is therefore called `frameVertical`. The second load case is a simulation of a wind load, under which the diagonal elements in the truss are in compression, and the class is therefore called `frameDiagonal`.

A graphical user interface (GUI) was devised, allowing the user to vary certain parameters critical to the investigations. As can be seen in Figure 4.2 the GUI is divided into sections, each performing a different function. The first section, referred to as 'File Management', enables the user to manage the different sessions, or analyses, generated. 'Truss Properties and Analysis' allows the user to define the truss height, the number of bays in the truss, the number of finite elements per member, the increment size with which the load factor is to be increased and the number of load increments or load steps. It also allows the user to define the type of connection, i.e. pinned, mixed or rigid (see Figure 4.1), and the profile size. The section sizes are all pre-defined as double angles.

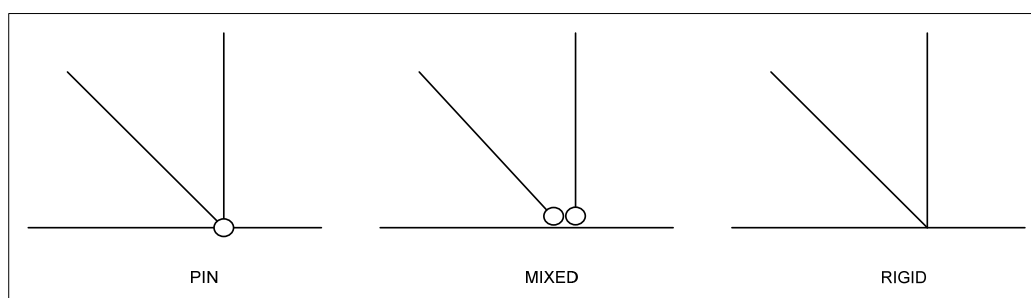


**Figure 4.1** : Definition of connection types

The following section, 'Loading of Lower Chord Nodes', allows the user to define the load pattern to be applied to the lower chord of the truss. The load application is restricted to the lower chord, as this same restriction is applicable in the laboratory, and it is important to apply the same conditions to the analyses as are imposed on the experimental situation. The load application is also restricted to the nodes. Again this is relevant, as the simplified method prescribed in SANS 10162-1:2005 assumes that loads are only applied to the nodes.

The last section enables the user to define the layout of the result file, which is where optimization of the output can be controlled. The result file generated is in the form of a text file, which can be exported to another program, such as Excel, for further processing. The output is limited to twelve columns, i.e. twelve different variables can be recorded per analysis. The variable type (displacement, axial force, bending moment, reaction force or load factor), the location (vertical, diagonal, upper chord, lower chord element or node) and exact point within the member can be specified. In addition to this the number of significant figures to which the result is to be displayed can also be defined.

Session Editor													
File Management													
file name	read from file			delete file									
S.Example	write to file			show file list									
Truss Properties and Analysis													
height	1.050			upper chord profile		60 x 60 x 6							
number of bays	6			lower chord profile		60 x 60 x 6							
elements per member	8			vertical profile		25 x 25 x 3							
load factor increment	0.100			diagonal profile		40 x 40 x 6							
number of load increments	10			joints	<input type="radio"/> pinned	<input checked="" type="radio"/> rigid	<input type="radio"/> mixed						
Loading of Lower Chord Nodes													
line	load	line	load	line	load	line	load	line	load				
2	10.000	4	10.000	6	10.000	8		10					
3	10.000	5	10.000	7		9							
Layout of the Result File													
column	width	digits	variable				location		number	distance			
6	9	3	<input type="radio"/> DX	<input checked="" type="radio"/> DY	<input type="radio"/> DZ	<input type="radio"/> A	<input type="radio"/> B	<input type="radio"/> L	<input type="radio"/> U	<input type="radio"/> V	<input type="radio"/> D	4	0.000
			<input type="radio"/> RX	<input type="radio"/> RY	<input type="radio"/> RZ	<input type="radio"/> LF		<input checked="" type="radio"/> NL		<input type="radio"/> NU			
1	6	3	load factor				point in lower chord member		0	0.000			
2	9	3	axial force in member				point in vertical member		1	0.500			
3	9	3	axial force in member				point in vertical member		7	0.500			
4	9	4	bending moment in member				point in vertical member		1	0.000			
5	9	4	bending moment in member				point in vertical member		7	0.000			
6	9	3	node displacement y-direction				node in lower chord member		4	0.000			
7													
8													
9													
10													
11													
12													
				confirm deletion			cancel deletion						

Figure 4.2 : Graphical user interface specifically developed for investigative analyses

Once the input is completed by the user and the analysis has been given a unique name, it can be graphically verified as follows:

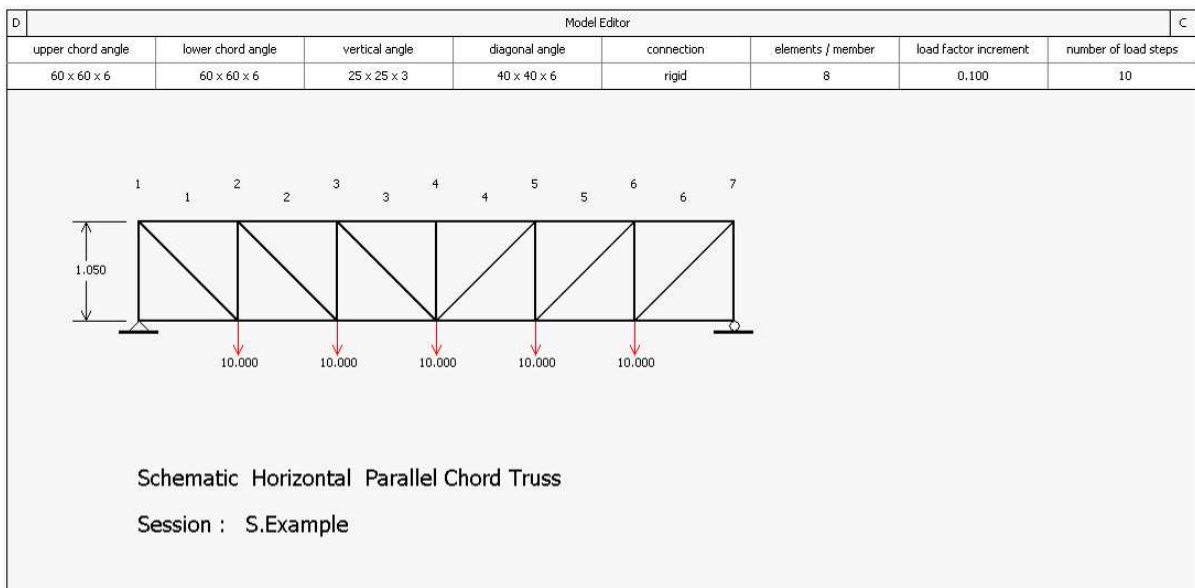


Figure 4.3 : Graphical verification of input specified for a specific analysis

The analysis is then performed by means of an iterative process. The number of load increments or load steps is refined until the singular point is achieved. Since the tangent stiffness of the frame configuration is singular, a minute displacement of the frame can take place without a minute change in the load acting on the frame. It must then be verified that this singular point occurred in the critical element. Each load step of the analysis, for each variable defined in the layout of the results file, is then written to the result file. The results can be shown graphically in a number of ways. The displacement, axial force, shear force or bending moment at a specific node, in a certain element or in the global truss can be specified as follows:

D	Result Editor				C
node	<input type="radio"/> displacement	<input type="radio"/> rotation	<input type="radio"/> reaction f	<input type="radio"/> reaction m	
member	<input type="radio"/> displacement	<input type="radio"/> axial force	<input type="radio"/> shear force	<input type="radio"/> bending mom.	
frame	<input checked="" type="radio"/> displacement	<input type="radio"/> axial force	<input type="radio"/> shear force	<input type="radio"/> bending mom.	
component name					
coordinate on axis					0.000
first state number					0
last state number					48
state number increment					2
displacement scale factor					38.111

**Figure 4.4** : Specification of graphical results to be shown

The following figures, Figures 4.5 to 4.7, show the displacements, axial forces and bending moments in the single configuration of the truss. Note the large displacement scale factor of 38.111, as can be seen in Figure 4.4. This strongly exaggerated displacement enables the user to detect displacements easily; however it may cause a distorted perception of the magnitude of displacement if not borne in mind.

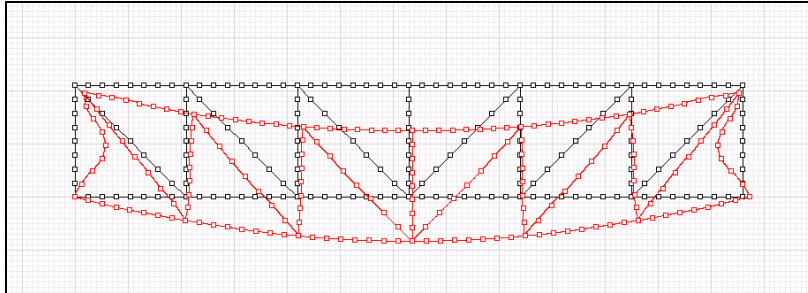


**Figure 4.5 :** Graphical representation of displacements

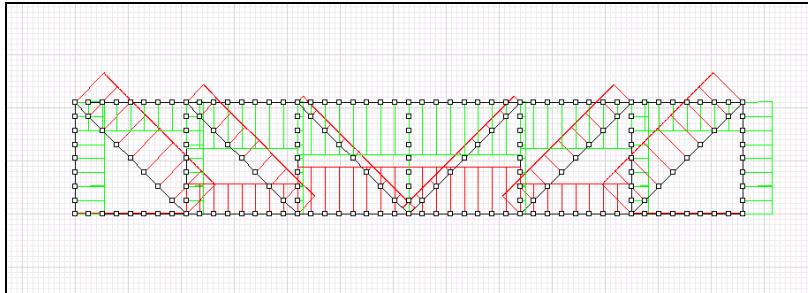


**Figure 4.6 :** Graphical representation of axial forces

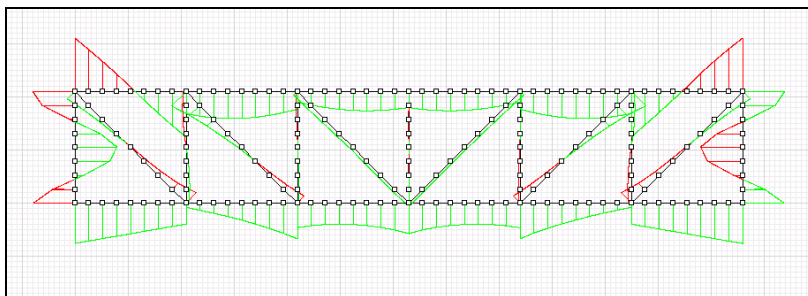


**Figure 4.7 :** Graphical representation of bending moments

In the example above the displacements, axial forces and bending moments occurring in the different bays can be easily compared, using the graphical user interface. The displacements indicate that the verticals above the supports are the elements which buckle first. These are also the elements which carry the largest bending moments. Although the vertical elements adjacent to those above the supports carry only a slightly lower axial force, the bending moments are significantly less.

**Table 4.1** : Excel sheet extract of results corresponding to input depicted in Figure 4.2

Step No	Load Factor	Axial V1 (kN)	Axial V7 (kN)	Bending V1 (kNm)	Bending V7 (kNm)	$\Delta y$ N4 (m)
0	0.000	0.000	0.000	0.0000	0.0000	0.000
1	0.100	-2.491	-2.491	-0.0015	0.0015	0.000
2	0.198	-4.933	-4.933	-0.0029	0.0029	-0.001
3	0.296	-7.375	-7.375	-0.0042	0.0042	-0.001
4	0.394	-9.817	-9.817	-0.0055	0.0055	-0.001
5	0.492	-12.259	-12.259	-0.0068	0.0068	-0.001
6	0.590	-14.700	-14.700	-0.0080	0.0080	-0.002
7	0.688	-17.141	-17.141	-0.0091	0.0091	-0.002
8	0.786	-19.581	-19.581	-0.0102	0.0102	-0.002
9	0.884	-22.022	-22.022	-0.0112	0.0112	-0.003
10	0.983	-24.462	-24.462	-0.0122	0.0122	-0.003
11	1.081	-26.902	-26.902	-0.0131	0.0131	-0.003
12	1.179	-29.341	-29.341	-0.0139	0.0139	-0.003
13	1.277	-31.781	-31.781	-0.0146	0.0146	-0.004
14	1.375	-34.220	-34.220	-0.0153	0.0153	-0.004
15	1.473	-36.659	-36.659	-0.0159	0.0159	-0.004
16	1.571	-39.097	-39.097	-0.0164	0.0164	-0.005
17	1.669	-41.536	-41.536	-0.0168	0.0168	-0.005
18	1.767	-43.974	-43.974	-0.0172	0.0172	-0.005
19	1.865	-46.413	-46.413	-0.0174	0.0174	-0.005
20	1.963	-48.851	-48.851	-0.0176	0.0176	-0.006
21	2.061	-51.288	-51.288	-0.0176	0.0176	-0.006
22	2.159	-53.726	-53.726	-0.0175	0.0175	-0.006
23	2.257	-56.164	-56.164	-0.0173	0.0173	-0.006
24	2.355	-58.601	-58.601	-0.0170	0.0170	-0.007
25	2.453	-61.038	-61.038	-0.0165	0.0165	-0.007
26	2.551	-63.475	-63.475	-0.0158	0.0158	-0.007
27	2.649	-65.913	-65.913	-0.0150	0.0150	-0.008
28	2.748	-68.349	-68.349	-0.0140	0.0140	-0.008
29	2.846	-70.786	-70.786	-0.0128	0.0128	-0.008
30	2.944	-73.223	-73.223	-0.0113	0.0113	-0.008
31	3.042	-75.660	-75.660	-0.0095	0.0095	-0.009
32	3.140	-78.097	-78.097	-0.0075	0.0075	-0.009
33	3.238	-80.533	-80.533	-0.0051	0.0051	-0.009
34	3.336	-82.970	-82.970	-0.0023	0.0023	-0.010
35	3.434	-85.406	-85.406	0.0011	-0.0011	-0.010
36	3.532	-87.842	-87.842	0.0050	-0.0050	-0.010
37	3.630	-90.278	-90.278	0.0098	-0.0098	-0.010
38	3.728	-92.714	-92.714	0.0155	-0.0155	-0.011
39	3.826	-95.149	-95.149	0.0225	-0.0225	-0.011
40	3.924	-97.583	-97.583	0.0313	-0.0313	-0.011
41	4.022	-100.014	-100.014	0.0426	-0.0426	-0.012
42	4.120	-102.439	-102.439	0.0577	-0.0577	-0.012
43	4.218	-104.853	-104.853	0.0833	-0.0833	-0.012
44	4.316	-107.229	-107.229	0.1202	-0.1202	-0.012
45	4.413	-109.467	-109.467	0.1936	-0.1936	-0.013
46	4.461	-110.364	-110.364	0.2679	-0.2679	-0.013
47	4.485	-110.606	-110.606	0.3302	-0.3302	-0.013

The effects investigated, as described previously, were as follows:

1. The effect of the rigidity of the node on the effective length of the compression element
2. The effect of the stiffness, and variation thereof, of neighbouring elements on the rigidity of the node
3. The effect of the rigidity of the node on the distribution of axial forces in the truss
4. The magnitude of bending moments caused by rigid nodal connections
5. The effect of reducing a distributed load over the length of the truss to a single point load applied at midspan

#### 4.6 INVESTIGATIVE ANALYSES PERFORMED

The main purpose of the investigative analyses is to determine the optimum truss design for the experiments to be performed, given certain practical limitations, yet allowing the critical behaviour to manifest during the experiments. Practical limitations include available space in the laboratory, the size of the existing multi-purpose beam/column testing apparatus and cost and time implications of the construction of trusses.

The existing multi-purpose testing apparatus can accommodate a maximum truss length of 10m and truss height of 1.5m. Therefore the 10 bay truss cannot be considered for experimental purposes as it is 10.5m long. The 10 bay truss was still included in the investigative analyses for several reasons. Inclusion of it attains a representative range of depth to span ratios of the trusses in the investigations. Additionally, the longer the truss the better the distribution of forces within the truss becomes i.e. large axial forces occur in the web at the extremes of the truss, and large axial forces in the chords are concentrated at midspan. This effect is illustrated in the Figures 4.8 and 4.9 below:

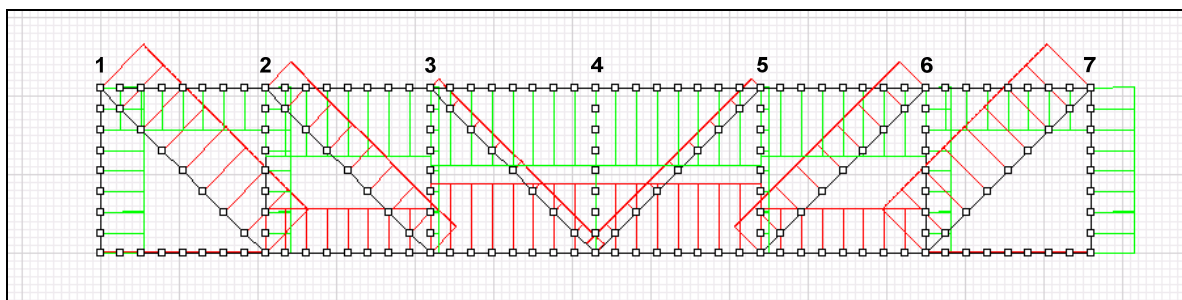


**Figure 4.8** : Distribution of axial forces in 6 bay truss

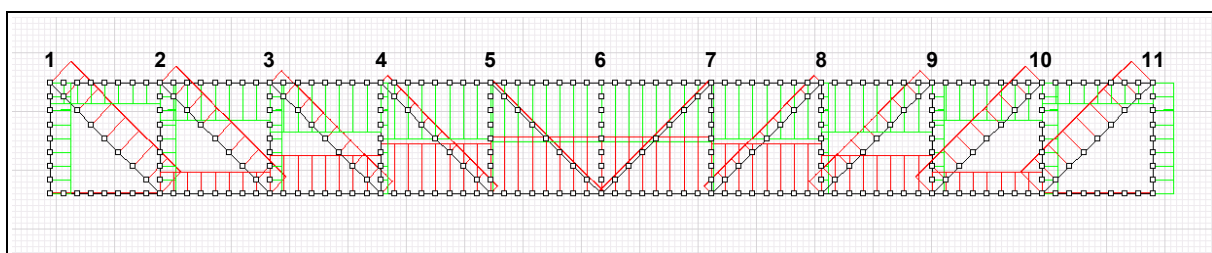


**Figure 4.9** : Distribution of axial forces in 10 bay truss

The following figures illustrate the load cases applied to the trusses in the investigative analyses. The figures only show frameVertical, however, the load cases applied are identical for frameDiagonal.

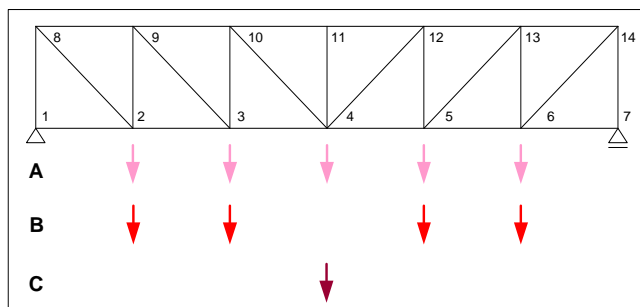


**Figure 4.10** : Load cases A, B and C for six bay truss

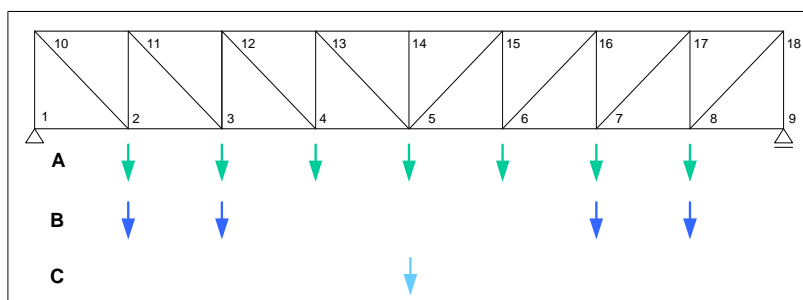


**Figure 4.11** : Load cases A, B and C for eight bay truss

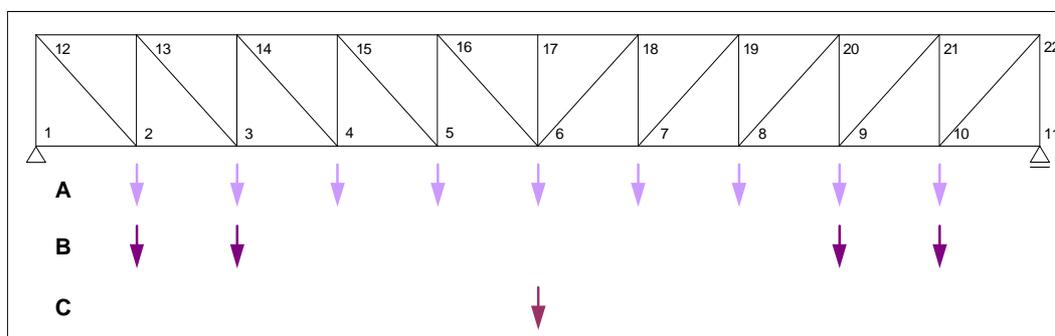


**Figure 4.12** : Load cases A, B and C for ten bay truss

Table 4.2 provides a summary of the analyses performed for frameVertical and frameDiagonal, totaling 90 analyses. A summary of the results of the analyses is provided in the following section.

**Table 4.2** : Summary of analyses performed in ANGELINE

	Load Case	Node Type	Number of Elements per Structural Member	Varying Stiffness of Chords	No of Analyses
Effect 1	A	pinned & rigid	8	No	12
Effect 2	B	rigid	8	Yes (x 3)	18
Effect 3	A	pinned & rigid	8	No	12
Effect 4	A	mixed & rigid	4 & 8	No	24
Effect 5	A & C	pinned & rigid	8	No	24
* Refer to Section 4.1 for definition of effects					<b>Total : 90</b>

## 4.7 RESULTS OF FRAMEVERTICAL ANALYSES

This section contains a summary of the results obtained of the investigative analyses performed in frameVertical. The results of each of the five effects investigated are presented separately.

### 4.7.1 EFFECT INVESTIGATED : NODE RIGIDITY ON THE EFFECTIVE LENGTH

In order to investigate the effect of the node fixity on the effective length Load Case A is applied, as this simulates a distributed load. The buckling loads achieved in the critical element, i.e. the first or last vertical element, for a pin-connected truss and a rigidly connected truss, are compared to the Euler load of a pin-connected column and the Euler load of a rigidly connected column respectively.

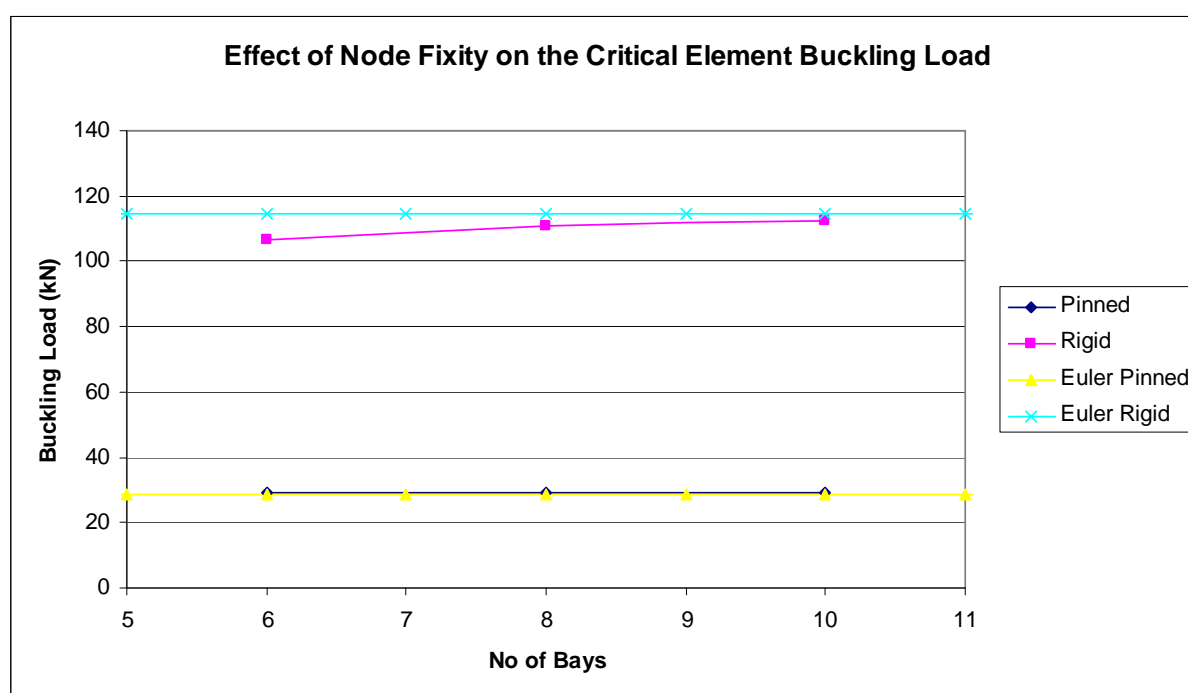


**Figure 4.13** : Effect of node fixity on the critical element buckling load

Figure 4.13 illustrates the fact that the degree of fixity of a node has a significant effect on the buckling load of an element. The rigidly connected truss exhibits buckling loads 3.6 to 3.9 times as large as those of the pin-connected truss. Apart from this, it can be seen that the number of bays in the truss has no effect in a pin-connected truss, but does play a role in a rigidly connected truss. The buckling load of the critical element in a 10 bay truss is 5.3% greater than that of a 6 bay truss.

### 4.7.2 EFFECT INVESTIGATED : STIFFNESS OF NEIGHBOURING ELEMENTS ON NODE FIXITY

In order to investigate the effect of the stiffness of neighbouring elements on the node fixity Load Case B is applied as this creates the situation in which the second nodes in both the top and bottom chords experience large axial forces in all elements connected at that node. The stiffness of the chords is

then varied by varying the section sizes of the chord elements. Varying the section size is the most practical way in which to vary the stiffness of the chords but it is by no means the only parameter which influences the stiffness.

The proposed section to be used for the chords in the experimental setup is a 60 x 60 x 6 double angle. Therefore this section as well as a weaker section, 50 x 50 x 6 double angle, and a stronger section, 70 x 70 x 6, are used. In this investigation only rigid nodes are considered in the investigation as this is the only connection type with which the phenomenon can be induced.

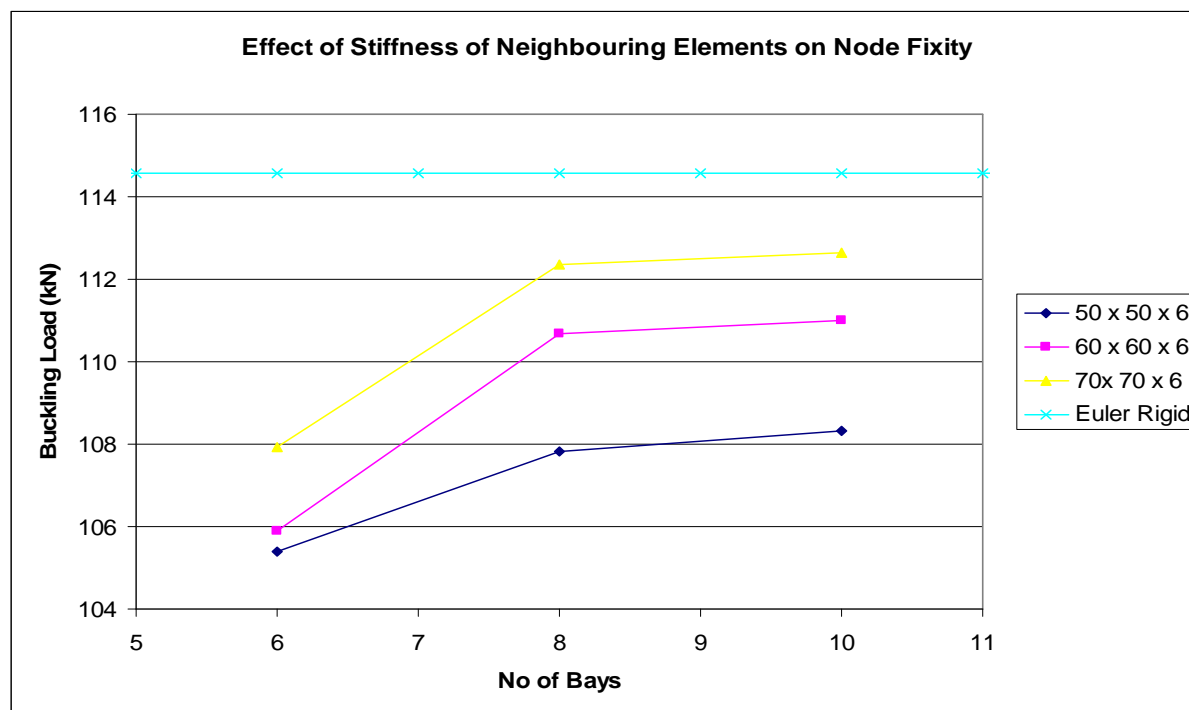


**Figure 4.14 :** Effect of stiffness of neighbouring elements on node fixity

From Figure 4.14 it is apparent that the stiffness of the chord element has a significant effect on the buckling load of the critical element. The load at which buckling occurs differs by as much as 4.2%, between the weakest and the stiffest chord elements. Again the number of bays plays a large role in the magnitude of the critical buckling load. Here the difference between a 6 bay and a 10 bay truss is as large as 4.8%.

#### 4.7.3 EFFECT INVESTIGATED : NODE FIXITY ON THE DISTRIBUTION OF AXIAL FORCES IN TRUSS

In order to investigate the effect of the node fixity on the distribution of axial forces in the truss Load Case A is applied as this simulates a distributed load. In order to compare the results of the different analyses, including the different node fixities and different number of bays, and to determine whether there is a significant change in the distribution of the axial forces throughout the truss, a common ground must be used to facilitate this.

The number of bays in the truss influences the magnitude of the forces in the elements and due to the varying number of elements a direct element for element comparison between the different trusses cannot be done. It is therefore more plausible, and of greater interest to this particular investigation, to establish a relationship between the pin connected and rigidly connected truss results for each truss configuration, and then establish whether this relationship holds true for all truss configurations.

In the analyses, all truss configurations are loaded until the buckling load in the critical element is achieved, for both the pin-connected and rigidly connected configurations. Certain elements are selected for the comparison, and each element's ratio between the load at buckling of the critical element for a pin-connected configuration and the load at buckling of the critical element for a rigidly connected configuration are determined.

This ratio of 'pin load' to 'rigid load' is determined for the vertical, diagonal and upper and lower chord elements at one extreme end of the truss, as well as at the middle of the truss as illustrated in Figure 4.15 below.

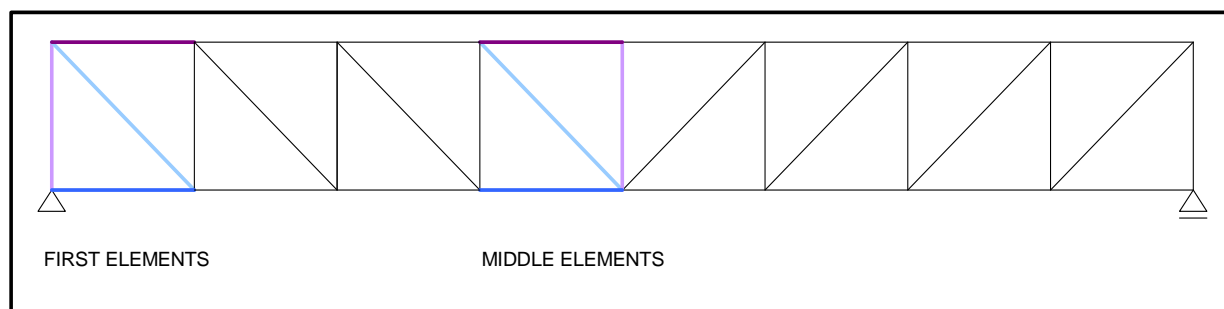


**Figure 4.15** : Illustration of first and middle elements of frame

The theoretical ratio of 'pin load' to 'rigid load' of an element according to Euler is 4.0. This ideal ratio is not achieved in true truss behaviour, due to insufficient restraint provided by the chords. A slightly lower value can be expected, within acceptable limits. If a consistent ratio is achieved between the first and middle element, of each element type, it can be shown that no significant change in axial force distribution occurs between a pin-connected and rigidly connected truss configuration.

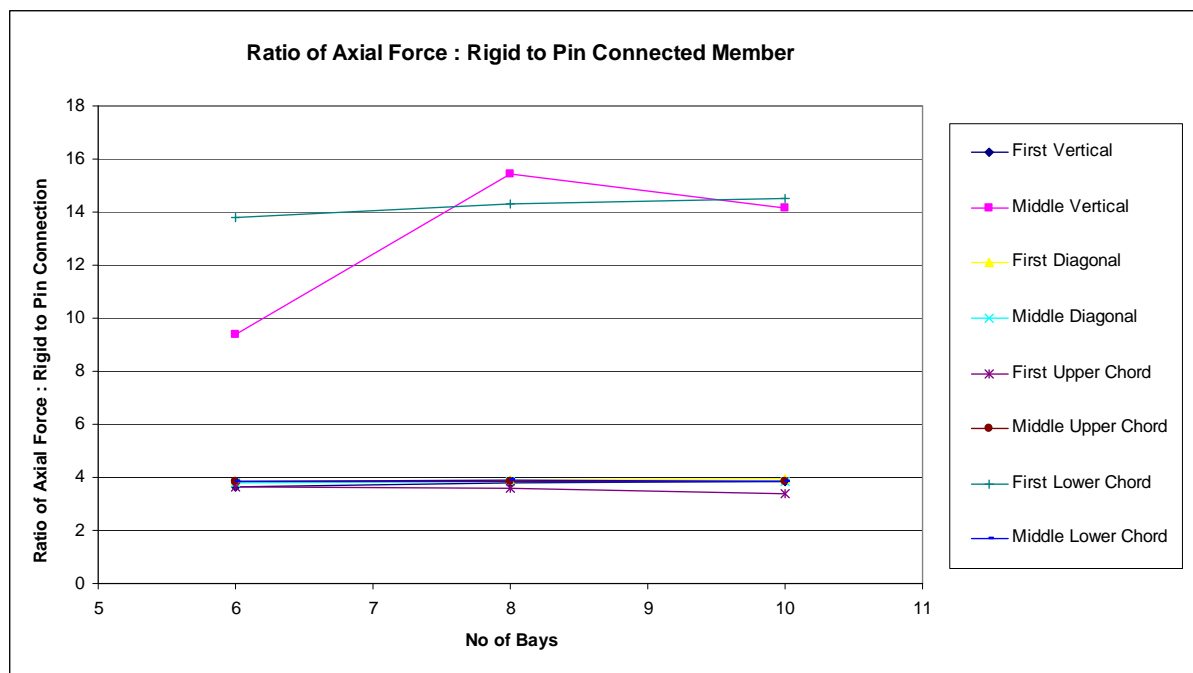


**Figure 4.16 :** Effect of node fixity on the distribution of axial forces in the truss

As can be seen in Figure 4.16 above the 'pin load' to 'rigid load' ratios of all elements fall within an acceptable band just below 4.0 and the first to middle element relationships compare well, except those of the middle vertical element and first lower chord element. These inconsistencies are easily explained. In ideal truss behaviour, the middle vertical element and first lower chord element experience zero axial force, under a gravity load equivalent load pattern. Realistically, however, they do carry very small loads. Typically these loads are negligible but for the purpose of the analyses they are included and a slight variance in these already small loads creates a large difference in the ratio of 'pin load' to 'rigid load'.

Apart from these anomalies there is little to suggest that a significant change in distribution of axial forces occurs. An increase in the number of bays of the truss configuration does result in an increase in the magnitude of the axial forces, especially in the middle of the upper and lower chords, however the ratio between the 'pin load' and 'rigid load' is unaffected.

#### 4.7.4 EFFECT INVESTIGATED : NODE FIXITY ON THE MAGNITUDE OF SUBSEQUENT BENDING MOMENTS

In order to investigate the effect of the node fixity on the magnitude of the subsequent bending moments in the truss elements Load Case A is applied as this simulates a distributed load. The investigation is done using rigid nodes only, as these create bending moments.

Each truss configuration is loaded up to the point where buckling of the critical vertical element occurs. The maximum bending moments which occur in each element type, i.e. vertical, diagonal and upper and lower chord members, at the point of critical buckling load, are shown below.

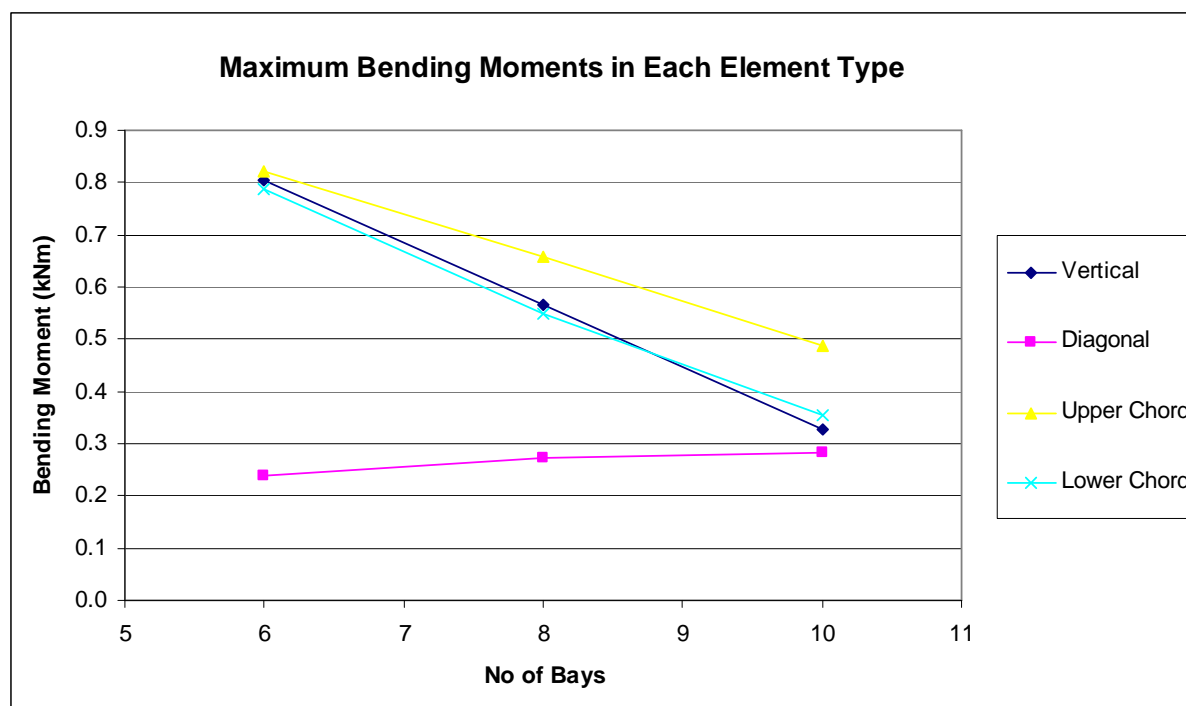


**Figure 4.17** : Maximum bending moments which occur in each element type

As can be seen in Figure 4.17, a fair amount of variance in bending moments occurs between the different truss configurations. The magnitude of the bending moments is also significant, in that a bending moment of 0.8kNm in a 25 x 25 x 3 double angle causes an elastic stress of approximately 890MPa, in a section with a yield stress of 200MPa.

#### 4.7.5 EFFECT INVESTIGATED : REDUCING DISTRIBUTED LOAD TO SINGLE POINT LOAD AT MIDSPAN

In order to investigate the effect of reducing a distributed load to an equivalent point load at midspan Load Cases A and C are applied. Load Case A simulates a distributed load whereas Load Case C applies a single point load at midspan. The buckling loads of the critical elements of the two load cases are compared to each other and to the theoretical values obtained from a pin-connected Euler column for the pin-connected truss, and a rigidly connected Euler column for the rigidly connected truss.

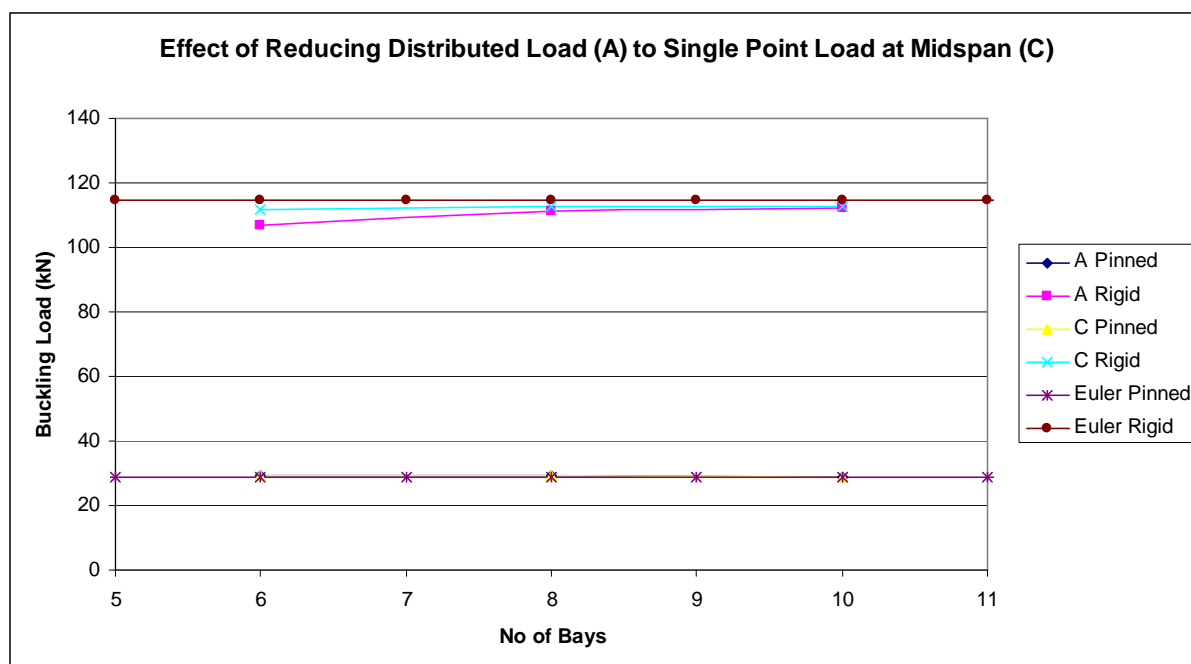


**Figure 4.18 :** Effect of reducing a distributed load to a single point load at midspan

Figure 4.18 illustrates that the pin-connected truss is unaffected by both the load application pattern and the number of bays in the truss. The rigidly connected truss is affected by both of these factors. It should be noted that the greater the number of bays used, the smaller the effect of reducing the distributed load to an equivalent point load becomes.

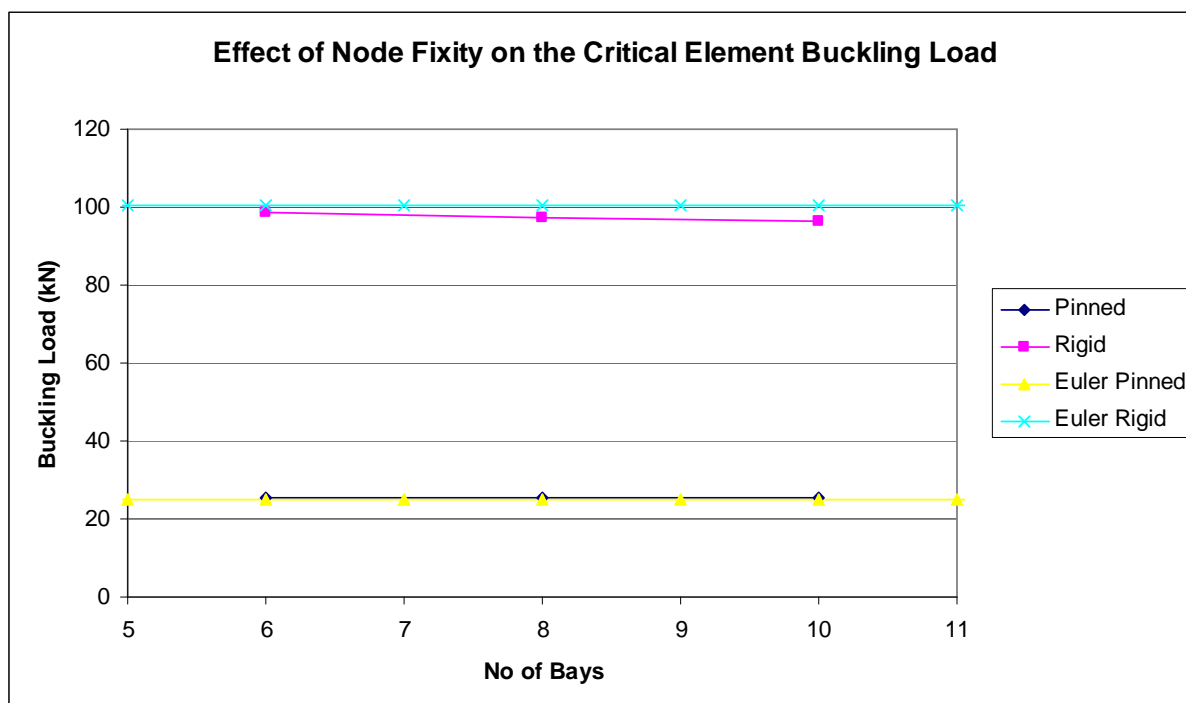
The greatest difference in buckling load of the critical element caused by changing the load application pattern is 4.9%, with the single point load at midspan inducing the greater buckling load. The difference in buckling load between a 6 bay and a 10 bay rigidly connected truss, for a uniformly distributed load is 5.3% whereas the difference for a single load applied at midspan is only 0.6%. Therefore, for experimental purposes, there is little difference between a 6 bay and a 10 bay truss, if a single point load is applied.

## 4.8 RESULTS OF FRAMEDIAGONAL ANALYSES

This section contains a summary of the results obtained of the investigative analyses performed in frameDiagonal. The results of each of the five effects investigated are presented separately.

### 4.8.1 EFFECT INVESTIGATED : NODE FIXITY ON THE EFFECTIVE LENGTH

In order to investigate the effect of the node fixity on the effective length Load Case A is applied, as this simulates a distributed load. The buckling loads achieved in the critical element, i.e. the first or last diagonal element, for a pin-connected truss and a rigidly connected truss, are compared to the theoretical values obtained from a pin-connected Euler column and a rigidly connected Euler column respectively.



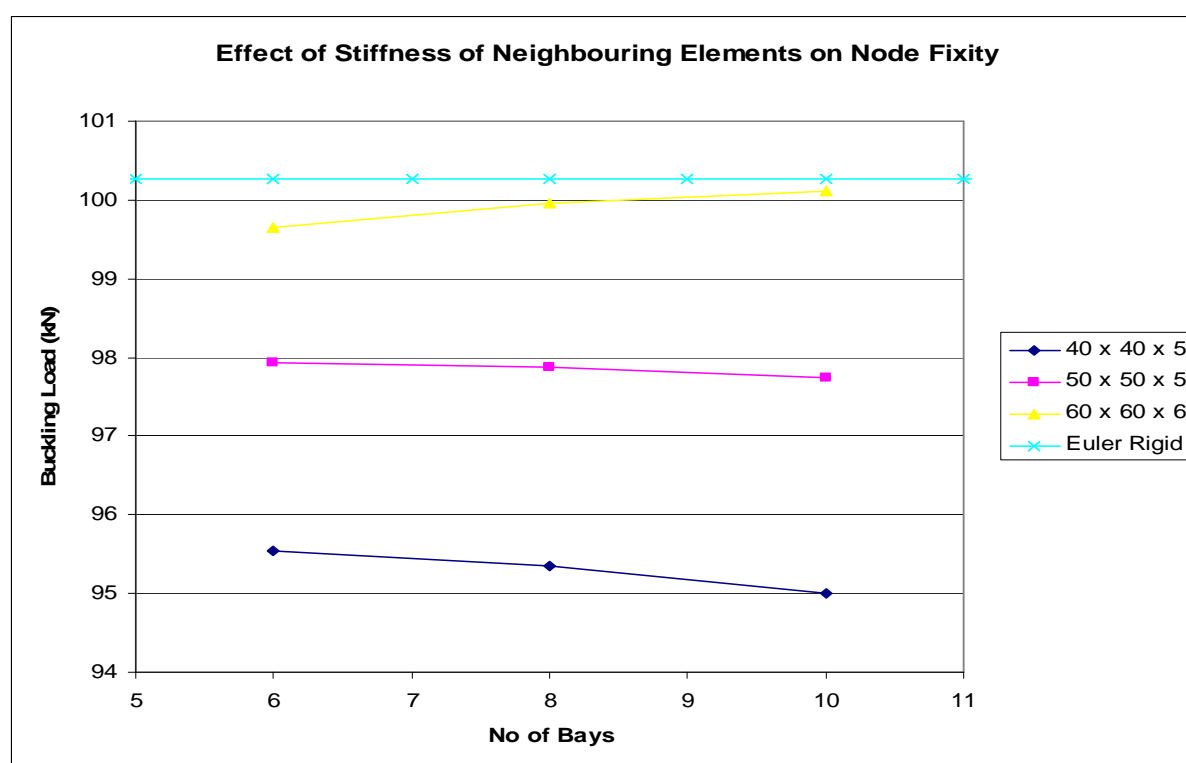
**Figure 4.19** : Effect of Node fixity on the critical element buckling load

Figure 4.19 illustrates the fact that the degree of fixity of a node has a significant effect on the buckling load of an element, similar to the results of frameVertical. The rigidly connected truss exhibits buckling loads 3.8 to 3.9 times as large as those of the pin-connected truss. Apart from this, it can be seen that the number of bays in the truss has no effect in a pin-connected truss, but does play a role in a rigidly connected truss. Unlike the results of frameVertical the buckling load decreases with an increase in the number of bays. The buckling load of the critical element in a 10 bay truss is 2.2% less than that of a 6 bay truss.

#### 4.8.2 EFFECT INVESTIGATED : STIFFNESS OF NEIGHBOURING ELEMENTS ON NODE FIXITY

In order to investigate the effect of the stiffness of neighbouring elements on the node fixity Load Case B is applied as this creates the situation in which the second nodes in both the top and bottom chords experience large axial forces in all elements connected at that node. The stiffness of the chords is then varied by varying the section sizes of the elements.

The proposed section to be used for the diagonal elements in the experimental setup is a 50 x 50 x 5 double angle. Therefore this section as well a weaker section, 40 x 40 x 5 double angle, and a stronger section, 60 x 60 x 5, are used. Only rigid nodes are considered in the investigation as this is the only connection type with which the phenomenon can be induced.



**Figure 4.20 :** Effect of stiffness of neighbouring elements on node fixity

From Figure 4.20 it is apparent that the stiffness of the chord element has a significant effect on the buckling load of the critical element. However the trends are not as uniform as was the case in frameVertical. The stiffest section, 60 x 60 x 5 double angle, increases the buckling load and hence the node fixity. However the two weaker sections, 40 x 40 x 5 and 50 x 50 x 5 double angles, decrease the buckling load and node fixity. The load at which buckling occurs differs between 4.3% and 5.4%, between the weakest and the stiffest chord elements. Again the number of bays plays a role in the magnitude of the critical buckling load but the effect is much less severe that in the results of frameVertical. Here the difference between a 6 bay and a 10 bay truss is 0.6% at its maximum.

#### 4.8.3 EFFECT INVESTIGATED : NODE FIXITY ON THE DISTRIBUTION OF AXIAL FORCES IN TRUSS

In order to investigate the effect of the node fixity on the distribution of axial forces in the truss Load Case A is applied as this simulates a distributed load. In order to compare the results of the different analyses, including the different node fixities and different number of bays, and to determine whether there is a significant change in the distribution of the axial forces throughout the truss, a common ground must be used to facilitate this.

The approach taken is similar to that of the results obtained in frameVertical. This ratio of 'pin load' to 'rigid load' is determined for the vertical, diagonal and upper and lower chord elements at one extreme end of the truss, as well as at the middle of the truss as illustrated in Figure 4.21 below.

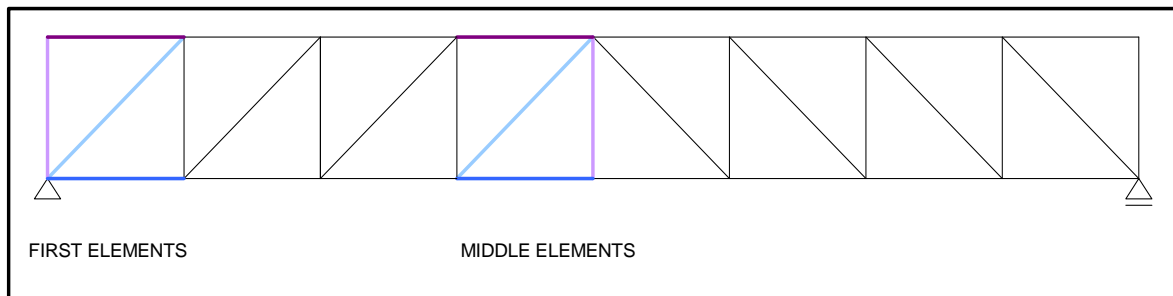


**Figure 4.21** : Illustration of first and middle elements of frameDiagonal

As in frameVertical, if a consistent ratio of 'pin load' to 'rigid load' is achieved between the first and middle element, of each element type, it can be shown that no significant change in axial force distribution occurs between a pin-connected and rigidly connected truss configuration.

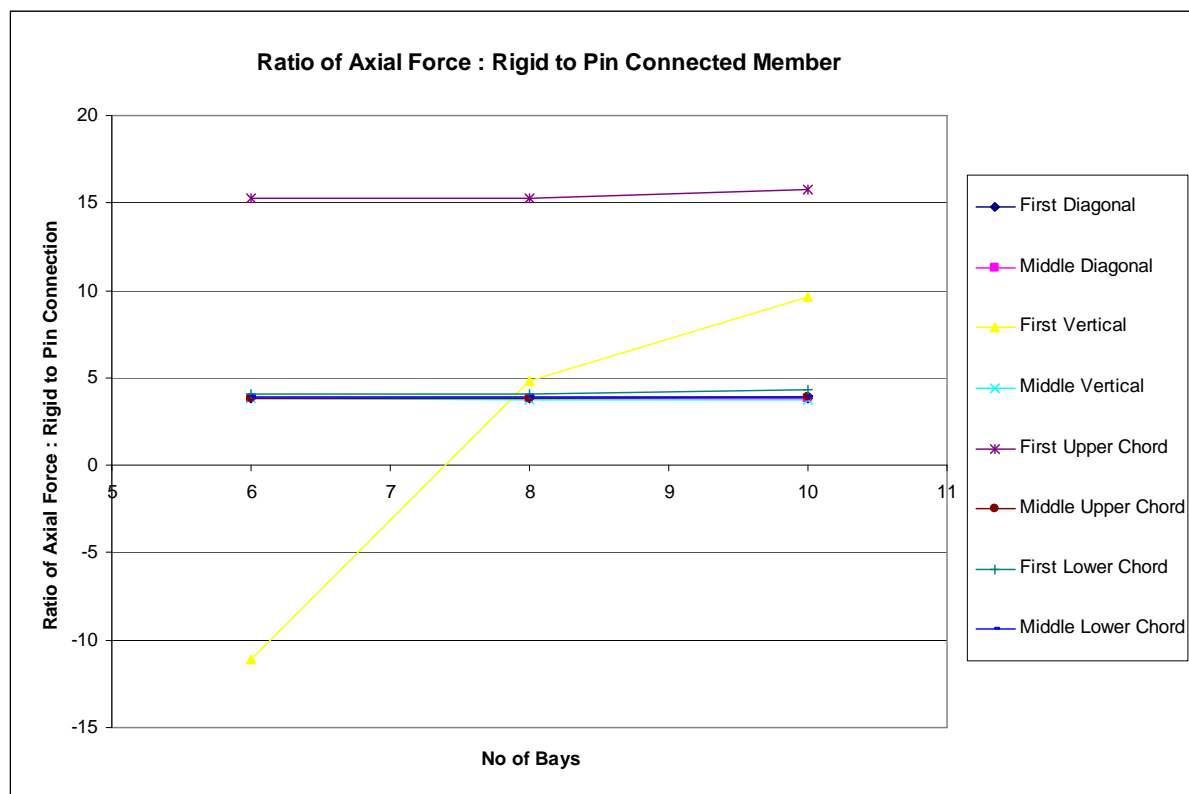


**Figure 4.22 :** Effect of node rigidity on distribution of axial forces in the truss

As can be seen in Figure 4.22 above the 'pin load' to 'rigid load' ratios of all elements again fall within an acceptable band just below 4.0 and the first to middle element relationships compare well, except those of the first vertical element and middle upper chord element. Similarly to the results of frameVertical these inconsistencies are easily explained. In ideal truss behaviour, the first vertical element and middle lower chord element experience virtually zero axial force, under a wind load equivalent load pattern. Realistically, however, they do carry very small loads. Typically these loads are negligible but for the purpose of the analyses they are included and a slight variance in these already small loads creates a large difference in the ratio of 'pin load' to 'rigid load'.

Apart from these anomalies there is little to suggest that a significant change in distribution of axial forces occurs. An increase in the number of bays of the truss configuration does result in an increase in the magnitude of the axial forces, especially in the middle upper and lower chord elements, however the ratio between the 'pin load' and 'rigid load' is unaffected.

#### 4.8.4 EFFECT INVESTIGATED : NODE FIXITY ON MAGNITUDE OF SUBSEQUENT BENDING MOMENTS

In order to investigate the effect of the node fixity on the magnitude of the subsequent bending moments Load Case A is applied as this simulates a distributed load. The investigation is done using rigid nodes only, as these create bending moments.

Each truss configuration is loaded up to the point where buckling of the critical vertical element occurs. The maximum bending moments which occur in each element type, i.e. vertical, diagonal and upper and lower chord members, at the point of critical buckling load, are shown below in Figure 4.22.

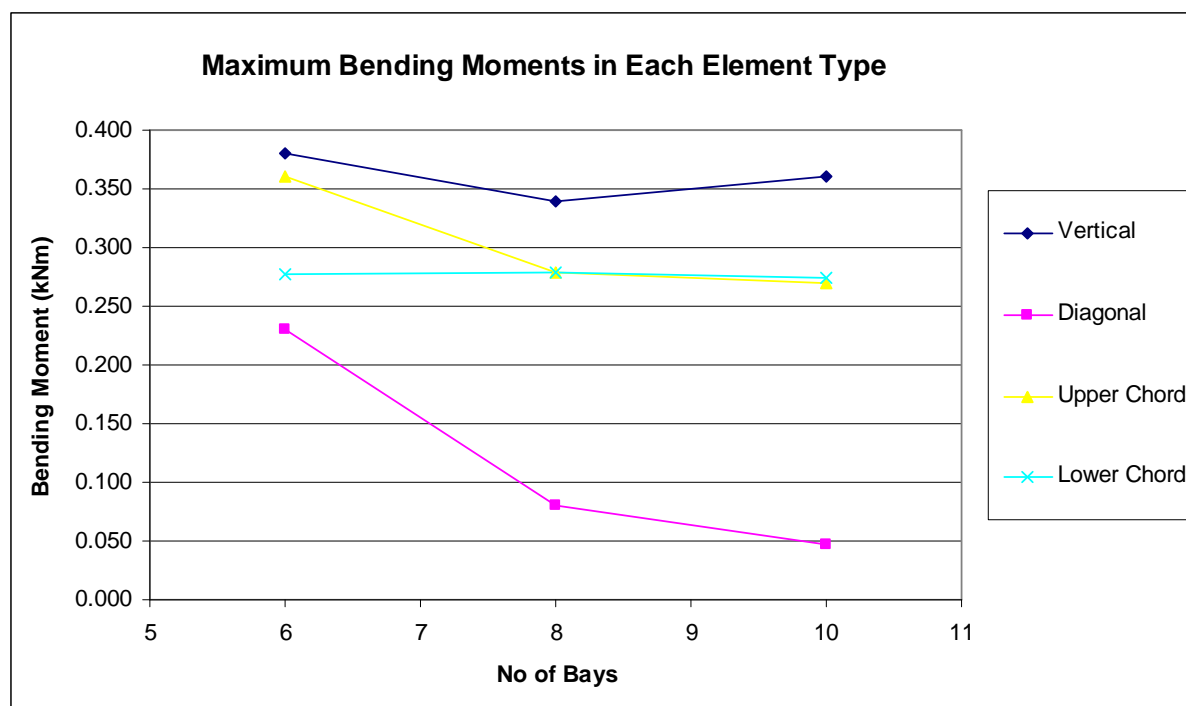


**Figure 4.23 :** Maximum bending moments which occur in each element type

As can be seen in Figure 4.23 above, a fair amount of variance in bending moment occurs between the different truss configurations. Again the magnitude of the bending moments is significant, but not as critical as the results obtained in frameVertical. In this case the bending moment in the critical diagonal elements, 30 x 30 x 3 double angles, is 0.23kNm, which results in an elastic stress of 178MPa, below the yield stress of 200MPa.

#### 4.8.5 EFFECT INVESTIGATED : REDUCING DISTRIBUTED LOAD TO SINGLE POINT LOAD AT MIDSPAN

In order to investigate the effect of reducing a uniformly distributed load to a single point load applied at midspan Load Cases A and C are applied. Load Case A simulates a distributed load whereas Load Case C applies a single point load at midspan. The buckling loads of the critical elements of the two load cases are compared to each other and to the theoretical values obtained from a pin-connected Euler column for the pin-connected truss, and a rigidly connected Euler column for the rigidly connected truss.

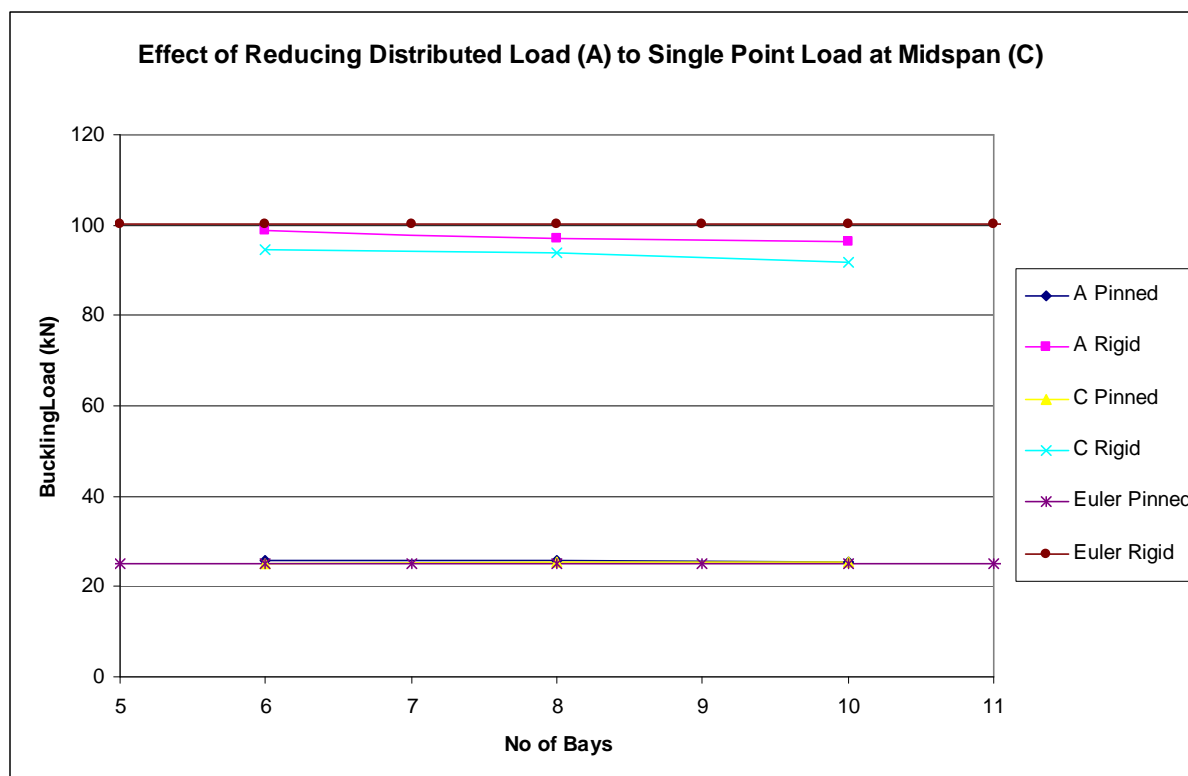


**Figure 4.24 :** Effect of reducing a distributed load to a single point load at midspan

Figure 4.24 above illustrates that the pin-connected truss is unaffected by both the load application pattern and the number of bays in the truss, similar to the results obtained from frameVertical. The rigidly connected truss is affected by both of these factors. It should be noted that, unlike frameVertical, the relationship between the two load cases of a rigidly connected truss remains fairly constant.

The greatest difference in buckling load of the critical element caused by changing the load application pattern is 5.0%, with the uniformly distributed load inducing the greater buckling load. The results of frameVertical indicated that single point load at midspan induces a greater buckling load. The difference in buckling load between a 6 bay and a 10 bay rigidly connected truss, for a uniformly distributed load is 2.3% whereas the difference for a single load applied at midspan is 3.7%. For experimental purposes, this difference is somewhat more significant than the one obtained in frameVertical, namely 0.6%.

## 4.9 CONCLUSIONS OF ANALYSES

As mentioned in the previous section the main purpose of the investigative analyses was to be able to analytically justify the decisions made in the design of the experimental trusses. On the whole the analyses revealed that the different truss layouts and dimensions only have minor influences on the effects which were investigated, which can be seen in the following table and are discussed in greater detail further on.

### 4.9.1 SUMMARY OF RESULTS

The results of the investigations into the effects of the node fixity on the distribution of axial forces and on the magnitude of subsequent bending moments, i.e. effects 3 and 4, are not included in Table 4.3 below as their results are more easily summarized, and do not require a table format.

**Table 4.3** : Summary of results obtained for frameVertical and frameDiagonal

Effect		frameVertical	frameDiagonal
1	a) ratio of buckling load of rigidly connected truss to pin-connected truss	3.6 – 3.9	3.8 – 3.9
	b) rigidly connected truss in which greatest buckling load occurs	10 bay	6 bay
	c) % difference in buckling load between 10 bay and 6 bay rigidly connected truss	5.3%	2.2%
2	a) % difference in buckling load between stiffest and weakest chord	4.2%	5.4%
	b) greatest % difference in buckling load between 6 bay and 10 bay	4.8%	0.6%
5	a) load pattern which causes greatest buckling load in rigidly connected truss	single point load applied at midspan	uniformly distributed load
	b) greatest % difference in buckling load of rigidly connected truss between load patterns	4.9%	5.0%
	c) % difference in buckling load between 6 bay and 10 bay rigidly connected truss for uniformly distributed load	5.3%	2.3%
	d) % difference in buckling load between 6 bay and 10 bay rigidly connected truss for single point load applied at midspan	0.6%	3.7%
* buckling load refers to the load required for buckling of the critical element of the truss, i.e. the first vertical elements in frameVertical or the first diagonal elements in frameDiagonal			

#### 4.9.2 CONCLUSIONS OF INVESTIGATIVE ANALYSES

The results of the effects investigated, as summarized in Table 4.3 above, illustrate that despite the interesting nature of the results, the variance in buckling load of the critical elements is relatively small, hardly above 5%. Greater variance of the buckling load can be expected in the execution of the experiments due to external influences, such as material quality or initial imperfections. Therefore the practical considerations and limitations have a more weighted influence on the final design of the trusses. However, this in itself is a valuable conclusion to arrive at.

The six bay truss was selected for various practical reasons. As mentioned before the existing multi-purpose testing apparatus can only accommodate the six or eight bay trusses. Standard lengths available for the chord sections are 6.0m, 6.5m and 13.0m. Choosing a six bay truss, i.e. a 6.3m truss, minimizes the amount of material off-cuts. This has a significant impact on the cost of materials, thereby increasing the number of trusses that can be built and tested. This ultimately benefits the integrity of the results obtained.

Some of the minor differences observed between the different truss configurations are as follows. A six bay truss configuration results in a lower buckling load in the vertical elements in frameVertical, than in larger trusses, as can be seen in Figure 4.18. Therefore a smaller load can be applied during the execution of the experiment, which holds various benefits.

The longer the truss, the greater the axial forces generated in the chords at midspan. The chord elements are designed to be non-critical elements, therefore lesser loads in these elements are preferred. Another notable benefit of a shorter truss is that the longer the truss, the greater the load becomes in the second web compression element, in both frameVertical and frameDiagonal. The first and second web compression elements then carry very similar loads, which reduces the probability of the first element buckling first during the execution of the experiments. This inability to safely predict which element will buckle first makes it difficult to decide on the placement of the strain gauges in the experiment.

A disadvantage of using a shorter truss is that the elements in frameVertical carry greater bending moments, as can be seen in Figure 4.17. There is approximately a 50% decrease in bending moments in the elements between the 6 bay truss and the 10 bay truss. However, even this lesser bending moment in the 10 bay truss causes a stress greater than the yield stress in the critical element and, taking the other factors into consideration, this alone does not warrant increasing the bay number from 6 to 10.

Approximating a uniformly distributed load with a single point load at midspan creates a negligible change in the distribution of the axial forces throughout the truss, as can be seen in Figures 4.18 and 4.24. Therefore this is an acceptable load application method in the experiment.

### 4.9.3 OPEN QUESTIONS

The following aspects could not be determined conclusively from the investigative analyses for a number of reasons. The first concerns the possibility of material failure of the critical member, prior to geometrical failure. As the investigative analyses were conducted using software designed for geometrically nonlinear structural analysis, material behaviour is not taken into direct consideration.

Considering the relatively large bending moments identified in the investigative analyses, in comparison to the size of the member sections employed, this is quite likely to be a critical factor. Further investigation into this matter is undertaken in Chapter 5. Coupled to this matter, is the possibility of material imperfections, as well as eccentricities due to fabrication of the sections and construction of the trusses.

The analyses, as well as the research as a whole, are restricted to in-plane behaviour of the truss. A number of measures have been taken to ensure that the experiment conforms to this. Therefore any out-of-plane behaviour, such as out-of-plane buckling of the critical elements or large lateral displacements of the upper chord, is unanticipated and unlikely but a possibility none the less.

### 4.9.4 FINAL TRUSS CONFIGURATIONS

The final truss configurations as decided upon based on the conclusions of the investigative analyses, as well as practical considerations, are as follows:

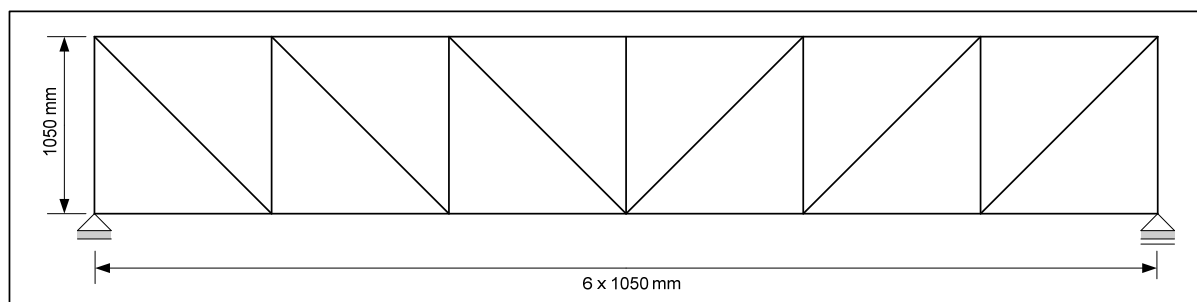


**Figure 4.25** : Truss configuration for gravity load case

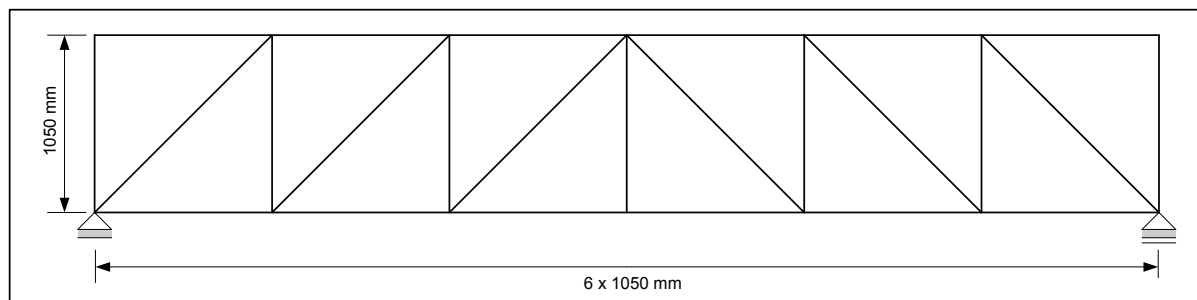


**Figure 4.26** : Truss configuration for wind load case

**Table 4.4 :** Section sizes of truss elements for both truss configurations

<b>Section</b>	<b>Gravity Load Case</b>	<b>Wind Load Case</b>
<b>Top Chord</b>	60 x 60 x 6	50 x 50 x 5
<b>Bottom Chord</b>	60 x 60 x 6	50 x 50 x 5
<b>Vertical Members</b>	25 x 25 x 3	40 x 40 x 6
<b>Diagonal Members</b>	40 x 40 x 6	30 x 30 x 3
* All sections comprise of double angles		

## **5. STRUCTURAL ANALYSES**

The previous chapter investigated a number of different factors which may influence the truss behaviour during the execution of experiments in unexpected ways and thereby establish an optimum truss configuration to be used for the test frames. In order to facilitate a direct comparison between the analytical and experimental results obtained, the same truss configuration is used for the structural analyses.

These analyses were performed using both ANGELINE and Prokon to facilitate a verification of the accuracy and validity of the results gained from Prokon. This is done in order to determine whether the eventual results and conclusions of the research could be reconstructed using one of the most commonly used structural analysis softwares in the South African industry. The methodologies employed in the structural analyses as well as their results are presented in this chapter.

### **5.1 PROKON STRUCTURAL ANALYSES**

#### **5.1.1 BACKGROUND TO PROKON**

The Prokon suite of structural analysis and design software includes frame and finite element analysis as well as design packages for a number of different materials, including steel, reinforced and pre-stressed concrete, timber and masonry.

It is one of the most widely used structural design software packages in the South African industry. For this reason it is important to compare any results achieved to those generated by Prokon. Possible correlation of Prokon and research results would enable the results of the research to be more easily applied in the context of the South African industry.

#### **5.1.2 ANALYSIS TYPES**

- **Buckling Analysis**

Performing a buckling analysis determines the Eigenvectors and Eigenvalues due to buckling. The Eigenvectors indicate the buckling mode shape whereas the Eigenvalue reflects the load factor. The load factor, multiplied by the applied load, results in the buckling load. Buckling analyses were performed to identify the critical elements in the truss.

By applying an initial point load at midspan to the bottom chord of the truss and multiplying this with the load factor obtained for the buckling mode from the analysis, the load required to achieve buckling of the critical element is determined. This buckling load is then used in the second order analyses performed.

#### - Second order Analysis

A second order analysis models sway behaviour by incorporating P-delta effects. The solution is obtained by iterative analysis. Second order analyses were performed to verify the overall stability of the structure.

In performing a second order analysis, using the buckling load obtained from the buckling analysis, the effects of the bending moments induced in the elements are not taken into account. It is likely that the axial load required to cause buckling of the critical element far exceeds the material capacity of the element. In other words, the element may have already yielded in combined axial / flexural mode.

The following results therefore include the axial forces in the elements at the point of buckling, as well as the bending moments in the elements at this stage. Once these results are obtained it is necessary to determine whether material or geometrical failure occurs first. If it is a case of material failure, i.e. yielding, this point must be found.

### 5.1.3 RESULTS OF GRAVITY LOAD CASE ANALYSES

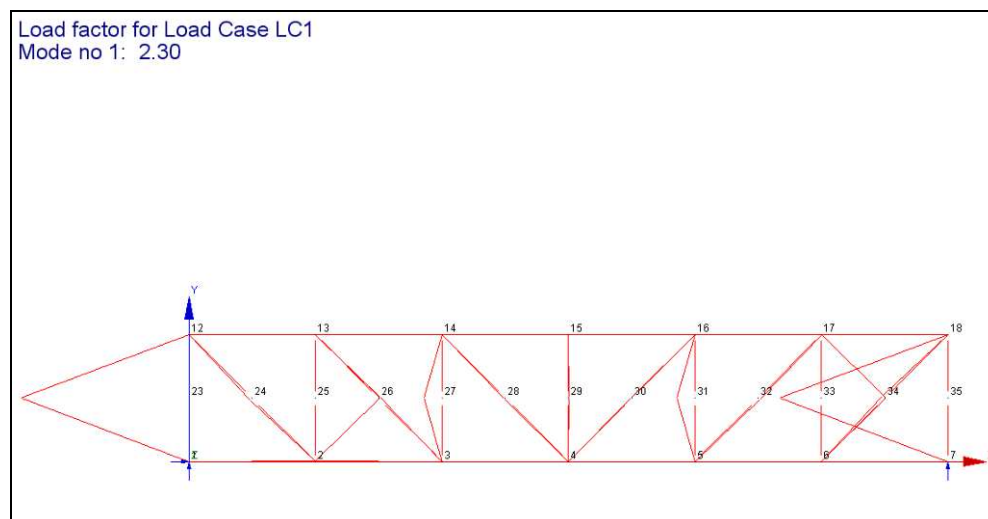


**Figure 5.1** : Output of buckling analysis for gravity load case

The initial load applied to the bottom chord at midspan was 100kN. Therefore the buckling load should be in the vicinity of 230kN, the applied 100kN multiplied by the load factor, 2.30. The critical element, the element which buckles first, is the first vertical member from the left.

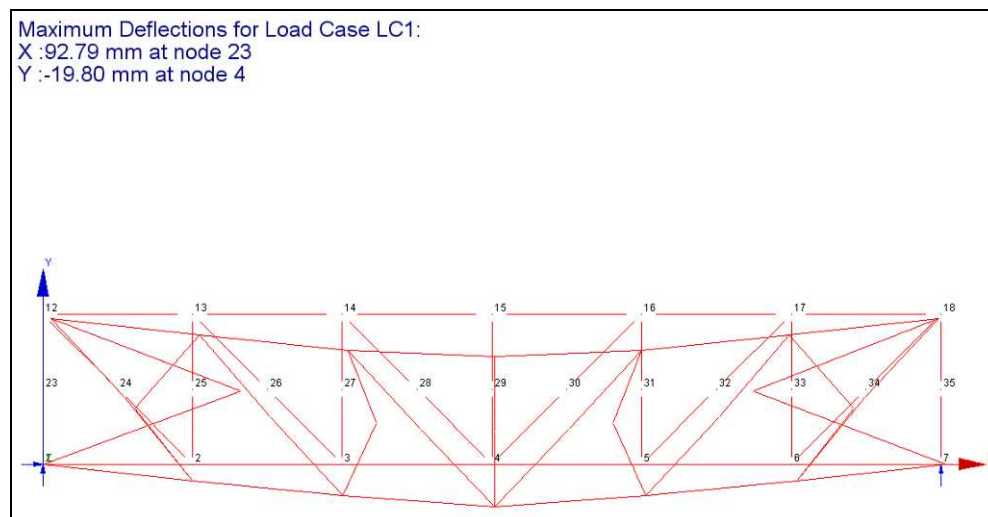


Figure 5.2 : Output of second order analysis for gravity load case

Table 5.1 : Member forces in vertical elements at buckling point of critical element

Vertical Element No	1	2	3	4	5	6	7
Axial Load (kN)	119.8	108.44	116.34	1.25	116.29	108.58	119.66
Bending Moment (kNm)	5.89	1.66	1.37	0	1.33	1.63	5.87
Stress (MPa)	6970.8	2227.5	1932.9	4.4	1888.3	2194.7	6948.0

The load applied at midspan to the bottom chord in the second order analysis in order to achieve buckling was indeed 228.3kN, corresponding to the value obtained by means of the buckling analysis. As can be seen in the Table 5.1, the stress in the elements at the point of buckling far exceeds the yield limit of the material. Therefore material failure occurs before geometrical failure. The yielding point under combined axial / flexural behaviour is determined in Section 5.3.

#### 5.1.4 RESULTS OF WIND LOAD CASE ANALYSES

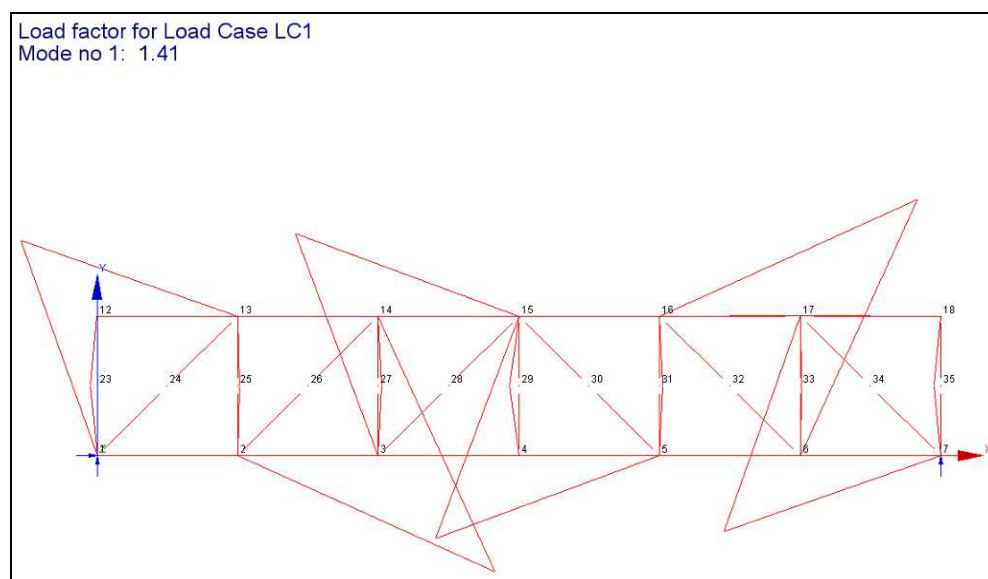


Figure 5.3 : Output of buckling analysis for wind load case

The initial load applied to the bottom chord at midspan was 100kN. Therefore the buckling load should be in the vicinity of 141.0kN, the applied 100kN multiplied by the load factor, 1.41.

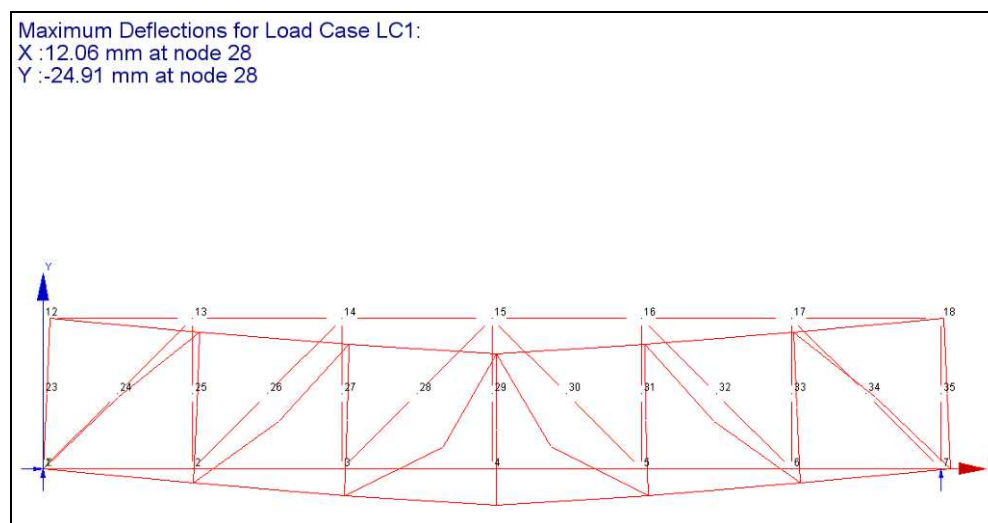


Figure 5.4 : Output of second order analysis for wind load case

Table 5.2 : Member forces in diagonal elements at buckling point of critical element

Diagonal Element No	1	2	3	4	5	6
Axial Load (kN)	97.66	99.19	97.25	97.25	99.19	97.66
Bending Moment (kNm)	0.12	0.29	0.73	0.73	0.29	0.12
Stress (MPa)	373.4	509.3	843.9	843.9	509.3	373.4

The load applied at midspan to the bottom chord in the second order analysis in order to achieve buckling of the critical elements, namely the central diagonals, was indeed 139.3kN, slightly lower than the value obtained by means of the buckling analysis.

As is the case for the gravity load case, the stresses in the elements at the point of buckling exceed the yield limit of the material. Therefore material failure occurs before geometrical failure. The yielding point under combined axial / flexural behaviour is determined in Section 5.3.

## 5.2 ANGELINE STRUCTURAL ANALYSES

The origin and basis of ANGELINE were discussed in Chapter 4, with regards to the investigative analyses. Analyses of the truss configurations decided upon, as described at the beginning of this chapter, are done using frameVertical for the gravity load case and frameDiagonal for the wind load case.

### 5.2.1 RESULTS OF GRAVITY LOAD CASE ANALYSES

For the analysis of the gravity load case using frameVertical, a 100kN point load is applied at midspan. As can be seen in Figure 5.5 below, a load factor of 2.256 is achieved at the buckling point of the critical element, namely the first vertical elements. This means that a load of 2.256 x 100kN causes buckling of the critical elements.

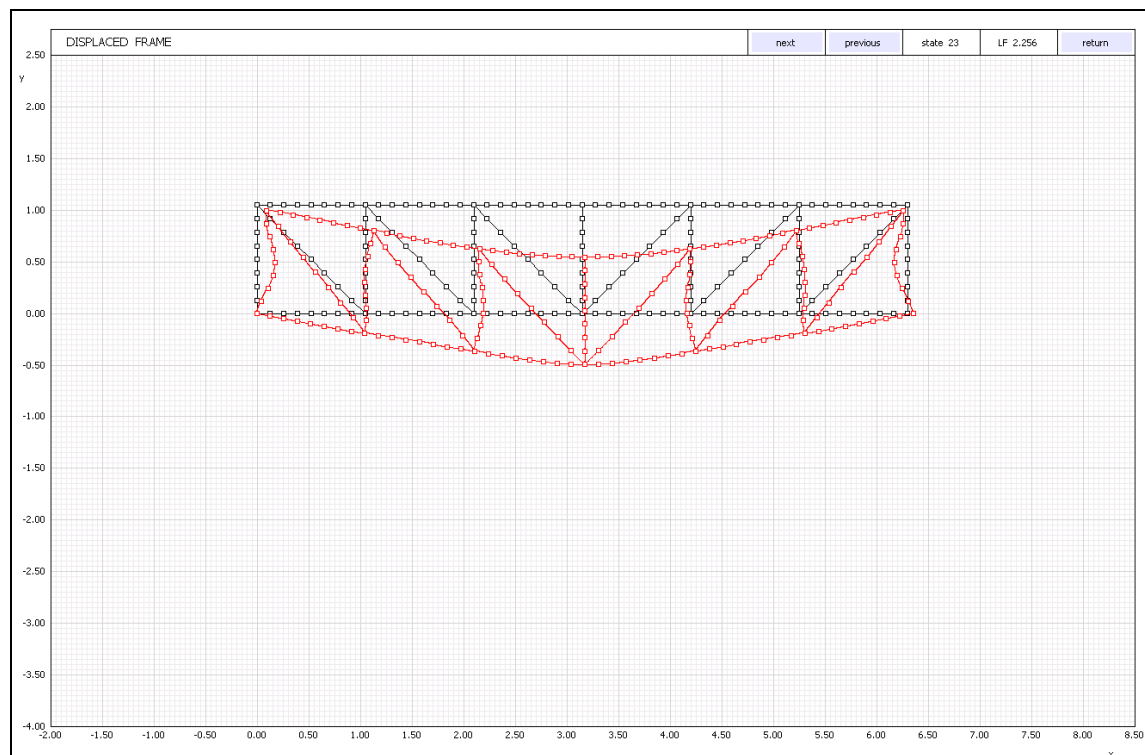


Figure 5.5 : Output of frameVertical analysis

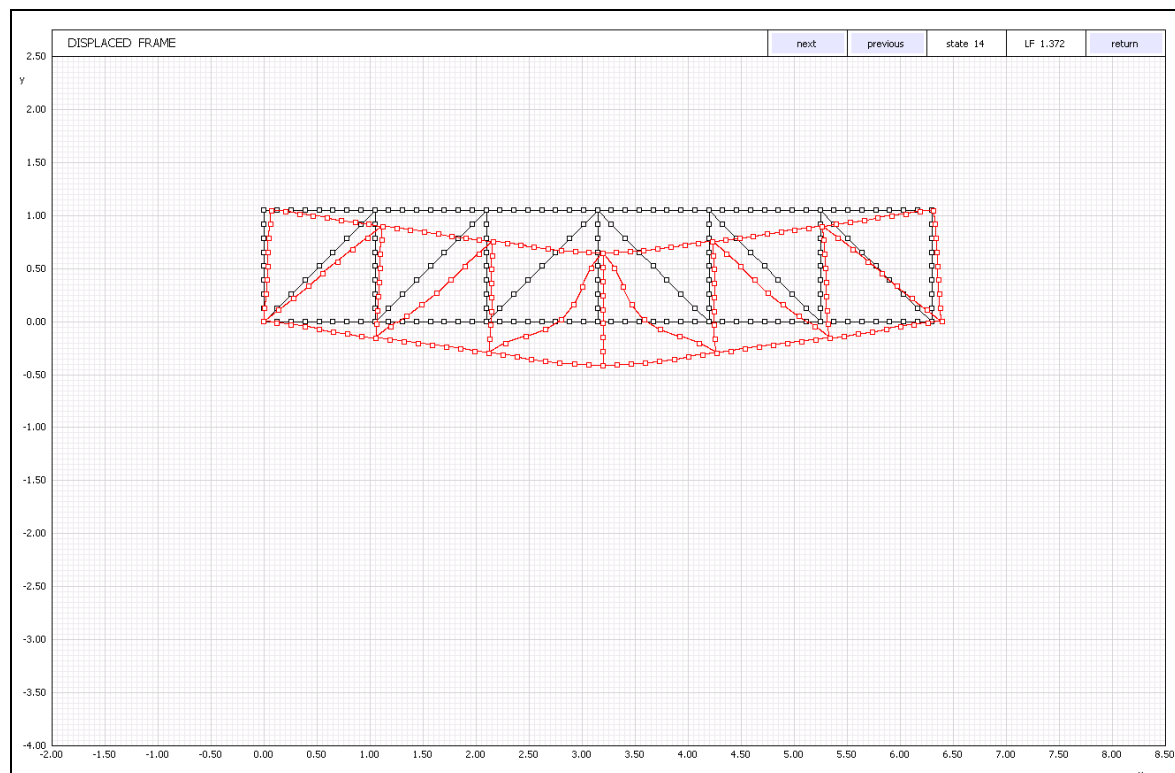
Table 5.3 contains the axial loads, bending moments and subsequent stresses in each of the vertical members of the truss at the point of buckling of the critical vertical member, according to the results obtained from ANGELINE.

Table 5.3 : Member forces in vertical elements at buckling point of critical element

Vertical Element No	1	2	3	4	5	6	7
Axial Load (kN)	112.59	111.67	110.78	1.07	110.78	111.68	112.58
Bending Moment (kNm)	0.30	0.12	0.15	0.00	0.15	0.12	0.31
Stress (MPa)	730.0	526.6	556.9	3.8	556.9	526.7	741.1

## 5.2.2 RESULTS OF WIND LOAD CASE ANALYSES

For the analysis of the wind load case using frameDiagonal, a 100kN point load is applied at midspan. As can be seen in Figure 5.6 below, a load factor of 1.372 is achieved at the buckling point of the critical element, namely the central diagonal elements.



**Figure 5.6** : Output of frameDiagonal analysis

Although the GUI indicates that the central diagonal elements buckled first, it is important to note that all diagonal elements are carrying very similar axial loads. However, the bending moments are greatest in the central diagonals. Table 5.4 contains the axial loads, bending moments and subsequent stresses in each of the diagonal members of the truss at the point of buckling of the critical diagonal member, according to the results obtained from ANGELINE.

**Table 5.4** : Member forces in diagonal elements at buckling point of critical element

Diagonal Element No	1	2	3	4	5	6
<b>Axial Load (kN)</b>	95.33	96.10	93.98	93.98	96.13	95.33
<b>Bending Moment (kNm)</b>	0.02	0.07	0.41	0.41	0.07	0.02
<b>Stress (MPa)</b>	289.4	330.3	587.1	587.1	330.4	289.4

This means that a load of  $1.372 \times 100\text{kN}$  causes buckling of the critical elements. At the point at which buckling occurs, the axial load in the critical element is 93.98kN.

### 5.3 COMPARISON OF RESULTS

In order to determine the stress in the critical element due combined axial / flexural behaviour, the following equation is applied:

$$\sigma = \frac{F}{A} + \frac{My}{I} \quad (\text{Equation 5.1})$$

Where  $\sigma$  is the stress,  $F$  the axial force in the element,  $A$  the cross-sectional area of the element,  $M$  the bending moment in the element,  $y$  the greatest distance from the centroid to the furthest compression fiber of the section and  $I$  is the moment of inertia about the weak axis of the section.

**Table 5.5** : Comparison of results obtained from structural analyses

	Gravity Load Case		Wind Load Case	
	Prokon	ANGELINE	Prokon	ANGELINE
Load Applied to Achieve Failure	228.3 kN	225.6 kN	139.3 kN	137.2 kN
Critical Element (visual inspection)	1 <sup>st</sup> Vertical	1 <sup>st</sup> Vertical	3 <sup>rd</sup> Diagonal	3 <sup>rd</sup> Diagonal
Buckling Load of Critical Element	119.80 kN	112.59 kN	97.25 kN	93.98 kN
Bending Moment in Critical Element	5.89 kNm	0.30 kNm	0.73 kNm	0.41 kNm
Stress in Critical Element	6970.8 MPa	730.0 MPa	843.9 MPa	587.1 MPa

The results obtained from the Prokon and ANGELINE analyses are consistent, in terms of the load applied in order to achieve failure, as well as the axial load in the critical element at the point of buckling. The bending moments in the critical elements at the point of buckling, and hence the stress, differ greatly. However, this is mainly due to the fact that the bending moments are very sensitive to the buckling failure mode, as can be seen in Figures 5.7 and 5.8. Therefore a slight difference in the singular point located in the analyses performed in ANGELINE and Prokon will lead to a large difference in the bending moments.

Given the stresses in the above table, material failure precedes geometrical failure in both the gravity load case and the wind load case. It is necessary to determine the point at which this failure occurs, due to combined axial / flexural behaviour. Figures 5.7 and 5.8 below illustrate the anticipated behaviour of the critical elements and the following description applies to both figures.

The pink line indicates the axial load at which the element buckles. The yellow line indicates the bending moment at which the material yields, assuming a yield stress equal to 200MPa. The turquoise line indicates the bending moment at which the material yields, assuming a yield stress equal to 326

MPa. The blue line indicates the level of bending moment in the critical element, as the axial load in the element increases. The red dot indicates the point at which yielding occurs under combined axial / flexural loading, assuming a yield stress equal to 200MPa. The green dot indicates the point at which yielding occurs under a combined axial / flexural loading, assuming a yield stress equal to 326MPa.

Commercial grade steel, used for the web members of the truss, is guaranteed to have a minimum yield stress of 200MPa. However, it could be considerably higher. Tensile tests were performed on samples of the steel used to determine the true material properties. An average yield stress of 341MPa was achieved. For the purposes of the experiment the lowest 5 percentile of the distribution of the results was taken as the yield stress, namely 326MPa. Detailed results are presented in Section 6.4. Therefore the following figures include data for yield stresses of both 200MPa and 326MPa.

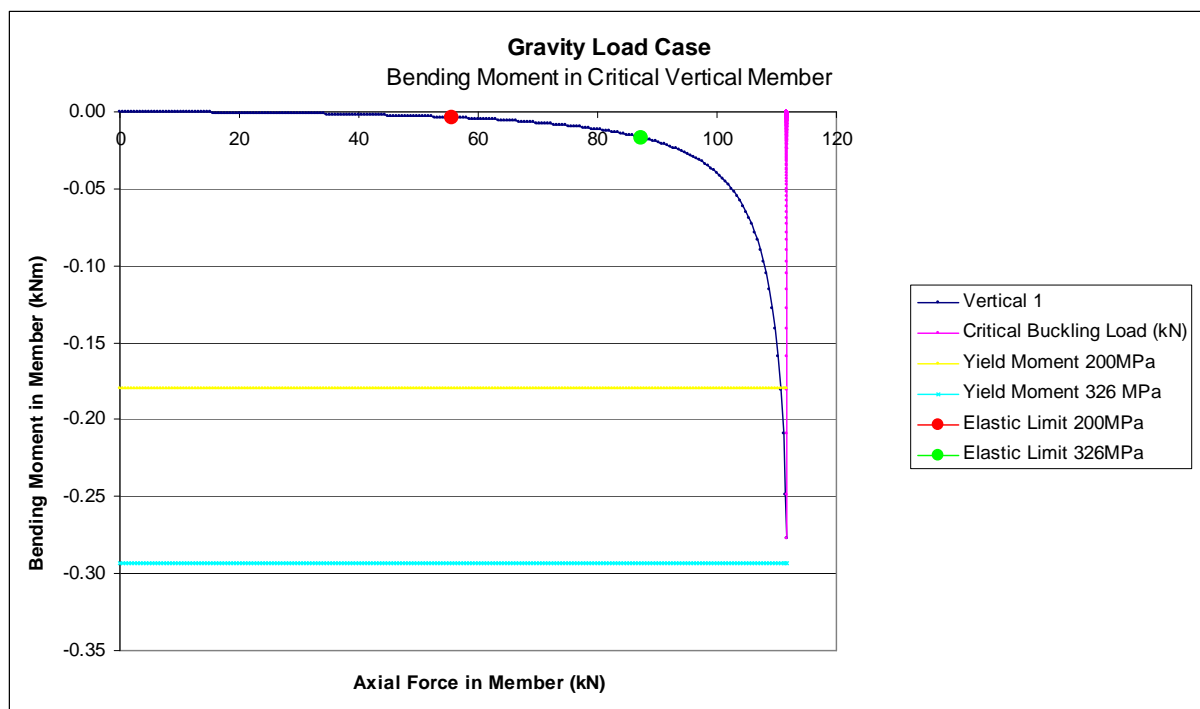


**Figure 5.7 :** Identification of material failure point for gravity load case

The green dot in Figure 5.7 indicates the most likely point of failure for the experiments. For the gravity load case, the axial load in the critical element at that point is 87.4kN, the bending moment is 0.017kNm and the applied load is 175.5kN.

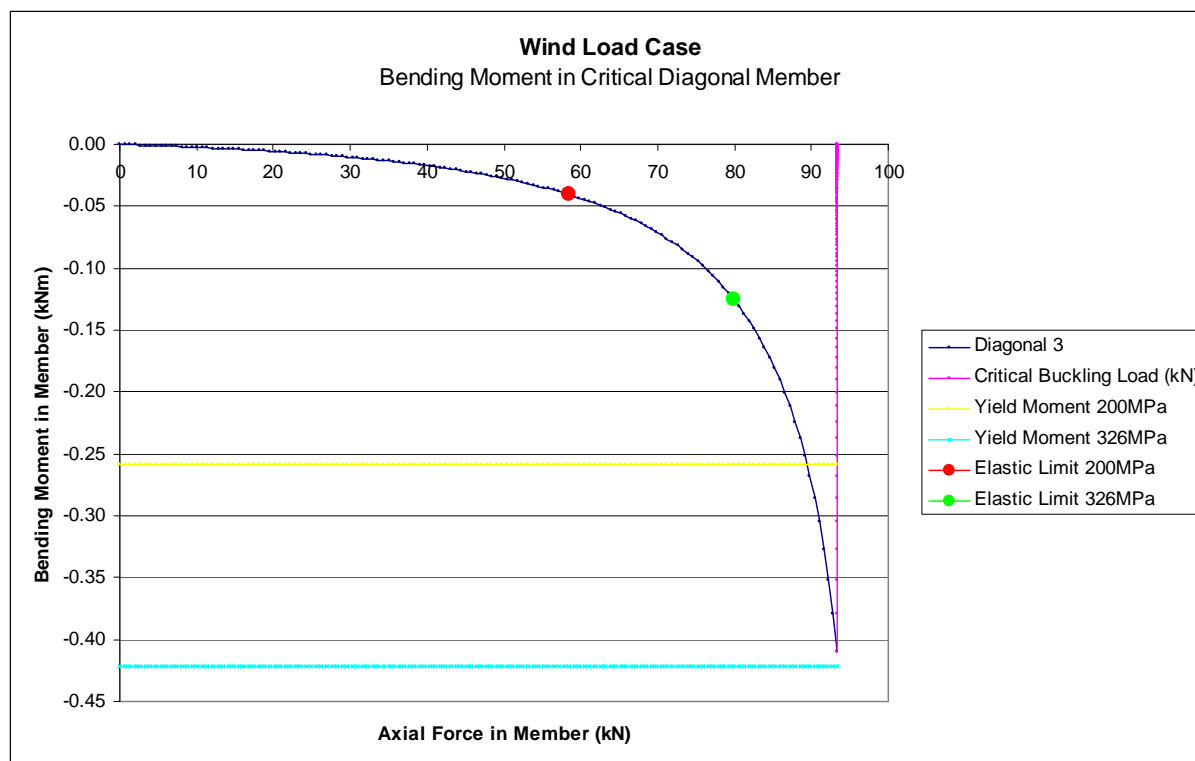


**Figure 5.8** : Identification of material failure point for wind load case

The green dot in Figure 5.8 once again indicates the most likely point of failure for the experiments. For the wind load case, the axial load in the critical element at that point is 80.0kN, the bending moment is 0.125kNm and the applied load is 116.7kN.

#### 5.4 INVESTIGATION INTO SIGNIFICANCE OF OWN WEIGHT ON BUCKLING LOAD

The premise on which the laboratory setup for the experiments and the specially developed classes of ANGELINE for the initial investigations were developed is that the own weight of the structure does not contribute significantly to the buckling load of the critical element. It is not presupposed that the own weight makes no contribution, but rather that this contribution is negligibly small.

This premise is necessary for a practical reason. In the laboratory setup of the experiment it is not possible to accurately measure the contribution of the own weight of the structure, with all measuring devices. Calibration of the strain gauges and load cells at the supports could be done before the truss is placed in position but calibration of the displacement transducers and the load application load cells can only be done once the truss is in position, at which point the own weight is automatically neglected.

Due to this practical restriction, two alternatives emerge to address the problem. The first would be to disregard the effect of the own weight altogether. Alternatively the own weight can be taken into

consideration by means of superposition, that the contribution to the buckling load of the critical element is determined separately and added to the buckling load achieved in the experiment.

Due to the fact that buckling is a nonlinear process, superposition cannot actually be applied. Despite the fact that this is not entirely correct, the second approach entails less of an error, than disregarding the effect of the own weight altogether.

An important factor to consider is the magnitude of the forces in the truss relative to the loads applied. Tables 5.6 and 5.7 below contain the axial forces for each element of a six bay truss, for both loading configurations, namely frameVertical and frameDiagonal, loaded purely with its own weight. The elements are numbered from left to right as they occur in the truss configuration.

**Table 5.6 :** Axial forces in elements due to own weight in gravity load case configuration

<b>Axial Load (kN)</b>	<b>1</b>	<b>2</b>	<b>3</b>	<b>4</b>	<b>5</b>	<b>6</b>	<b>7</b>
<b>Verticals</b>	<b>-1.001</b>	-0.705	-0.354	-0.139	-0.354	-0.705	<b>-1.001</b>
<b>Diagonals</b>	1.286	0.745	0.265	0.265	0.745	1.286	
<b>Upper Chord</b>	-0.902	-1.417	-1.593	-1.593	-1.417	-0.902	
<b>Lower Chord</b>	0.003	-0.902	1.418	1.418	0.902	0.003	

**Table 5.7 :** Axial forces in elements due to own weight in wind load case configuration

<b>Axial Load (kN)</b>	<b>1</b>	<b>2</b>	<b>3</b>	<b>4</b>	<b>5</b>	<b>6</b>	<b>7</b>
<b>Verticals</b>	0.095	0.549	0.284	0.134	0.284	0.549	0.095
<b>Diagonals</b>	-0.954	-0.566	<b>-0.194</b>	<b>-0.194</b>	-0.566	-0.954	
<b>Upper Chord</b>	-0.013	-0.687	-1.085	-1.085	-0.687	-0.013	
<b>Lower Chord</b>	0.683	1.082	1.217	1.217	1.082	0.683	

As can be seen in Tables 5.6 and 5.7 above, the own weight contributes approximately 1.0kN to the load in the critical compression elements for frameVertical and approximately 0.2kN for frameDiagonal. By comparison, for a vertical compression element with end connections assumed to be pinned the buckling load is approximately 29.0kN, i.e. the own weight contributes about 3.5% to the buckling load. For a vertical compression element with end connections assumed to be rigid the buckling load is approximately 116kN, i.e. the own weight contributes about 0.9% to the buckling load. The own weight contribution to the buckling load of the critical element in frameDiagonal is even less.

It is expected that the end connections are relatively rigid, and that the subsequent contribution by the own weight of the truss to the buckling load of the most critical element is about 0.9%. This is considered small enough to render the error, due to superposition of the experimental buckling load and the own weight load, negligible.

## 6. DESIGN, CONSTRUCTION AND EXECUTION OF EXPERIMENTS

### 6.1 DESIGN OF TRUSSES

As described in Chapter 4, the layout and dimensions of the truss to be designed for experimentation are influenced by a number of factors. Taking all of these factors into account, the following layouts and specifications, provided in Figures 6.1 and 6.2 and Tables 6.1 and 6.2, emerged as the optimum design for the two load cases.

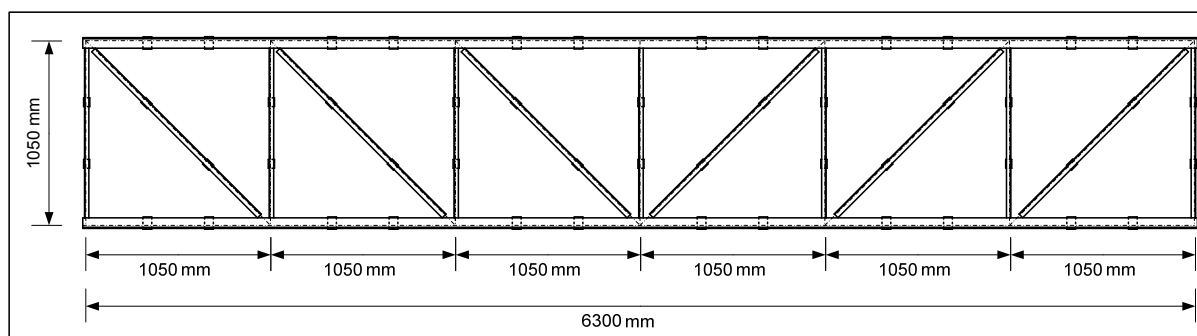


**Figure 6.1** : Truss layout for gravity load case as determined by frame Vertical analyses

**Table 6.1** : Truss dimensions and section sizes for gravity load case

<b>Number of Bays</b>	6
<b>Bay Size</b>	1050 mm x 1050 mm
<b>Length : centre-line to centre-line</b>	6300 mm
<b>Length : actual</b>	6334 mm
<b>Height : centre-line to centre-line</b>	1050 mm
<b>Height : actual</b>	1084 mm
<b>Top Chord</b>	60 x 60 x 6 double angles
<b>Bottom Chord</b>	60 x 60 x 6 double angles
<b>Vertical Elements</b>	25 x 25 x 3 double angles
<b>Diagonal Elements</b>	40 x 40 x 6 double angles
<b>Max Load Applied at Midspan</b>	225.6 kN

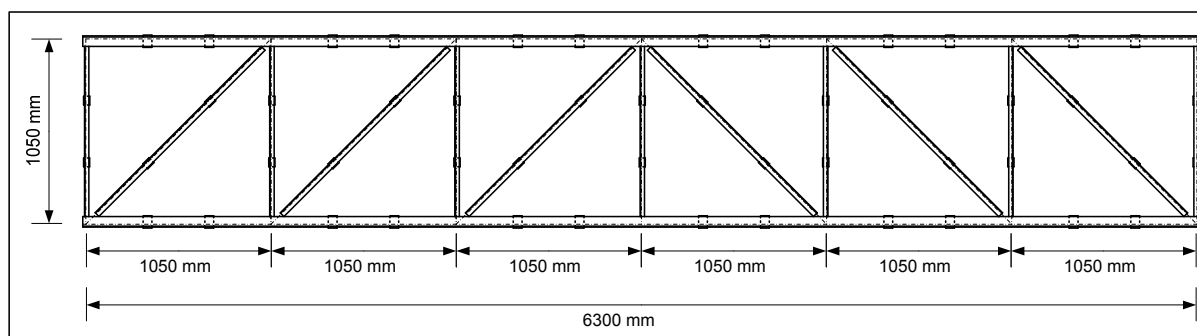


**Figure 6.2 :** Truss layout for wind load case as determined by frameDiagonal analyses

**Table 6.2 :** Truss dimensions and section sizes for wind load case:

<b>Number of Bays</b>	6
<b>Bay Size</b>	1050 mm x 1050 mm
<b>Length : centre-line to centre-line</b>	6300 mm
<b>Length : actual</b>	6344 mm
<b>Height : centre-line to centre-line</b>	1050 mm
<b>Height : actual</b>	1078 mm
<b>Top Chord</b>	50 x 50 x 5 double angles
<b>Bottom Chord</b>	50 x 50 x 5 double angles
<b>Vertical Elements</b>	40 x 40 x 6 double angles
<b>Diagonal Elements</b>	30 x 30 x 3 double angles
<b>Load Applied at Midspan</b>	137.2 kN

## 6.2 DESIGN OF CONNECTIONS

In practice two types of connections are employed, namely welded and bolted connections. However the decision was taken to restrict the experimentation to welded connections only. This was done for several reasons. Of the two connection types, welded connections are considerably more prevalent. For practical purposes, welded connections can be considered near rigid, whereas the rigidity of bolted connections is more difficult to define. In addition to this bolted connections may cause some slip during initial loading of the truss. Due to various constraints, concentrating on one connection type also allows more trusses to be constructed and therefore more experiments to be performed.

The connections are designed according to Clause 13.13 of SANS 10162-1:2005. All welds are fillet welds except those connecting the load application point to the bottom chord, which are full penetration welds. The weld leg length depends on the thickness of the section that is being connected and for all welds Afrox Vitamax welding rods with a 460MPa tensile capacity are used. For detailed connection drawings see Appendix C for the gravity load case drawings and Appendix D for the wind load case drawings.

### 6.3 DESIGN OF SUPPORTS

In order for the truss support conditions to be simply supported and behave as anticipated, the truss must be pin-supported at one end and roller-supported at the other. This is approximated with the use of Glacier pot supports, Teflon coated bearing supports, depicted in Figure 6.3. The Glacier at the roller-support end has an additional horizontal degree of freedom.

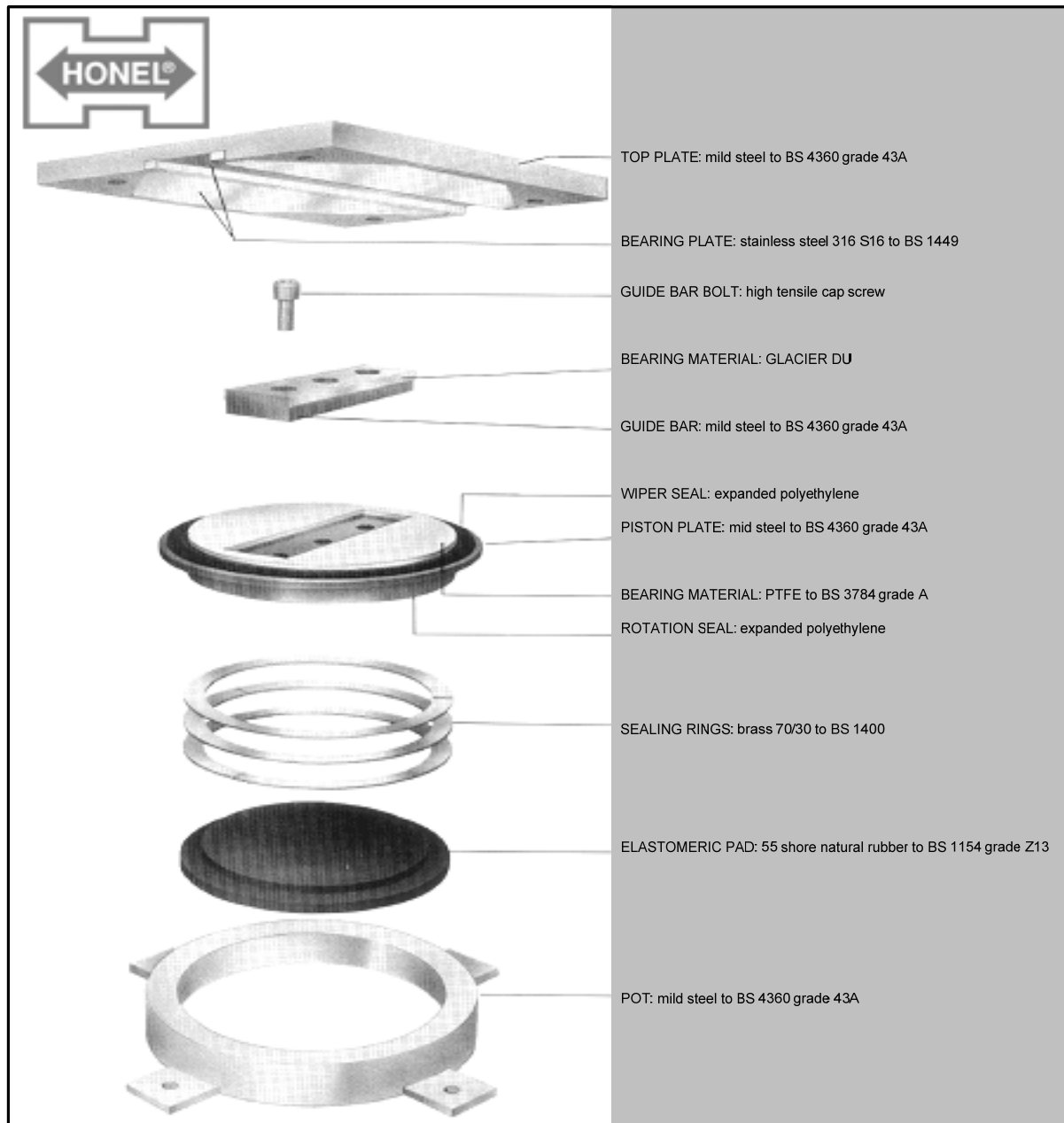


**Figure 6.3 :** Cross-section of Glacier pot supports

Figure 6.4 below depicts the Glacier pot supports installed beneath a truss test piece, as well as 20t load cells beneath the supports. The additional horizontal, in-plane degree of freedom for the roller support can be seen in the right photograph.

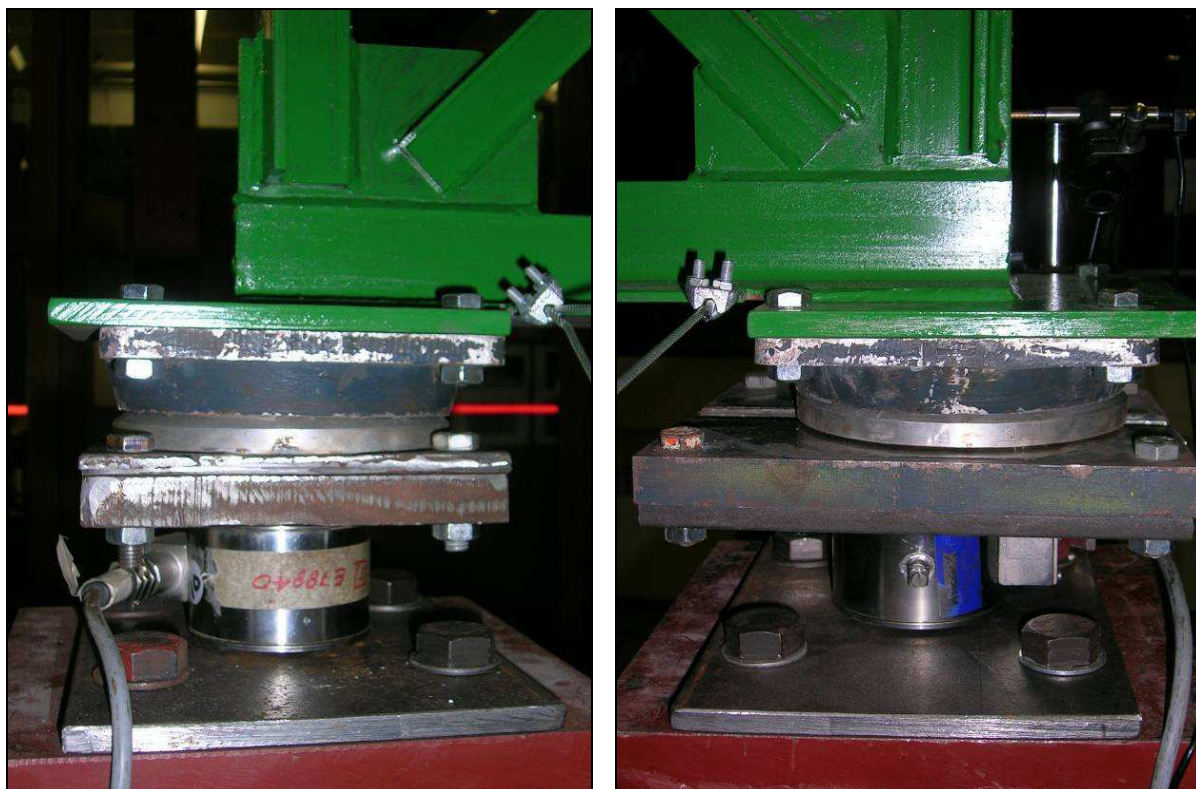


**Figure 6.4 :** Glacier pot support used to create pin support (left) and roller support (right)

The possibility of creating a truly pinned support was investigated. A steel rod passing through the web of the bottom chord at the point at which the centre-lines of all elements connected to that node intersect, at either end of the truss, would allow the truss to rotate freely about this point. However, the restricted geometry of the bottom chord and the required diameter of such a rod were not compatible.

## 6.4 DETERMINATION OF MATERIAL PROPERTIES

### 6.4.1 METHOD OF TESTING

In order to eliminate an additional source of error during the experiments, the material properties, specifically the yield and ultimate stresses as specified by the supplier, of the sections to be used, must be verified. This is done by means of tensile tests performed using the Zwick Z250 Universal Materials Testing Machine, as shown in Figure 6.5. For testing 15mm wide coupons are cut from the off cuts of the angle sections used to construct the trusses. An increasing load is applied to the sample until break point is achieved.

The material tests are restricted to the sections used as web elements, namely 25 x 25 x 3, 30 x 30 x 3 and 40 x 40 x 6 angles, all commercial grade steel. The existing multi-purpose beam/column testing apparatus restricts the bay size of the truss, which determines the web compression length. In order to achieve a sufficiently slender compression member, unusually small sections have to be selected, which are only manufactured using commercial grade steel.

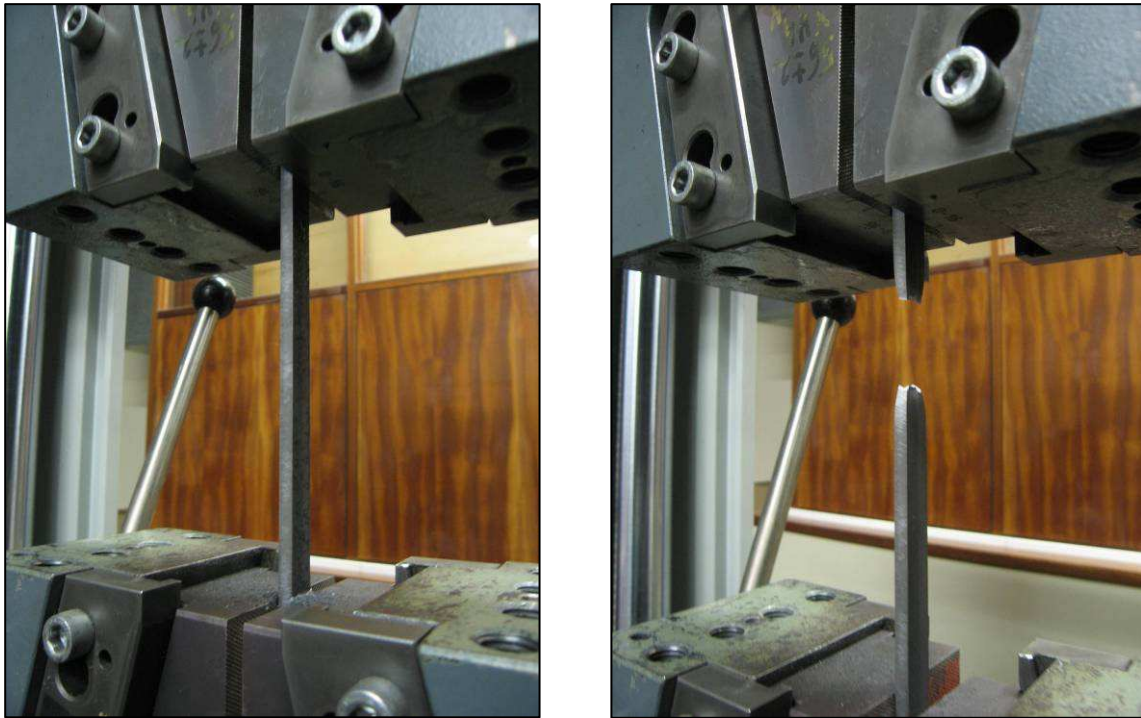


**Figure 6.5 :** Tensile test of coupon performed in Zwick Z250

The chord element sections are not tested for several reasons. The off cuts available are too short for testing in the Zwick, the chord elements are non-critical elements and the sections used for the chords, namely 50 x 50 x 5 and 60 x 60 x 6 angles, are produced using higher capacity steel with a yield stress of 350MPa and ultimate stress of 480MPa, as confirmed by the supplier.

**Table 6.3 :** Samples tested for material property verification

Angle Size	Number of	Strip Length	Strip Width	Expected $f_y$	Expected $f_u$
25 x 25 x 3	4	330mm	15mm	200MPa	365MPa
30 x 30 x 3	5	340mm	15mm	200MPa	365MPa
40 x 40 x 6	5	270mm	15mm	200MPa	365MPa

**Table 6.4 :** Summary of statistical data of yield stress

	$f_y$ (MPa)
<b>Minimum</b>	330.26
<b>Maximum</b>	358.05
<b>Mean</b>	341.14
<b>Standard Deviation</b>	8.964
<b>Variance</b>	80.347
<b>5 Percentile</b>	326.44

## 6.4.2 RESULTS OF MATERIAL TESTS

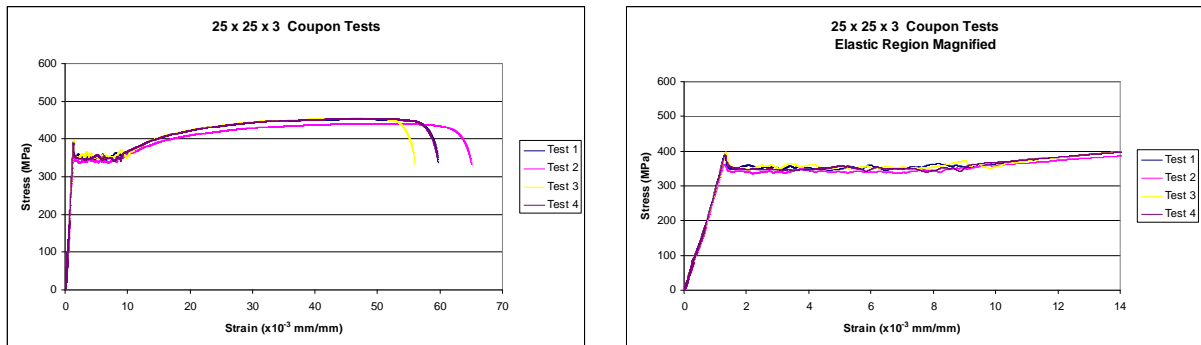


Figure 6.6 : Results of tensile tests of 25 x 25 x 3 angle coupons

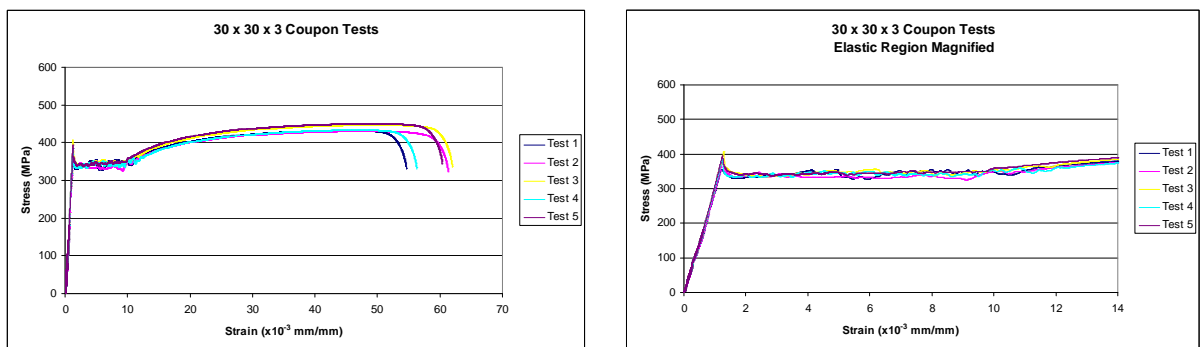


Figure 6.7 : Results of tensile tests of 30 x 30 x 3 angle coupons

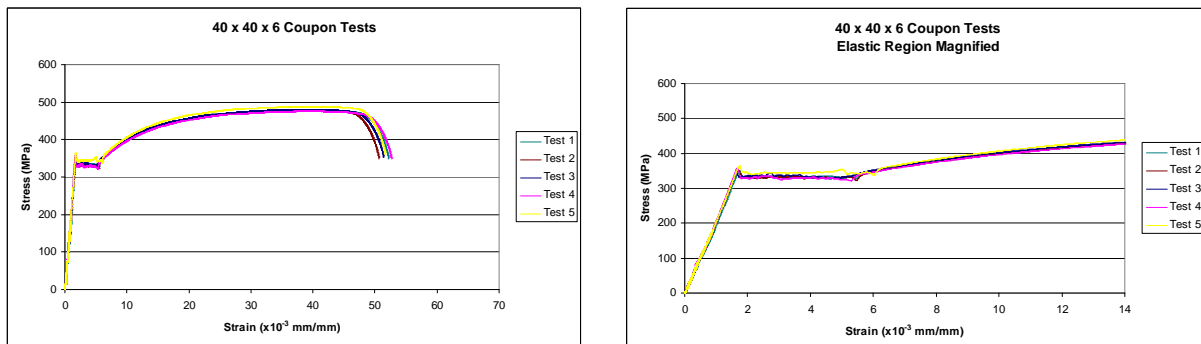


Figure 6.8 : Results of tensile tests of 40 x 40 x 6 angle coupons

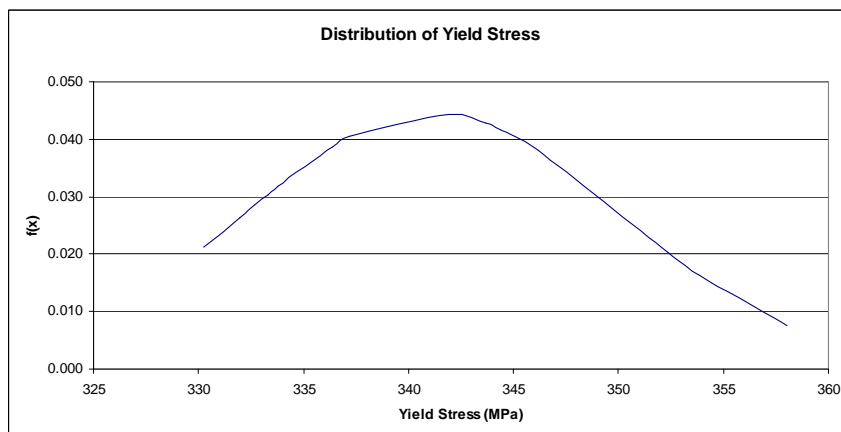
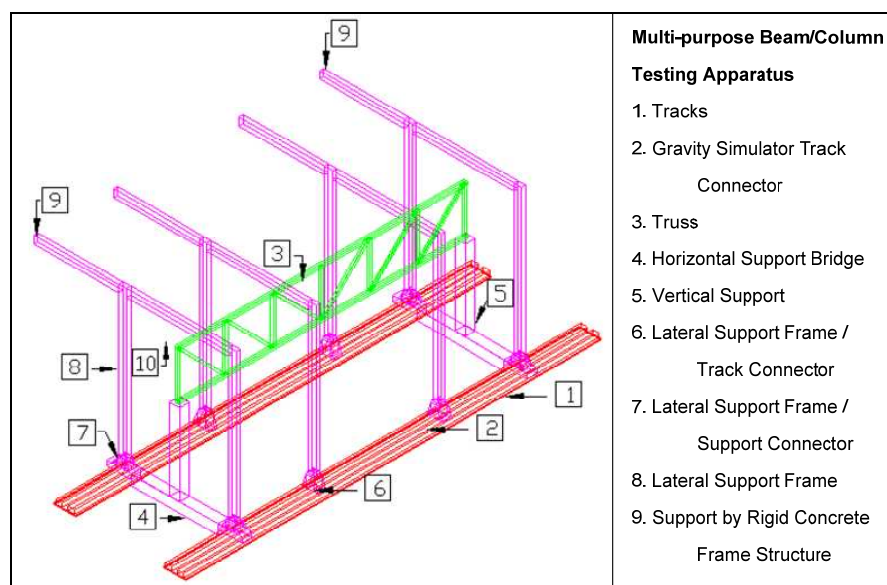


Figure 6.9 : Distribution of yield stresses achieved in material tests

## 6.5 SETUP OF TEST

### 6.5.1 MULTI-PURPOSE BEAM/COLUMN TESTING APPARATUS

As mentioned in Chapter 4, the truss is setup within the multi-purpose beam/column testing apparatus, developed by Colin Koen in his M.Eng thesis, "The Development of a Multi-Purpose Beam/Column Testing Apparatus" <sup>[17]</sup>.



**Figure 6.10 :** Setup of test frame within multi-purpose beam/column testing apparatus



**Figure 6.11 :** Setup of test frame within multi-purpose beam/column testing apparatus

As depicted in Figure 6.10, the truss is supported vertically on two stub columns. Lateral support of the truss is supplied at every node of the compression chord and at the extremes of the tension chord, by means of 5mm steel cables, to ensure that the truss behaviour is truly restricted to two-dimensional behaviour. Lateral support is provided to the multi-purpose testing apparatus by means of beams connected to the laboratory structure.

### 6.5.2 LOAD APPLICATION POINT

The load applied to the test frames is restricted to a single point load at midspan, due to practical restrictions in the laboratory. As discussed in Chapter 4, this is an acceptable approximation of a uniformly distributed load, resulting in negligible change in buckling load of the critical element.

The requirements of the load application point are as follows. The load applied by means of a 60t Enerpac hydraulic jack must be transferred to the bottom chord at midspan. The frame used to do this must accommodate the 60t hydraulic actuator, as well as a 20t or 50t load cell. All connections and supporting structures must be able to withstand a tensile force in excess of 225kN.

The force is transferred by means of a 30mm tensile rod. The rod is attached to the bottom chord, through an extended and reinforced gusset plate, by means of a fork and steel pin. The tensile rod feeds through both the hydraulic actuator and load cell, and is fastened with a washer and nut. The rod and pin are both made of 800MPa tensile strength steel.

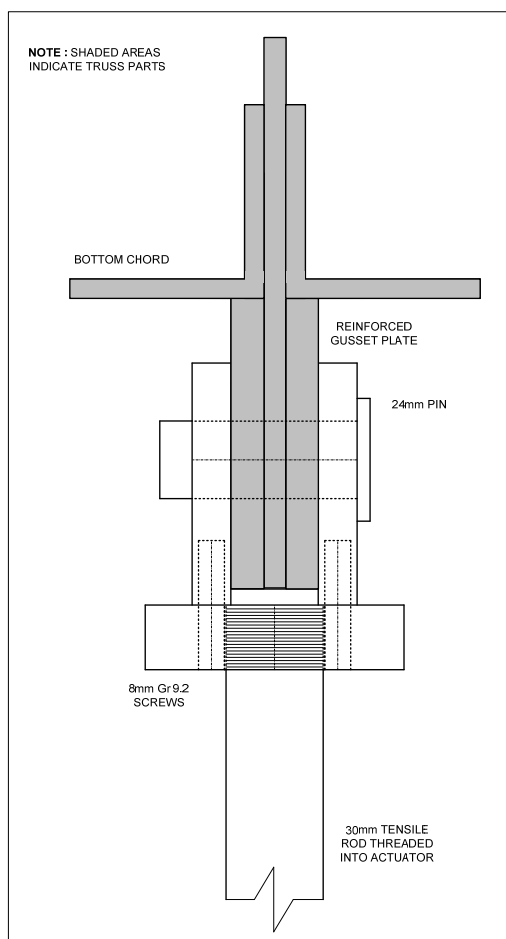


**Figure 6.12** : Fork and steel pin used to transfer load from tensile rod to bottom chord

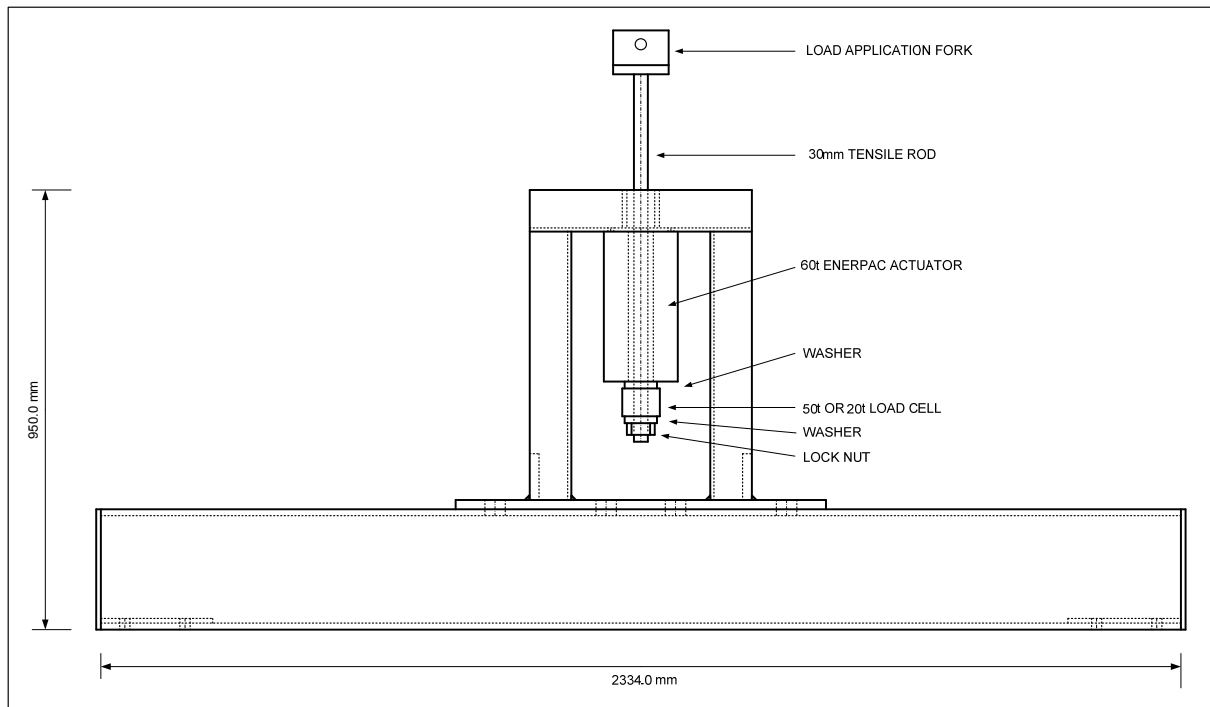


**Figure 6.13 :** Frame designed for load application and to support actuator and load cell



**Figure 6.14 :** Frame designed for load application and to support actuator and load cell

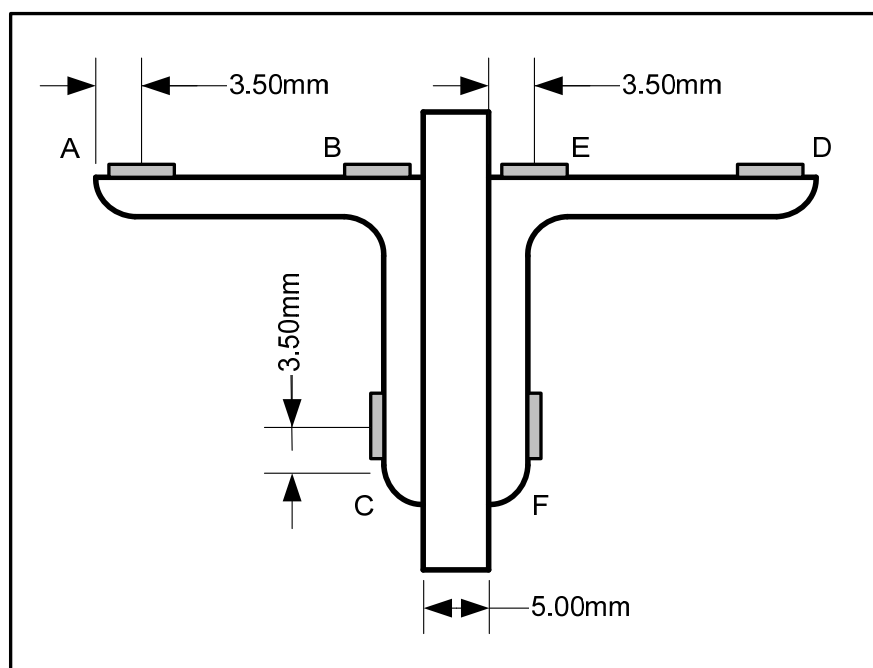
Figures 6.13 and 6.14 depict the frame which was designed and built specifically for the tests performed, for the application of the point load at midspan, as well as to support the 60t Enerpac hydraulic actuator and load cell.

### 6.5.3 MEASURING PROGRAM

Capturing and recording the necessary measurement data is critical to the success of the experiments performed. All analogue measurements taken are converted to digital data by means of Spider8 converters and the data is recorded using Catman software. Once the data is recorded it is processed further in Microsoft Excel.

The measurements taken are as follows. The load applied as well as the vertical support reactions are monitored and recorded by means of Hottinger Baldwin Messtechnik (HBM) load cells. Displacements at critical points are measured by means of a range of spring loaded linearly varying displacement transducers (LVDT's), also manufactured by HBM. The LVDT's are attached to an independent frame, not affected by the load application. The horizontal in-plane deflection of the truss (Channel 5, Table 6.5) is measured at the pinned support, solely for the purpose of monitoring the true behaviour of the Glacier pot.

The buckling point of the critical element is captured by monitoring and recording the strain at mid-length of the critical elements. A sudden change in the direction or magnitude of strain experienced by the extreme fibres of the section indicates the buckling point. Figure 6.15 below indicates the placement of the 10mm strain gauges, manufactured by Kyowa, on the double angle section.



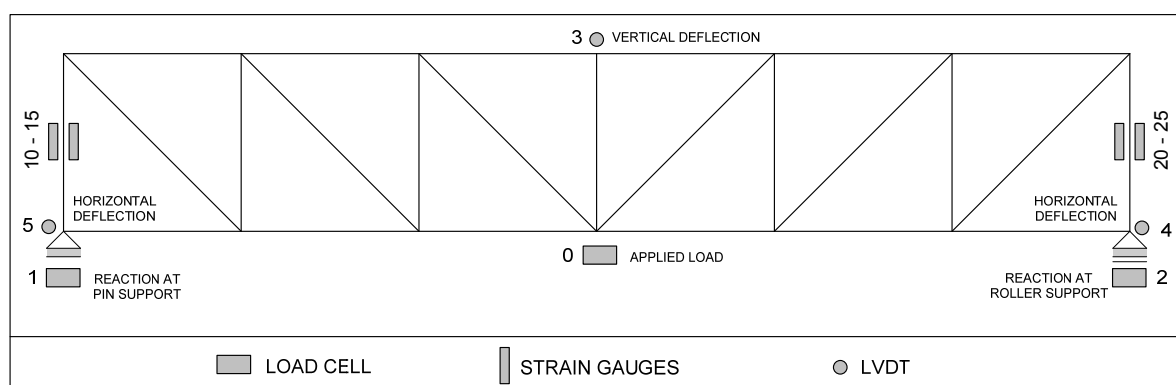
**Figure 6.15** : Positioning of strain gauges at mid-length of critical elements

Table 6.5 which follows provides a summary of the measurements taken, including the channel number to which each variable is associated for the Spider8 converter, the position of the measuring instrument, the units of measurement as well as a short description of the instrument.

**Table 6.5** : Summary of measuring program

Spider#	Channel	Device	Abbreviation	Variable	Location	Units	Description
1	0	Load Cell	ALC	applied load	load application	kN	50t Tension
1	1	Load Cell	PLC	support reaction	pin support	kN	20t compression
1	2	Load Cell	RLC	support reaction	roller support	kN	20t compression
1	3	LVDT	MV	vertical in-plane deflection	midspan top chord	mm	W20tk (spring), 40mm range
1	4	LVDT	RBOT	horizontal in-plane deflection	roller support bottom chord	mm	W110 (spring), 10mm range
1	5	LVDT	RPIN	horizontal in-plane deflection	pin support bottom chord	mm	W110 (spring), 10mm range
1	6	SG	STEMP	strain temperature	temperature compensation	$\mu\text{m}/\mu\text{m}$	-12mV to 12mV (plastic range)
2	10	SG	SAP	strain AP	midlength of first critical element	$\mu\text{m}/\mu\text{m}$	-12mV to 12mV (plastic range)
2	11	SG	SBP	strain BP	midlength of first critical element	$\mu\text{m}/\mu\text{m}$	-12mV to 12mV (plastic range)
2	12	SG	SCP	strain CP	midlength of first critical element	$\mu\text{m}/\mu\text{m}$	-12mV to 12mV (plastic range)
2	13	SG	SDP	strain DP	midlength of first critical element	$\mu\text{m}/\mu\text{m}$	-12mV to 12mV (plastic range)
2	14	SG	SEP	strain EP	midlength of first critical element	$\mu\text{m}/\mu\text{m}$	-12mV to 12mV (plastic range)
2	15	SG	SFP	strain FP	midlength of first critical element	$\mu\text{m}/\mu\text{m}$	-12mV to 12mV (plastic range)
3	20	SG	SAR	strain AR	midlength of last critical element	$\mu\text{m}/\mu\text{m}$	-12mV to 12mV (plastic range)
3	21	SG	SBR	strain BR	midlength of last critical element	$\mu\text{m}/\mu\text{m}$	-12mV to 12mV (plastic range)
3	22	SG	SCR	strain CR	midlength of last critical element	$\mu\text{m}/\mu\text{m}$	-12mV to 12mV (plastic range)
3	23	SG	SDR	strain DR	midlength of last critical element	$\mu\text{m}/\mu\text{m}$	-12mV to 12mV (plastic range)
3	24	SG	SER	strain ER	midlength of last critical element	$\mu\text{m}/\mu\text{m}$	-12mV to 12mV (plastic range)
3	25	SG	SFR	strain FR	midlength of last critical element	$\mu\text{m}/\mu\text{m}$	-12mV to 12mV (plastic range)

Figure 6.16, in conjunction with the Table 6.5 above, indicates the location of each measuring instrument. The figure indicates the positioning for the gravity load case tests. However, the same measuring configuration is used for the wind load case tests. The only difference is in the load cell used at the point of load application. The wind load case tests only require an applied force of 137.0kN. A 20t load cell is therefore sufficient. The gravity load case tests require an applied load of 225.0kN. Therefore a 50t load cell is required. The 50t load cell is not used for the wind load case test as this would compromise the sensitivity of the measurements taken.

**Figure 6.16** : Positioning of measuring devices for the gravity load case tests

## 6.6 TEST PROCEDURE

The test frame is secured in place in the multipurpose beam/column testing apparatus, all measuring devices are connected and set to taken an initial reading of zero, in order to exclude the effect of the own weight on the readings. An initial load is applied to the truss, which is approximately the serviceability load for the truss. The serviceability load and design load are determined according to SANS 10162-1:2005. See Appendix B for the determination of the design load of the critical section. The design load, i.e. the code determined capacity of the truss, is considerably lower than the load required to cause ultimate failure of the truss. Once the serviceability load is reached, the total load is removed. Finally a load is applied at a constant rate until failure occurs.

The serviceability load is applied for several reasons. It ensures that any slip present in the connections of the truss is removed. This would be of far greater importance in a truss with bolted connections than with welded connections, as is the case, but it is important to avoid all errors wherever possible. It allows for a comparison between strains and displacements measured at the design load, and those measured at the buckling load.

**Table 6.6** : Expected values of measurements during testing of gravity load case

	<b>Force in Member</b>	<b>Applied Force</b>	<b>Bending Moment in Member</b>	<b>Midspan Vertical Deflection</b>
	<b>kN</b>	<b>kN</b>	<b>kNm</b>	<b>mm</b>
<b>Serviceability Load</b>	12.50	25.51	0.0004	2.2
<b>Design Load</b>	22.3	45.13	0.0008	4.0
<b>200 MPa</b>	55.67	111.80	0.004	9.9
<b>325 MPa</b>	87.39	<b>175.54</b>	0.017	15.5
<b>Ultimate Buckling</b>	111.60	224.98	0.277	19.9

The expected values of the measurements taken during testing of the gravity load case, presented in Table 6.6, are obtained by the same means as Figure 6.17. The development of Figure 6.17 was discussed in detail in Section 5.3.

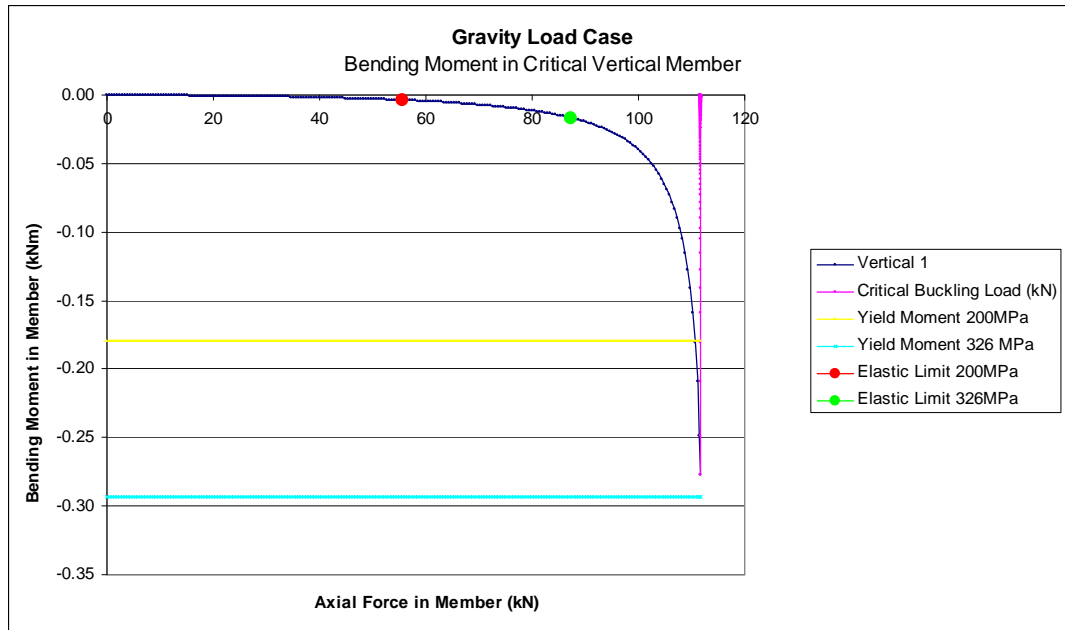


Figure 6.17 : Expected behaviour during testing of gravity load case

Table 6.7 : Expected values of measurements during testing of wind load case

	Force in Member kN	Applied Force kN	Bending Moment in Member kNm	Midspan Vertical Deflection mm
<b>Initial Load</b>	11.90	16.69	0.003	2.0
<b>Design Load</b>	20.64	30.42	0.006	3.7
<b>200 MPa</b>	58.50	85.32	0.041	10.3
<b>325 MPa</b>	79.96	<b>116.66</b>	0.125	14.1
<b>Ultimate Buckling</b>	93.29	137.04	0.410	16.7

The expected values of the measurements taken during testing of the gravity load case, presented in Table 6.7, are obtained by the same means as Figure 6.18. The development of Figure 6.18 was discussed in detail in Section 5.3.

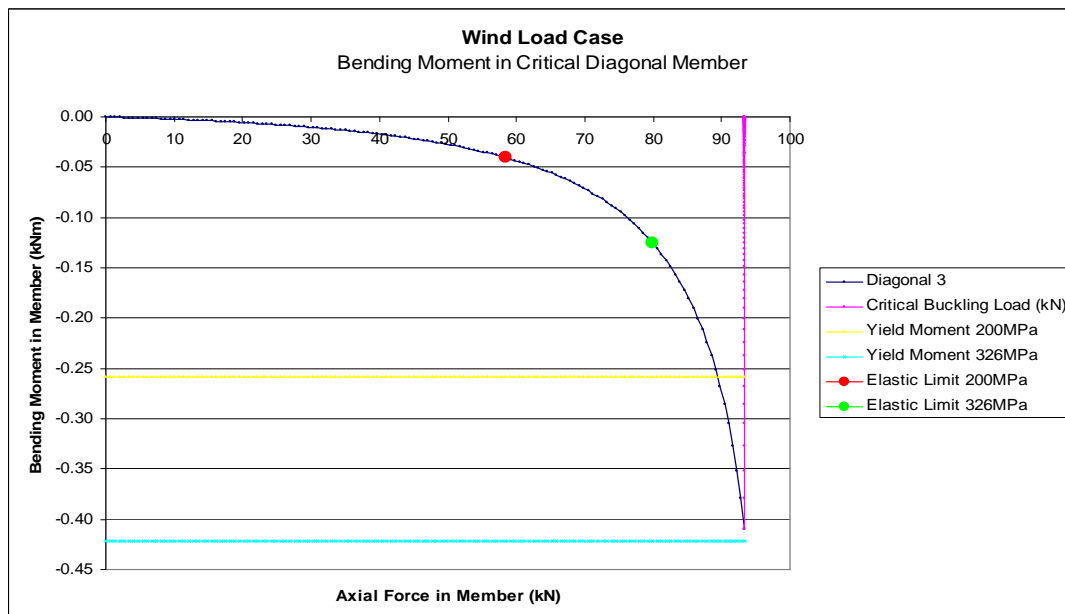


Figure 6.18 : Expected behaviour during testing of wind load case

## 6.7 RESULTS OF WIND LOAD CASE TESTS

The following results are presented in the chronological order of the execution of the tests. The green truss was tested first, followed by the yellow truss and finally the orange. A summary of the three test results is given. Greater details of the results are presented in Appendix F. The results of the wind load case are presented before those of the gravity load case as these were the first set of tests to be performed in the laboratory.

It should be noted that all references to either stress or strain followed by any letter A to E are references to the position of the strain gauges A to E used to determine the stress or strain in the critical element, as illustrated in Figure 6.15.

### 6.7.1 MODE OF FAILURE

The dominant mode of failure of the wind load case tests was out-of-plane buckling of a diagonal compression member, at an axial load approaching the member's Euler buckling load. Out-of-plane buckling implies that the members buckled about their stronger axis, an unanticipated failure mode. It was expected that the members would buckle in-plane, i.e. about their weaker axis. However, it is due to the stiffness of the connections that out-of-plane buckling became the dominant failure mode.



**Figure 6.19:** Out-of-plane buckling mode of failed diagonal compression members

The connections used are typical of a welded truss in practice, as shown in Figure 6.20. The gusset plates at either ends of the member are orientated so that the stronger axes of the gusset plates coincide with the weaker axis of the member. Hence the effective length of the member about the weak axis is reduced due to the stiffness of the end connections. Subsequently the weaker axes of the gusset plates coincided with the stronger axis of the member, allowing for strong axis buckling of the member.

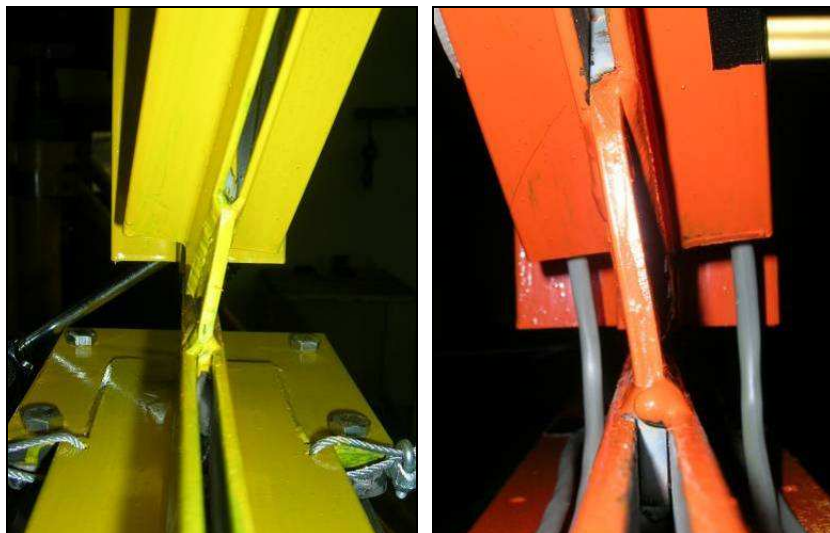


**Figure 6.20** : Post-buckling condition of gusset plates supporting failed diagonal members

Figure 6.21 illustrates the failed compression members of each of the three tests performed. As can be seen, each test resulted in a different diagonal member failing, whereas all structural analyses indicated that the central, i.e. 3<sup>rd</sup> or 4<sup>th</sup> diagonal members would be critical. This is ascribed to a combination of factors. Each of the diagonal members carries the same axial load. The in-plane buckling mode, and hence in-plane bending moments, proved to be non-critical. Therefore the greater in-plane bending moments in the 3<sup>rd</sup> and 4<sup>th</sup> diagonal members which were initially thought to be the catalysts in causing these members to be the critical ones, did not come into play. Therefore the variability in material and geometric tolerances of the sections play a large role in determining which member is the critical one.

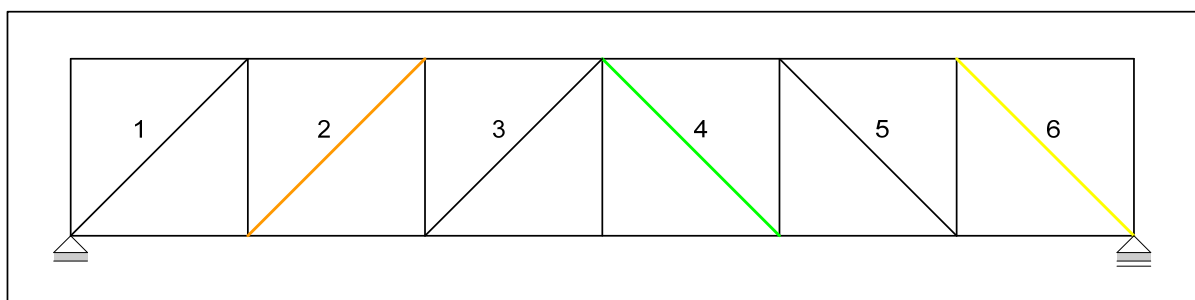


**Figure 6.21** : Comparison of location of failed diagonal compression members

### 6.7.2 STRAIN GAUGE CONFIGURATION

The first test performed, the green test, failed at the 4<sup>th</sup> diagonal member thereby reinforcing the expectation of failure of one of the central diagonals. It was therefore not considered necessary to alter the strain gauge configuration for the next test.

At the time all twelve strain gauges were concentrated on the 3<sup>rd</sup> and 4<sup>th</sup> diagonal members, with six strain gauges placed on each member in order to measure the extreme stresses expected in in-plane buckling, illustrated in Figure 6.15. However, after the yellow test failed at the 6<sup>th</sup> diagonal member it was considered pertinent to revise the strain gauge configuration.

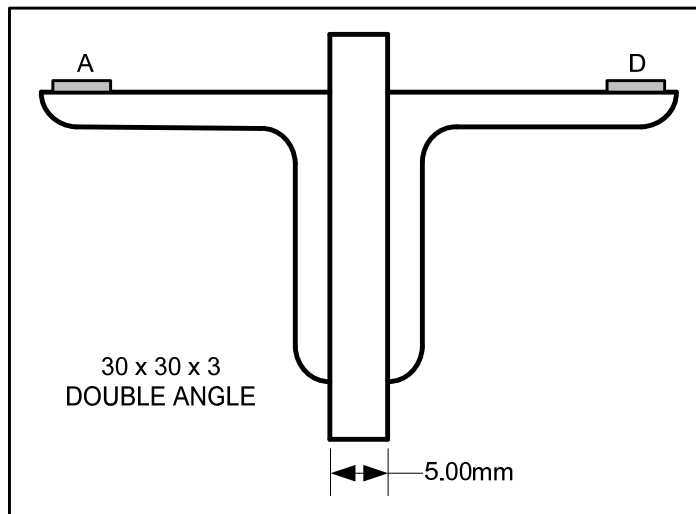


**Figure 6.22** : Revised strain gauge configuration

As the dominant failure mode was out-of-plane buckling, two strain gauges were sufficient to measure the stresses at the extremes of the section. Therefore the twelve strain gauges were redistributed to two strain gauges on each diagonal compression member, in order to monitor the strains in every diagonal. The revised strain gauge configuration is illustrated in Figure 6.22. This decision was ratified by the results of the orange test, in which a diagonal in yet another location failed.

### 6.7.3 RESULTS OF PRINCIPLE MEASUREMENTS

Despite the location of the critical member varying, all three critical diagonal compression members failed in the same mode, namely out-of-plane buckling, about the weak axis of the gusset plates at the end connections of the members. All three members failed at an applied load between 102.9kN and 119.1kN, well above the design load of the truss of 30.4kN. All three members failed at a vertical deflection, measured at midspan of the top chord of between 12.7mm and 14.1mm.

**Table 6.8** : Comparison of principle measurement results of wind load case tests

30 x 30 x 3 Double Angle	Applied Force			Axial Force in Failed Member			Midspan Vertical Deflection		
	kN			kN			mm		
	Green	Yellow	Orange	Green	Yellow	Orange	Green	Yellow	Orange
<b>Failed Diagonal Member</b>	4th	6th	2nd	4th	6th	2nd	4th	6th	2nd
<b>Initial Load</b>	16.91	16.57	16.75	11.60	11.50	11.71	2.02	2.02	2.20
<b>Design Load</b>	27.62	27.48	27.59	18.95	19.07	19.29	3.26	3.30	3.51
<b>200 MPa</b>	85.29	85.30	85.49	58.51	59.20	59.76	9.86	9.96	10.42
<b>Failure</b>	115.72	119.13	102.85	<b>79.15</b>	<b>82.68</b>	<b>71.89</b>	13.56	14.05	12.71

The axial force in the failed member could not be measured directly from the strain gauges applied to it, because it is not possible to ascertain to which degree the strain in the member is due to axial load or due to bending. Therefore the detailed results obtained from the ANGELINE analyses were used to obtain a ratio between the load applied and the axial load in the critical member, and hence the applied load was used to determine the axial load in the critical member. This approach is considered justifiable given that the displacement/load relationship of the tests compare very well with those obtained from ANGELINE, as illustrated in Figure 7.5.

What is most important to note is that the calculated axial load in the critical members, at the onset of buckling lay between 71.9kN and 82.7kN, again well above the design load of such a section of 20.6kN. As discussed in Section 5.4 the own weight of the truss was not taken into consideration for the test purposes and it was determined that superposition of the own weight would be satisfactory. If this is done, the buckling axial loads increase to 79.3kN for the green test, 83.6kN for the yellow test and 72.5kN for the orange test.

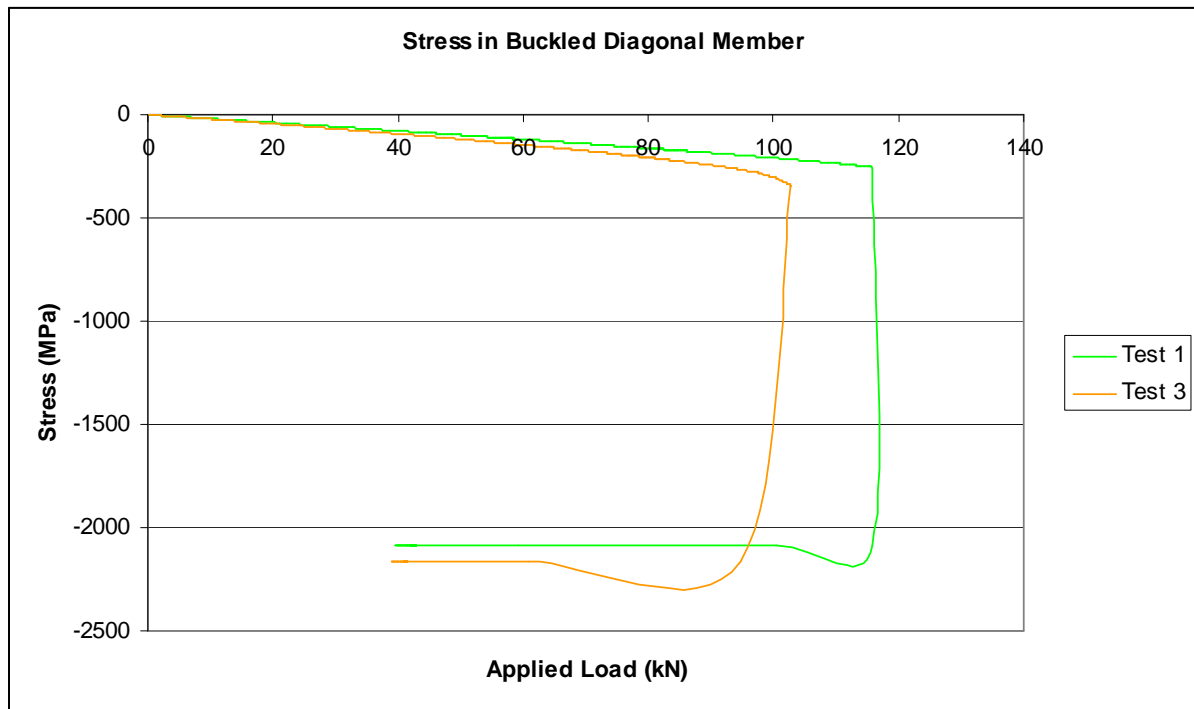


**Figure 6.23** : Stresses in buckled diagonal compression members

Figures 6.23 and 6.24 demonstrate the stresses in the buckled members and the vertical deflection of the truss respectively, for each of the tests performed. Figure 6.23 does not contain the results for the second test, in which the 6<sup>th</sup> diagonal buckled, as failure of the central diagonals was still the anticipated failure mode at this point in time, and no strain gauges had been placed on the other diagonal members of the truss.

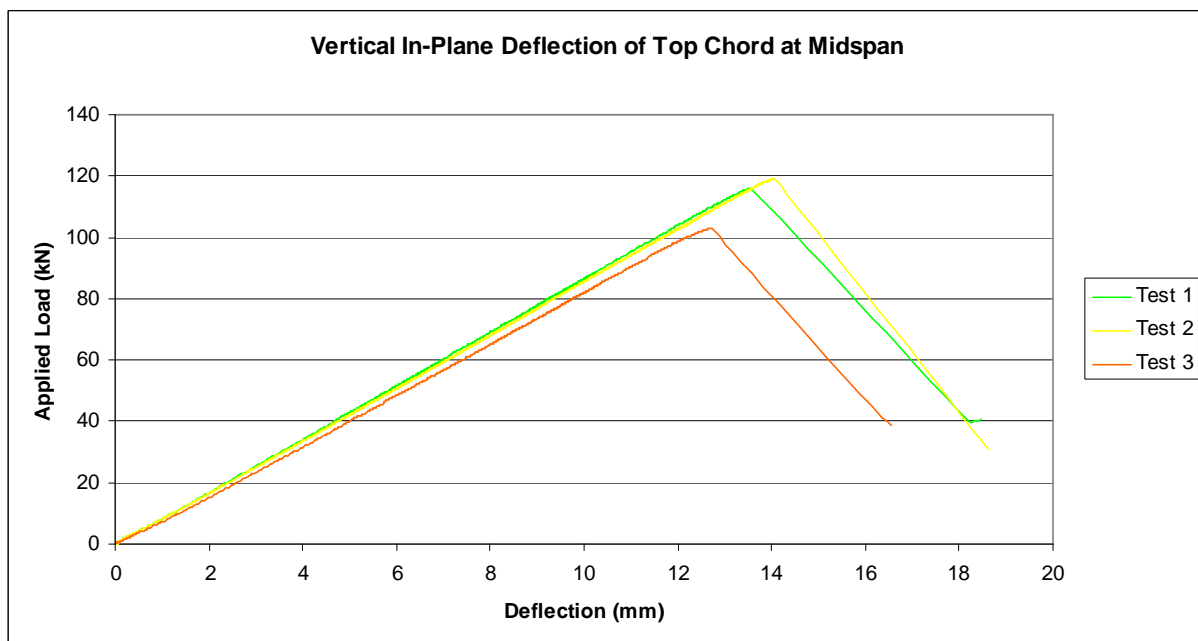


**Figure 6.24** : Comparison of vertical deflection of top chord at midspan

## 6.8 RESULTS OF GRAVITY LOAD CASE TESTS

The following results are presented in the chronological order of the execution of the tests. Again the green truss was tested first, followed by the yellow truss and finally the orange. A summary of the three test results is given. Greater details of the results are given in Appendix E.

### 6.8.1 STRAIN GAUGE CONFIGURATION

As was the case for the compression members of the wind load case, the vertical compression members of the gravity load case also carry very similar axial loads. The structural analyses indicated that the critical members would be the 1<sup>st</sup> or 7<sup>th</sup> vertical compression member, mainly due to the greater bending moments in these members. However, due to the experience gained from the execution of the wind load case tests, these in-plane bending moments do not contribute to the out-of-plane failure mode of the buckled members. Therefore the strain gauge configuration for the gravity load case was adapted, to monitor the strains in each of the potentially critical vertical compression members.

It was shown that two strain gauges are sufficient to measure the extreme stresses of out-of-plane buckling. Therefore two strain gauges, as illustrated in Figure 6.25, were placed on the vertical compression members, numbers 1 to 3 and 5 to 7. Vertical member number 4, i.e. the central vertical member, carries a negligibly small axial load.

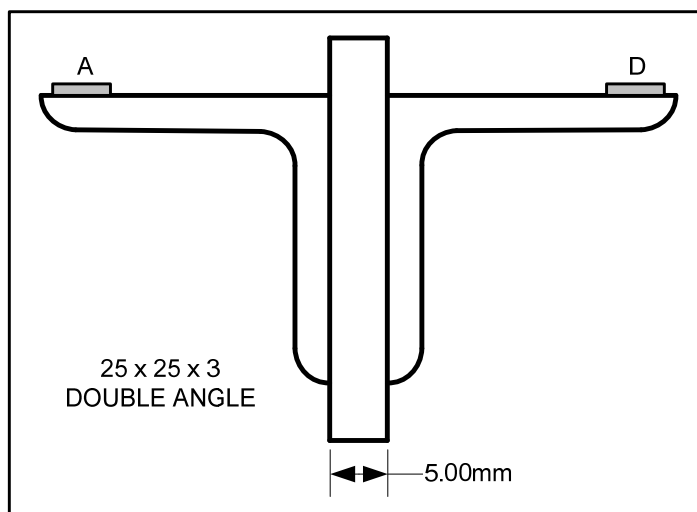


**Figure 6.25** : Strain gauge configuration for vertical members

### 6.8.2 MODE OF FAILURE

The dominant mode of failure of the gravity load case tests was out-of-plane buckling of a vertical compression member, as was the case for the wind load case. Weak axis bending of the gusset plates at the end connections of the compression members caused strong axis buckling of the vertical compression members, at an axial load approaching the Euler buckling load of the member.



**Figure 6.26 :** Out-of-plane buckling mode of failed vertical compression members

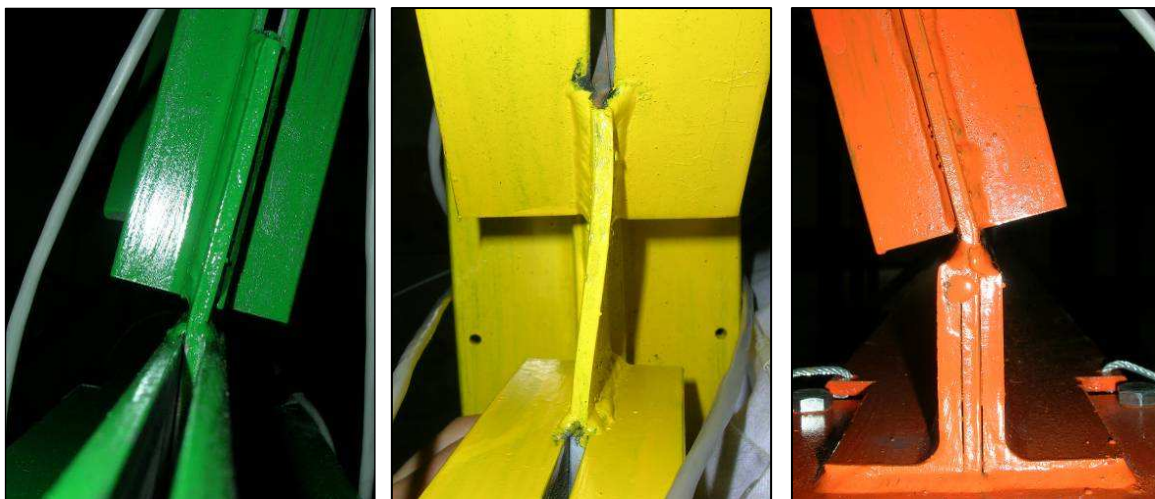


**Figure 6.27 :** Post-buckling condition of gusset plates supporting failed vertical members

Figure 6.28 identifies the failed compression members of each of the three tests performed. As was the case for the wind load case, the location of the failed member was not consistent between the three tests. The first two tests both failed at the 5<sup>th</sup> vertical compression member at very similar applied loads, 142kN and 140kN respectively. The final test failed at the 7<sup>th</sup> vertical compression member at a significantly lower applied load of 131kN.

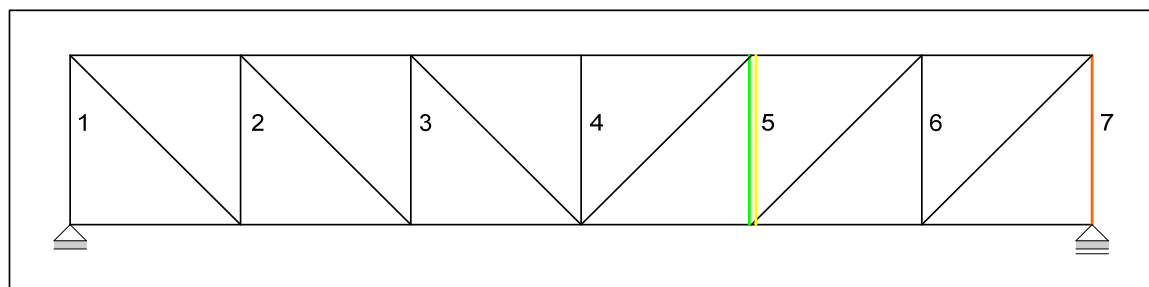


**Figure 6.28** : Comparison of location of failed vertical compression members

Despite all of the vertical compression members, except the central one, carrying a very similar axial load, it was still initially anticipated that the 1<sup>st</sup> or 7<sup>th</sup> vertical members would be the critical ones. This is due to the fact that the outer vertical members are supported the least by the chords, because the chords terminate at their positions, and the gusset plates supporting the outer verticals are also the smallest, therefore providing the least support against out-of-plane buckling. It is therefore only the third test which behaved as anticipated. These results can only lead to the conclusion that material or geometric initial imperfections of the members play a much larger role in determining the critical member than initially anticipated.

**Table 6.9** : Comparison of principle measurement results of gravity load case tests

25 x 25 x 3 Double Angle	Applied Force			Axial Force in Failed Member			Midspan Vertical Deflection		
	kN			kN			mm		
	Green	Yellow	Orange	Green	Yellow	Orange	Green	Yellow	Orange
<b>Failed Vertical Member</b>	5 <sup>th</sup>	5 <sup>th</sup>	7 <sup>th</sup>	5 <sup>th</sup>	5 <sup>th</sup>	7 <sup>th</sup>	5 <sup>th</sup>	5 <sup>th</sup>	7 <sup>th</sup>
<b>Initial Load</b>	25.58	25.56	25.54	12.53	12.52	12.72	2.35	2.46	2.57
<b>Design Load</b>	40.14	40.36	40.21	19.67	19.77	20.02	3.58	3.78	3.85
<b>200 MPa</b>	111.79	111.92	111.73	54.78	54.84	55.64	9.66	9.95	10.05
<b>Failure</b>	141.93	139.95	131.17	<b>69.54</b>	<b>68.58</b>	<b>65.32</b>	12.45	12.61	11.87

As discussed for the results of the wind load case the axial force in the failed member could not be measured directly from the two strain gauges applied to it, because it is not possible to ascertain to which degree the strain in the member is due to axial load or due to bending. Again the detailed results obtained from the ANGELINE analyses were used to obtain a ratio between the load applied and the axial load in the critical member, and hence the applied load was used to determine the axial load in the critical member. This approach is considered justifiable given that the displacement/load relationship of the tests compare well with those obtained from ANGELINE, as illustrated in Figure 7.3.

What is most important to note is that the calculated axial load in the critical members, at the onset of buckling lay between 65.3kN and 69.5kN, again well above the design load of such a section of

22.3kN. See Appendix B for the determination of the design load of the critical section. As discussed in Section 5.4, the own weight of the truss was not taken into consideration for the test purposes and it was determined that superposition of the own weight would be satisfactory. If this is done, the buckling axial loads increase to 69.9kN for the green test, 68.9kN for the yellow test and 66.3kN for the orange test. Figures 6.29 and 6.30 demonstrate the stresses in the buckled members and the vertical deflection of the truss respectively, for each of the tests performed.

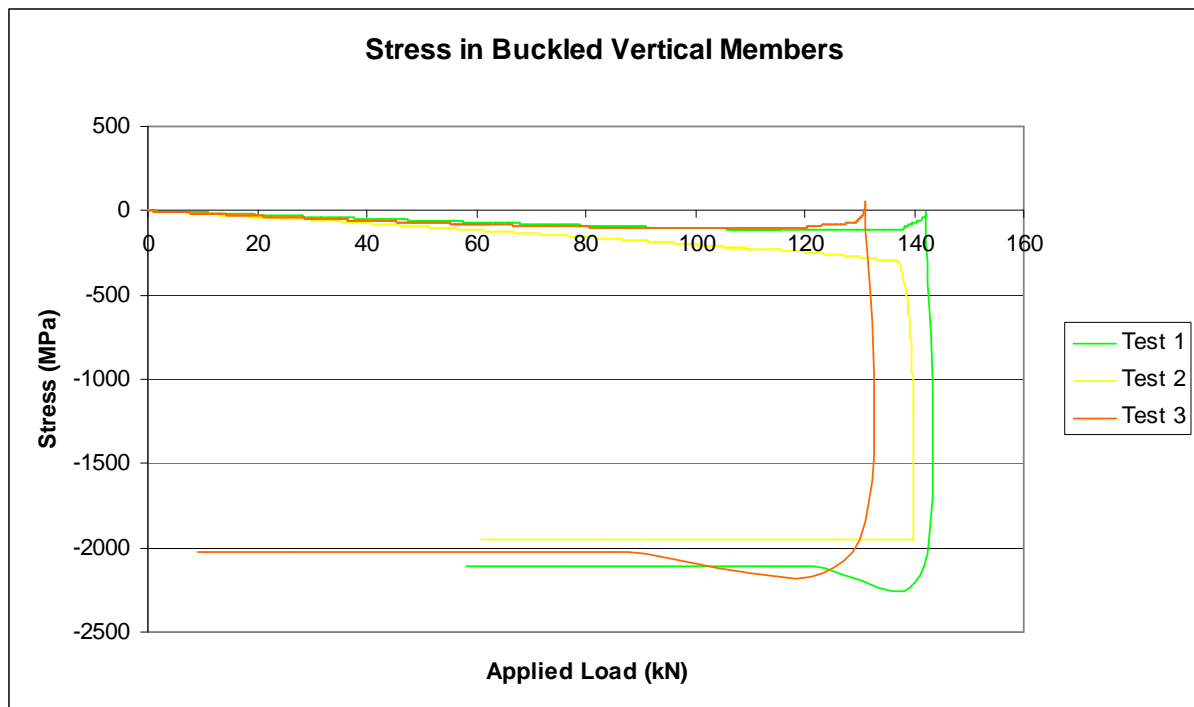


Figure 6.29 : Stresses in buckled vertical compression members

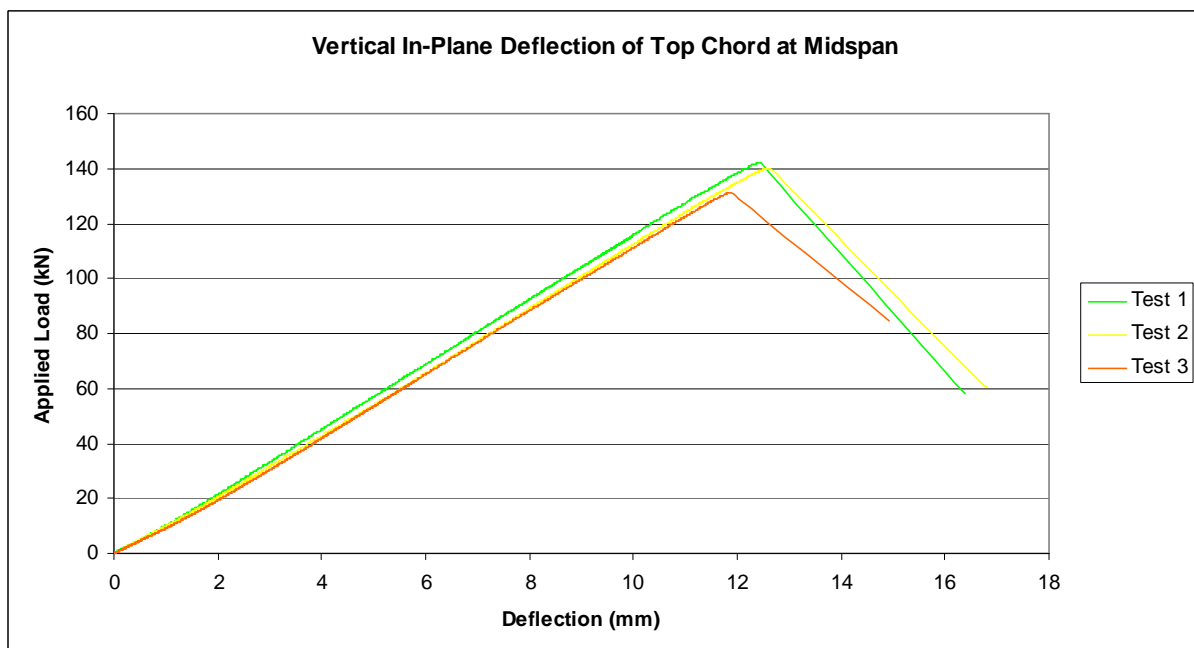


Figure 6.30 : Comparison of test results of vertical deflection of top chord at midspan

## 7. COMPARISON OF ANALYTICAL AND EXPERIMENTAL RESULTS

As has been discussed in Chapter 6, the anticipated failure mode of in-plane buckling of the critical compression members, as determined by the structural analyses, did not occur. The dominant failure mode was out-of-plane buckling of the web compression members and the location of the critical members varied. Therefore the following comparisons between the analytical and experimental results cannot be made between the individual critical compression members, because the mode of failure differs, but the comparison can still be made in terms of the global stability of the truss.

The effective length factors,  $K$ , as provided in Tables 7.1 and 7.2, were determined using two different approaches. The first is a theoretical approach using Euler's buckling formula:

$$K = \sqrt{\frac{\pi^2 EI}{C_r}} / L \quad (\text{Equation 7.1})$$

The second approach applies the formula used to determine the axial compressive resistance in Clause 13.3 of SANS 10162-1:2005. A similar approach was followed by Ding et al <sup>[13]</sup> in determining the effective lengths of solid round diagonals in lattice towers.

$$K = \left[ \left( \frac{Af_y}{C_r} \right)^n - 1 \right]^{\frac{1}{2n}} \frac{r}{L} \sqrt{\frac{\pi^2 E}{f_y}} \quad (\text{Equation 7.2})$$

The elastic modulus is taken as 200GPa and the yield stress as 326MPa, as determined by the material tests explained in Section 6.5. The regression factor  $n$  in Equation 7.2 is taken as 1.34 as stipulated by Clause 13.3 of SANS 10162-1:2005, for hot-rolled structural sections. The moment of inertia,  $I$ , and radius of gyration,  $r$ , are taken about the x-axis for the in-plane effective length factor and about the y-axis of the section for the out-of-plane effective length factor, as shown in Figure 7.1.

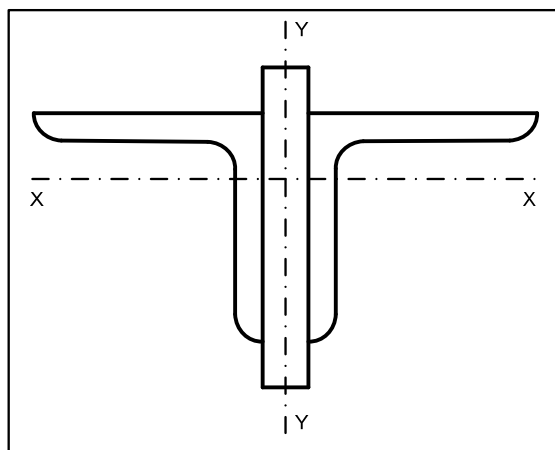


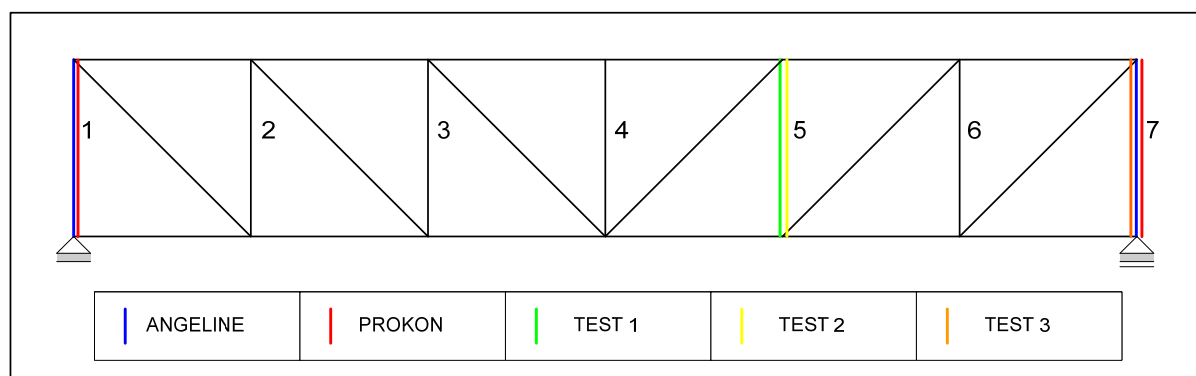
**Figure 7.1** : Definition of axes of double-angle sections used for web compression members

The length of the member is taken as the distance between the points of intersection of the centerlines of the members, at their end connections. The critical load,  $C_r$ , is taken as the axial load in the failed member at the onset of buckling. Therefore the effective length factors determined are only true for the out-of-plane case, because all the members failed in an out-of-plane buckling mode. However, this implies that the effective length factors determined for the in-plane case are at least that low, because at that particular axial load, failure had not occurred yet about the x-axis, i.e. these are larger than the actual effective length factors for in-plane buckling.

The effective length factors determined according to Equation 7.1 are referred to as Euler K and those determined according to Equation 7.2 are referred to as SANS K. As shown in Tables 7.1 and 7.2 the SANS K factors determined for in-plane buckling lie below 0.5. This is due to the fact that the SANS approach includes factors which take into account imperfections and residual stresses in the section. Of the two approaches, the Euler K factor is therefore the more realistic representation of the physical because the critical loads used to determine the K factors are the actual buckling loads and therefore intrinsically include the effects of imperfections and residual stresses.

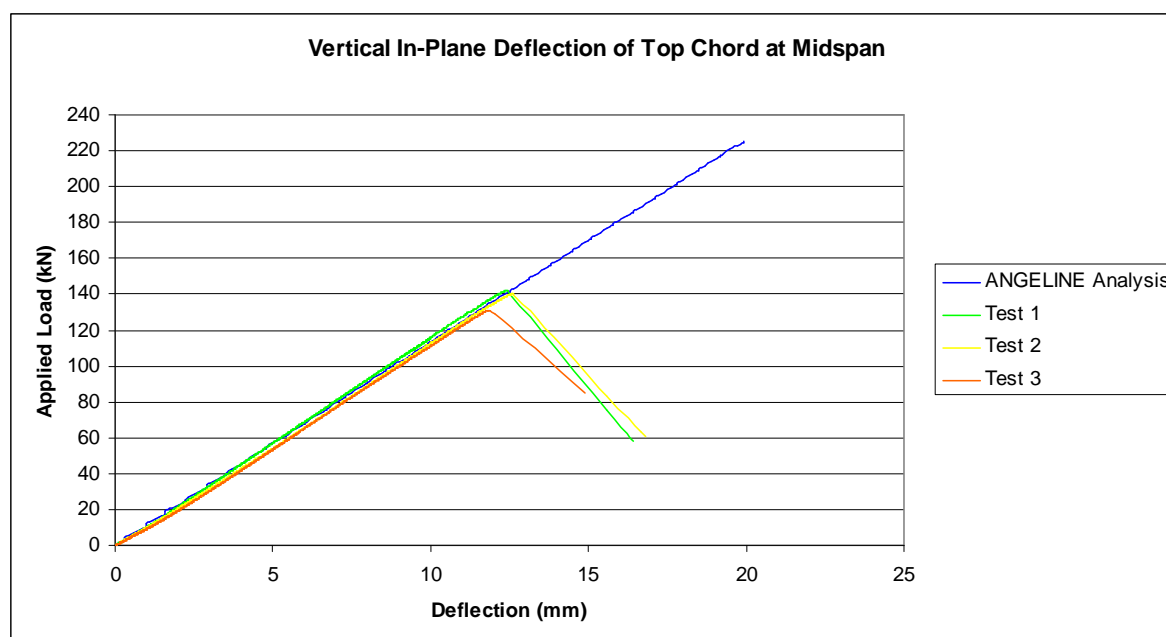
## 7.1 GRAVITY LOAD CASE

Figure 7.1 below identifies the location of the buckled web compression member for the structural analyses performed in ANGELINE and Prokon, as well as for each of the tests performed.



**Figure 7.2 :** Comparison of location of failed vertical compression members

The inconsistency in the location of the failed compression members between the analytical and experimental results is due to the difference in failure modes. The axial load carried by each of the vertical compression members is very similar. Initial curvature of the members was not measured but it is proposed that the location of the failed member is determined to a greater degree by initial imperfections of each member.



**Figure 7.3** : Comparison of analytical and experimental vertical deflection of top chord

The general load/deflection behaviour of the truss is well reflected by the analytical results, as shown in Figure 7.3. The analyses only deviate from the true behaviour of the truss in describing the actual failure mode. This is due to the fact that the analysis is restricted to two-dimensional or in-plane behaviour of the truss and therefore does not detect out-of-plane buckling as a potential, and in this case dominant, failure mode. Out-of-plane buckling of the web compression members occurs at a lower applied load than in-plane buckling, due to the stiffness of the connections. This is discussed in greater detail in Section 7.3.

**Table 7.1** : Comparison of principle analytical and experimental results of gravity load case

25 x 25 x 3 Double Angle		ANGELINE	Prokon	Green Test	Yellow Test	Orange Test
Failed Vertical Member		1 <sup>st</sup> / 7 <sup>th</sup>	1 <sup>st</sup> / 7 <sup>th</sup>	5 <sup>th</sup>	5 <sup>th</sup>	7 <sup>th</sup>
Buckling Load of Failed Member		112.6 kN	119.8 kN	69.5 kN	68.6 kN	65.3 kN
Applied Load		225.6 kN	228.3 kN	141.9 kN	140.0 kN	131.2 kN
Midspan Vertical Deflection		19.9 mm	19.8 mm	12.5 mm	12.6 mm	11.9 mm
X – Axis	Euler K	“rigid”	“fixed”	0.642	0.646	0.662
	SANS K			0.419	0.428	0.459
Y – Axis	Euler K	not analysed	not analysed	1.049	1.057	1.083
	SANS K			0.685	0.700	0.750

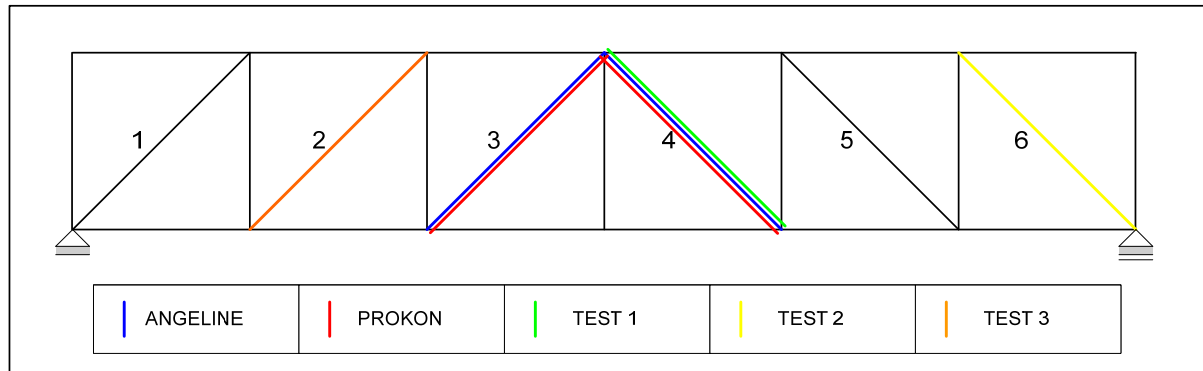
\* “rigid” refers to the type of node definition used in the ANGELINE analyses

\* “fixed” refers to the type of node definition used in the Prokon analyses

The Euler K factor, determined for out-of plane buckling, in Table 7.1 are greater than 1.0. This is most likely due a combination of insufficient lateral support provided by the bottom chord and initial out-of-straightness of the chords, causing relative displacement between the ends of the web compression members.

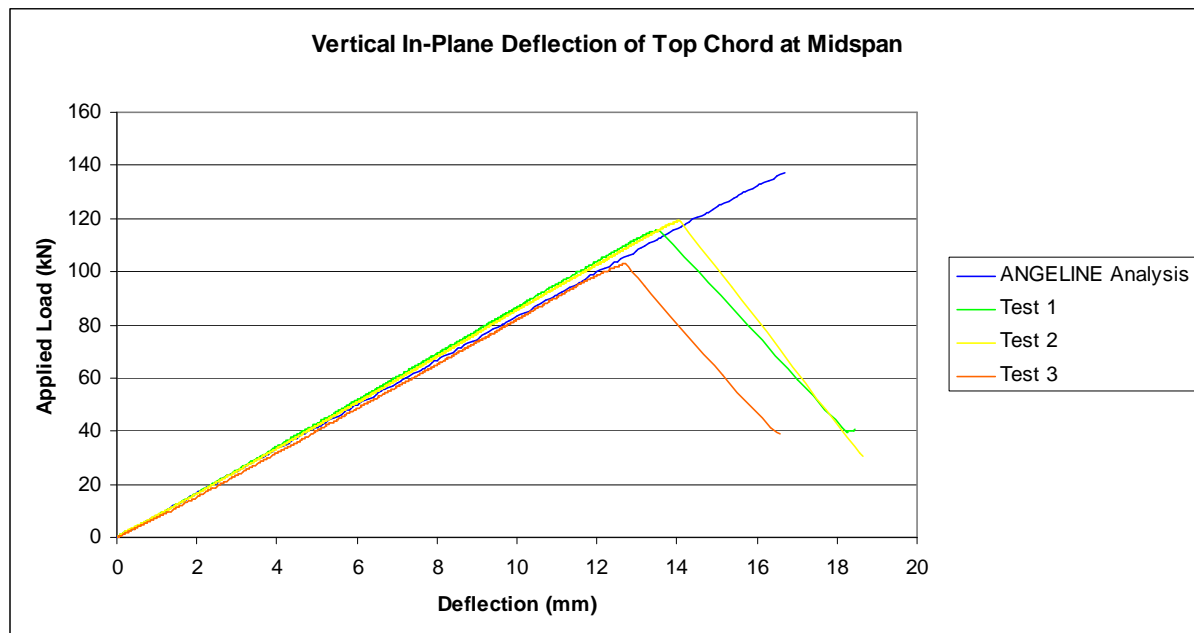
## 7.2 WIND LOAD CASE

Figure 7.3 below identifies the location of the buckled web compression member for the structural analyses performed in ANGELINE and Prokon, as well as for each of the tests performed.



**Figure 7.4** : Comparison of location of failed diagonal compression members

As was the case for the gravity load case test results, the inconsistency in the location of the failed compression members between the analytical and experimental results is due to the difference in failure modes. The location of the failed member is determined by a greater degree by initial imperfections of each individual member.



**Figure 7.5** : Comparison of analytical and experimental vertical deflection of top chord

As was the case for the gravity load case the general load/deflection behaviour of the truss is well reflected by the analytical results. The analyses again deviate from the true behaviour of the truss in describing the actual failure mode. Out-of-plane buckling of the web compression members occurs at a lower applied load than in-plane buckling, due to the stiffness of the connections.

**Table 7.2** : Comparison of principle analytical and experimental results of wind load case

30 x 30 x 3 Double Angle		ANGELINE	Prokon	Green Test	Yellow Test	Orange Test
Failed Vertical Member		3 <sup>rd</sup> / 4 <sup>th</sup>	3 <sup>rd</sup> / 4 <sup>th</sup>	4 <sup>th</sup>	6 <sup>th</sup>	2 <sup>nd</sup>
Buckling Load of Failed Member		94.0 kN	97.3 kN	79.4 kN	82.7 kN	71.9 kN
Applied Load		137.2 kN	139.3 kN	115.7 kN	119.1 kN	102.9 kN
Midspan Vertical Deflection		16.7 mm	16.5 mm	13.6 mm	14.1 mm	12.7 mm
X – Axis	Euler K	“rigid”	“fixed”	0.563	0.551	0.590
	SANS K			0.393	0.370	0.441
Y – Axis	Euler K	not analysed	not analysed	0.883	0.864	0.927
	SANS K			0.617	0.581	0.692

\* “rigid” refers to the type of node definition used in the ANGELINE analyses

\* “fixed” refers to the type of node definition used in the Prokon analyses

### 7.3 COMPARISON OF EXPERIMENTAL RESULTS TO CODE APPROACH

The following two tables, Tables 7.3 and 7.4, contain a comparison of the design loads obtained using the approach prescribed in SANS 10162-1:2005, and the loads and effective length factors obtained from the tests performed, for both the gravity and wind load cases. The SANS critical axial load is determined according to Clause 13.3 of SANS 10162-1:2005, detailed calculations of which are presented in Appendix B. The SANS critical axial load is determined for a yield stress of 200MPa as well as 326MPa.

The applied load is the load required at midspan of the bottom chord to induce the critical axial load in the critical member. The effective length factor is determined according the Euler K approach as defined in Section 7.2. However only the effective length factors about the x-axis, i.e. for in-plane buckling of the section, are provided, because the uncertainty with respect to Clause 15 of SANS 10162-1:2005 only concerns the effective length factors for in-plane buckling.

**Table 7.3** : Comparison of critical loads and effective length factors for gravity load case

25 x 25 x 3 Double Angle	SANS		Average of Tests	Tests		
	200 MPa	326 MPa		Green	Yellow	Orange
<b>Critical Axial Load</b>	20.0 kN	22.3 kN	67.8 kN	69.5 kN	68.6 kN	65.3 kN
<b>Applied Load</b>	40.2 kN	45.2 kN	137.7	141.9 kN	140.0 kN	131.2 kN
<b>Effective Length Factor</b>	1.0		0.650	0.642	0.646	0.662

**Table 7.4** : Comparison of critical loads and effective length factors for wind load case

30 x 30 x Double Angle	SANS		Average of Tests	Tests		
	200 MPa	326 MPa		Green	Yellow	Orange
<b>Critical Axial Load</b>	19.1 kN	20.6 kN	76.5kN	79.4 kN	82.7 kN	71.9 kN
<b>Applied Load</b>	27.5 kN	30.4 kN	112.6 kN	115.7 kN	119.1 kN	102.9 kN
<b>Effective Length Factor</b>	1.0		0.568	0.563	0.551	0.590

The most important findings to note are the differences between the design axial loads as obtained by SANS 10162-1:2005, of 22.3kN and 20.6kN for the gravity load case and the wind load case respectively, and the actual axial loads carried by the web members during testing, of 67.8kN and 76.5kN respectively. Subsequently the effective length factors also vary greatly. The K factor for in-plane buckling is prescribed as 1.0, but realistically found to be at least between 0.55 and 0.66. In practice these could be expected to be even lower for in-plane buckling, due to the fact that the failure mode experienced was out-of-plane buckling and not in-plane.

The effective length of the web compression is therefore much closer to that of a column with rigid boundary conditions, than to that of a simply supported column, i.e. the requirements of the code are unnecessarily conservative. This result could have a significant effect on the economy of large parallel chord trusses. In addition to this, the fact that the critical web compression member of each of the tests performed buckled out of the plane of the truss indicates that, contrary to common opinion, the load bearing capacity of a truss may well be governed by the out-of-plane behaviour of the web compression members, and not the in-plane. This effect is not taken into consideration in current engineering practice.

The following is a direct comparison between the individual prescriptions relevant to the research conducted of Clause 15 of SANS 10162-1:2005, and the findings based on the tests performed.

Clause	Relevant Clause Content	Experimental Findings
15.2.1	<i>The simplified method assumes that all members are pin-connected.</i>	None of the compression members, with respect to in-plane behaviour, exhibited behaviour associated with pin-connected end restraints. All results indicate resistance to rotation to some degree.
15.2.1 a)	<i>This method (the simplified method) may be used when the out-of-plane resistance of all compression members is larger than the in-plane resistance.</i>	In all six tests performed the out-of-plane buckling capacity of the web compression members was found to be critical. Therefore the out-of-plane resistance of the compression members was not larger than the in-plane resistance.
15.3.1	<i>The effective length for buckling in the plane of the truss shall be taken as the distance between the lines of intersection of the working points of the web members and the chord.</i>	The simplified method therefore prescribes an effective length factor of 1.0. The tests performed obtained effective length factors for the buckled web compression members in the range of at least as low as 0.55 to 0.66.
15.3.1 (cont.)	<i>The effective length for buckling perpendicular to the plane of the truss shall be equal to the distance between the points of lateral support.</i>	The effective length of the web compression members is taken as the distance between the lines of intersection of the working points of the web members and the chords because they are supported laterally at their end points by the chords. However, the effective lateral support offered by the chords is not absolute. The K-factors determined experimentally range between 0.86 and 1.08.
15.3.4	<i>The factored resistances of the first compression web member and its connections shall be determined with their respective resistance factors, <math>\phi</math>, multiplied by 0.85.</i>	The results indicated that the weakest first web compression member of all tests performed, only failed at an axial load more than 3 times greater than the design load. However, the failure mode was not in-plane buckling, therefore it is inconclusive whether a reduced resistance of 0.85 is necessary when considering in-plane behaviour.

## 8. CONCLUSIONS AND RECOMMENDATIONS

### 8.1 CONCLUSIONS

The main results of the numerical analyses were confirmed, namely that the effective length factor of web compression members is closer to that of a rigidly connected column than to a simply supported column, i.e. closer to 0.5 than 1.0. This can have a significant impact on the economy of large parallel chord trusses. A reduction in the effective length factor leads to a significant reduction in the cross-section of the member.

In addition to this it was found that, contrary to common opinion, the capacity of web compression members may be governed by out-of-plane behaviour, and not by in-plane behaviour. The mind set of general practice is that, assuming an effective length factor of 1.0 for in-plane buckling of the web compression members and provided that the moment of inertia out-of-plane is greater than that for in-plane, which is often the case, then out-of-plane stability of the web compression members is of no concern. However, it is this out-of-plane stability of the web compression members which has proven to be critical. Therefore both in- and out-of-plane stability should be taken into consideration.

In the introduction to this thesis, several questions were put forward with the intention of obtaining answers to them by means of the research conducted, most of which can be answered satisfactorily. However, the unanticipated strong-axis buckling behaviour leads to some inconclusive answers.

---

*What is the influence of the node fixity on the effective length of the compression elements and the distribution of the forces through the truss?*

#### **In-Plane**

Node fixity, due to the stiffness of the gusset plates, introduces significant restraint at the end connections of the compression members, thereby reducing the effective length of the member considerably. Investigative analyses performed in ANGELINE showed no significant difference in the distribution of axial forces through the truss between pin-connected and rigidly connected trusses.

#### **Out-of-Plane**

The gusset plates offer little restraint against buckling out of the plane of the truss at the end connections of the truss and for practical purposes these connections must be considered pinned. Although the analyses performed in ANGELINE was restricted to in-plane behaviour, the same conclusion, namely that there is no significant difference in distribution of axial forces, as for in-plane behaviour can be made.

*Does the fixity of the nodes induce significant bending moments in the elements and would the elements subsequently have to be designed as beam-columns instead of simple columns?*

**In-Plane**

All analytical results showed that bending moments are generated and contribute to reducing the ultimate capacity of the compression members. To take these bending moments into account the elements should be designed as beam-columns instead of simple columns. However, the bending moments are insignificant compared to the considerable amount of design effort required to design the elements as beam-columns, it is therefore considered unjustifiable.

**Out-of-Plane**

It was not possible to investigate analytically the out-of-plane behaviour of the truss. However, it is suggested that, similar to in-plane behaviour, the additional design effort required in designing beam-columns is not justified by the magnitude of the bending moments.

---

*Can the effective length factor  $K$ , as defined in SANS 10162-1:2005, be reduced to less than 1.0?*

**In-Plane**

For the gravity load case average effective length factors of 0.650 were achieved. For the wind load case effective length factors of at least 0.568 were determined. Therefore the results of the tests performed indicate that an effective factor of less than 1.0 would be justified.

**Out-of-Plane**

In the tests performed effective length factors as high as 1.08 were determined. Therefore the effective length factor for out-of-plane behaviour can not be reduced to less than 1.0.

---

*Is the reduced resistance by a factor of 0.85 of the first web compression elements necessary?*

**In-Plane**

In two of the six tests, it was the first web compression elements that failed but at an axial load three times greater than the design load. However, the 0.85 resistance reduction factor pertains to in-plane buckling of the members and, as the consistent failure mode was out-of-plane buckling, no conclusions can be drawn with regards to the 0.85 resistance reduction factor.

**Out-of-Plane**

As the 0.85 resistance reduction factor specifically pertains to in-plane buckling of the web compression members, it is not clear whether this factor would also apply to the out-of-plane resistance of the members. No conclusion can therefore be drawn in this regard.

## 8.2 RECOMMENDATIONS

### 8.2.1 EFFECTIVE LENGTH FACTORS

Most importantly, in considering the aim of the research, it has been found that designing web compression members of trusses with welded gusset plates, using an effective length factor of 1.0 for in-plane buckling is overly conservative. It is recommended that an effective length factor of 0.8 is used. This recommendation is jointly based on the results of the tests performed, as well as the approach to the design of web compression members of trusses in SIA 263 : Steel Construction (2003) <sup>[31]</sup>.

This approach, as described in Chapter 3, recommends the reduction of the effective length factor to 0.8 provided that the end restraints justify such a reduction and that the maximum compression loads do not act simultaneously on the adjacent members. The disadvantage of this approach is that the onus still rests with the designer to decide whether the end restraints are sufficiently rigid. However, for very little additional design effort, a more realistic design is achieved.

However, it is recommended that the effective length factor for out-of-plane buckling of web compression members, for trusses with welded gusset plates, is to be increased to 1.1. The effective length factor for out-of-plane buckling was experimentally found to be greater than 1.0 in some cases. Therefore employing an effective length factor of 1.0 could be unconservative. In addition to this it is considered necessary to maintain the 0.85 resistance reduction factor of the first web compression members, until further research is conducted with respect to in-plane behaviour specifically.

It is important to note that these recommendations are solely based on a relatively limited set of experiments. In order to make conclusive changes to the relevant sections of SANS 10162-1:2005 <sup>[30]</sup> a great amount of theoretical research, supported by experimental work, which investigates a range of different truss configurations, as well specifically the in-plane behaviour of web compression members, is necessary. It is expected that, given more extensive testing which induces in-plane buckling and a subsequent reliability analysis, an effective length factor for in-plane buckling of the web compression members, lower than 0.8 could be recommended. The reliability analysis would be done most effectively by performing a preposterior analysis to determine the optimal sample size, as a function of the accuracy required and the cost of construction and testing.

### 8.2.2 TRUSS TESTING

A number of recommendations can be made pertaining to the execution of the experimental work. Certain restrictions rendered a truss with a number of bays greater than six impractical to test. It is however recommended that a truss design with a greater number of bays, ideally ten as illustrated by the investigative analyses performed in ANGELINE, would be of great benefit to better simulate full

truss behaviour. The greater the number of bays used, the greater the variation in axial loads and bending moments along the length of the truss will be. Subsequently the critical compression member can be predicted with greater certainty.

In addition to this, full scale testing would improve the recreation of practice related truss behaviour. Full scale testing would allow for the use of structural elements of grade 350W steel, as opposed to commercial grade steel, and subsequently lower variability of material quality, a large contributing factor to the variation in the location of the buckled web compression member.

It is recommended that a methodology is developed to measure the initial imperfections of the members, and thereby verify the degree to which initial imperfections play a role.

One of the principle aims of the research was to investigate the behaviour of the web compression members, specifically using practice-related design procedures of trusses. The out-of-plane failure mode of the compression members was unexpected, but a valuable observation to make in itself. The intended study of in-plane buckling behaviour could therefore not be tested. However, it is an important realization that, despite several measures taken to ensure in-plane buckling, out-of-plane buckling was still the dominant failure mode. It is therefore necessary to take both the in-plane and out-of-plane behaviour of web compression members into consideration when designing large parallel chord trusses, using welded gusset plates.

### **8.2.3 PROKON**

A stated objective of including Prokon in the structural analysis of the representative truss was to have the opportunity to correlate the results obtained from Prokon with the research results. As Prokon is one of the most widely used structural analysis software packages in the South African industry, it is important to establish whether the same analytical results could be achieved in the local design context, and hence whether or not the recommendations made with regards to the adjustments of the effective length factor could be easily applied.

As was discussed in Section 5.3, the results obtained from the ANGELINE and Prokon analyses compare very well in all aspects, except in determining the magnitude of the bending moments in the compression members, at the point at which buckling occurs. As mentioned, the bending moments at this point are very sensitive to the exact determination of the singular point, and relatively large variations can be expected. In all other aspects Prokon obtained satisfactory results, with respect to the analyses performed. It is therefore concluded that Prokon would provide sufficiently similar analytical results in the local design context for the scope of truss configurations investigated.

## 9. REFERENCES

### 9.1 BOOKS

1. Bleich, F (1952). **Buckling Strength of Metal Structures**, , McGraw-Hill, New York.
2. Dowling, Harding, Bjorhovde (1992). **Constructional Steel Design : An International Guide**. Essex : Elsevier Science Publishers Ltd.  
Chapter 2.9 : Trusses
3. Fisher, BH. (2002). **Manual for the design of steelwork building structures**. London: Institution of Structural Engineers.  
Chapter 12 : Lattice Girders or Truss with Pin-Base Columns.
4. Galambos, Theodore V. (1988). **Guide to Stability Design Criteria for Metal Structures**. Canada: John Wiley & Sons.  
Chapter 15 : Members with Elastic Lateral Restraints
5. Galishnikova, Pahl and Dunaiski. **Geometrically Nonlinear Analysis of Plane Trusses and Frames**. To be published.  
Chapter 1 : State of the Art in Nonlinear Structural Analysis  
Chapter 2 : Nonlinear Behaviour of Plane Trusses and Frames  
Chapter 4 : Plane Trusses
6. Mahachi, J. (2004). **Design of Structural Steelwork to SANS 10162**. Pretoria: Council for Industrial and Scientific Research.  
Chapter 9 : Trusses and Lattice Girders
7. Tall, Lambert (1974). **Structural Steel Design, Second Edition**. New York : John Wiley & Sons.  
Chapter 10 : Compression Members in Frames and Trusses
8. The South African Institute of Steel Construction (1992). **Structural Steelwork Connections, Limit State Design**. Johannesburg: The South African Institute of Steel Construction.

## 9.2 PUBLICATIONS

9. Blandford, G.E. **Progressive failure analysis of inelastic space truss structures.** Computers and Structures, Volume 58, No 5 (981 – 990), 1996.
10. Chan, S.L. and Cho, S.H. **Second-order analysis and design of angle trusses, Part I : Elastic analysis and design.** Engineering Structures, Volume 30 (616 – 625), 2008.
11. Chan, S.L. and Cho, S.H. **Second-order analysis and design of angle trusses, Part II : Plastic analysis and design.** Engineering Structures, Volume 30 (626 – 631), 2008.
12. Chen, Shaofan. **Buckling of T-strut subject to compressive force on its shear centre.** Journal of Constructional Steel Research, Volume 63 (332 – 336), 2007.
13. Chen, Shaofan and Su, Mingzhou. **Out-of-plane buckling and bracing requirement in double-angle trusses.** Steel and Composite Structures, Volume 3, Number 4, August 2003.
14. Ding, Yoncong, Jaboo, Kalid S, Sun, Yean and Madugula, Murty, K.S. **Experimental basis for the effective length factors of steel solid round cross-braced diagonals in CSA Standard S37-01.** Canadian Journal of Civil Engineering, Volume 29 (430 – 435), 2002.
15. Kennedy, D.J. Laurie and Brattland, Anita. **Flexural tests of two full-scale composite trusses.** Canadian Journal of Civil Engineering, Volume 19 (279 – 295), 1992.
16. Kennedy, D.J. Laurie et al. **Inelastic incremental analysis of an industrial Pratt truss.** Engineering Structures, Volume 22, No 2 (146 – 154), February 2000.
17. Koen, Colin B. **The Development of a Multi-Purpose Beam/Column Testing Apparatus.** Masters Thesis in Civil Engineering at University of Stellenbosch, March 2003.
18. Ogawa, Koji et al. **Effective length for web members in tubular trusses.** Journal of Structural and Construction Engineering, No 338 (70 – 76).
19. Sun, H et al. **Comparison of theories for stability of truss structures, Part I : Computation of critical load.** Commun Nonlinear Sci Numer Simulat, Volume 3, 2008.
20. Temple, Murray C., Petretta, Davide M. and Morand, Catherine. **Influence of the assumed effective length factor on the load carrying capacity of steel angles in compression.** Canadian Journal of Civil Engineering, Volume 22, 1995.

21. Temple, Murray C. and Sakla, Sherief S.S. **Considerations for the design of single-angle compression members attached by one leg.** Canadian Journal of Civil Engineering, Volume 23, 1996.
22. Temple, Murray C. and Sakla, Sherief S.S. **Single-angle compression members welded by one leg to a gusset plate, Part 1: Experimental study.** Canadian Journal of Civil Engineering, Volume 25, 1998.
23. Trahair, N.S., Usami, T., and Galambos, T.V. 1969. **Eccentrically loaded single-angle columns.** Civil and Environmental Engineering Department, Washington University, St. Louis, Mo., Research Report No.11.
24. Woolcock, Scott T. and Kitipornchai, Sritawat. **Design of Single Angle Web Struts in Trusses.** Journal of Structural Engineering, Volume 112, June 1986.
25. Yam, Michael C.H. and Cheng, J.J. Roger. **Experimental investigation of the compressive behaviour of gusset plate connections.** University of Alberta, Department of Civil Engineering, September 1993.
26. Yeong-Bin, Chang et al. **Effects of member buckling and yielding on ultimate strengths of space trusses.** Engineering Structures, Volume 19, No 2 (179 – 191), 1997.

### 9.3 DESIGN CODES

27. American Institute of Steel Construction (2005). **ANSI/AISC 360-05 : Specification for Structural Steel Buildings.** Chicago, Illinois : American Institute of Steel Construction.
28. British Standards Institute (2000). **BS 5950-1:2000 : Structural use of steelwork in building – Part 1 : Code of practice for design – Rolled and welded sections.** United Kingdom : British Standards Institute.
29. Canadian Standards Association (2005). **CAN/CSA-S16-01 : Limit States Design Of Steel Structures.** Ontario, Canada : Canadian Standards Association.
30. Standards South Africa (2005). **SANS 10162-1:2005, The structural use of steel, Part 1 : Limit-state design of hot-rolled steelwork.** Pretoria : Standards South Africa.
31. Swiss Society of Engineers and Architects (2003). **SIA 263 : Steel Construction.** Zürich : Swiss Society of Engineers and Architects.

## A. APPENDIX : DETAILED BENCHMARK PROBLEM CALCULATIONS

### GENERAL SECTION PROPERTIES : 60 x 60 x 5 DOUBLE ANGLE

$$E = 200 \times 10^3 \text{ MPa}$$

$$f_y = 200 \text{ MPa}$$

$$f_u = 365 \text{ MPa}$$

$$G = 77 \times 10^3 \text{ MPa}$$

$$\phi = 0.90$$

$$A = 1164 \text{ mm}^2$$

$$I_x = 388.0 \times 10^3 \text{ mm}^4$$

$$I_y = 803.8 \times 10^3 \text{ mm}^4$$

$$r_x = 18.3 \text{ mm}$$

$$r_y = 26.3 \text{ mm}$$

$$C_w = 0 \text{ mm}^4$$

$$J = 11.28 \times 10^3 \text{ mm}^4$$

The benchmark problem was applied to each code approach, for a range of different section lengths. These range from 1000mm to 3000mm, in 500mm increments. The calculations provided in this appendix are only those for the 1500mm length of section.

**SANS 10162-1 : 2005 & CSA/CAN S16-01****15.2.1 Effective Length Factor**

$$K_x = K_y = 1.0$$

**Table 3 Classification of Section**

$$\frac{b}{t} = \frac{60}{5} = 12 < \frac{200}{\sqrt{f_y}} = \frac{200}{\sqrt{200}} = 14.14 \quad \therefore \text{not Class 4 section}$$

**13.3 Axial Compression****13.3.2 b) Torsional or Torsional-Flexural Buckling (Singly Symmetric)**

$f_e$  : lesser of  $f_{ex}$  and  $f_{eyz}$

$$f_{ex} = \frac{\pi^2 E}{\left(\frac{K_x L_x}{r_x}\right)^2} = \frac{\pi^2 \times 200 \times 10^3}{\left(\frac{1.0 \times 1500}{18.3}\right)^2} = 293.8 \text{MPa}$$

$$f_{ey} = \frac{\pi^2 E}{\left(\frac{K_y L_y}{r_y}\right)^2} = \frac{\pi^2 \times 200 \times 10^3}{\left(\frac{1.0 \times 1500}{26.3}\right)^2} = 606.8 \text{MPa}$$

$$x_o = 0.0 \text{mm} \text{ and } y_o = 13.9 \text{mm}$$

$$r_o^2 = x_o^2 + y_o^2 + r_x^2 + r_y^2 = 0.0^2 + 13.9^2 + 18.3^2 + 26.3^2 = 1219.8 \text{mm}^2$$

$$\Omega = 1 - \left(\frac{x_o^2 + y_o^2}{r_o^2}\right) = 1 - \left(\frac{0.0^2 + 13.9^2}{1219.8}\right) = 0.842$$

$$f_{ez} = \left(\frac{\pi^2 E C_w}{K_z^2 L_z^2} + GJ\right) \frac{1}{A r_o^2} = \frac{77 \times 10^3 \times 11.28 \times 10^3}{1164 \times 1219.8} = 611.7 \text{MPa}$$

$$f_{eyz} = \frac{f_{ey} + f_{ez}}{2\Omega} \left(1 - \sqrt{1 - \frac{4f_{ey}f_{ez}\Omega}{(f_{ey} + f_{ez})^2}}\right)$$

$$= \frac{606.8 + 611.7}{2 \times 0.842} \left(1 - \sqrt{1 - \frac{4 \times 606.8 \times 611.7 \times 0.842}{(606.8 + 611.7)^2}}\right) = 435.9 \text{MPa}$$

$$\therefore f_e = f_{ex} = 293.8 \text{MPa}$$

$$\therefore \lambda = \sqrt{\frac{f_y}{f_e}} = \sqrt{\frac{200}{293.8}} = 0.825$$

$$C_r = \phi A f_y (1 + \lambda^{2n})^{-1/n} = 0.90 \times 1164 \times 200 \times (1 + 0.825^{2 \times 1.34})^{-1/1.34} \times 10^{-3} = 147.7 \text{ kN}$$

$$\therefore C_r = 147.7 \text{ kN}$$

---

**BS 5950-1 : 2000****4.7.10.3 c) Effective Length**

$$\lambda_x = \frac{0.85L_x}{r_x} \text{ but } \geq \frac{0.7L_x}{r_x} + 30$$

$$\frac{0.85 \times 1500}{18.3} = 69.7 \text{ and } \frac{0.7 \times 1500}{18.3} + 30 = 87.4$$

$$\therefore \lambda_x = 87.4$$

$$\lambda_y = \left[ \left( \frac{L_y}{r_y} \right)^2 + \lambda_c^2 \right]^{0.5} \text{ but } \geq 1.4\lambda_c$$

$$\text{Where } \lambda_c = \frac{L_v}{r_v}$$

$L_v$  : distance between intermediate connectors = 500mm

$r_v$  : radius of gyration of single angle = 11.7mm

$$\therefore \lambda_c = \frac{500}{11.7} = 42.7$$

$$\left[ \left( \frac{1500}{26.3} \right)^2 + 42.7^2 \right]^{0.5} = 71.3 \text{ and } 1.4 \times 42.7 = 59.8$$

$$\therefore \lambda_y = 71.3$$

**Table 23 Allocation of Strut Curve**

Rolled angle, channel or T-section : Strut curve c)

**3.5 Classification of Cross-Sections**

$$\text{Table 11 } \varepsilon = \left( \frac{275}{p_y} \right)^{0.5} = \left( \frac{275}{200} \right)^{0.5} = 1.173$$

$$\frac{b}{t} = \frac{60}{5} = 12 < 15\varepsilon = 17.6$$

$$\frac{d}{t} = \frac{60}{5} = 12 < 15\varepsilon = 17.6$$

$$\frac{(b+d)}{t} = \frac{(60+60)}{5} = 24 < 24\varepsilon = 28.1$$

$\therefore$  all 3 conditions satisfy conditions for Class 3 semi-compact

**Annex C.1 Compressive Strength**

$$\alpha = 5.5$$

$$\lambda_o = 0.2 \left( \frac{\pi^2 E}{p_y} \right)^{0.5} = 0.2 \times \left( \frac{\pi^2 \times 200 \times 10^3}{200} \right)^{0.5} = 19.869$$

$$\eta = \frac{\alpha(\lambda - \lambda_o)}{1000}$$

**About x-axis**

$$\therefore \eta = \frac{\alpha(\lambda_x - \lambda_o)}{1000} = \frac{5.5 \times (87.4 - 19.9)}{1000} = 0.371$$

$$p_E = \left( \frac{\pi^2 E}{\lambda^2} \right) = \left( \frac{\pi^2 \times 200 \times 10^3}{87.4^2} \right) = 258.5 \text{ MPa}$$

$$\Phi = \frac{p_y + (\eta + 1)p_E}{2} = \frac{200 + (0.371 + 1) \times 258.5}{2} = 277.2 \text{ MPa}$$

$$p_c = \frac{p_E p_y}{\Phi + (\Phi^2 - p_E p_y)^{0.5}} = \frac{258.5 \times 200}{277.2 + (277.2^2 - 258.5 \times 200)^{0.5}} = 118.6 \text{ MPa}$$

**About y-axis**

$$\therefore \eta = \frac{\alpha(\lambda_y - \lambda_o)}{1000} = \frac{5.5 \times (71.3 - 19.9)}{1000} = 0.283$$

$$p_E = \left( \frac{\pi^2 E}{\lambda^2} \right) = \left( \frac{\pi^2 \times 200 \times 10^3}{71.3^2} \right) = 388.6 \text{ MPa}$$

$$\Phi = \frac{p_y + (\eta + 1)p_E}{2} = \frac{200 + (0.283 + 1) \times 388.6}{2} = 349.3 \text{ MPa}$$

$$p_c = \frac{p_E p_y}{\Phi + (\Phi^2 - p_E p_y)^{0.5}} = \frac{388.6 \times 200}{349.3 + (349.3^2 - 388.6 \times 200)^{0.5}} = 138.8 \text{ MPa}$$

$$\therefore \text{critical } p_c = 118.6 \text{ MPa}$$

**4.7.4 a) Compression Resistance**

$$P_c = A_g p_c = 1164 \times 118.6 \times 10^{-3} = 138.1 \text{ kN}$$

**SIA 263 : 2003****Table 13 | Effective Length**

$$L_K = 0.8L$$

**4.5.1 Buckling of Centrally Loaded Compression Members**

Figure 7 Buckling Curve (c) : sections with compressive residual stresses in the extreme fibres

Table 7  $\therefore \alpha = 0.49$ **Critical elastic buckling stress about x-axis**

$$\sigma_{cr,K} = \frac{\pi^2 E}{\lambda_K^2} = \frac{\pi^2 EI}{L_K^2 A} = \frac{\pi^2 \times 200 \times 10^3 \times 388.0 \times 10^3}{(0.8 \times 1500)^2 \times 1164} = 456.9 \text{ MPa}$$

**Critical elastic buckling stress about y-axis**

$$\sigma_{cr,K} = \frac{\pi^2 E}{\lambda_K^2} = \frac{\pi^2 EI}{L_K^2 A} = \frac{\pi^2 \times 200 \times 10^3 \times 803.8 \times 10^3}{(0.8 \times 1500)^2 \times 1164} = 946.6 \text{ MPa}$$

$$\therefore \sigma_{cr,K} = 456.9 \text{ MPa}$$

$$\therefore \bar{\lambda}_K = \sqrt{\frac{f_y}{\sigma_{cr,K}}} = \sqrt{\frac{200}{456.9}} = 0.662$$

$$\Phi_K = 0.5 \left[ 1 + \alpha (\bar{\lambda}_K - 0.2) + \bar{\lambda}_K^2 \right] = 0.5 \times \left[ 1 + 0.49 \times (0.662 - 0.2) + 0.662^2 \right] = 0.832$$

$$\chi_K = \frac{1}{\Phi_K + \sqrt{\Phi_K^2 - \bar{\lambda}_K^2}} = \frac{1}{0.832 + \sqrt{0.832^2 - 0.662^2}} = 0.748 \leq 1.0$$

$$\therefore N_{K,Rd} = \frac{\chi_K f_y A}{\gamma_{M1}} = \frac{0.748 \times 200 \times 1164 \times 10^{-3}}{1.05} = 165.8 \text{ kN}$$

**ANSI / AISC 360 - 05****C2. Effective Length**

$K_1 = 1.0$  : in-plane bending, unless analysis indicates that a smaller value may be used

**E6. Built-Up Members**

1. (a)

Compressive Strength

(ii)

distance between connectors :  $a = 500\text{mm}$

radius of gyration of individual component relative to its centroidal axis parallel to member axis of buckling :  $r_{ib,x} = 18.3\text{mm}$  and  $r_{ib,y} = 26.3\text{mm}$

distance between centroids of individual components perpendicular to the member axis of buckling :  $h = 37.8\text{mm}$

**E3. Compressive Strength for Flexural Buckling of Members Without Slender Elements**

$$\alpha = \frac{h}{2r_{ib}} = \frac{37.8}{2 \times 18.3} = 1.033$$

$$\left(\frac{KL}{r}\right)_o = \frac{1.0 \times 1500}{18.3} = 81.967$$

$$\left(\frac{KL}{r}\right)_m = \sqrt{\left(\frac{KL}{r}\right)_o^2 + 0.82 \frac{\alpha^2}{1 + \alpha^2} \left(\frac{a}{r_{ib}}\right)^2} = \sqrt{81.967^2 + 0.82 \times \frac{1.033^2}{1 + 1.033^2} \left(\frac{500}{18.3}\right)^2} = 83.813$$

$$F_e = \frac{\pi^2 E}{\left(\frac{KL}{r}\right)_m^2} = \frac{\pi^2 \times 200 \times 10^3}{83.813^2} = 281.0\text{MPa}$$

$$\left(\frac{KL}{r}\right)_m = 83.813 < 4.71 \sqrt{\frac{E}{F_y}} = 4.71 \times \sqrt{\frac{200 \times 10^3}{200}} = 148.94$$

$$\therefore F_{cr} = \left[0.658^{F_y/F_e}\right] F_y = \left[0.658^{200/281.0}\right] \times 200 = 148.5\text{MPa}$$

**E4. Compressive Strength for Torsional and Flexural-Torsional Buckling of Members Without Slender Elements**

$$\alpha = \frac{h}{2r_{ib}} = \frac{37.8}{2 \times 26.3} = 0.719$$

$$\left(\frac{KL}{r}\right)_o = \frac{1.0 \times 1500}{26.3} = 57.034$$

$$\left(\frac{KL}{r}\right)_m = \sqrt{\left(\frac{KL}{r}\right)_o^2 + 0.82 \frac{\alpha^2}{1 + \alpha^2} \left(\frac{a}{r_{ib}}\right)^2} = \sqrt{57.034^2 + 0.82 \times \frac{0.719^2}{1 + 0.719^2} \left(\frac{500}{26.3}\right)^2} = 57.891$$

$$F_e = \frac{\pi^2 E}{\left(\frac{KL}{r}\right)_m^2} = \frac{\pi^2 \times 200 \times 10^3}{57.891^2} = 589.0 \text{ MPa}$$

$$\left(\frac{KL}{r}\right)_m = 57.891 < 4.71 \sqrt{\frac{E}{F_y}} = 4.71 \times \sqrt{\frac{200 \times 10^3}{200}} = 148.94$$

$$\therefore F_{cry} = \left[0.658^{F_y/F_e}\right] F_y = \left[0.658^{200/589.0}\right] \times 200 = 173.5 \text{ MPa}$$

$$r_o^2 = x_o^2 + y_o^2 + \frac{I_x + I_y}{A} = 0.0^2 + 13.9^2 + \frac{388.0 \times 10^3 + 803.8 \times 10^3}{1164} = 1217.1 \text{ mm}^2$$

$$H = 1 - \frac{x_o^2 + y_o^2}{r_o^2} = 1 - \frac{0.0^2 + 13.9^2}{1217.1} = 0.841$$

$$F_{crz} = \frac{GJ}{A_g r_o^2} = \frac{77 \times 10^3 \times 11.28 \times 10^3}{1164 \times 1217.1} = 613.1 \text{ MPa}$$

$$\therefore F_{cr} = \left(\frac{F_{cry} + F_{crz}}{2H}\right) \left[1 - \sqrt{1 - \frac{4F_{cry}F_{crz}H}{(F_{cry} + F_{crz})^2}}\right]$$

$$\therefore F_{cr} = \left(\frac{173.5 + 613.1}{2 \times 0.841}\right) \left[1 - \sqrt{1 - \frac{4 \times 173.5 \times 613.1 \times 0.841}{(173.5 + 613.1)^2}}\right] = 164.0 \text{ MPa}$$

**Lesser of  $F_{cr}$  for flexural buckling and  $F_{cr}$  for torsional-flexural buckling:**

$$\therefore F_{cr} = 148.5 \text{ MPa}$$

$$\therefore P_n = AF_{cr} = 1164 \times 148.5 \times 10^{-3} = 172.8 \text{ kN}$$

## B. APPENDIX : DETERMINATION OF CRITICAL ELEMENT DESIGN LOADS

### GRAVITY LOAD CASE

#### GENERAL SECTION PROPERTIES : 25 x 25 x 3 DOUBLE ANGLE

$$E = 200 \times 10^3 \text{ MPa}$$

$$f_y = 200 \text{ MPa}$$

$$f_u = 365 \text{ MPa}$$

$$G = 77 \times 10^3 \text{ MPa}$$

$$\phi = 0.90$$

$$A = 284 \text{ mm}^2$$

$$I_x = 16.0 \times 10^3 \text{ mm}^4$$

$$I_y = 42.8 \times 10^3 \text{ mm}^4$$

$$r_x = 7.49 \text{ mm}$$

$$r_y = 12.27 \text{ mm}$$

$$C_w = 0 \text{ mm}^4$$

$$J = 952 \text{ mm}^4$$

#### SANS 10162-1 : 2005 DESIGN LOAD CALCULATIONS

##### 15.2.1 Effective Length Factor

$$K_x = K_y = 1.0$$

##### Table 3 Classification of Section

$$\frac{b}{t} = \frac{25}{3} = 8.33 < \frac{200}{\sqrt{f_y}} = \frac{200}{\sqrt{200}} = 14.14 \quad \therefore \text{not Class 4 section}$$

##### 13.3 Axial Compression

##### 13.3.2 b) Torsional or Torsional-Flexural Buckling (Singly Symmetric)

$$f_e : \text{lesser of } f_{ex} \text{ and } f_{eyz}$$

$$f_{ex} = \frac{\pi^2 E}{\left(\frac{K_x L_x}{r_x}\right)^2} = \frac{\pi^2 \times 200 \times 10^3}{\left(\frac{1.0 \times 1050}{7.49}\right)^2} = 100.4 \text{MPa}$$

$$f_{ey} = \frac{\pi^2 E}{\left(\frac{K_y L_y}{r_y}\right)^2} = \frac{\pi^2 \times 200 \times 10^3}{\left(\frac{1.0 \times 1050}{12.27}\right)^2} = 269.6 \text{MPa}$$

$$x_o = 0.0 \text{mm} \text{ and } y_o = 5.71 \text{mm}$$

$$r_o^2 = x_o^2 + y_o^2 + r_x^2 + r_y^2 = 0.0^2 + 5.71^2 + 7.49^2 + 12.27^2 = 239.26 \text{mm}^2$$

$$\Omega = 1 - \left(\frac{x_o^2 + y_o^2}{r_o^2}\right) = 1 - \left(\frac{0.0^2 + 5.71^2}{239.26}\right) = 0.864$$

$$f_{ez} = \left(\frac{\pi^2 E C_w}{K_z^2 L_z^2} + GJ\right) \frac{1}{A r_o^2} = \frac{77 \times 10^3 \times 952}{284 \times 239.26} = 1078.8 \text{MPa}$$

$$f_{eyz} = \frac{f_{ey} + f_{ez}}{2\Omega} \left(1 - \sqrt{1 - \frac{4f_{ey}f_{ez}\Omega}{(f_{ey} + f_{ez})^2}}\right)$$

$$= \frac{269.6 + 1078.8}{2 \times 0.864} \left(1 - \sqrt{1 - \frac{4 \times 269.6 \times 1078.8 \times 0.864}{(269.6 + 1078.8)^2}}\right) = 258.5 \text{MPa}$$

$$\therefore f_e = f_{ex} = 100.4 \text{MPa}$$

$$= \lambda = \sqrt{\frac{f_y}{f_e}} = \sqrt{\frac{200}{100.4}} = 1.411$$

$$C_r = \phi A f_y (1 + \lambda^{2n})^{-1/n} = 0.90 \times 284 \times 200 \times (1 + 1.411^{2 \times 1.34})^{-1/1.34} \times 10^{-3} = 20.0 \text{kN}$$

$$\therefore C_r = 20.0 \text{kN}$$

The section under consideration complies with the requirements for built-up members in compression according to Clause 19.1 of SANS 10162-1:2005.

The above calculations were also performed using a yield stress of  $f_y$  of 326MPa as determined by means of the material tests described in Section 6.4. In this case the critical axial load becomes 22.3kN.

**WIND LOAD CASE****GENERAL SECTION PROPERTIES : 30 x 30 x 3 DOUBLE ANGLE**

$$E = 200 \times 10^3 \text{ MPa}$$

$$f_y = 200 \text{ MPa}$$

$$f_u = 365 \text{ MPa}$$

$$G = 77 \times 10^3 \text{ MPa}$$

$$\phi = 0.90$$

$$A = 348 \text{ mm}^2$$

$$I_x = 28.0 \times 10^3 \text{ mm}^4$$

$$I_y = 69.0 \times 10^3 \text{ mm}^4$$

$$r_x = 8.99 \text{ mm}$$

$$r_y = 14.08 \text{ mm}$$

$$C_w = 0 \text{ mm}^4$$

$$J = 1270 \text{ mm}^4$$

**SANS 10162-1 : 2005 DESIGN LOAD CALCULATIONS****15.2.1 Effective Length Factor**

$$K_x = K_y = 1.0$$

**Table 3 Classification of Section**

$$\frac{b}{t} = \frac{30}{3} = 10.0 < \frac{200}{\sqrt{f_y}} = \frac{200}{\sqrt{200}} = 14.14 \quad \therefore \text{not Class 4 section}$$

**13.3 Axial Compression****13.3.2 b) Torsional or Torsional-Flexural Buckling (Singly Symmetric)**

$f_e$  : lesser of  $f_{ex}$  and  $f_{eyz}$

$$f_{ex} = \frac{\pi^2 E}{\left( \frac{K_x L_x}{r_x} \right)^2} = \frac{\pi^2 \times 200 \times 10^3}{\left( \frac{1.0 \times 1485}{8.99} \right)^2} = 72.3 \text{ MPa}$$

$$f_{ey} = \frac{\pi^2 E}{\left(\frac{K_y L_y}{r_y}\right)^2} = \frac{\pi^2 \times 200 \times 10^3}{\left(\frac{1.0 \times 1485}{14.08}\right)^2} = 177.5 \text{MPa}$$

$$x_o = 0.0 \text{mm and } y_o = 6.85 \text{mm}$$

$$r_o^2 = x_o^2 + y_o^2 + r_x^2 + r_y^2 = 0.0^2 + 6.85^2 + 8.99^2 + 14.08^2 = 326.0 \text{mm}^2$$

$$\Omega = 1 - \left(\frac{x_o^2 + y_o^2}{r_o^2}\right) = 1 - \left(\frac{0.0^2 + 6.85^2}{326.0}\right) = 0.856$$

$$f_{ez} = \left(\frac{\pi^2 E C_w}{K_z^2 L_z^2} + GJ\right) \frac{1}{A r_o^2} = \frac{77 \times 10^3 \times 1270}{348 \times 326.0} = 862.0 \text{MPa}$$

$$f_{eyz} = \frac{f_{ey} + f_{ez}}{2\Omega} \left(1 - \sqrt{1 - \frac{4f_{ey}f_{ez}\Omega}{(f_{ey} + f_{ez})^2}}\right)$$

$$= \frac{117.5 + 862.0}{2 \times 0.856} \left(1 - \sqrt{1 - \frac{4 \times 177.5 \times 862.0 \times 0.856}{(177.5 + 862.0)^2}}\right) = 171.4 \text{MPa}$$

$$\therefore f_e = f_{ex} = 72.3 \text{MPa}$$

$$\lambda = \sqrt{\frac{f_y}{f_e}} = \sqrt{\frac{200}{72.3}} = 1.663$$

$$C_r = \phi A f_y (1 + \lambda^{2n})^{-1/n} = 0.90 \times 348 \times 200 \times (1 + 1.663^{2 \times 1.34})^{-1/1.34} \times 10^{-3} = 19.1 \text{kN}$$

$$\therefore C_r = 19.1 \text{kN}$$

The section under consideration complies with the requirements for built-up members in compression according to Clause 19.1 of SANS 10162-1:2005.

The above calculations were also performed using a yield stress of  $f_y$  of 326MPa as determined by means of the material tests described in Section 6.4. In this case the critical axial load becomes 20.6kN.

## **C. APPENDIX : DRAWINGS FOR GRAVITY LOAD CASE TRUSS**

### **GENERAL NOTES TO WORKSHOP DRAWINGS**

#### **TRUSS DIMENSIONS**

- 6300mm x 1050mm
- 6 bays

#### **SECTIONS**

- All sections double angles
- All sections 200W (Commercial Grade) Steel, except 60x60x6 angles (350W)

#### **CONNECTING PLATES**

- All connecting plates 5mm thick and 50mm long
- Width of plate determined by angle width, plus 10mm

#### **GUSSET PLATES**

- All gusset plates 5mm thick, cut from plates
- Grade 300W steel

#### **SUPPORT PLATES**

- All support plates 10mm thick, cut from plates
- Grade 300W steel

#### **BUILT-UP PLATES**

- All built-up plates consist of 5mm gusset plate, between two 10mm thick plates, cut from plates
- Grade 300W steel, welded

### **LIST OF WORKSHOP DRAWINGS**

- |                                   |                             |
|-----------------------------------|-----------------------------|
| - Truss Layout – Gravity Load.vsd | - Connection H.vsd          |
| - Connection A.vsd                | - Connection I & J.vsd      |
| - Connection B & C.vsd            | - Connection K.vsd          |
| - Connection D.vsd                | - Connection K Sideview.vsd |
| - Connection E & F.vsd            | - Connection L & M.vsd      |
| - Connection G.vsd                | - Connection N.vsd          |

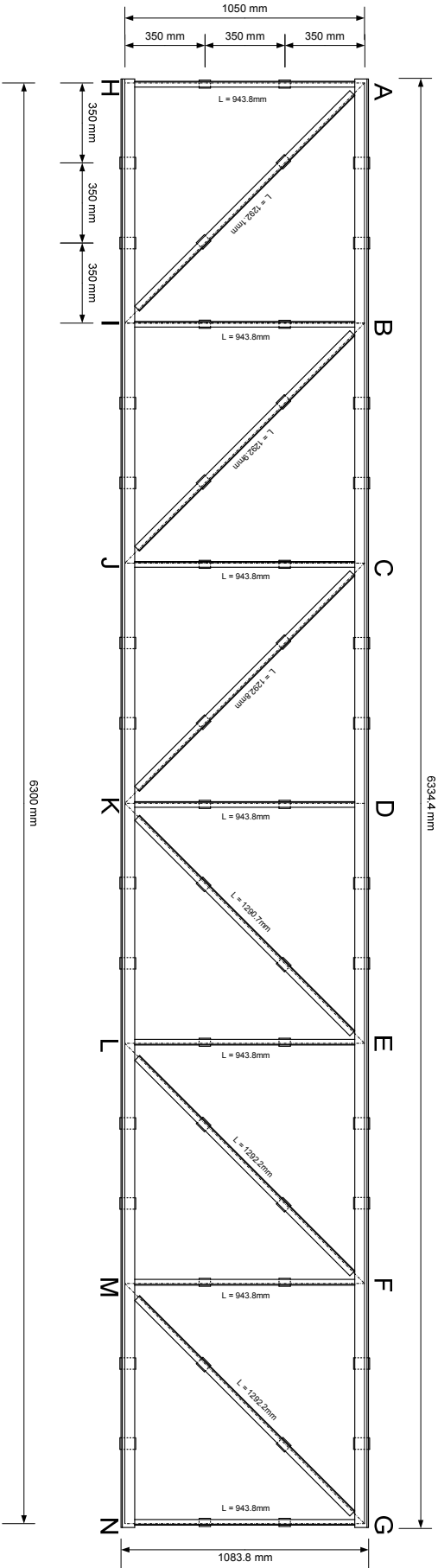
### Truss Layout | Gravity Load

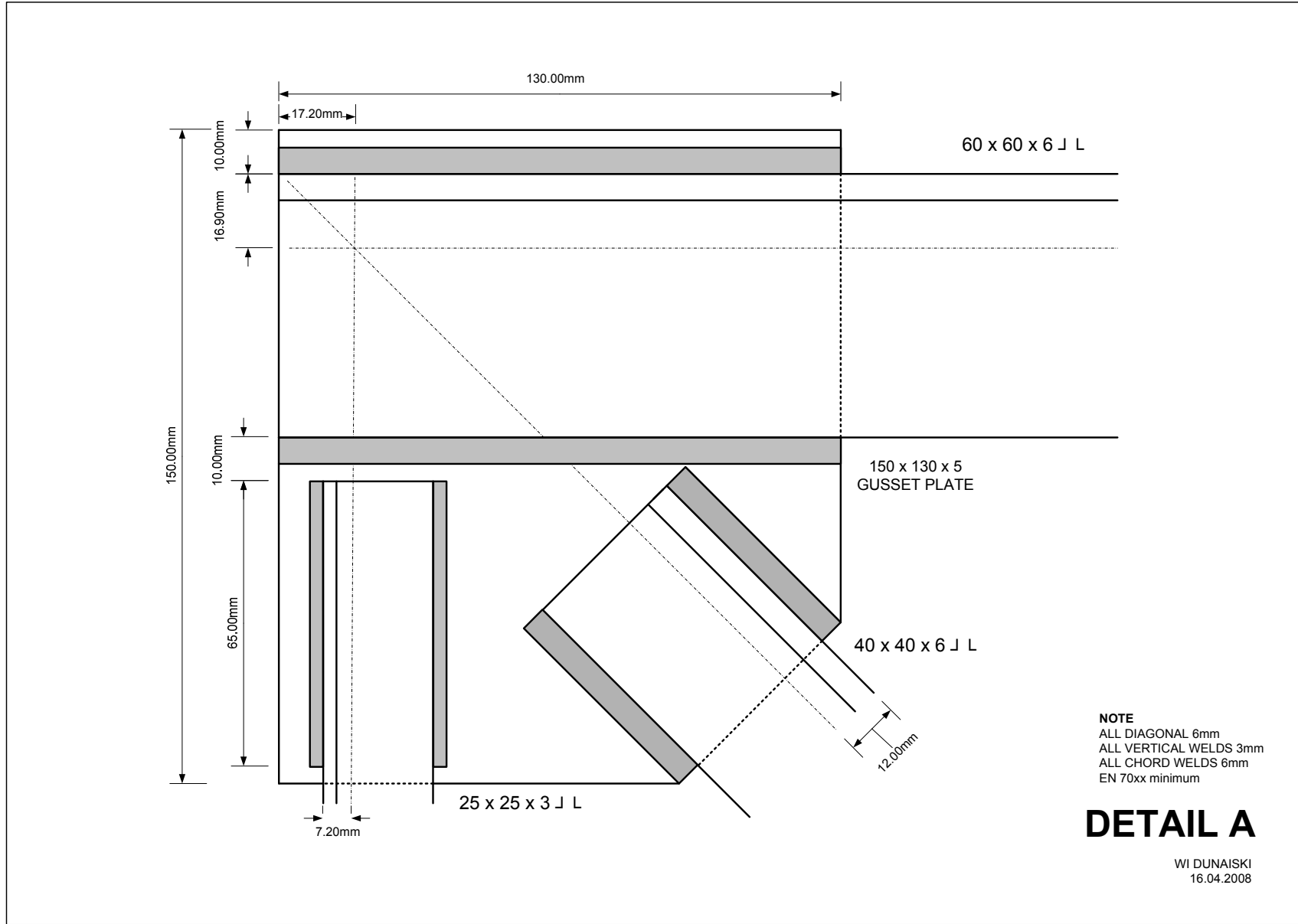
6300mm x 1050mm

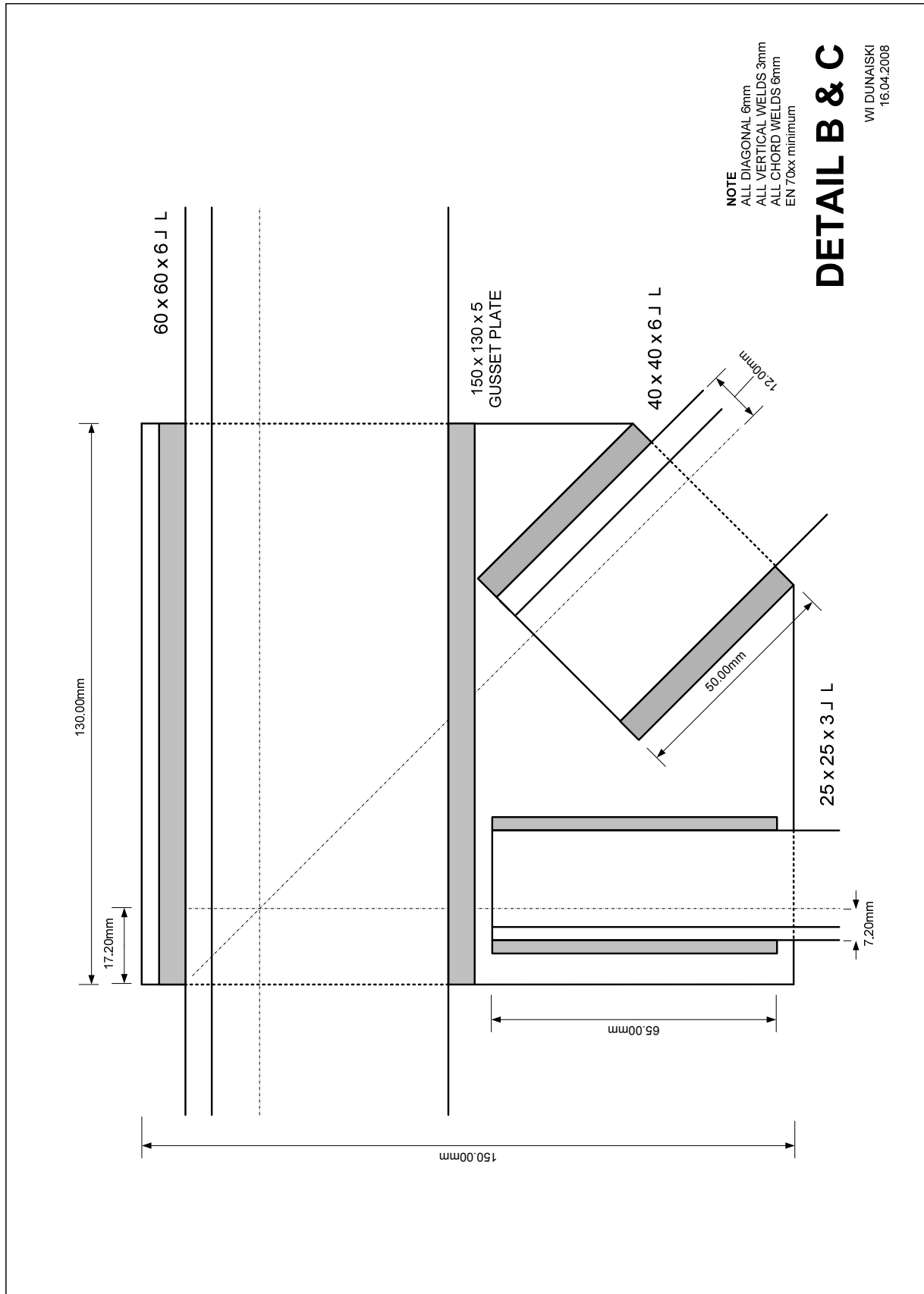
6 Bays

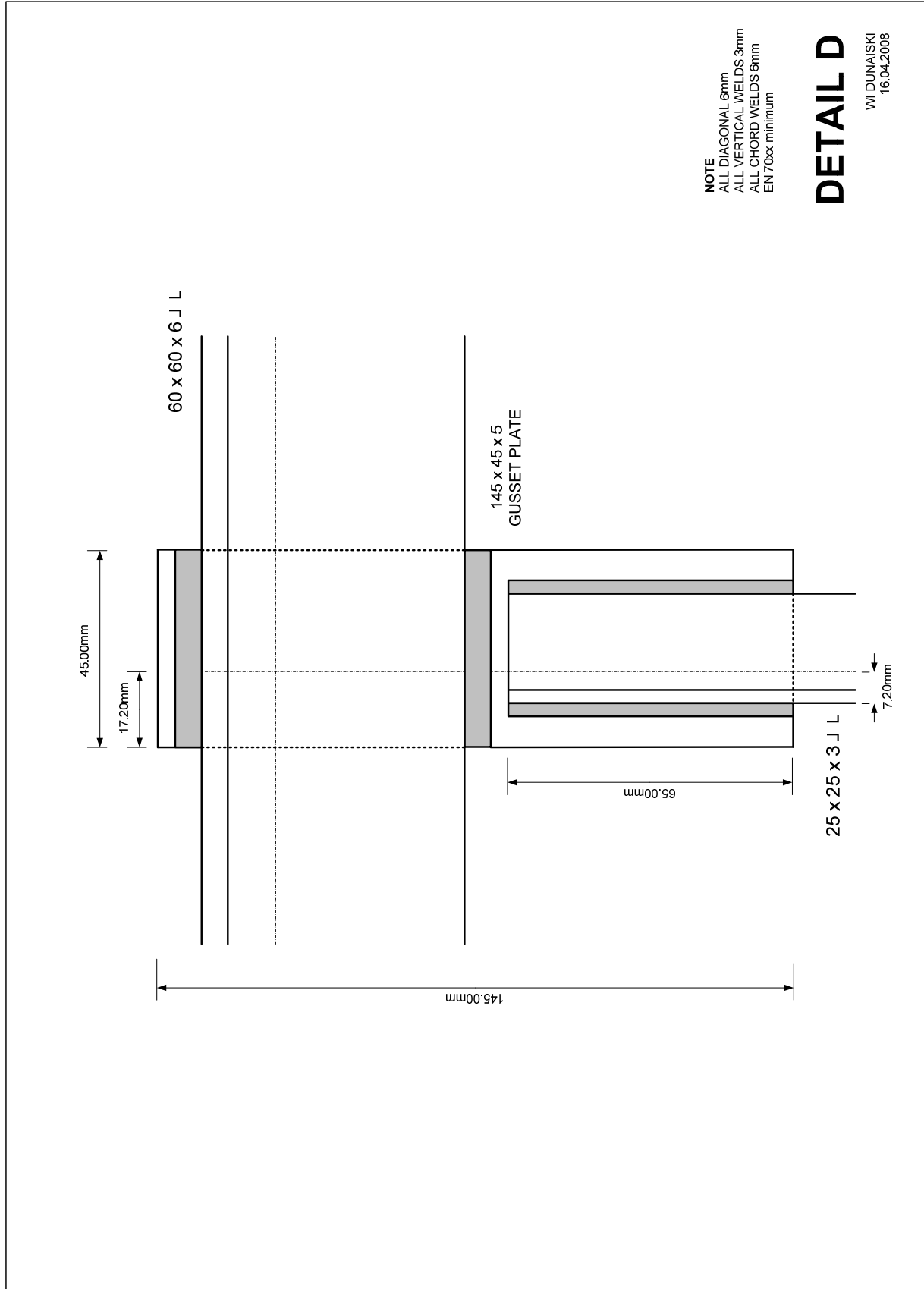
All sections double angles

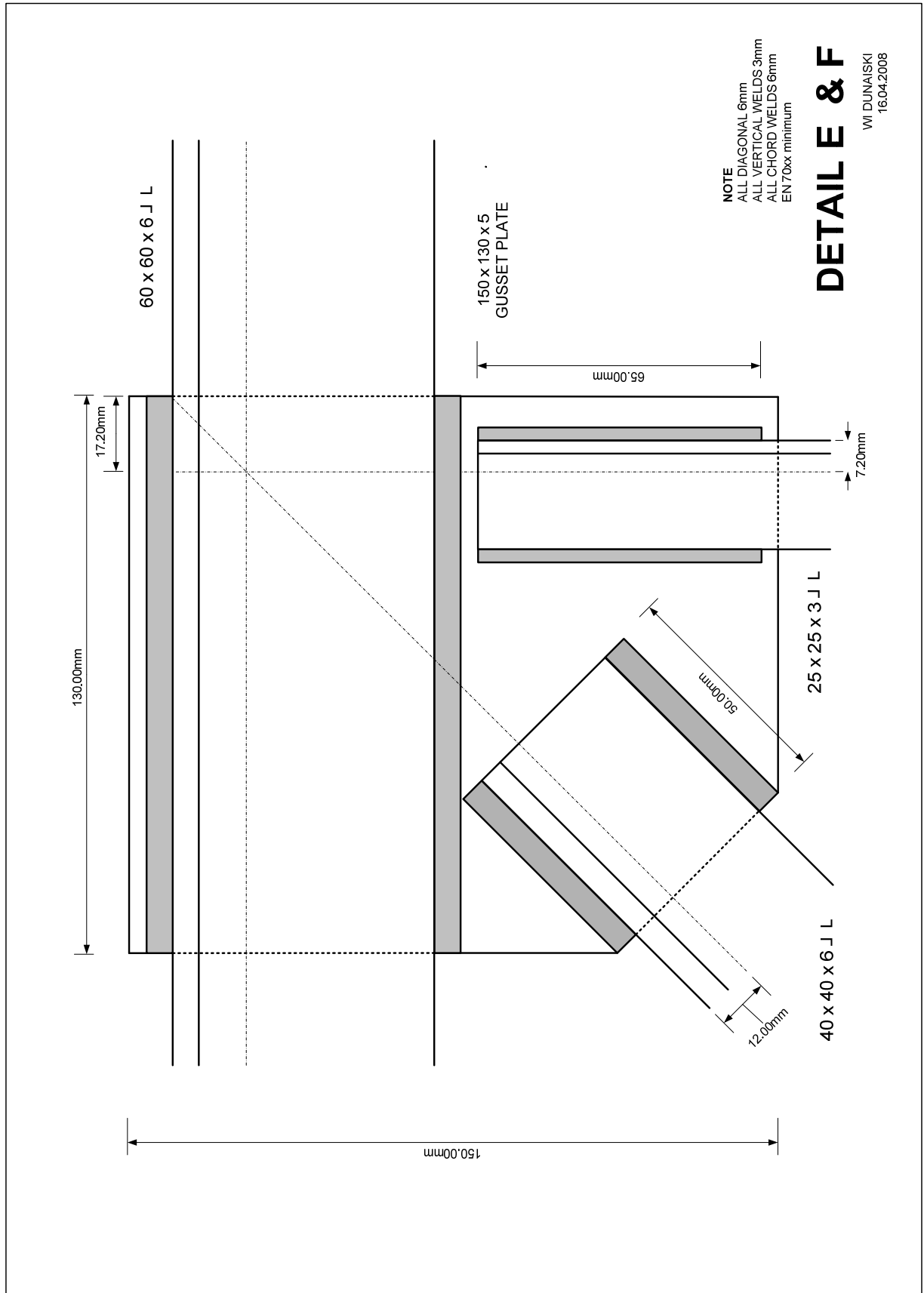
Top Chord	60 x 60 x 6
Bottom Chord	60 x 60 x 6
Diagonals	40 x 40 x 6
Verticals	25 x 25 x 3

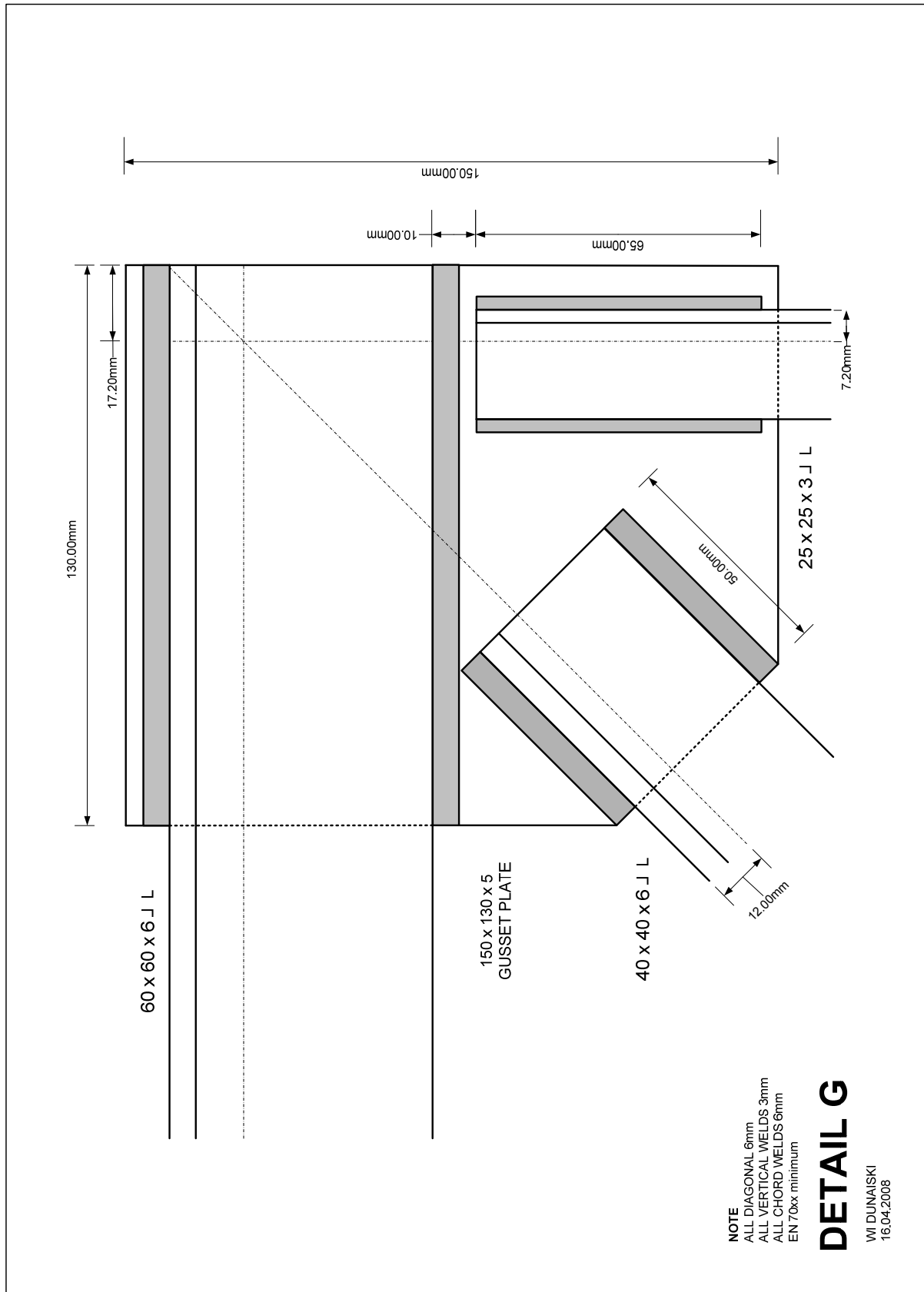


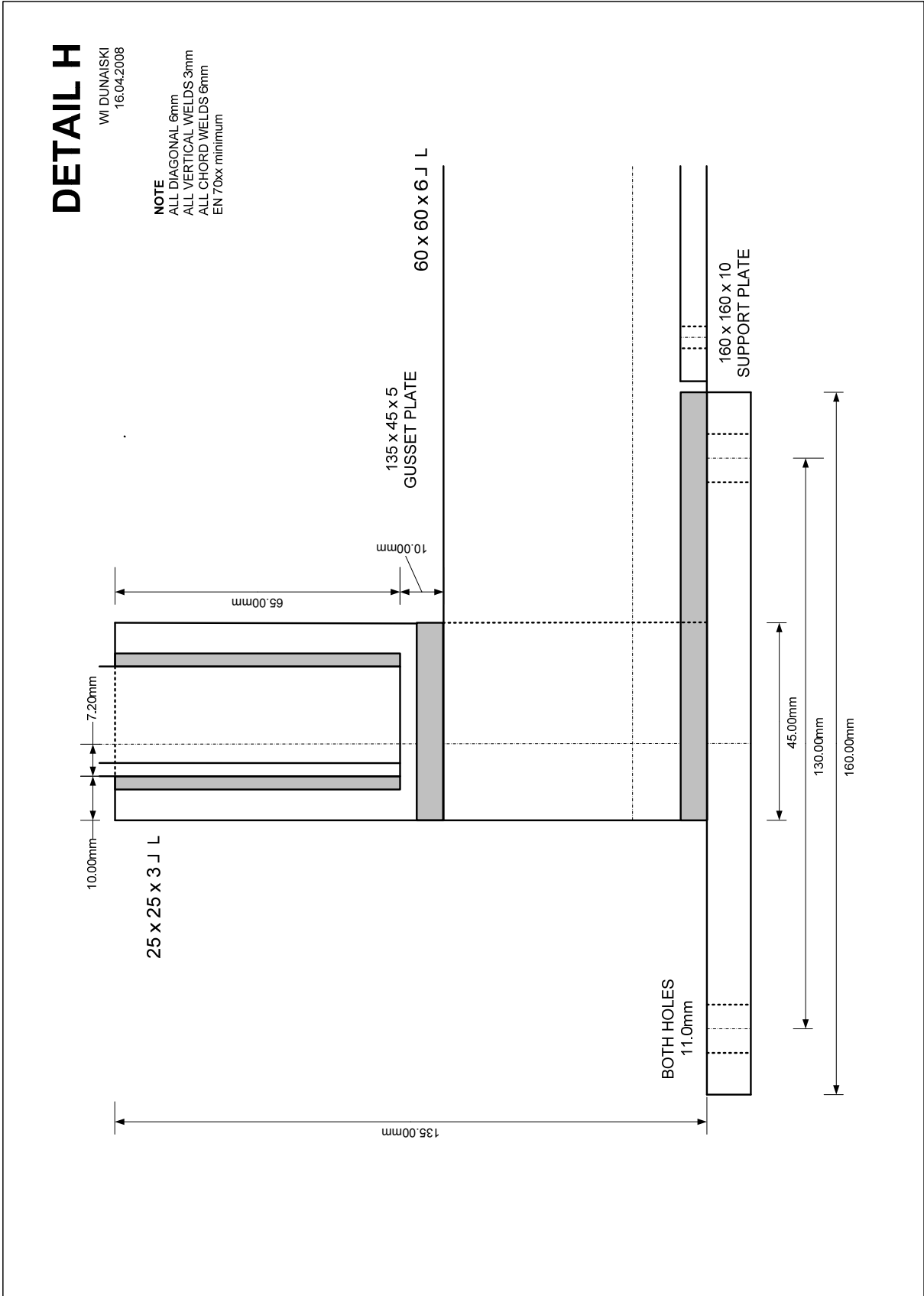


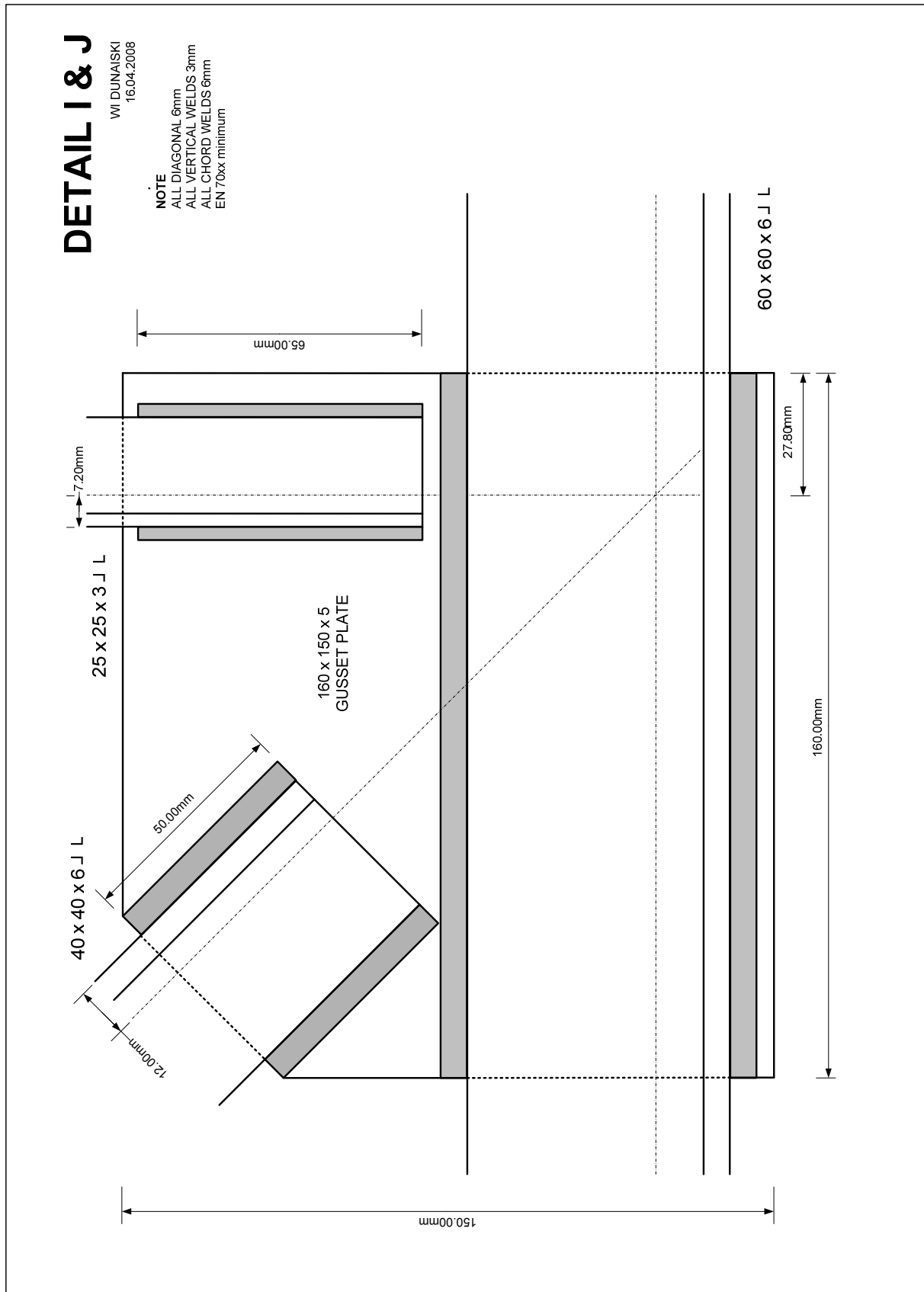


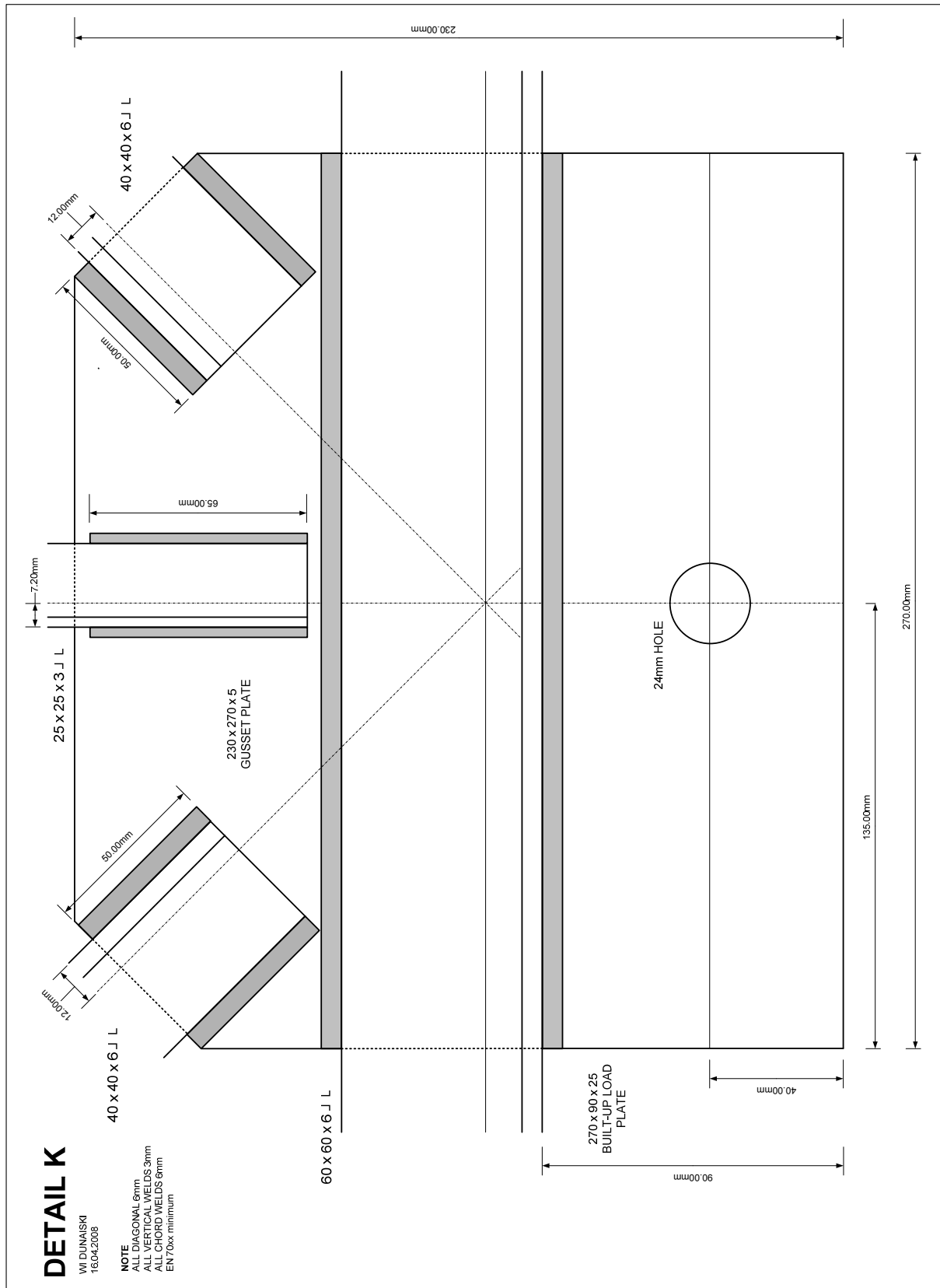


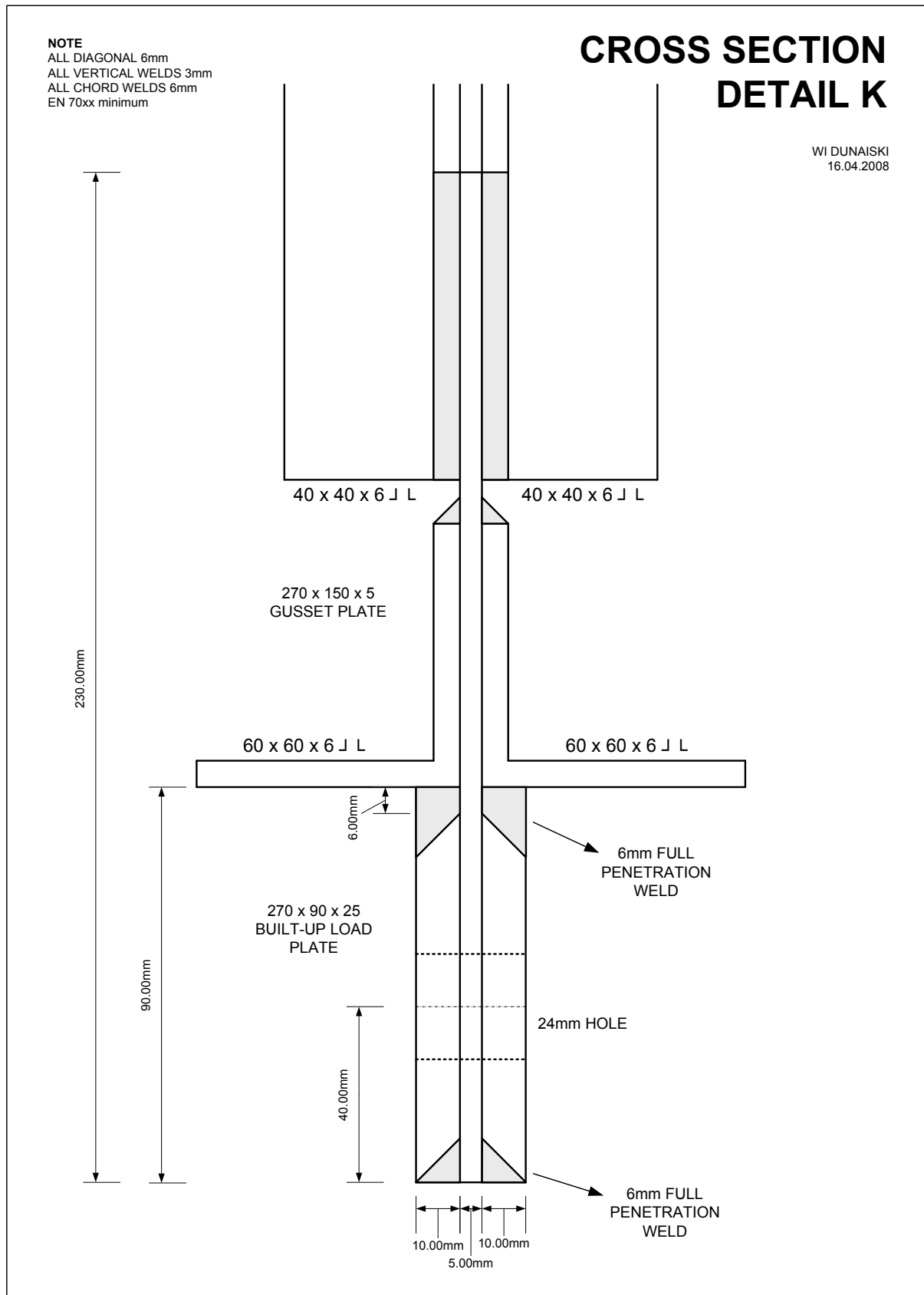


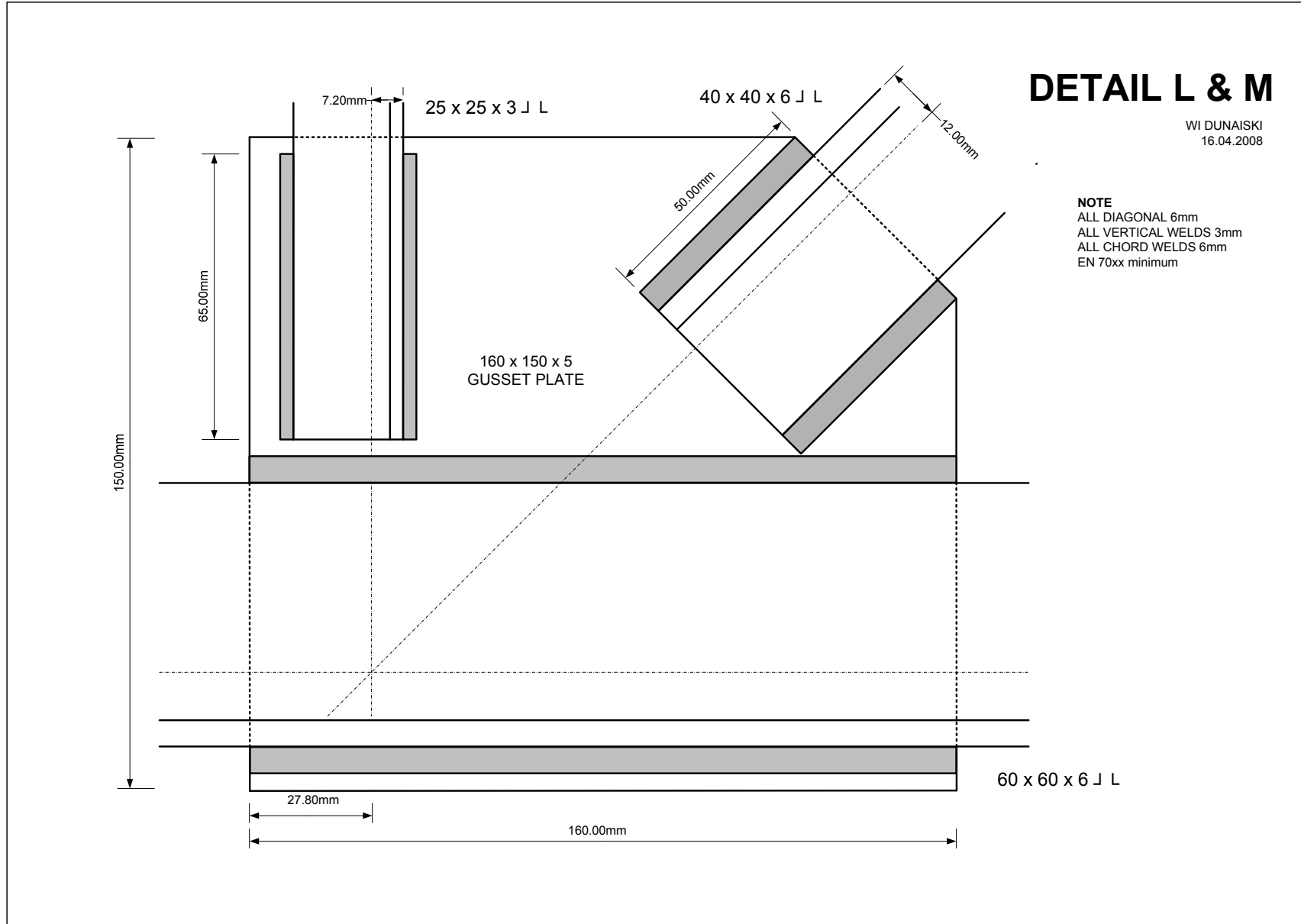


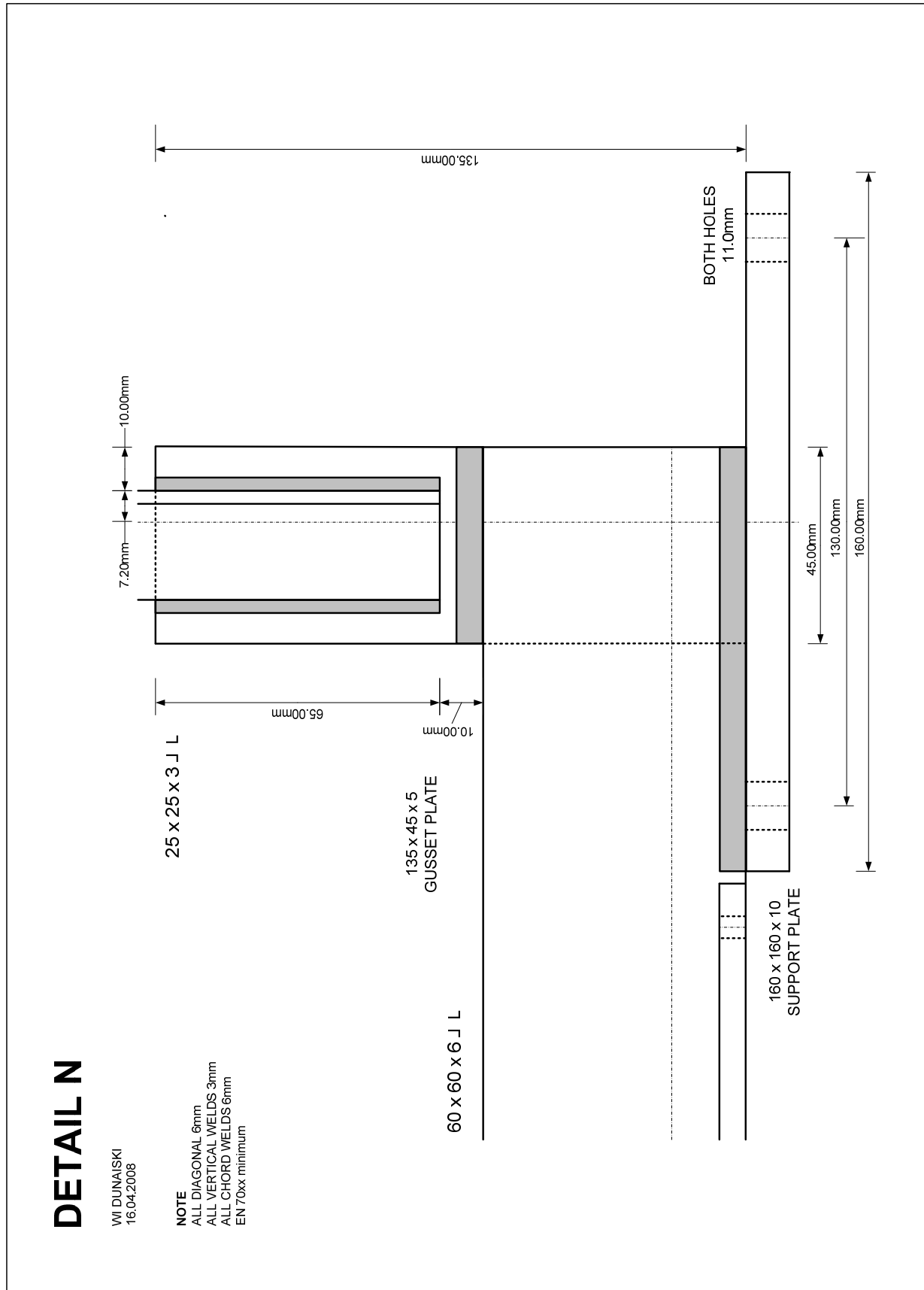












## **D. APPENDIX : DRAWINGS FOR WIND LOAD CASE TRUSS**

### **GENERAL NOTES TO WORKSHOP DRAWINGS**

#### **TRUSS DIMENSIONS**

- 6300mm x 1050mm
- 6 bays

#### **SECTIONS**

- All sections double angles
- All sections 200W (Commercial Grade) Steel, except 60x60x6 angles (350W)

#### **CONNECTING PLATES**

- All connecting plates 5mm thick and 50mm long
- Width of plate determined by angle width, plus 10mm

#### **GUSSET PLATES**

- All gusset plates 5mm thick, cut from plates
- Grade 300W steel

#### **SUPPORT PLATES**

- All support plates 10mm thick, cut from plates
- Grade 300W steel

#### **BUILT-UP PLATES**

- All built-up plates consist of 5mm gusset plate, between two 10mm thick plates, cut from plates
- Grade 300W steel, welded

### **LIST OF WORKSHOP DRAWINGS**

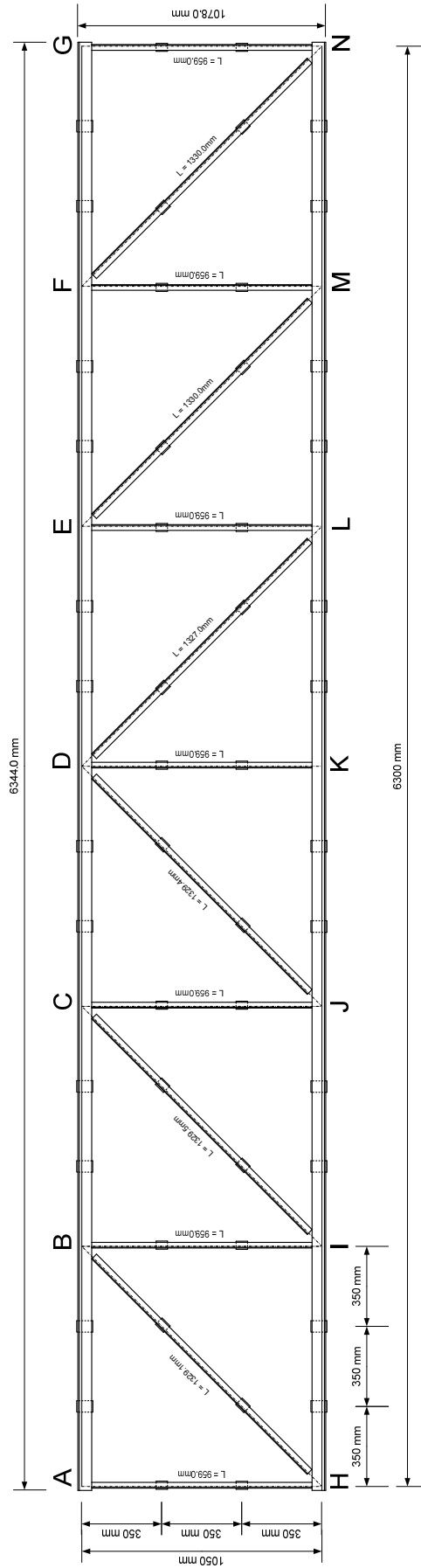
- |                                |                             |
|--------------------------------|-----------------------------|
| - Truss Layout – Wind Load.vsd | - Connection H.vsd          |
| - Connection A.vsd             | - Connection I & J.vsd      |
| - Connection B & C.vsd         | - Connection K.vsd          |
| - Connection D.vsd             | - Connection K Sideview.vsd |
| - Connection E & F.vsd         | - Connection L & M.vsd      |
| - Connection G.vsd             | - Connection N.vsd          |

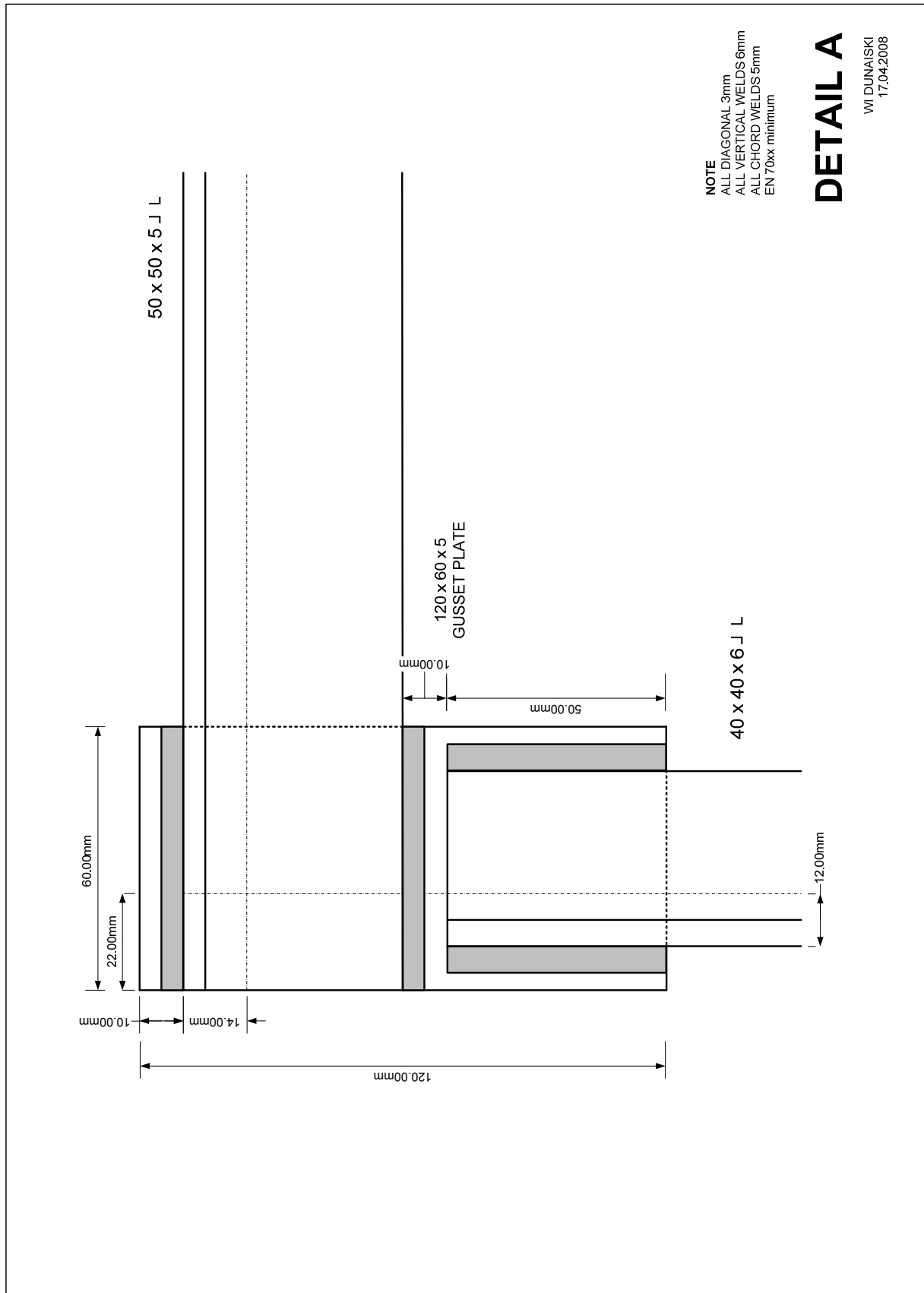
**Truss Layout | Wind Load**

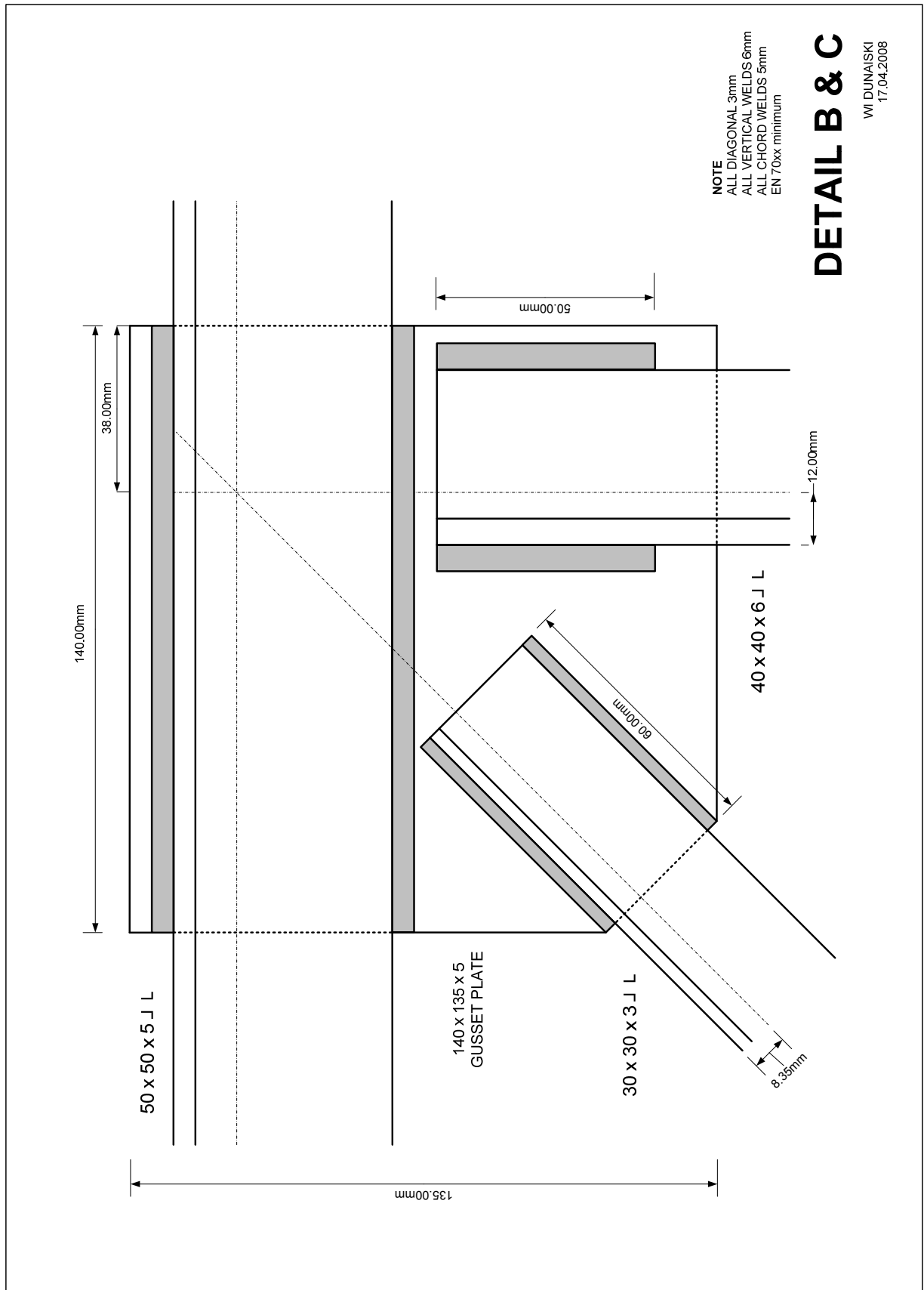
6300mm x 1050mm  
6 Bays

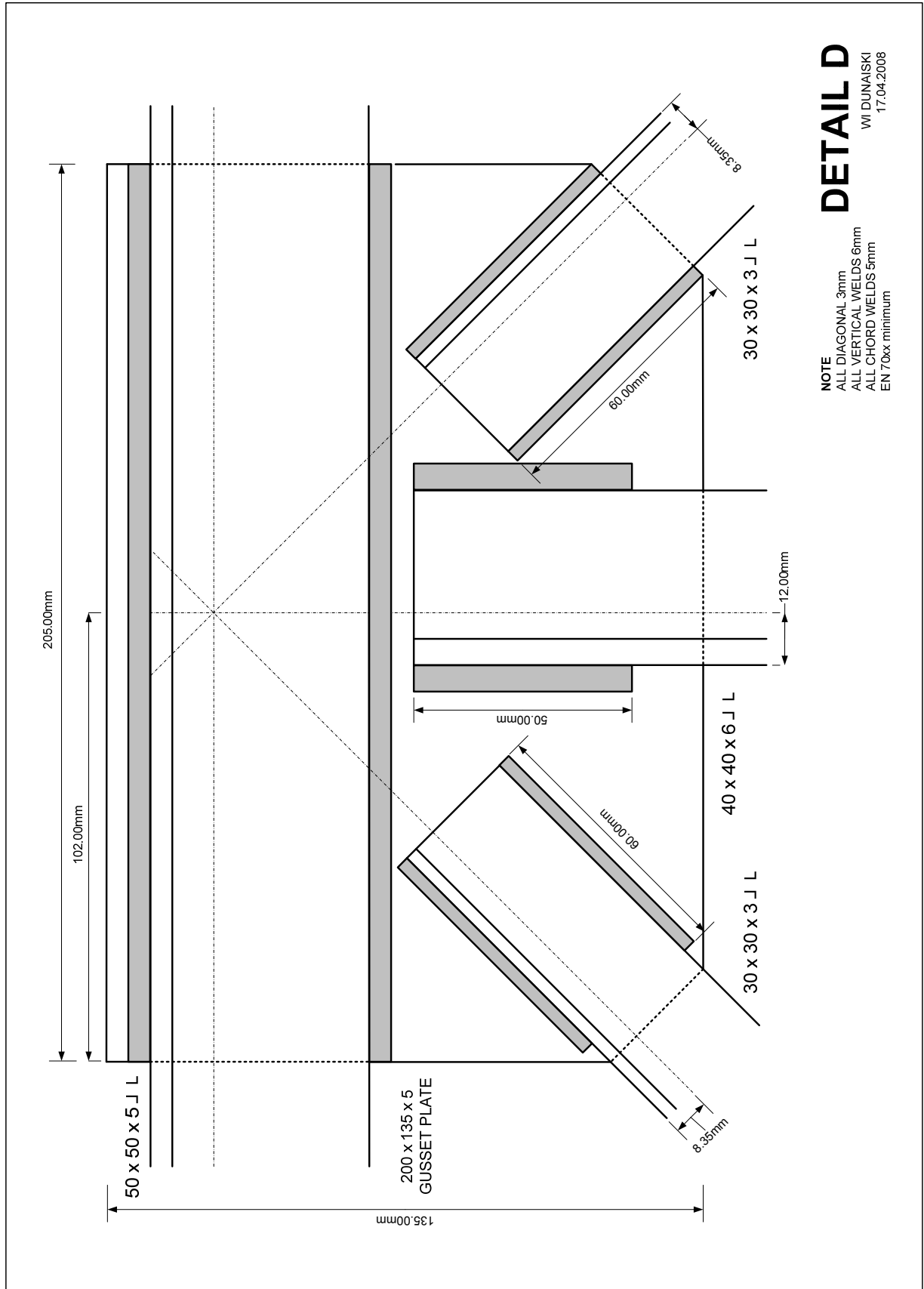
All sections double angles

Top Chord 50 x 50 x 5  
 Bottom Chord 50 x 50 x 5  
 Diagonals 30 x 30 x 3  
 Verticals 40 x 40 x 6





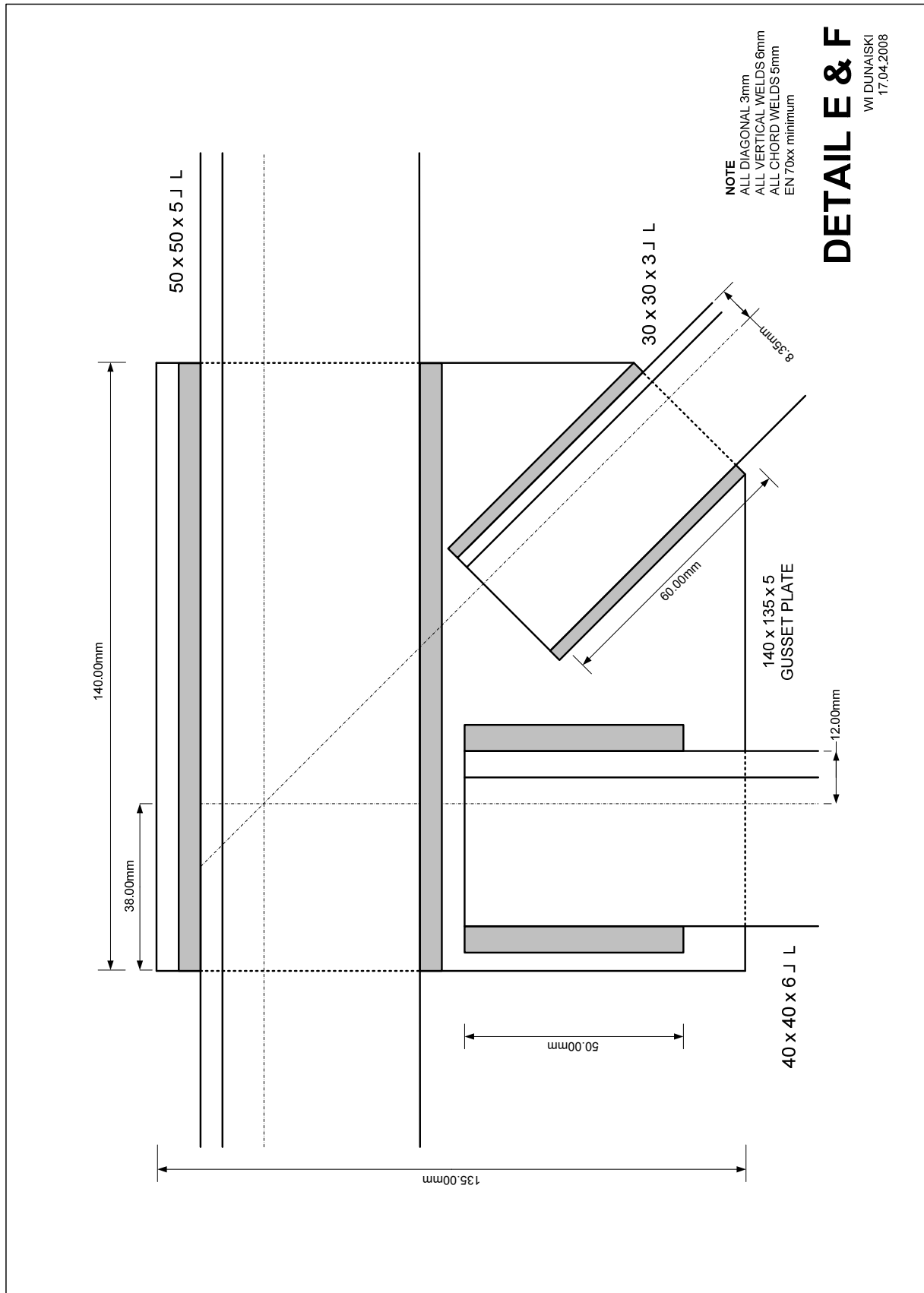




# DETAIL D

**NOTE**  
 ALL DIAGONAL 3mm  
 ALL VERTICAL WELDS 6mm  
 ALL CHORD WELDS 5mm  
 EN 70xx minimum

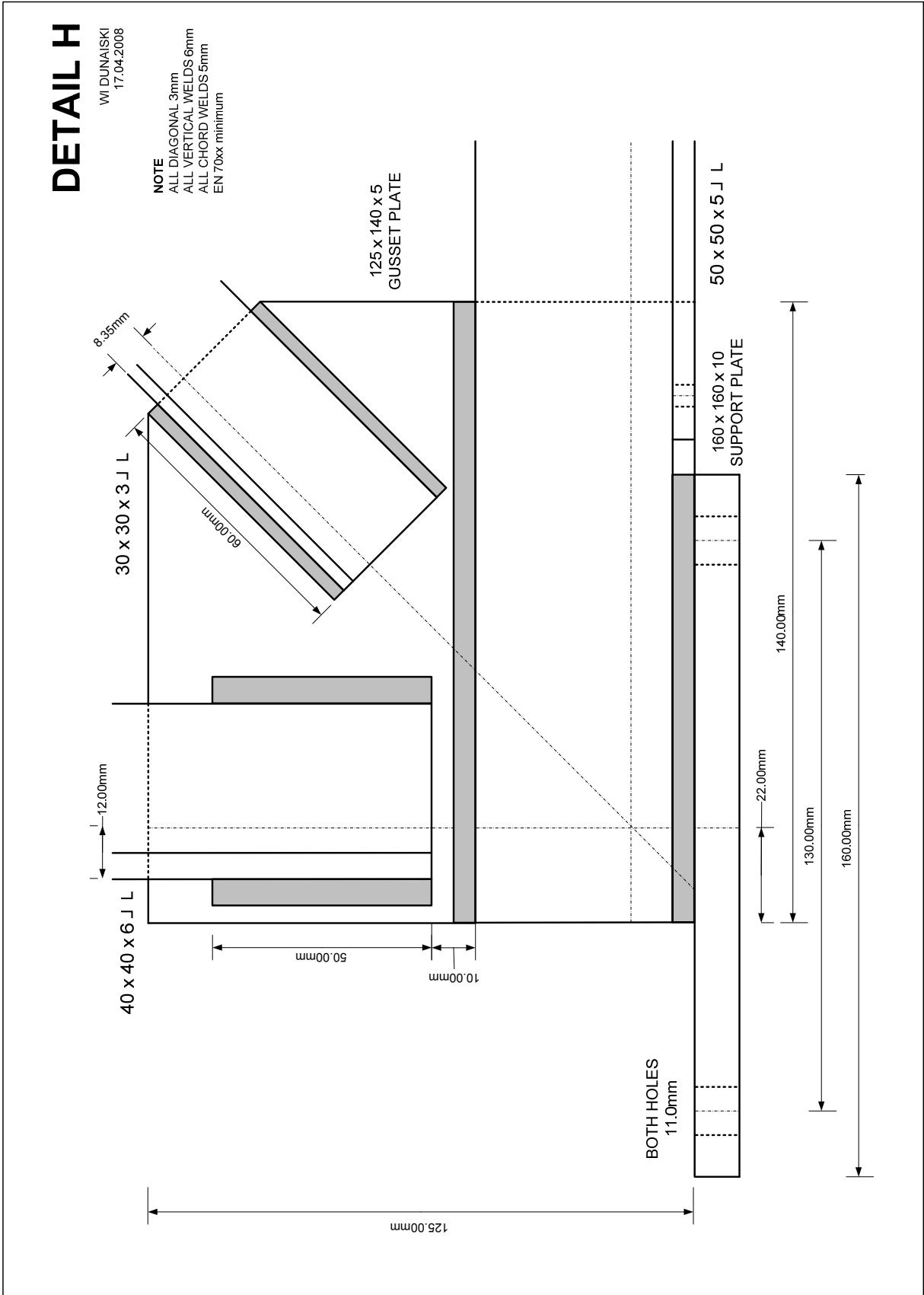
WI DUNAISKI  
 17.04.2008



# DETAIL E & F

WI. DUNAISKI  
 17.04.2008



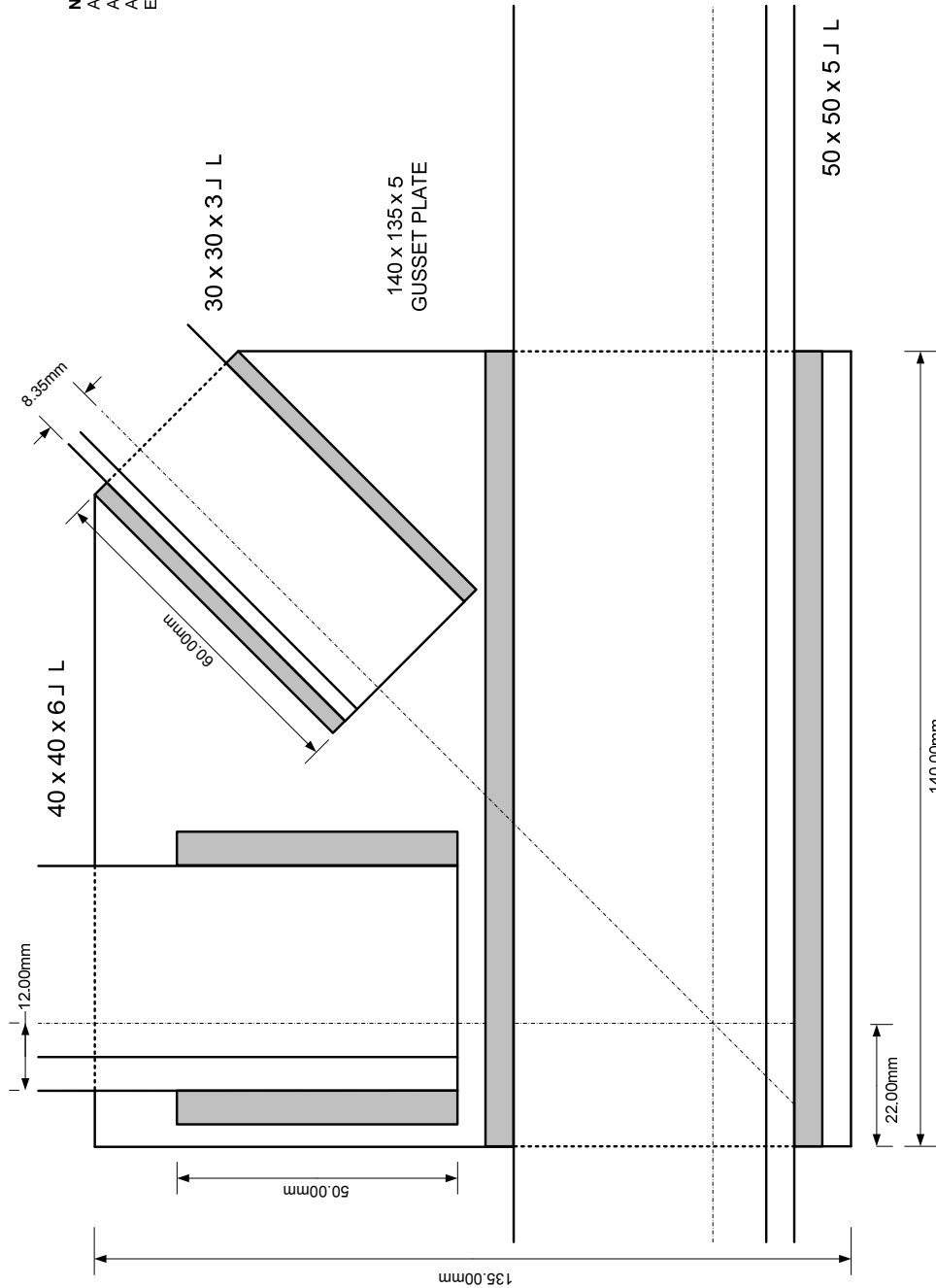


# DETAIL I & J

WI DUNAISKI  
17.04.2008

**NOTE**

ALL DIAGONAL 3mm  
ALL VERTICAL WELDS 6mm  
ALL CHORD WELDS 5mm  
EN 70xx minimum

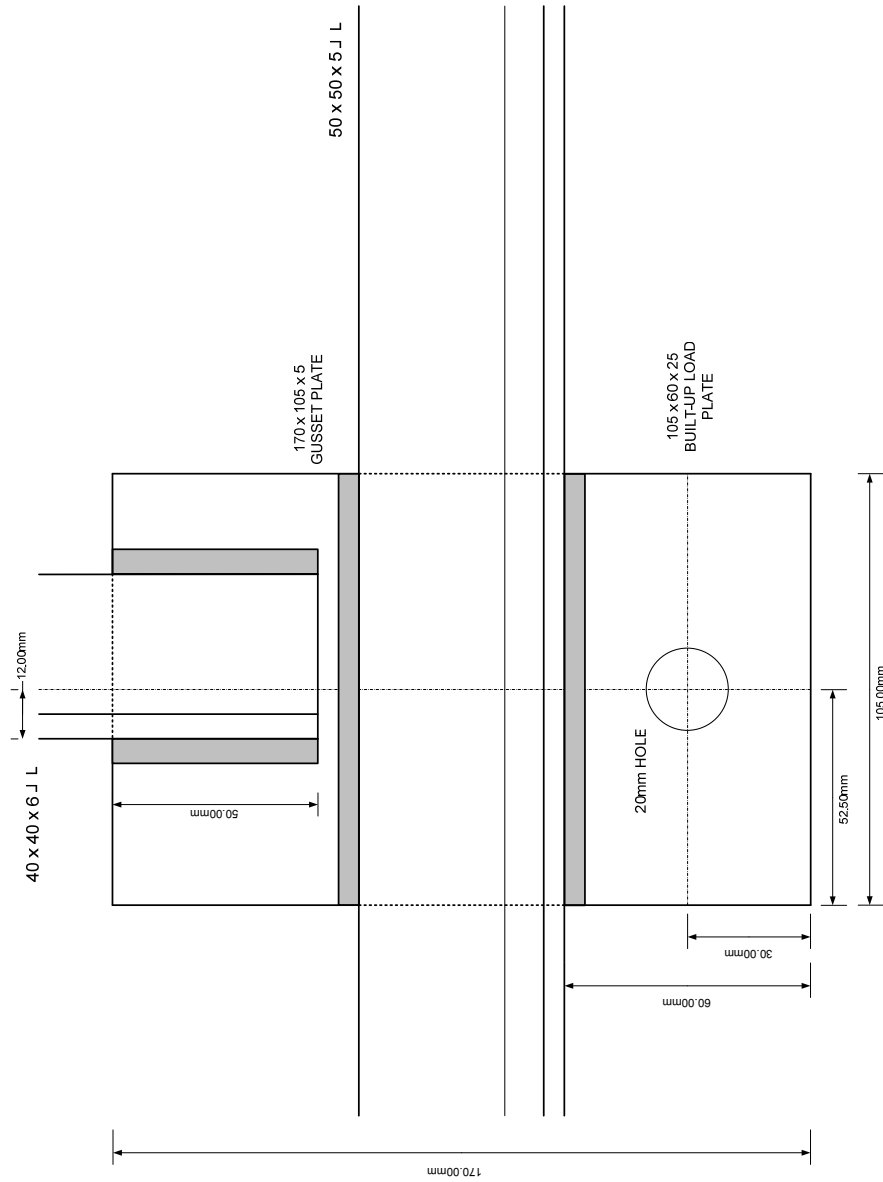


# DETAIL K

WI DUNAISKI  
17.04.2008

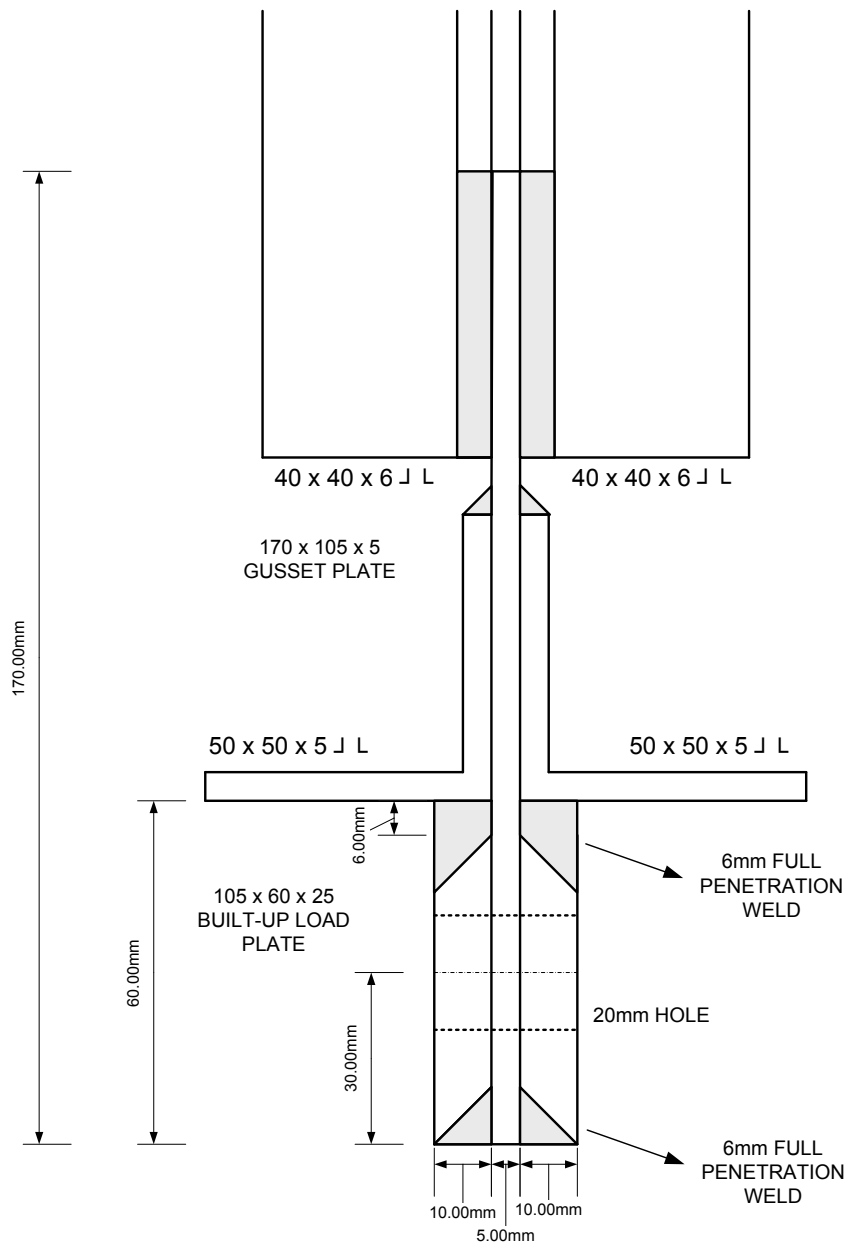
**NOTE**

ALL DIAGONAL 3mm  
ALL VERTICAL WELDS 6mm  
ALL CHORD WELDS 3mm  
EN 78x minimum

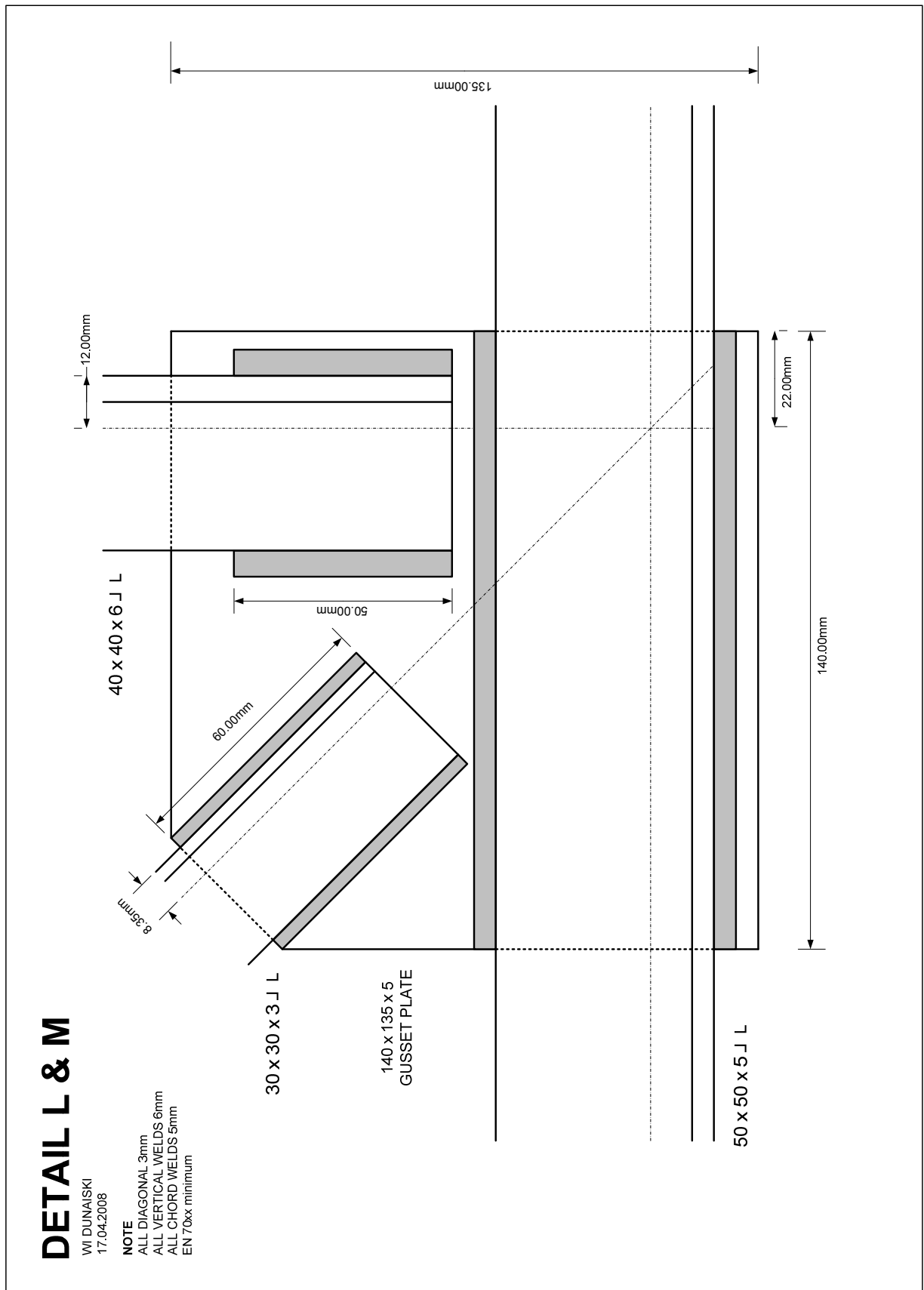


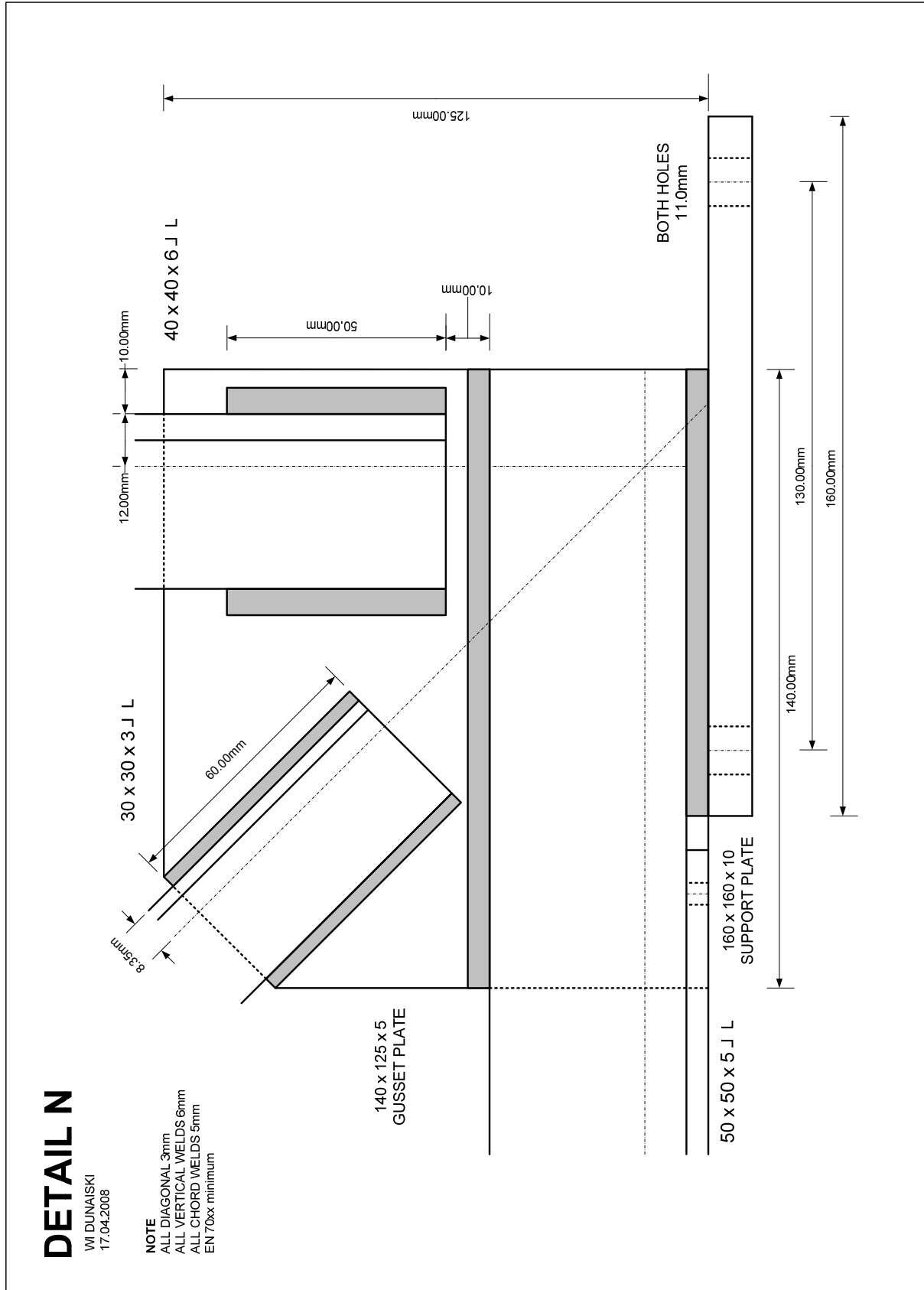
# CROSS SECTION DETAIL K

WI DUNAISKI  
16.04.2008



**NOTE**  
ALL DIAGONAL 6mm  
ALL VERTICAL WELDS 3mm  
ALL CHORD WELDS 5mm  
EN 70xx minimum

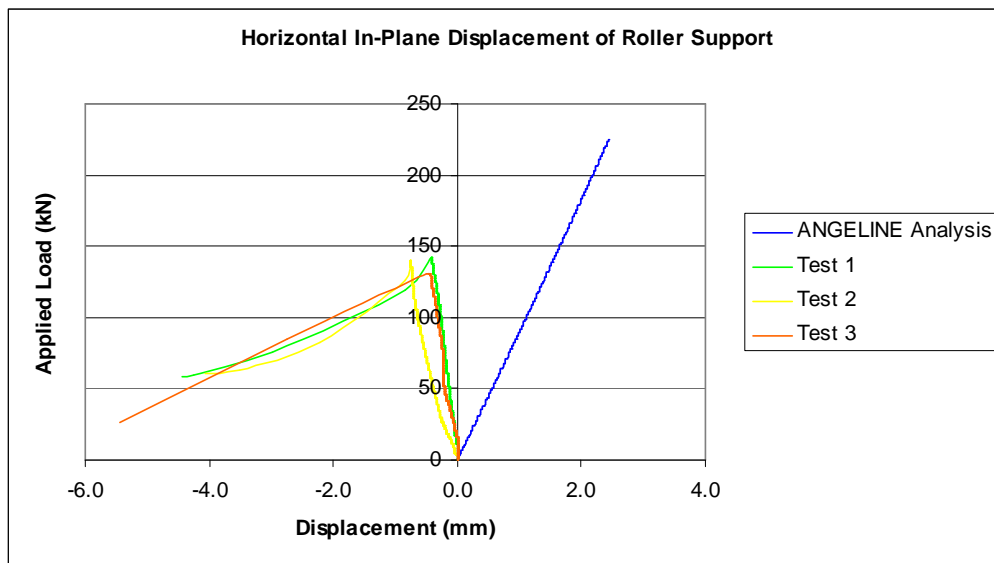




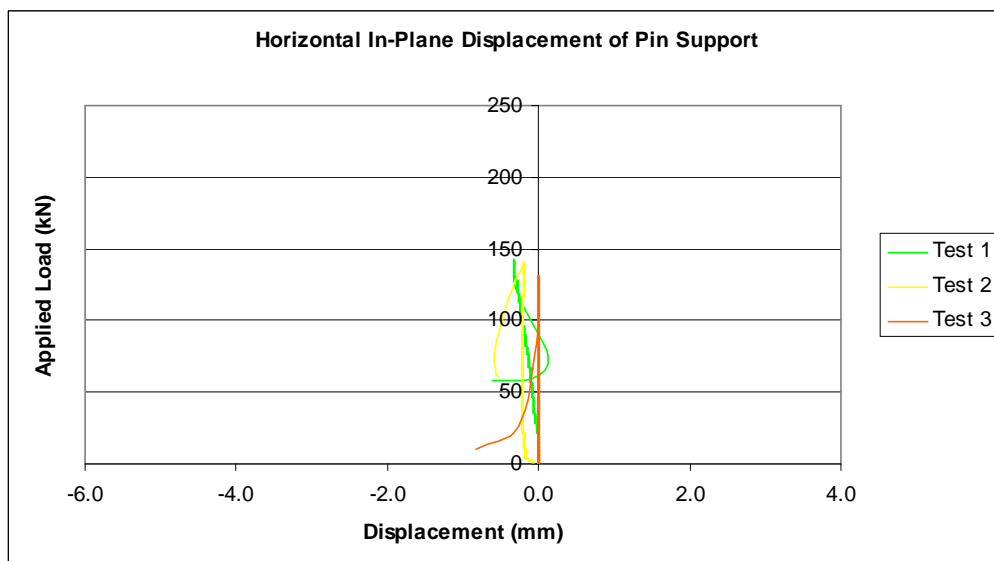
## E. APPENDIX : RESULTS OF GRAVITY LOAD CASE TESTS

### DISPLACEMENT OF SUPPORTS

The following two graphs depict the in-plane movement of the truss at both the roller support as well as the pin support. A maximum displacement of 2.4mm was expected at the roller support. However displacements of up to -5.8mm were measured. This large negative displacement is due to the large deformations of the truss following the buckling of the critical element.

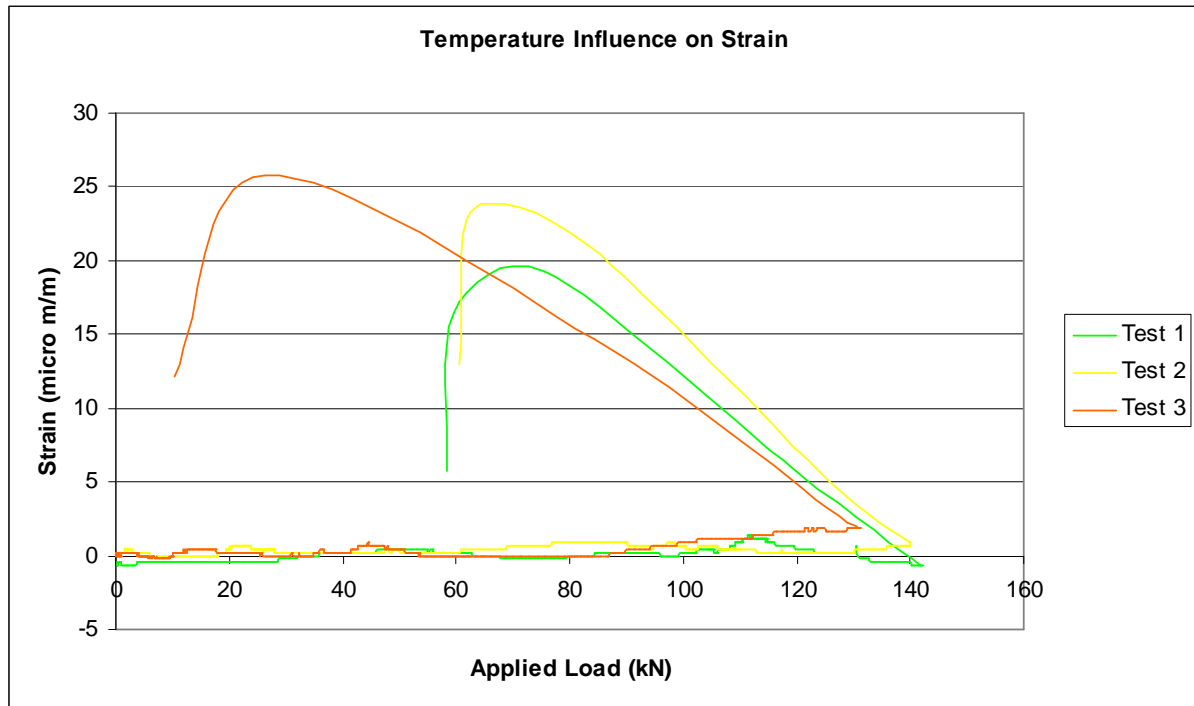


Theoretically no movement of the pin support should occur. Some displacements were measured, however, they were considered negligibly small. The maximum displacement measured of the pin support was -0.8mm.



## INFLUENCE OF TEMPERATURE ON STRAIN MEASUREMENTS

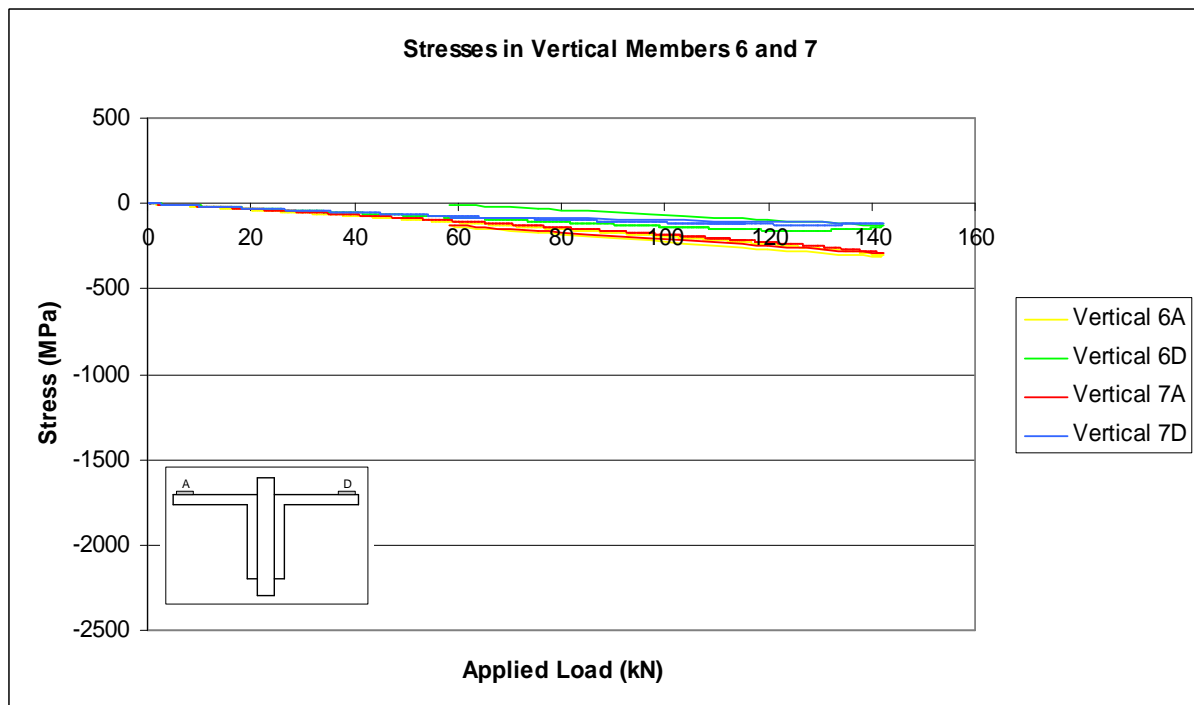
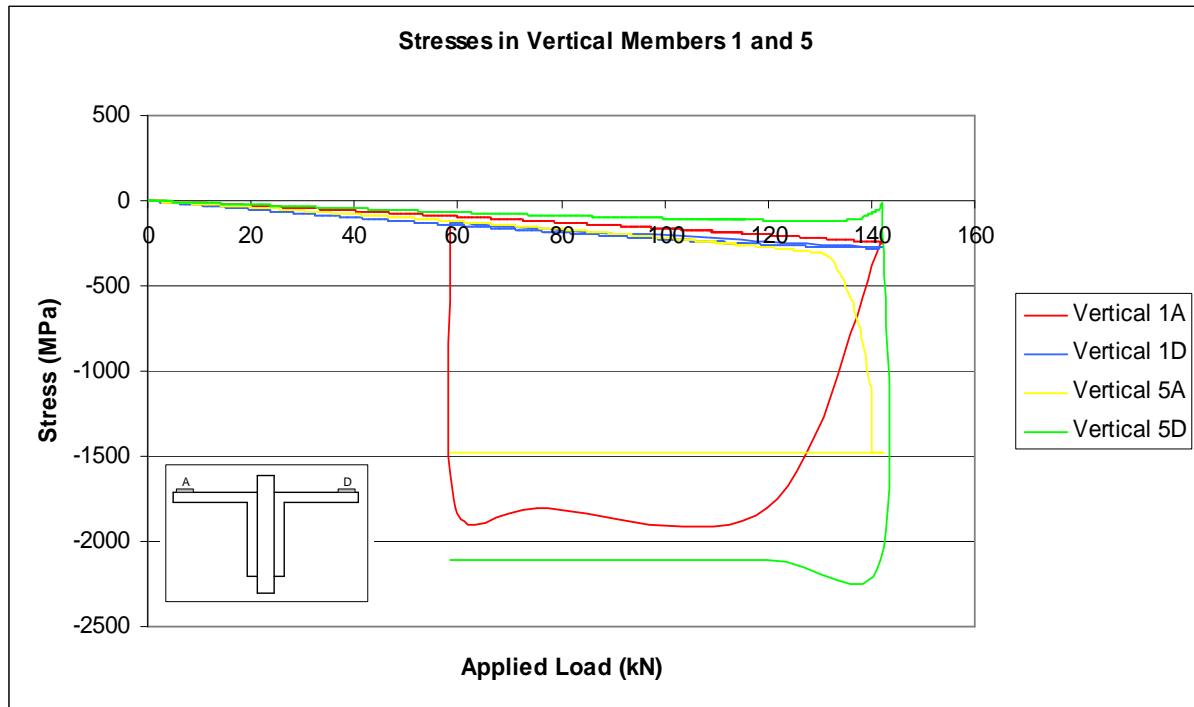
In order to ensure that ambient temperature fluctuations did not significantly influence the strain measurements taken during the tests, a separate strain gauge was placed in the same environment to monitor such possible fluctuations. The readings taken by this strain gauge are presented below.



It is interesting to note the sudden increase in strain, indicating an expansion and hence increase in temperature in the steel, at the point of failure of the trusses until a sudden decrease again which coincides with the load removal. The strain gauge monitoring the temperature was placed on the frame supporting the fork with which the load was applied to the trusses. This indicates that the energy released in the buckling process is partially converted to heat energy, dissipated through the supporting structure. However, it is important to note that the strain variations due to ambient temperature fluctuations are negligibly small, in the order of magnitude of 0.05%.

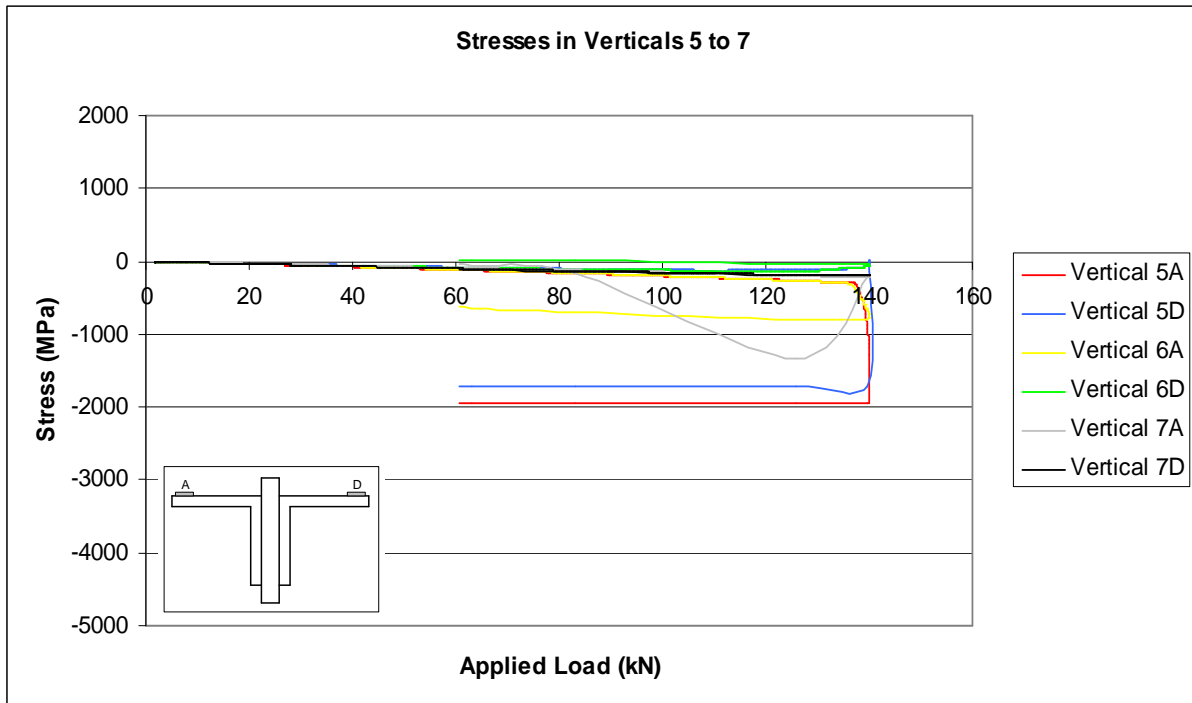
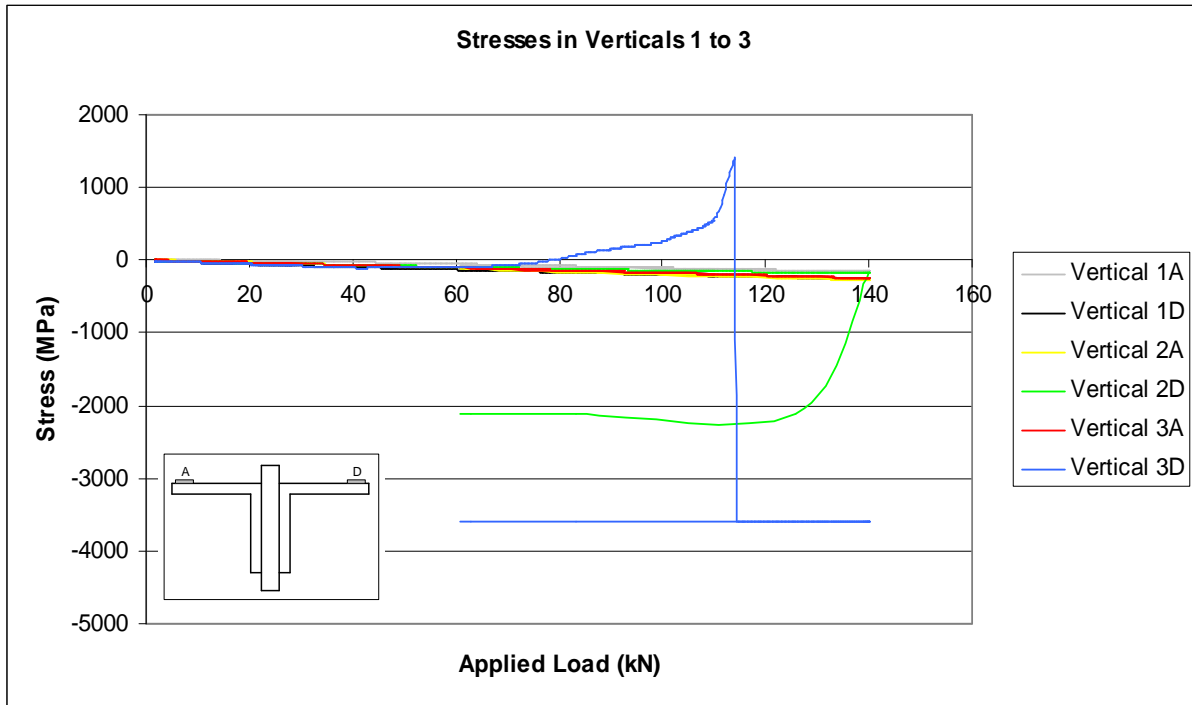
**TEST 1 : GREEN**

- Vertical 5 failed at 142kN applied load



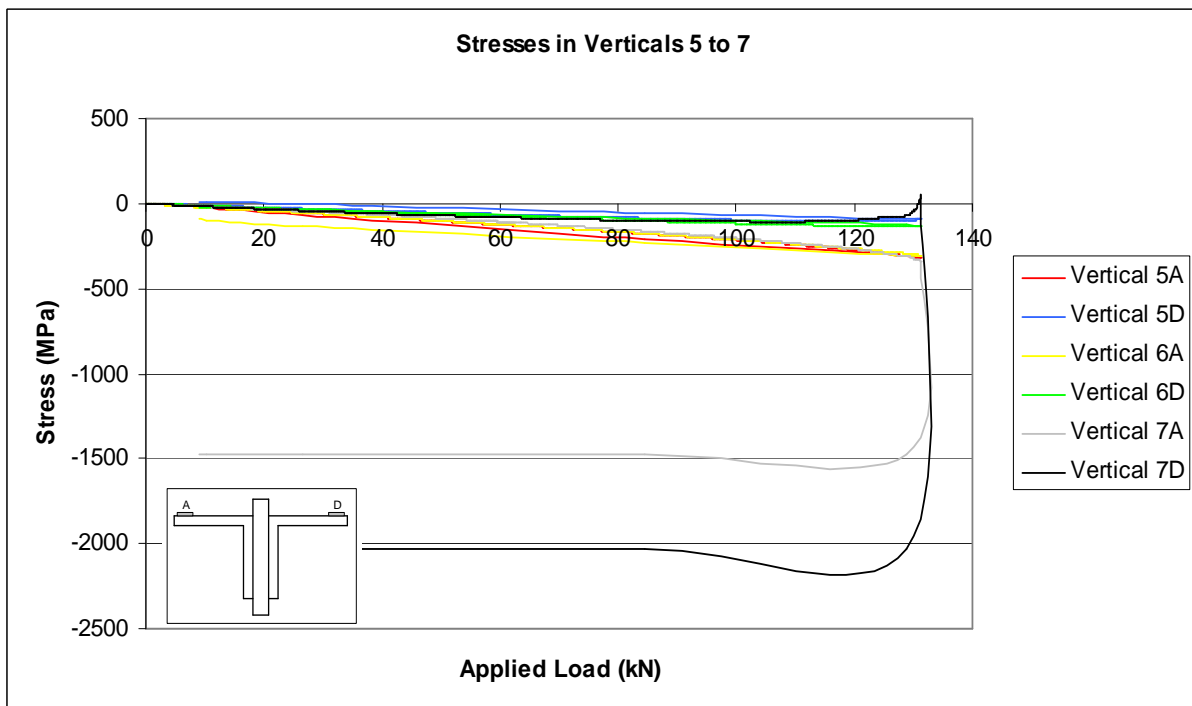
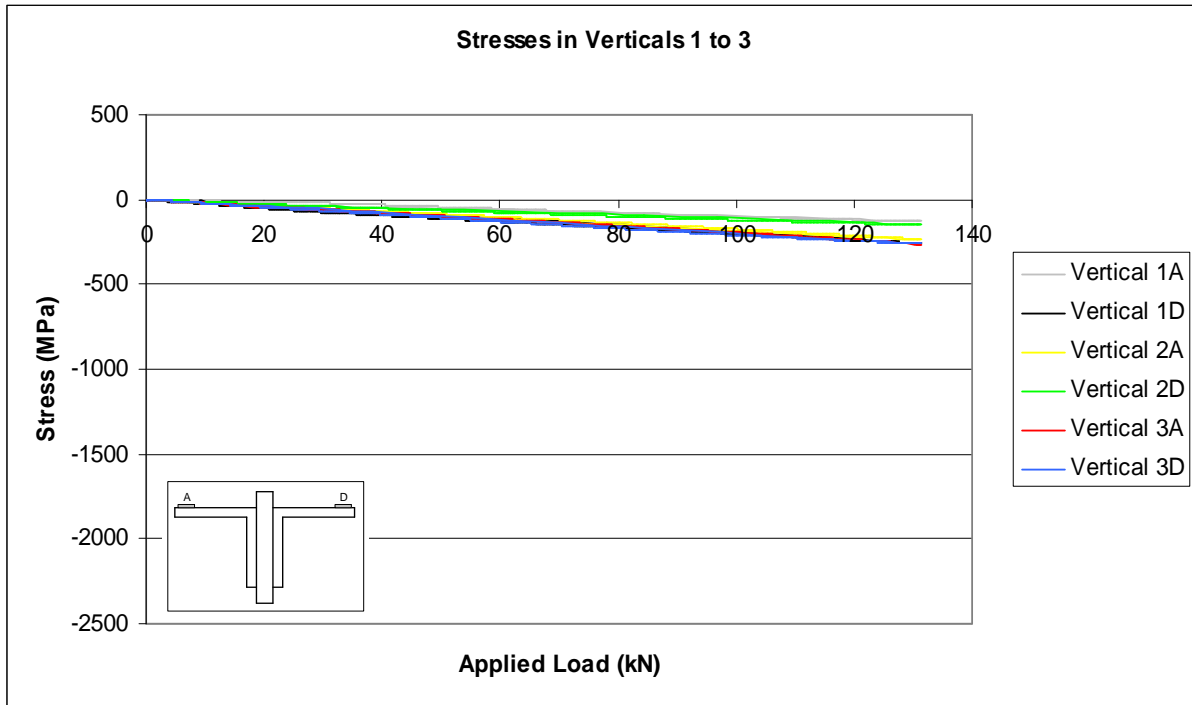
**TEST 2 : YELLOW**

- Vertical 5 failed at 140kN applied load



**TEST 3 : ORANGE**

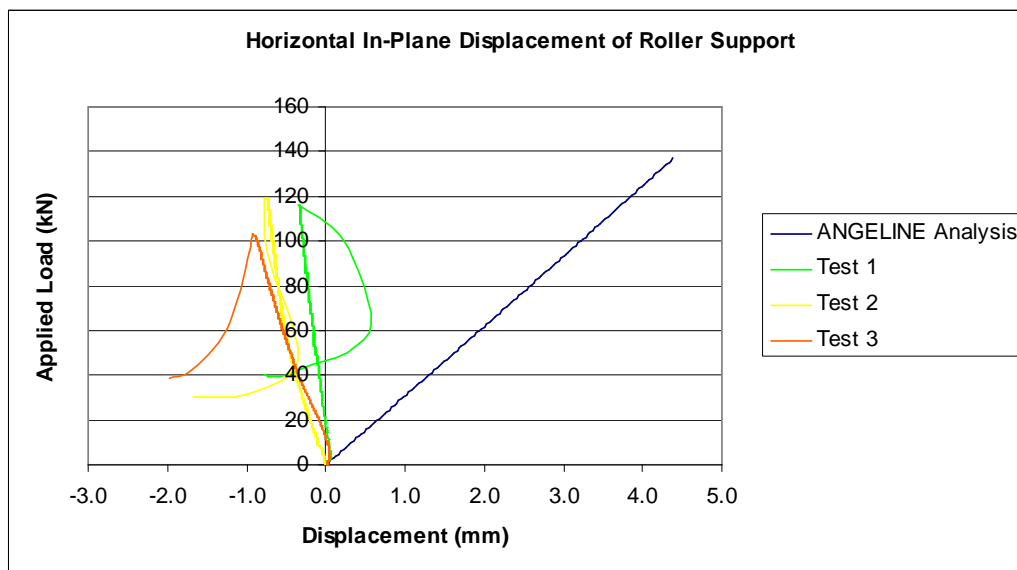
- Vertical 7 failed at 131kN applied load



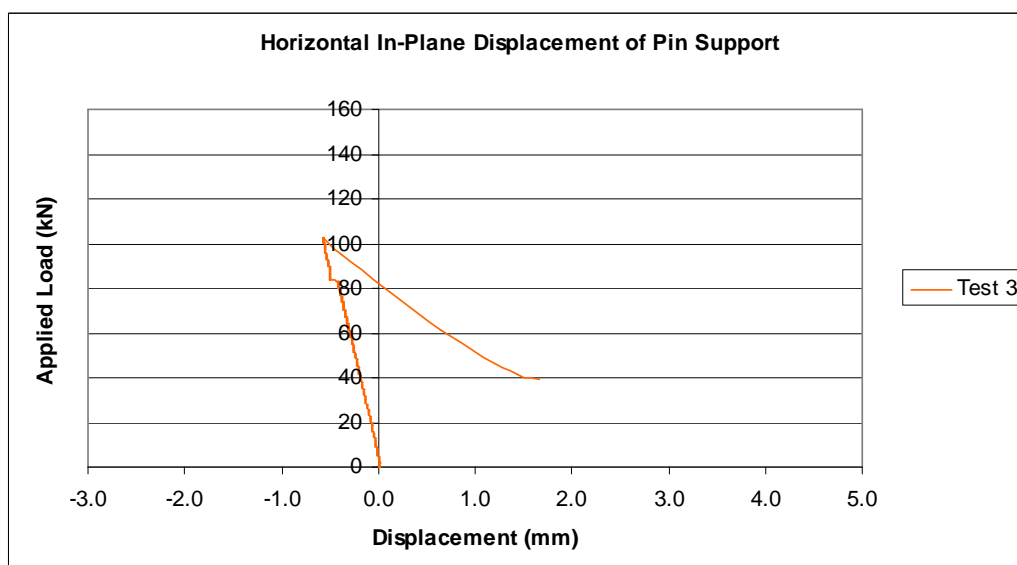
## F. APPENDIX : RESULTS OF WIND LOAD CASE

### DISPLACEMENT OF SUPPORTS

The following two graphs depict the in-plane movement of the truss at both the roller support as well as the pin support. A maximum displacement of 4.4mm was expected at the roller support. However displacements of up to -2.0mm were measured. This large negative displacement is due to the large deformations of the truss following the buckling of the critical element.

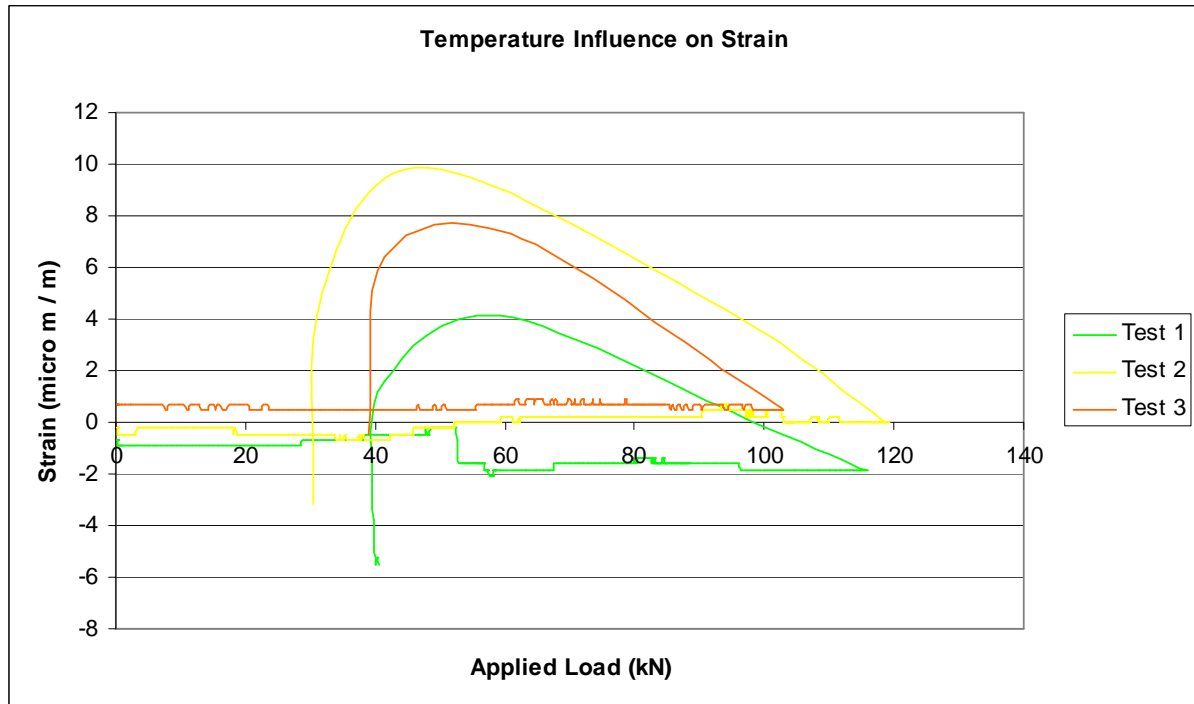


Theoretically no movement of the pin support should occur. Some displacements were measured, however, they were considered negligibly small. The maximum displacement measured of the pin support was 1.6mm.



## INFLUENCE OF TEMPERATURE ON STRAIN MEASUREMENTS

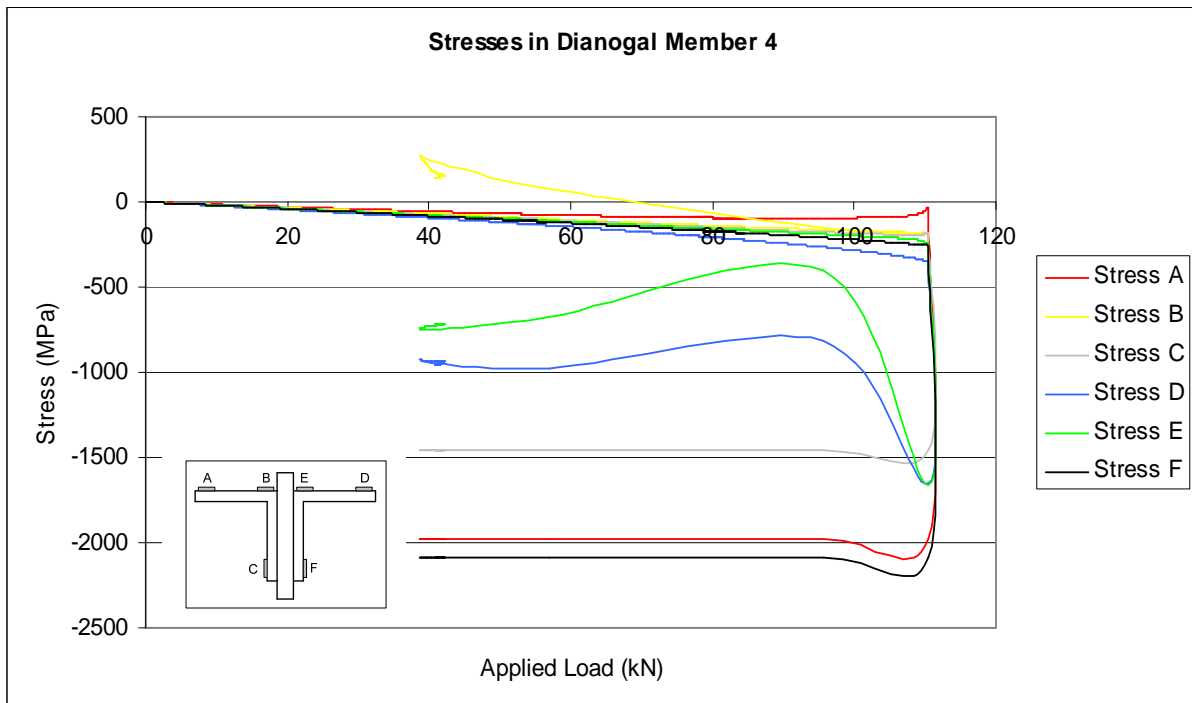
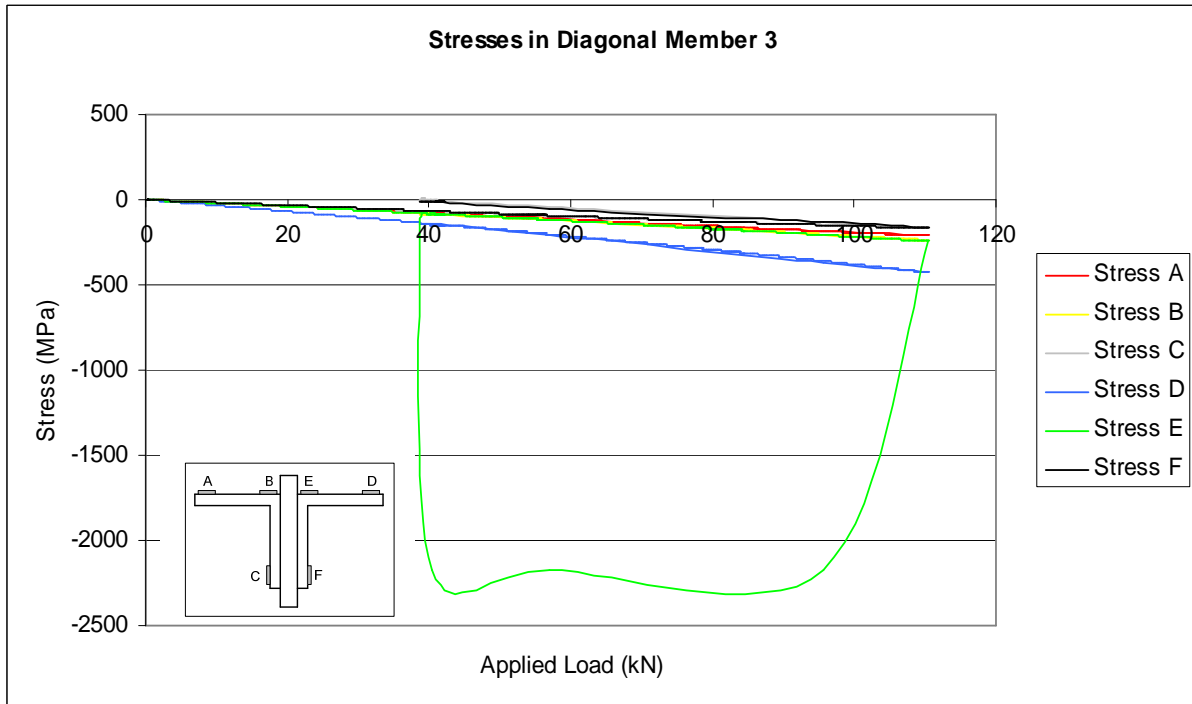
In order to ensure that ambient temperature fluctuations did not significantly influence the strain measurements taken during the tests, a separate strain gauge was again placed in the same environment to monitor such possible fluctuations. The readings taken by this strain gauge are presented below.



Similar to the wind load case test results, it is interesting to note the sudden increase in strain at the point of failure of the trusses. This again indicates that the energy released in the buckling process is partially converted to heat energy, dissipated through the supporting structure. However, it is important to note that the strain variations due to ambient temperature fluctuations are still negligibly small, in the order of magnitude of 0.05%.

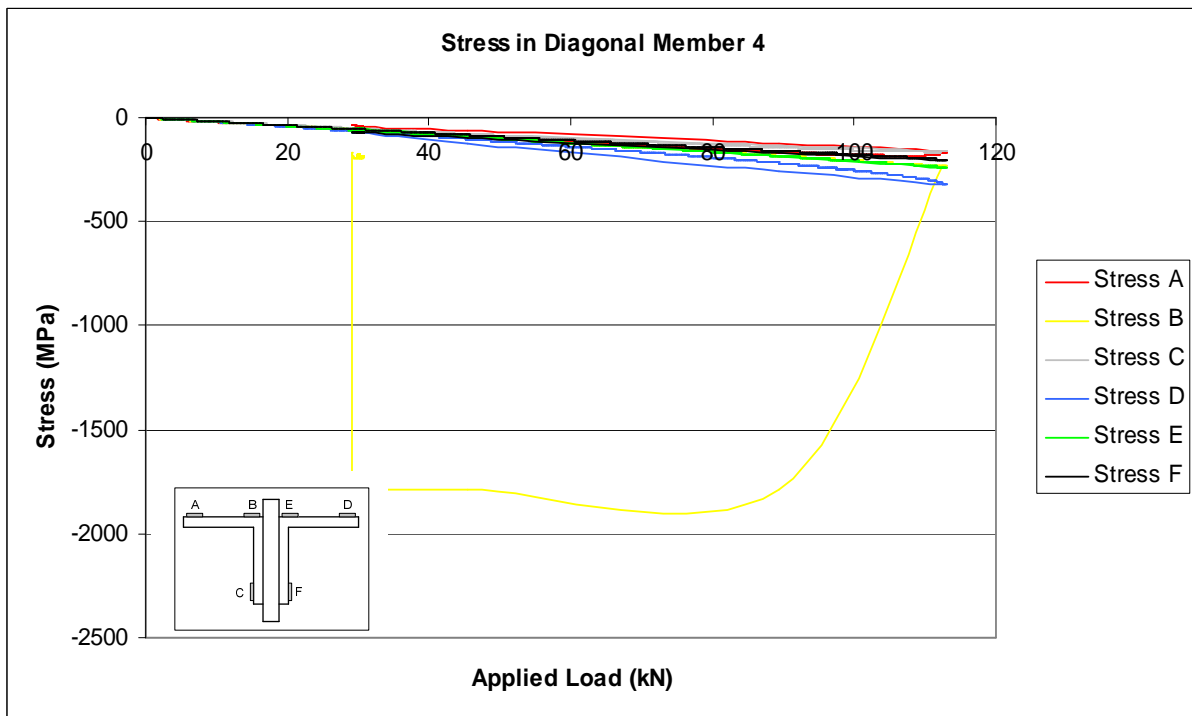
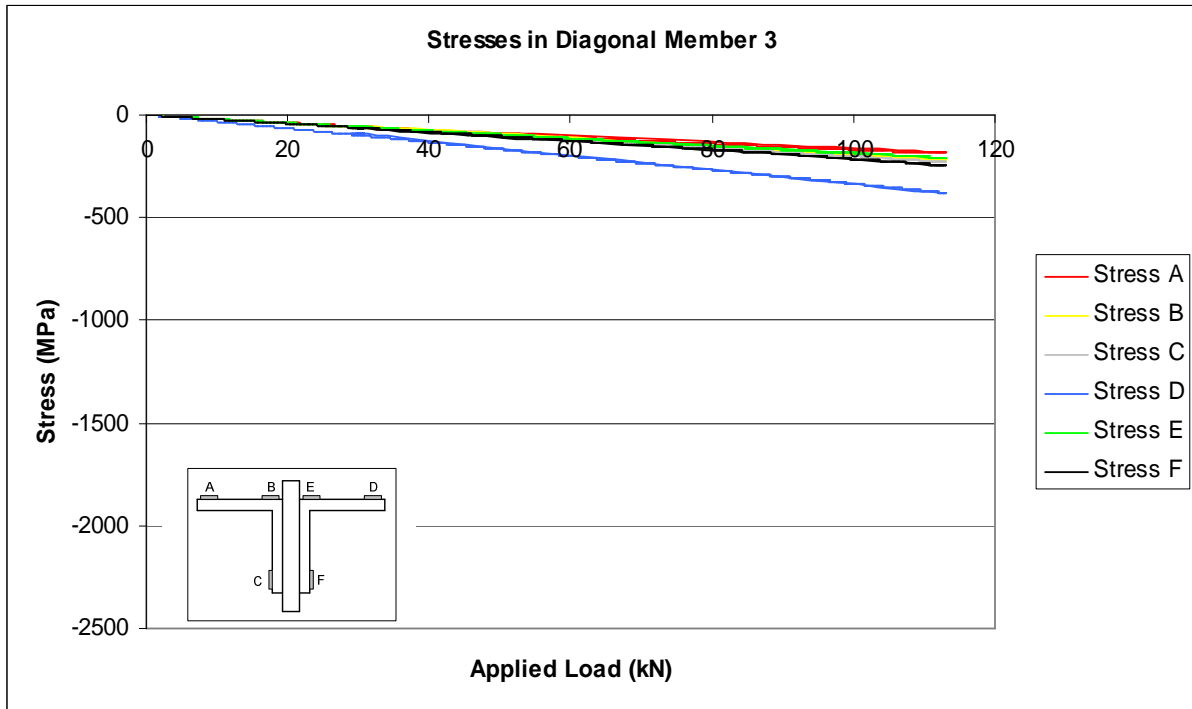
**TEST 1 : GREEN**

- Diagonal 4 failed at 119kN applied load



**TEST 2 : YELLOW**

- Diagonal 6 failed at 115kN applied load



**TEST 3 : ORANGE**

- Diagonal 2 failed at 102kN applied load

